Human Lysosomal Sulphate Transport

Martin David LEWIS B.Sc. (Hons)

Thesis Submitted For the Degree Of
Doctor of Philosophy

in

The University of Adelaide
(Faculty of Medicine)

May 2001

Lysosomal Diseases Research Unit
Department of Chemical Pathology
Women's and Children's Hospital
South Australia

and

Department of Paediatrics
Faculty of Medicine
Women's and Children's Hospital
South Australia

Elliot, Samuel and Millie

Table of Contents

Abstract

The lysosome is a cytoplasmic organelle that contains hydrolytic enzymes in a suitable environment for the degradation of macromolecules. The products of hydrolysis need to be transported out of the lysosome and into the cytosol. Approximately twenty substrate-specific transporters have been described which perform this important role. Defects in lysosomal transporters cause serious diseases. The clinical severity of lysosomal storage diseases resulting from a transport defect correlates with the degree of storage, and four have been described to date. Cystinosis results from the failure to transport cystine from the lysosome, and Salla disease is a consequence of a defective sialic acid transporter. Niemann-Pick type C disease results from the failure of cholesterol to be removed from the lysosome; the normal mechanism for this is still not clear. The fourth storage disease of hydrolytic products results from the failure to clear cobalamin from the lysosome.

The lysosomal hydrolases, in a coordinated manner, sequentially degrade glycosaminoglycans, glycolipids, glycoproteins and hydroxysteroids. Eight of these lysosomal hydrolytic enzymes are sulphatases, which liberate inorganic sulphate from sulphated macromolecules such as heparan sulphate. Inorganic sulphate, which can inhibit sulphatase activities, is transported from the lysosome for re-utilisation in the cytosol. Neither the transporter for sulphate nor any other substrate had been isolated from the lysosome, although the gene encoding the cystine transporter has recently been identified. Isolation of this integral membrane protein would unravel more of the basic biology of lysosomal degradation.

To purify this transporter, lysosomes were isolated from human placenta in a manner that maintained the sulphate transporter's activity. The integral membrane proteins were isolated

and fractionated. Chemical probes that inhibited the transporter and antibodies produced to a functionally and characteristically similar protein, the erythrocyte anion exchanger (Band 3), were used in an attempt to identify related proteins (the sulphate transporter) in the lysosomal membrane. Integral membrane proteins were separated by two-dimensional electrophoresis and identified by *N*-terminal sequence. The sulphate transporter was reconstituted into artificial phospholipid vesicles. At this time a new family of sulphate transporters with the same characteristics as the lysosomal sulphate transporter were reported. Antibodies against synthetic peptides of the SAT-1 member of this family were then produced and used to continue the search for the lysosomal sulphate transporter. A mutation in the SAT-1 transporter that coincided with a particularly severe form of the lysosomal storage disorder known as Hurler's syndrome was investigated. No difference in lysosomal sulphate transport could be measured in the fibroblasts with the particularly severe form of Hurler's syndrome.

Declaration (of Authenticity)

This work contains no material which has been accepted for the award of any other degree or diploma in any university or other tertiary institution and, to the best of my knowledge and belief, contains no material previously published or written by another person, except where due reference has been made in the text.

I give consent to this copy of my thesis, when deposited in the University Library, being available for loan and photocopying.

Acknowledgments.

My far from exhaustive personal acknowledgments are chronological.

Many thanks go to John Hopwood and Peter Meikle for supervising me throughout this study. John your unpredictable contributions and reminders of the bigger picture are appreciated. Thanks Peter for your energy at the bench particularly in the earlier stages of this study.

Warren Hill and Angela Taylor your friendship was truly valued. Thanks Doug Brooks for being the catalyst of spontaneous social opportunities. Tessa Bradford your presence in the lab consistently contributed to a positive environment.

Viv Muller thanks for giving time to entertain my thoughts and distractions. Tim Chataway thanks for the technical, theoretical, hypothetical and jovial discourses.

Thank you Mike Brisco for your successful effort in constructively reading my thesis without familiarity in the area.

Thank you, to my parents, siblings and friends for their encouragement and support.

Words however, cannot describe the thanks that go to Nicola for sticking it out through thick and thin. Elliot, Samuel and Millie, who will one day be old enough to read this, I'm sorry a cost of this study, has been not having spent more time with you.

Abbreviations

2-D	two-dimensional
2-DE	two-dimensional electrophoresis
ABTS	2,2'-Azino *bis* (3-ethylbenzothiazoline-6-sulphonic acid) diammonium salt
ADP	adenosine diphosphate
AE	anion exchanger
AMPS	ammonium persulphate
APMB	2-(4'-amino phenyl)-6-methylbenzene thiazol-3',7-disulphonic acid
APS	adenosine phosphosulphate
ATP	adenosine triphosphate
BCA	bicinchoninic acid
BME	Basal Medium Eagle
BSA	bovine serum albumin
cAMP	cyclic adenosine monophosphate
CAPS	3-cyclohexylamino-1-propanesulphonic acid
CCCP	carbonyl cyanide m-chlorophenylhydrazone
cDNA	complementary DNA
Con A	Concanavalin A
CS	chondroitin sulphate
DAS	4,4'-diacetamido stilbene-2,2'-disulphonic acid
DCCD	*N,N'*-dicyclohexylcarbodiimide
DIDS	diisothiocyanatostilbene disulphonic acid
DMG	3,3-dimethyl glutaric acid
DMSO	dimethylsulphoxide

DPM	disintegrations per minute
DRA	down regulated in adenoma
DT	diphtheria toxoid
DTD	diastrophic dysplasia
DTDST	diastrophic dysplasia sulphate transporter
DTT	dithiothreitol
ECL	enhanced chemiluminescence
EM	electron microscopy
ELISA	enzyme-linked immuno-sorbant assay
EDTA	ethylenediaminetetra acetic acid
ER	endoplasmic reticulum
DS	dermatan sulphate
FCS	foetal calf serum
FCCP	carbonyl cyanide *p*-trifluoromethoxyphyenylhydrazone
GAG	glycosaminoglycan
Gal	galactose
GalN	galactosamine
GalNAc4, 6diS	*N*-acetylgalactosamine-4, 6-disulphate
GalNAc4S	*N*-acetylgalactosamine-4-sulphate
GF	glass fibre
GlcA	gluconic acid
GlcN	glucosamine
GlcUA	glucuronic acid
GlcNAc	*N*-acetylglucosamine

GlcNAc6S	*N*-acetylglucosamine 6-sulphate
GNAT	acetyl coenzyme A-α-glucosaminide *N*-acetyltransferase
H_2DIDS	4,4'-diisothiocyanodihydrostilbene-2, 2'-disulphonic acid
HEPES	*N*-2-hydroxyethylpiperazine-N'-2-ethanesulphonic acid
HRP	horse radish peroxidase
HS	heparan sulphate
HSP	heat shock protein
ID	identification
IDUA	α-L-iduronidase
IEF	isoelectric focusing
IgG	immunoglobulin class G
LA-GMA	low acid glycol methacrylate
LAMP	lysosomal associated membrane protein
LEP	lysosomal endosomal plasma membrane protein
LIMP	lysosomal integral membrane protein
lgp	lysosomal granule protein
LSD	lysosomal storage disorder
LST	lysosomal sulphate transporter
K_m	Michaelis-Menten affinity constant
KS	keratan sulphate
MCS	6-maleimido caproic acyl *N*-hydroxy succinimide ester
MES	4-moroholine-ethanesulphonic acid
MHS	6-(*N*-maleimido)-*n*-hexanoate
mRNA	messenger RNA

mol	moles
MPS	mucopolysaccharidosis
Mr	relative molecular mass
MSD	multiple sulphatase deficiency
NP40	nonylphenoxy polyethoxy ethanol
NR	non-redundant
PAM	point accepted mutation
PAPS	phosphoadenosine phosphosulphate
PAGE	polyacrylamide gel electrophoresis
PBS	phosphate buffered saline
PC	phosphatidylcholine
PCR	polymerase chain reaction
PG	phenylglyoxal
PHYLIP	Phylogeny Inference Package
pI	isoelectric point
P_i	phosphate (inorganic)
PIR	Protein Information Resource
PLAP	placental alkaline phosphatase
pmol	pico mole
PPi	pyrophosphate
psi	pounds per square inch
PVDF	polyvinylidene difluoride
SAT	sulphate anion transporter
SDS	sodium dodecyl sulphate

SITS	acetamido isothiocyanatostilbene disulphonic acid
TBS	Tris-buffered saline
Thesit®	polyoxethylene 9-laural ether
TLC	thin-layer chromatography
Tris	Tris (hydroxymethyl) methylamine
Tween-20	polyoxyethylenesorbitan monolaurate
UV	ultraviolet
v/v	volume per volume
w/v	weight per volume

List of figures.

List of tables

1. Introduction.

This chapter reviews the literature to enable the appreciation of the study's initial objectives, those that evolved with the advent of newly published work and the approaches taken to reach those aims. Literature that emerged during the preparation of this manuscript has also been included. Chapter two comprises the general materials and methods employed in the study. Chapters three to six report results; the latter two were influenced by the emergence of a new family of candidate sulphate transporters. This new family of sulphate transporters, whose emergence altered the path and approach of the study, spanned 1994 to 1998. Concluding remarks are presented in chapter seven.

The lysosome, in its course of degrading macromolecules, liberates inorganic sulphate. A specific protein then transports this anion across the lysosomal membrane into the cytoplasm. This review makes evident the importance of this process and the specific proteins involved. The current knowledge of the role of sulphate in the cell, its metabolism and intracellular pools is reviewed. A critique of the lysosome, the substrates it degrades, the products produced, and some of the known storage disorders that can arise from failure of either the catabolism of substrates or the egress of products are presented. The transport processes involved in lysosomal product clearance are discussed, with particular emphasis on saturable transporters involved in removal of monomeric subunits such as sulphate. The final part of this introductory chapter looks at the anion transporters that have been characterised and cloned. The recently identified sulphate-specific transporters and diseases with which they are associated are also described.

1.1 Transporters.

Transporters are membrane proteins that allow the controlled passage across a phospholipid membrane of a single molecule or defined group of molecules. Transporters function to supply or remove compounds, regulate cell volume and the pH of membrane-bound spaces. These functions are achieved by working in concert with other transporters, enzymes or in isolation. Transporters also facilitate cell communication by providing a means of chemical or electrical exchange. The lysosomal sulphate transporter allows sulphate produced by numerous sulphatases to escape from the lysosome.

1.1.1 Nomenclature.

The net direction of substrate transport can be described by a number of terms. If the direction of transport is from the extracellular space across the plasma membrane into the cytoplasm, it is referred to as uptake or influx. Transport out of the cell in the opposite direction across the plasma membrane is known as egress or efflux. Just as these terms describe the direction of transport in and out of the cell, they also describe the direction of transport in and out of intracellular organelles and vesicles.

1.1.2 Membrane proteins.

There are membrane-associated or peripheral proteins, and integral membrane proteins. The peripheral membrane proteins are bound to the membrane surface by interactions with proteins or the lipid polar groups. This interaction can be disrupted by high salt or extreme pH. Integral membrane proteins are embedded into the phospholipid bilayer interacting directly with the lipophilic hydrocarbon region of the lipid. Integral membrane proteins are

displaced by disrupting the membrane with organic solvents or detergents (Finean *et al.* 1984; Sabatini and Adesnik 1998).

The relatively few membrane proteins crystallised attests to the hurdles involved when membrane or hydrophobic proteins are removed from their phospholipid bilayer. When integral membrane proteins are removed from a phospholipid bilayer, aggregation and possible precipitation of the protein may occur. Non-ionic detergents such as Triton X-100 can prevent such aggregation by taking the place of the lipid yet enable the protein to be manipulated in an aqueous system (Finean *et al.* 1984).

Integral membrane proteins are divided into three groups, *type I* proteins have one hydrophobic membrane-anchoring domain with the *N*-terminal in the extracellular or a luminal organelle space and the *C*-terminal in the cytoplasmic space. Proteins that have one trans-membrane domain with the terminals in reverse to *type I* are *type II* proteins. When a protein such as a transporter crosses a phospholipid membrane more than once, it is a *type III* protein. This third class of proteins can have its terminals in any orientation including both terminals on the same side of the membrane (Sabatini and Adesnik 1998). The number of *type III* proteins that have had their structure determined is very low when compared with soluble proteins. The hydrophobic nature of membrane proteins does not allow their structure to be easily preserved after their extraction from phospholipid membranes. Detergent-protein complexes are a strategy used to control stability and aggregation of membrane proteins. This results in more complicated crystallisation conditions, which need to be optimised to accommodate the presence of detergents (Garavito *et al.* 1996). Transporters are *type III* membrane proteins.

1.1.3 Types of transporters.

Transporters can be divided into three categories based on how they function, namely channels, pumps and carriers. These groups cannot be ascertained by sequence alone as some channels and carriers are structurally very similar (Simon and Blobel 1991).

Channels transport extremely fast, in the order of 10^6-10^8 ions /sec (Stein 1986) generating a measurable membrane potential. This membrane potential is measured by patch-clamping where electrophysiological data is collected (Hamill *et al.* 1981; Neher and Sakmann 1976). Channels are either voltage- or ligand-operated (Stanfield 1987) and do not undergo conformational change during transport. Ions are able to interact with binding sites at both sides of the membrane at the same time (Neher and Sakmann 1976). Pumps such as a proton pump (*Section 1.3.3.1*) are primary active transporters using nucleotide hydrolysis (ATP for example) or the energy from redox reactions directly. Pumps usually function in a unidirectional manner against an electrochemical gradient. A pump is demonstrated by its energy dependence (Forgac *et al.* 1983; Stevens and Forgac 1997). Carriers also known as permeases or translocases allow hydrophilic substrates to diffuse across phospholipid membranes. They differ from channels in that they are saturable with a finite number of binding sites. The rate of carrier-mediated transport is also limited by the transporter's conformational changes during substrate transport (Addison and Scarborough 1982; Hamill *et al.* 1981; Stein 1986). The lysosomal sulphate transporter in rat liver has been described as a saturable carrier (Jonas and Jobe 1990).

Carrier-mediated transport can be expressed like an enzyme reaction by the Michaelis-Menten kinetics (*Equation 1*). With transporters, however, the affinity constant is often denoted as K_t instead of K_m. Carriers can also be subject to inhibition either in a competitive or non-competitive mode.

$$v = SV_{max} / [K_m + S]$$

Equation 1 *The symbol v is the velocity of the reaction, S is the substrate concentration, V_{max} is the maximal rate of velocity, and K_m is equal to the substrate concentration at which the reaction rate is half of its maximal rate.*

1.1.4 Carrier transport mechanisms.

Transporters facilitate the passage of their substrates by either a passive or an active mechanism. Passive transport, as the name suggests, is not driven but allows the diffusion of its specific substrate down an electrochemical gradient. Active transport by a carrier is not primary active transport, as the energy driving the transport is derived from the concentration gradient of another ion. An ion that binds to another ion species during carrier-mediated transport is said to be co-transported. The co-transported ion can influence the direction of the anion transport. This influence of the chemical gradient of one substrate on the direction of transport of another substrate is known as secondary active transport (Geck and Heinz 1976, 1989; Geck *et al.* 1978; Heinz *et al.* 1972).

Secondary active carrier transport can be coupled to chemical gradients in several ways (*Figure 1.1*). The substrate can be co-transported after binding to another ion (*Figure 1.1A*), alternatively a co-transporter could be a symporter or an antiporter where the different substrates are transported in the same or different directions (*Figure 1.1B and C*). If the same substrate is on both sides of the carrier with a higher concentration on one side and a lower radio-labelled concentration on the other, the transport of labelled substrate can be measured moving against its own concentration gradient and is called counter-transport (*Figure 1.1D*).

The rate of transport is determined by the highest concentration present. If a substrate exchanges with a substrate analogue, it is known as *trans*-stimulation. A characteristic of carriers is their ability to be involved in countertransport (Gennis 1989; Turner 1983). The stimulated transport of a substrate by co-transport is referred to as *cis*-stimulation.

1.1.5 Transporter families.

Transporters can also be grouped into families based on a structural homology or function. A well-known super-family is the ABC transporter, so named because they contain an 'ATP binding cassette'. These transporters utilise ATP hydrolysis as an energy source, hence the highly conserved ATP-binding motif. An example of an eukaryotic member of this family is the cystic fibrosis conductance regulator protein (Fath and Kolter 1993).

The sodium / solute symporters comprise another super-family which is divided into eleven sub-families based on functionality and sequence analysis. Briefly, the eleven sub-families are the: (1) ubiquitous broad specificity solute symporters; (2) eukaryotic-specific neurotransmitter family; (3) ubiquitous dicarboxylate family; (4) ubiquitous inorganic phosphate family; (5) bacterial galactoside family; (6) bacterial citrate family; (7-9) bacterial amino acid transporters specific for alanine, branched chain and glutamate; (10) mammalian bile acid transporter; and (11) mammalian sodium chloride transporter (Reizer *et al.* 1994).

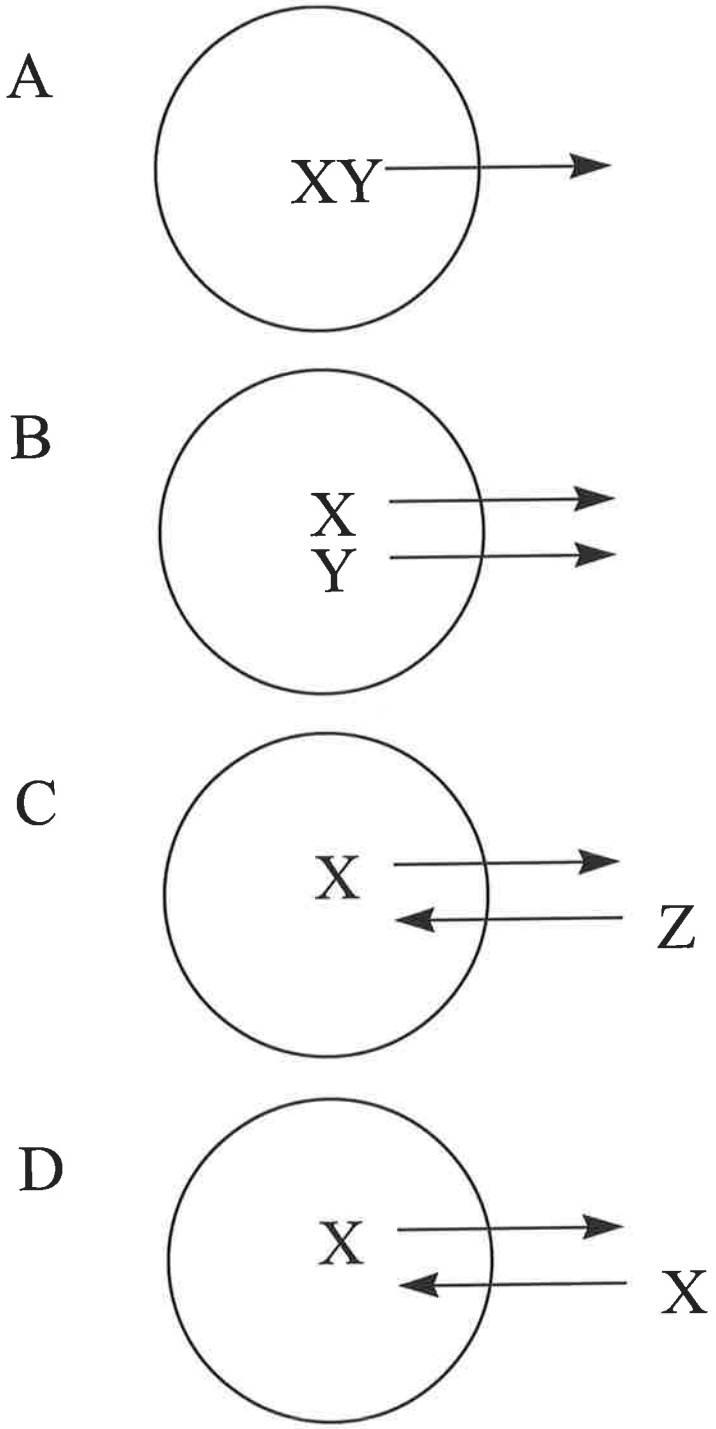

Figure 1.1 Carrier transport mechanisms.

A substrate bound to another substrate during transport is co-transported (A); a symporter transports two substrates in the same direction (B); and the transport of substrates in opposite direction is counter-transport, either with a different substrate (C) or the same substrate (D).

1.2 Sulphate metabolism.

The cellular roles of sulphate, its metabolism and transport have long been studied. Sulphation of xenobiotics for detoxification, and drug metabolism of steroids and neurotransmitters are some of the important processes in which it is involved (Mulder *et al.* 1982). The sulphation of structural proteins is also a vital process closely connected with sulphate availability and its transport. Sulphation requires the universal sulphate donor phosphoadenosine phosphosulphate (PAPS). The synthesis of PAPS in turn requires a supply of intracellular sulphate, which results from the catabolism of intracellular and dietary compounds. Inorganic sulphate is transported from serum into cells and from organelles into the cytoplasm. Sulphate transport is a vital process in the maintenance of these intracellular sulphate pools.

1.2.1 Phosphoadenosine phosphosulphate synthesis.

Due to the integral part PAPS plays in the sulphate metabolism cycle, a brief description of its synthesis is warranted. The synthesis of PAPS is described here as three reactions (*Figure 1.2*). The enzyme adenosine triphosphate (ATP) sulphurylase converts sulphate and ATP to adenosine phosphosulphate (APS) and pyrophosphate (PPi); APS is then converted to PAPS by APS kinase; and the PPi is converted into inorganic phosphate (Schmidt *et al.* 1982). The importance of PAPS synthesis is illustrated by dwarfism in the brachymorphic mouse (characterised by a disproportionately short stature), which is caused by a defective APS kinase (Sugahara and Schwartz 1979).

PAPS is the sulphate donor for the sulphation of glycoproteins, glycosaminoglycans and glycolipids (Liau and Horowitz 1976). Sulphate availability influences the level of PAPS

synthesis, which in turn affects the level of sulphation (*Section 1.2.2.1*). The sulphate pool drawn upon by the synthesis of PAPS is derived from a number of sources (*Section 1.2.3.1*). One of these sources is generated by the lysosomal sulphatases (*Table 1.2*), which liberate inorganic sulphate during the catabolism of sulphated macromolecules. The liberated sulphate is subsequently transported back to the cytosol. The contribution of sulphate from the catabolism of cysteine in the mitochondria to produce PAPS has been shown to be very small (Hill 1995; Imai *et al.* 1994) even in sulphate-depleted cells. In another study however, it has been shown that cysteine, as a source of sulphate was adequate in maintaining normal levels of glomerular proteoglycan sulphation (Templeton and Wang 1992). This difference may be due to the different requirements of the cell types investigated (*Section 1.2.2.1*).

Reaction 1

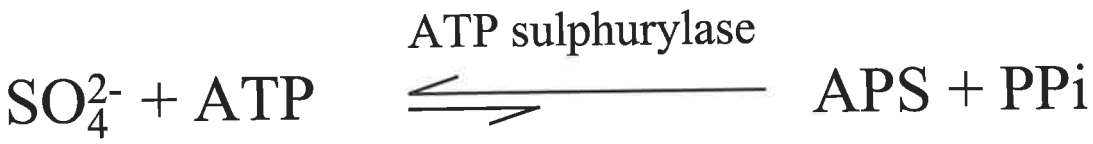

Reaction 2

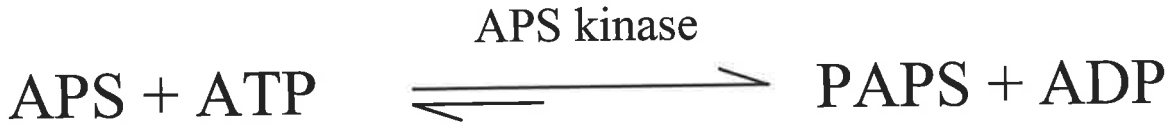

Reaction 3

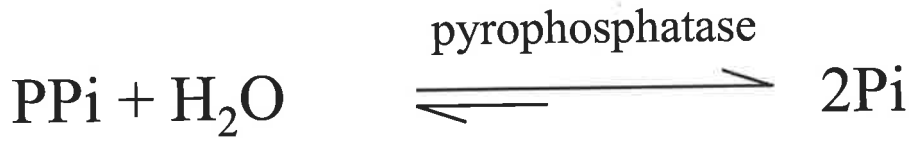

Figure 1.2 Synthesis of phosphoadenosine phosphosulphate.

The equilibrium of reaction 1 lies far to the left, however, the hydrolysis of pyrophosphate (PPi) in reaction 3 and the action of APS kinase in reaction 2 promote the production of PAPS.

Abbreviations: adenosine triphosphate (ATP); adenosine phosphosulphate (APS); phosphoadenosine phosphosulphate (PAPS); adenosine diphosphate (ADP); pyrophosphate (PPi); and inorganic phosphate (Pi).

1.2.2 The roles of sulphate within the cell.

The cellular roles of sulphate can be divided into structural, metabolic and regulatory, although these are often interrelated. The structural roles have been illustrated by either a low availability of sulphate or a defective enzyme involved in sulphate metabolism. The metabolic and regulatory roles of sulphate include drug and hormone metabolism, and the modulation of neurotransmitters.

1.2.2.1 A structural role of sulphation.

Under-sulphation of glycosaminoglycans causes the pathology in a number of diseases. Diastrophic dysplasia (osteochondrodysplasia) for example, results from under-sulphation of proteoglycans in cartilage and bone (*Section 1.5.2.2*). The clinical features include dwarfism, spinal deformation and joint abnormalities (Walker *et al.* 1972).

Extracellular matrix, which is composed of collagens, glycoproteins and proteoglycans, interacts with receptors. These interactions affect cell recognition and adhesion, signal transduction and cytoskeletal organisation, which in turn regulates cell locomotion (McCarthy and Turley 1993).

Cartilage-producing cells have a very large sulphate requirement for the synthesis of proteoglycans (Esko *et al.* 1986) which is why they are profoundly affected by sulphate availability. A number of workers have shown that decreases in extracellular and intracellular sulphate result in under-sulphated proteoglycans (Estep *et al.* 1981; Humphries *et al.* 1986; Krijgsheld *et al.* 1982; Sobue *et al.* 1978). Intracellular levels of sulphate regulate PAPS synthesis directly, due to the pathway's relatively high overall K_m, which is in the same range as the serum concentration (Muelder and Kuelemans 1978). In turn the level of PAPS has

been shown to determine the amount of sulphation (Hart 1978; Muelder and Kuelemans 1978), hence the undersulphation in the brachymorphic mouse (*Section 1.2.1*).

1.2.2.2 Metabolic and regulatory roles of sulphate.

Sulphation plays a large role in detoxification and drug metabolism. Non-microsomal enzymes perform most drug biotransformations. These reactions occur primarily in liver but also in plasma and other tissues. Included in these non-microsomal reactions are the sulphate conjugations of phenolic compounds including steroids. These sulphate conjugations of drugs and environmental substances utilise PAPS as the sulphate donor (Benet and Sheiner 1985). These detoxifying reactions are catalysed by members of the sulphotransferase and sulphatase enzyme super-families (Coughtrie *et al.* 1998; Varin *et al.* 1997).

1.2.3 Intracellular sulphate pools.

1.2.3.1 The origins of intracellular sulphate pools.

The origins of inorganic sulphate pools are complex and involve the metabolism of sulphur-containing compounds. There are still many questions that need answering before this field can be better understood. The human diet contains a large amount of sulphate; it has been quantitated in breast milk (McPhee *et al.* 1990) that 87% of the total sulphate could be derived from acid-labile sulphoesters (220 μmol/L), while inorganic sulphate (35 μmol/L) was only a small part of the dietary sulphate pool. It has been estimated that dietary sulphate intakes in the population range between 1.5 and 16 mmol/day (Florin *et al.* 1991). Sulphate absorption in the upper gastrointestinal tract however, plateaus at 5 mmol/day in subjects on a high sulphate diet, which is consistent with low capacity, high affinity active transport in the

mucosa. Sulphate derived from sulphur-containing amino acids was calculated to be 23 mmol/day.

In humans, the turnover of glycosaminoglycans (*Figure 1.3*) has been determined as 250 mg/day, which would generate 0.5 mmol, or 48 mg/day (Curtis 1982). Endogenous sulphate from intestinal secretions (0.96-2.6 mmol/day) is esterified with glycoproteins (mainly mucins), and to a lesser extent with steroids and glycolipids. Of urinary sulphate, 12% is bound as esters of phenol, indole and p-cresol, which are derived from bacterial degradation of aromatic amino acids in the gut. There is little sulphatase activity in the mucosa of the gastrointestinal tract; the free sulphate in the ileum is likely to be dietary, whereas the bound sulphate is largely endogenous. In mammals filtered sulphate is effectively reabsorbed by the kidney. Only 10-15% of the filtered load is excreted in the urine (Pritchard 1987).

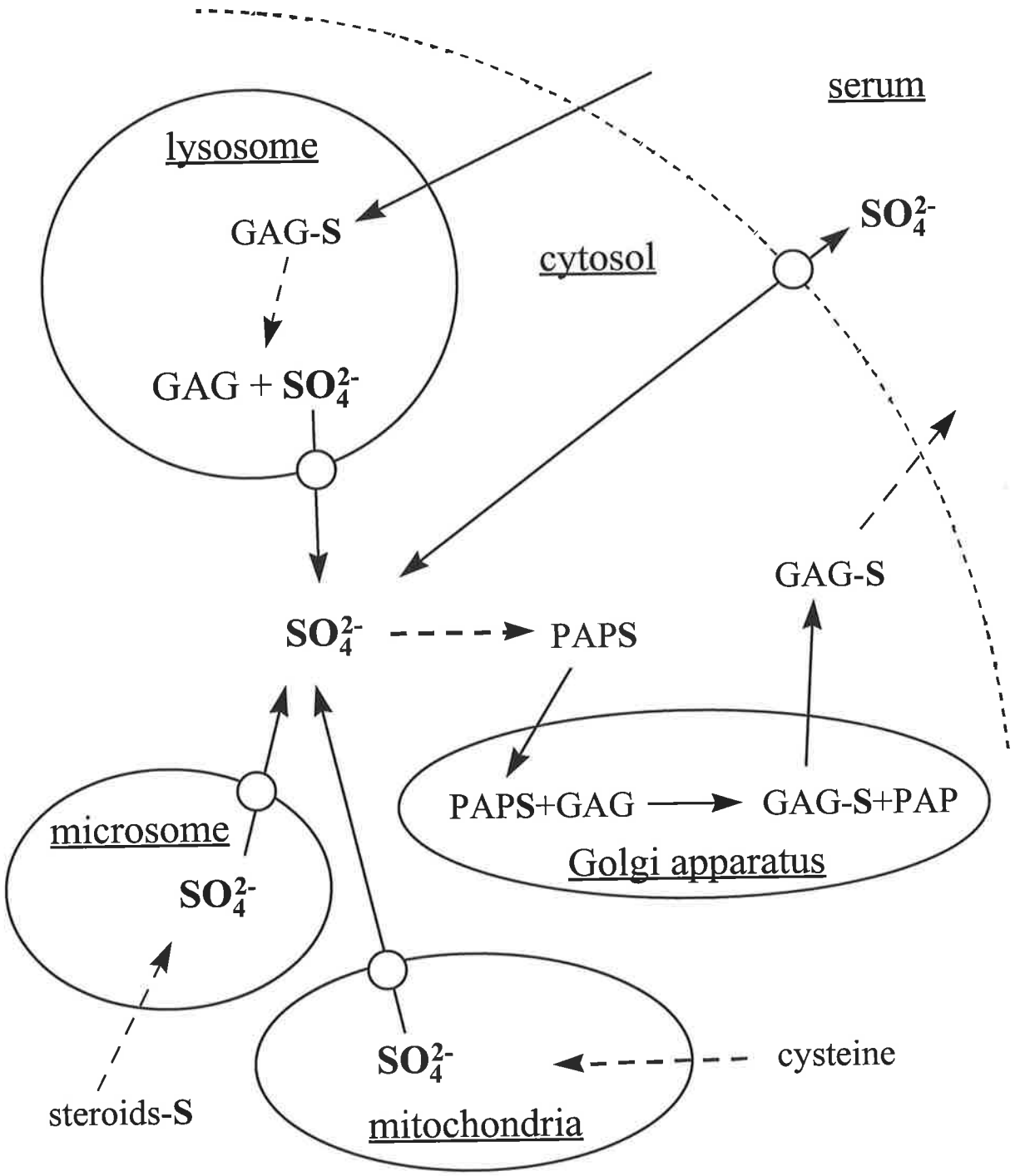

Figure 1.3 Sulphate cycling and generation from organelle macromolecular catalysis.

Sulphation of glycosaminoglycans (GAG) occurs in the Golgi apparatus. Sulphate is liberated from sulphated macromolecules by lysosomal and microsomal sulphatase activity and the catabolism of cysteine in the mitochondria. These pools of sulphate are transported to the cytoplasm. Abbreviations: phosphoadenosine phosphosulphate (PAPS); and phosphoadenosine phosphate (PAPS).

1.2.3.2 Metabolism of sulphate from cysteine.

The intracellular metabolism of sulphate (*Figure 1.4*) occurs in the cytosol, mitochondria, microsomes and the lysosomes. Thiosulphate can be oxidised to sulphate in animal cells. Decomposition of cysteine by cystathionase leads to the formation of sulphide, and transamination of cysteine-sulphinic acid is the main source of sulphite. Both of these products (sulphide and sulphite) can enter the thiosulphate cycle before complete oxidation to sulphate occurs (Koj *et al.* 1967; Recasens and Mandel 1979; Templeton and Wang 1992). Cysteine can also form sulphide via cystine and thiocystine before oxidation to sulphate. Another route to produce sulphate from cysteine is the cysteamine to taurine pathway into which cysteine-sulphinic acid can also contribute.

The sulphinic acid pathway in sulphate metabolism has been extensively studied, however, its importance as a source of sulphate appears to be negligible (Hill 1995; Imai *et al.* 1994). Two far more important sources of sulphate are derived from the degradation of sulphated macromolecules predominantly in the lysosome (*Section 1.3.1.1*) and transport of sulphate from intracellular and extracellular pools (*Section 1.2.3*). The convoluted pathways involved in sulphate metabolism illustrate the complexity of defining sulphate pools.

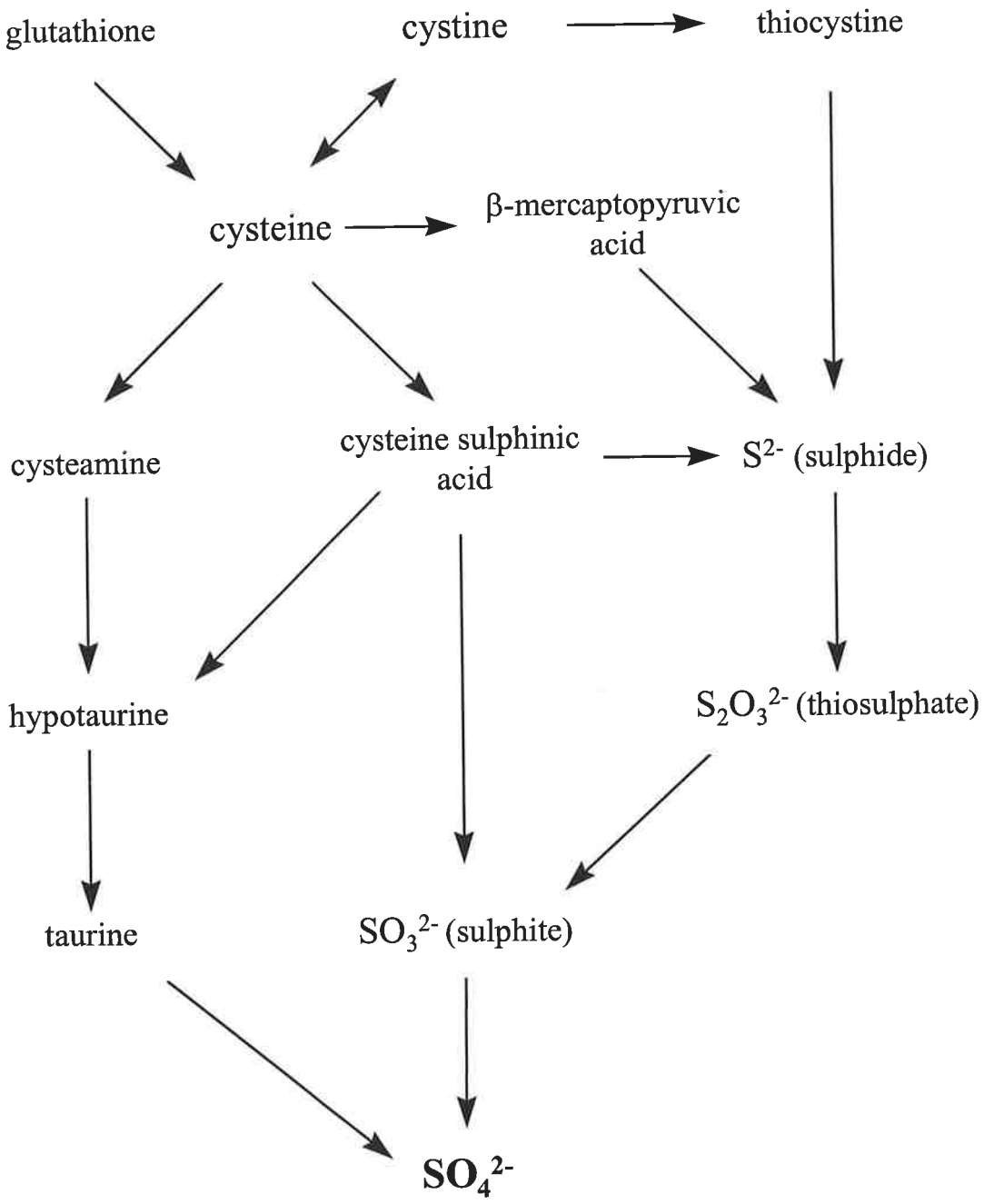

Figure 1.4 The metabolism of sulphate from cysteine.

The metabolism of sulphate from cysteine occurs in the cytosol and mitochondria. The figure is based on those by Koj *et al.* (1967) and Vadgama and Jonas (1992). This figure has been simplified by omitting some by-products and intermediate compounds.

1.2.3.3 Regulation of sulphate pools.

The significance of changes to sulphate pools by various regulators is not well understood. Progesterone for example has been shown to increase the intracellular inorganic sulphate pool of uterine epithelial cells (Mahfoudi *et al.* 1991). In diabetes there is an under-sulphation of proteoglycans and an increase in intracellular sulphate pools and renal clearance (Fan and Templeton 1992). The level of glycosaminoglycan sulphation is upset in cystic fibrosis with an increase in sulphation (Frates *et al.* 1983) which is thought to increase respiratory infection (Hill 1995). Mohapatra *et al.* (1993) believed, from experiments in bronchial epithelia cells, that there are two intracellular sulphate pools, a large slowly exchangeable one and a small one that can become very large if the level of extracellular chloride is lowered. This hypothesis of two intracellular sulphate pools has also been supported by Hill (1995) and Hill *et al.* (1997a,b).

Serum sulphate concentration varies considerably between species (*Table 1.1*). Human serum has the lowest sulphate level, which is coupled, to the lowest level of sulphate excreted in urine. Therefore, the importance of a change in serum sulphate concentration between species may also be different. This difference between species will not aid the understanding of sulphate pools. It has been shown in rat serum that sulphate can be significantly reduced by a low-protein diet or administration of a substrate of sulphation such as paracetamol (Krijgsheld and Mulder 1982). This means that data on sulphate pools must be taken in context of the animal system under study.

Table 1.1 Sulphate concentrations in serum.

Data from Krijgsheld *et al.* (1980) and Krijgsheld and Mulder (1982).

Species	Serum sulphate (mM)	Urinary excretion of sulphate (μmol/hr/kg)
Human	0.3	15
Rat	0.9	70
Mouse	1.2	
Dog	1.4	25
Cow	1.8	
Rabbit	2.0	25

In plants, glutathione is an important storage and transport form of organic sulphur (Noctor *et al.* 1997) and is described as the most abundant low-molecular weight thiol compound in plants (Hell 1997). The importance of glutathione as a sulphur store or sulphate intermediary still needs to be investigated in animal systems.

1.3 The definition and function of the lysosome.

The lysosome is the major digestive organelle in an animal cell that is specialised in the orderly destruction of cellular components. It is an intracellular single membrane organelle, which ranges from 25 nm to over 1 μm in diameter and varies in number with cell type. The enzymes housed in this compartment have optimal activities at an acid pH, hence the term acid hydrolases. A proton pump (H^+-ATPase) in the lysosomal membrane maintains a pH of approximately 4.6, suitable for these catalytic enzymes. Lysosomes are involved in phagocytosis, endocytosis and autophagy (Karp 1999; Storrie 1988).

Phagocytosis is uptake by a cell of large particulate material by engulfment with cytoplasmic extensions of the plasma membrane, which pinches free to produce a phagosome and then fuses with a lysosome to digest its content. In mammals examples of this process are performed by Kupffer cells in the liver that engulf aging erythrocytes, and macrophages which engulf unwelcome microorganisms. Endocytosis is the non-specific uptake of extracellular fluids or the receptor-mediated uptake of specific ligands such as hormones and growth factors into endosomes. This extracellular material is enclosed by the invagination of plasma membrane budding off into the cell as a vesicle. These vacuoles can then fuse with lysosomes through the endocytic pathway. Autophagy is the recycling of the cell's own organelles. Mitochondria for example, are enclosed by the endoplasmic reticulum which then fuse with a lysosome. Cells deprived of nutrients show a marked increase in autophagy, where it cannibalises its own organelles to remain alive (Karp 1999; Klionsky and Ohsumi 1999; Sabatini and Adesnik 1998). An unusual role of lysosomal activity is played out during fertilisation. A packet of lysosomal enzymes (the acrosome) in the head of a sperm fuses with its plasma membrane as it reaches the egg and digests a hole in the outer covering of the egg through which the sperm can pass (Karp 1999).

Storrie (1988) defined a lysosome, in addition to that just described, as an organelle rich in a range of mature forms of recognised lysosomal proteins including acid hydrolases; the terminal compartment in the endocytic pathway, distinct from the pre-lysosomal compartment which contains the mannose-6-phosphate receptors; and a lysosome must behave as a high density organelle in fractionation experiments.

The lysosomal enzymes hydrolyse a wide range of macromolecules including proteins, nucleic acids, carbohydrates, glycoproteins, glycolipids, neutral lipids, phospholipids and phosphoesters (Finean *et al.* 1984; Rome and Hill 1986). The resulting monomeric subunits, including sugars, amino acids, purines and pyrimidines, inorganic phosphate, fatty acids and sulphate are transported back to the cytoplasm for reutilisation in biosynthetic pathways.

The lysosome is also a major site of degradation for polypeptides. Polypeptides with a KFERQ-like peptide motif are recognised by a heat shock cognate protein, which mediates their transport to the lysosome for degradation (Terlecky and Dice 1993). Polypeptides that have this motif, are cytosolic, and their degradation which is mediated by the heat shock cognate protein, is induced under conditions of stress, such as starvation.

1.3.1 Structure of the lysosome.

Electron micrographs show lysosomes to be neither distinctive nor uniform in appearance making their identification by morphology alone difficult (Karp 1999). The single phospholipid bilayers or membranes of the lysosomes are largely phosphatidylcholine (41% w/w), phosphatidylethanolamine (26%), phosphatidylinositol (10%), sphingomyelin (8%), and cholesterol with a molar ratio of cholesterol to total phospholipid of 0.3:1 (Henning and

Heidrich 1974). Lysosomes also have a unique acidic phospholipid bis (monoacylglycerol) phosphate, also known as lysobisphosphatidic acid (Matsuzawa and Hostetler 1980; Tjiong and Debuch 1978; Tjiong *et al.* 1978; Wherrett and Huterer 1972). This phospholipid is resistant to degradation by lysosomal acid hydrolases (Matsuzawa and Hostetler 1979).

The phospholipid bilayer or lysosomal membrane plays an important role in this organelle's function. It not only provides an isolated intracellular acid environment required for the hydrolytic activity, but it contains the macromolecules for degradation, only allowing the egress of the end products of digestion. This egress of products is via specific lysosomal transporters (*Section 1.3.3*) either active or passive in nature (Fukuda 1991; Lloyd and Forster 1991). The failure of such a transporter results in lysosomal storage of an end product resulting in disease (*Table 1.6*).

Lysosomal proteins are either soluble hydrolytic enzymes, such as the sulphatases associated with the phospholipid membrane in a putatively structural role (*Section 1.3.2.3*), or embedded in the phospholipid membrane, as are the transporters (*Section 1.3.3*). These proteins in concert perform the functions of the lysosome, each group dependent on the others.

1.3.1.1 Lysosomal hydrolysis of glycosaminoglycans.

Degradation of glycosaminoglycans by the lysosome involves a number of sulphatases that generate sulphate. Sulphate has been shown *in-vitro* to inhibit sulphatase activity, indicating the importance of the sulphate transporter's function in allowing the egress of sulphate from the lysosome into the cytoplasm.

The lysosomal catabolism of glycosaminoglycans is a stepwise *exo*-degradative process. Each step is performed by a different enzyme, which requires the previous step to be completed. For example, the degradation of heparan sulphate, which requires five sulphatases, three glycosidases and an acetyl transferase illustrates this *exo*-degradative process (see *Figure 1.5*).

Figure 1.5 Degradation of heparan sulphate.

Stepwise *exo*-enzyme degradation of heparan sulphate oligosaccharides in the lysosome. Reproduced from Hopwood and Morris (1990). The sequence shown was chosen to demonstrate all bonds modified by the nine *exo*-enzymes required to degrade heparan sulphate.

The deficiency of an *exo*-enzyme results in the accumulation of an incompletely degraded GAG. A deficiency of one of these enzymes, can give rise to a specific disease, due to the accumulation in the lysosome of incompletely degraded GAG. The disease MPS II for example, is due to the deficiency of iduronate-2-sulphatase.

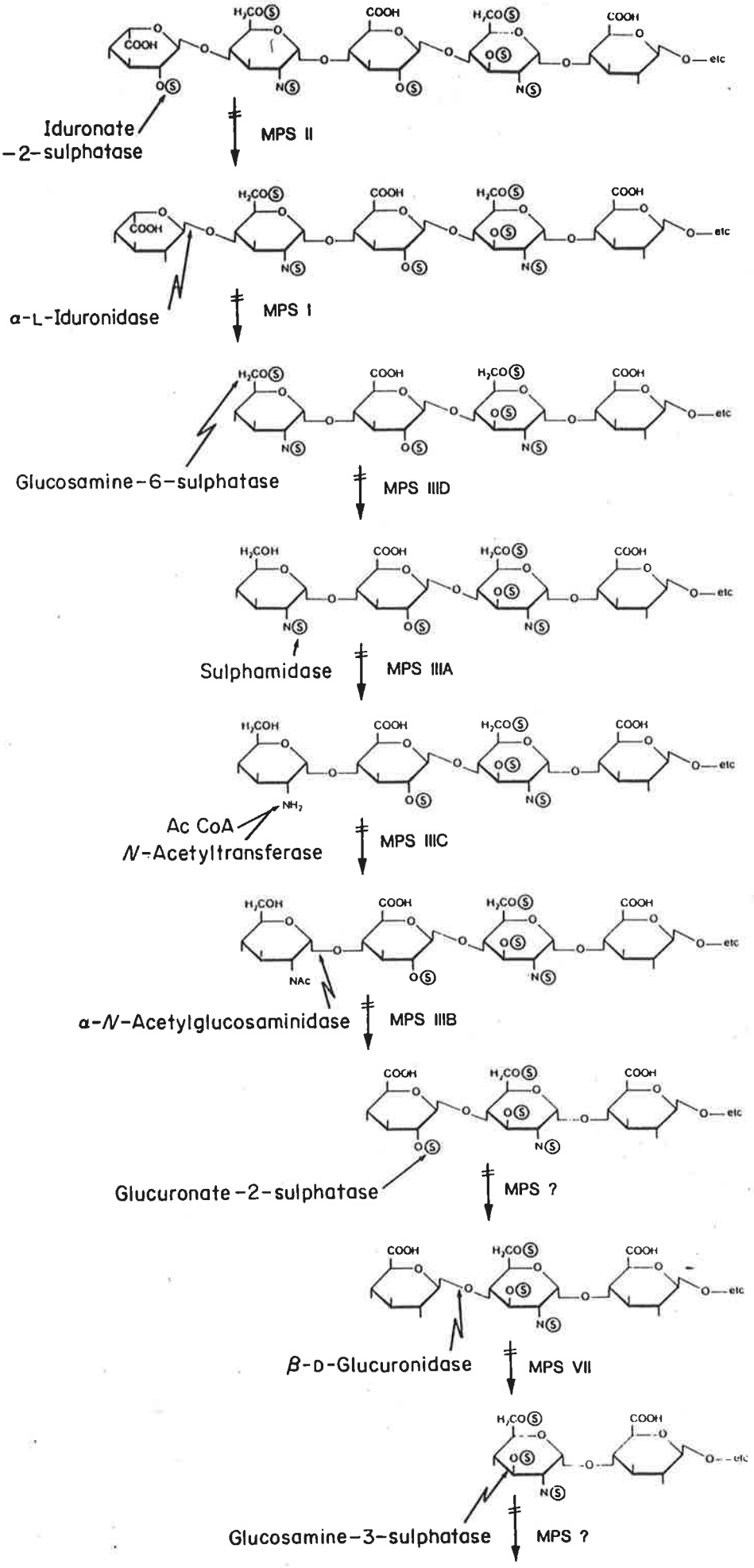
Iduronate
-2-sulphatase
MPS II
α-L-Iduronidase
MPS I
Glucosamine-6-sulphatase
MPS IIID
Sulphamidase
MPS IIIA
Ac CoA
N-Acetyltransferase
MPS IIIC
α-N-Acetylglucosaminidase
MPS IIIB
Glucuronate-2-sulphatase
MPS ?
β-D-Glucuronidase
MPS VII
Glucosamine-3-sulphatase
MPS ?

1.3.1.1.1 Sulphatases

Sulphatases hydrolyse sulphated glycosaminoglycans, glycolipids, glycoproteins and hydroxysteroids liberating inorganic sulphate. There is a high degree of amino acid homology along the entire length of this family of proteins. There are twelve reported sulphatases (*Table 1.2*), eight of which are lysosomal and four associated with microsomal fractions (Parenti *et al.* 1997; Scott *et al.* 1995). The structure of arylsulphatase B has been determined by X-ray crystallography showing the active site to be conserved in the sulphatase family (Bond *et al.* 1997). A range of diseases can arise when one or more sulphatases are defective. Disease is caused by the accumulation of partly degraded glycosaminoglycans (*Section 1.3.1.1*). The particular glycosaminoglycans stored are those that are substrates of the defective enzyme, which give rise to the clinical symptoms associated with that disease. In multiple sulphatase deficiency (MSD) all of the sulphatase substrates are stored.

Table 1.2 Human sulphatases.

(Parenti *et al.* 1997; Scott *et al.* 1995)

Enzyme	Location	Substrate	Disease
galactose-3-sulphatase ARS A (E.C. 3.1.6.8)	Lysosome	Cerebroside	metachromatic leukodystrophy, MSD
N-acetylgalactosamine-4-sulphatase ARS B (E.C. 3.1.6.12)	Lysosome	DS	MPS VI, MSD
ARS C / steroid sulphatase (E.C. 3.1.6.2)	Microsome	Sulphated steroids	Ichthyosis, metachromatic leukodystrophy
ARS D	Endoplasmic Reticulum	Unknown	Not established
ARS E	Golgi apparatus	Unknown	Chondrodysplasia punctata, MSD
ASR F	Endoplasmic Reticulum	Unknown	Not established
Iduronate-2-sulphatase (EC 3.1.6.13)	Lysosome	HS, DS	MPS II, MSD
Sulphamidase (EC 3.10.1.1)	Lysosome	HS	MPS IIIA, MSD
glucosamine-6-sulphatase (E.C. 3.1.6.14)	Lysosome	HS, GlcNAc6S	MPS IIID, MSD
glucuronate-2-sulphatase (E.C. 3.1.6.18)	Lysosome	HS	Not established
glucosamine-3-sulphatase (E.C. 3.1.6.15)	Lysosome	HS	Not established
galactose-6-sulphatase (E.C. 2.5.1.5)	Lysosome	KS, CS	MPS IV, MSD

Abbreviations: arylsulphatase (ARS); multiple sulphatase deficiency (MSD); mucopolysaccharidosis (MPS); dermatan sulphate (DS); heparan sulphate (HS); chondroitin sulphate (CS); *N*-acetylglucosamine-6-sulphate (GlcNAc6S); keratan sulphate (KS).

1.3.2 Lysosomal biogenesis.

The plasma membrane and cytoplasmic organelles, including the endoplasmic reticulum (ER), Golgi, secretory vesicles, endosomes and lysosomes, form an integrated endomembrane system. Mitochondria and peroxisomes do not communicate with the endomembrane system. This system transports macromolecules and membrane components to different parts of the cell, and in and out of the cell. Organelles and secretory granules or vesicles are formed by budding off from the endomembrane. The targeting of newly-synthesised proteins is by transport along the endomembrane or delivered by a vesicle that fuses with the membrane of its destination compartment. The luminal faces of endomembranes are topologically equivalent. That is, the extracellular and luminal faces are the same, and the organelle's and plasma membrane's cytoplasmic faces are the same (Sabatini and Adesnik 1998). The lipid component of the plasma membrane has a high cholesterol content and is relatively rich in sphingolipids. In contrast, mitochondria, nuclear membranes and ER contain little cholesterol and sphingolipids. Golgi, secretory vesicles and lysosomal membranes have lipid compositions intermediate between those of the plasma membrane and the major intracellular organelles, reflecting their role in the endomembrane system (Finean *et al.* 1984).

1.3.2.1 Targeting of lysosomal luminal proteins.

Soluble lysosomal enzymes are tagged for targeting by additions to asparagine-linked heterosaccharide chains of a phosphorylated mannose residue. This occurs in the *cis*-Golgi to the 6-position of a mannose residue by the addition of *N*-acetylglucosamine-1-phosphate followed by the hydrolytic removal of the *N*-acetylglucosamine (Finean *et al.* 1984). An acidic environment is required for certain post-translational processing reactions associated with secretion, such as proteolytic cleavage of proproteins and glycosylation, and also for proper sorting of membrane and secretory constituents (Andersson *et al.* 1989).

Mannose-6-phosphate receptors traffic these tagged proteins into the endosomal network and on to their lysosomal destiny (Hille-Rehfeld 1995; Kornfeld 1992; von Figura 1991). The mannose-6-phosphate receptor-linked lysosomal proteins leave the trans-Golgi network via vesicles, which bud off to join the endocytic network where vesicular fusion occurs (Geuze *et al.* 1988).

1.3.2.2 Targeting of lysosomal membrane proteins.

Membrane proteins do not reach the lysosome using the mannose-6-phosphate tag. A direct path to the lysosome and one via the plasma membrane has been observed. It is thought that a single glycine, tyrosine (GY) motif near the C-terminal may be responsible (Honing *et al.* 1996). This motif exists in the lysosomal-associated membrane proteins (lamp) and the lysosomal acid phosphatase and cystinosin proteins (Town *et al.* 1998). An alternative or more extensive targeting motif is yet to be found, which could be a useful tool for the remaining low abundant and elusive transporters.

1.3.2.3 Lysosomal membrane proteins.

A major group of lysosomal membrane proteins are the transporters (Section 1.3.3). Of the non-transporter lysosomal membrane proteins, relatively few sequences are known. Many functions have been ascribed as to the roles of these proteins, from protecting the phospholipid bilayer from degradation to contributing to the acid environment. Lysosomal membrane glycoproteins sequenced to date (*Table 1.3*) are rich in complex *N*-linked oligosaccharides that are rich in poly-*N*-acetyllactosamines bearing sialic acid. It is thought these oligosaccharides protect the phospholipid membrane from hydrolytic attack (Sabatini and Adesnik 1998).

Table 1.3 Sequenced lysosomal membrane proteins.

This is an expansion of the table reported by Hopwood and Brooks (1997).

Human	Mouse	Rat	Reference
cystine transporter			(Town *et al.* 1998)
lysosomal acid phosphatase			(Geier *et al.* 1989)
cation dependent mannose 6-phosphate receptor			(Pohlmann *et al.* 1987)
cation independent mannose 6-phosphate receptor			(Oshima *et al.* 1988)
Battenin protein (CLN3)			(Golabek *et al.* 1999)
Macrosialin / CD68			(Holness and Simmons 1993)
CD164	CD164	endolyn	(Ihrke *et al.* 2000)
lysosomal-associated multi-transmembrane protein			(Adra *et al.* 1996)
syntaxin 7			(Nakamura *et al.* 2000)
		lgp 107	(Akamine *et al.* 1993)
lamp 1	limp 3	lgp 100	(Carlsson *et al.* 1988; Mane *et al.* 1989)
lamp 2	limp 4	lgp 120	(Carlsson *et al.* 1988; Mane *et al.* 1989)
lamp 3 / CD63	limp 1		(Hopwood and Brooks 1997)
h_lgp 85	limp 2/ CD36	lgp 85	(Fujita *et al.* 1992)
H^+-ATPase			(Ohkuma and Poole 1978; Schneider 1979)

Abbreviations: lysosomal associated membrane protein (lamp); lysosomal integral membrane protein (limp); lysosomal granule protein (lgp); lysosomal endosomal plasma membrane protein (lep).

1.3.3 Lysosomal transporters.

The degradation of macromolecules by the lysosome can be divided into three parts: the acquisition of macromolecules, the coordinated digestion of the macromolecules, and the transport of the resulting products out of the lysosome. This thesis is most concerned with this third area of lysosomal function. Over the last twenty years as many lysosomal transporters have been described (Chou *et al.* 1992; Thoene 1992). Of the transporters listed in *Table 1.4* there is one channel, one pump, and the remainder is split between passive and active transporters (*Section 1.1.4*). The ubiquitous vacuolar proton pump (*Section 1.3.3.1*) and the cystine transporter (*Section 1.3.3.2*), however, are the only two transporters that have been isolated or cloned.

Table 1.4 Characterised lysosomal transporters.

Type of transporter	Reference
Channel	
Chloride	(Tilly *et al.* 1992)
Pump	
H^+-ATPase	(Ohkuma and Poole 1978; Schneider 1979)
Passive-Carrier	
Large neutral amino acids	(Bernar *et al.* 1986)
Tyr, Leu, Ileu, Try, Phe, His, Val, Met	
Small neutral amino acids	(Pisoni *et al.* 1987)
Ala, Ser, Thr, not Proline	
Pro and Ala	(Pisoni *et al.* 1987)
Proline, not Ala	(Pisoni *et al.* 1987)
Dicarboxylic amino acids	(Collarini *et al.* 1989)
Aspartate and Glutamate	
Nucleosides	(Pisoni and Thoene 1989)
Branched and aromatic amino acids	(Stewart *et al.* 1989)
N-acetylated hexoses	(Jonas *et al.* 1989)
N-acetyl-D-glucosamine, N-acetyl-D-galactosamine	
Neutral monosaccharides (hexoses)	(Jonas *et al.* 1990; Mancini *et al.* 1990)
D-Glucose, L-Fructose	
Phosphate	(Pisoni 1991)
Calcium	(Lemons and Thoene 1991)
Folypolyglutamates	(Barrueco and Sirotnak 1991)

(continued)

Table 1.4 (continued)

Active Carrier	
Cystine	(Gahl *et al.* 1982)
Cationic amino acids	(Pisoni *et al.* 1985)
Lys, Arg	
Acidic sugars	(Mancini *et al.* 1989; Renlund *et al.* 1986)
Sialic acid, glucuronate, gluconate, galactonate and galactuonate.	
Sulphate	(Jonas and Jobe 1990)
Cysteine	(Pisoni *et al.* 1990; Town *et al.* 1998)
Cobalamin	(Idriss and Jonas 1991; Rosenblatt *et al.* 1985)
Taurine	(Vadgama *et al.* 1991)
Unknown	
Cholesterol	(Liscum *et al.* 1989)
Small dipeptides	(Bird and Lloyd 1990)
Biotin	(Idriss *et al.* 1991)

1.3.3.1 Proton pump (H^+-ATPase).

The intralysosomal pH, measured to be 4.6 (Ohkuma and Poole 1978), is generated by a proton pump (Schneider 1979, 1981). The lysosomal proton pump was found to be Mg^{2+} and ATP dependent (Ohkuma *et al.* 1982), and is the only active transporter (pump) isolated from lysosomes (Schneider 1983). The lysosomal acidification, which was measured by fluorescein fluorescence, required a membrane-permeant anion such as chloride and was reversed by the protonophore carbonyl cyanide *p*-trifluoromethoxyphyenylhydrazone (FCCP). It differed from the mitochondrial oligomycin-sensitive ATPase, the Na^+/K^+-ATPase by its insensitivity to ouabain, and the microsomal Ca^{2+}-ATPase by not requiring calcium. Moriyama *et al.* (1984) used acridine orange as a fluorescent probe to observe the Mg^{2+}-ATPase-generated pH gradient in tritosome membrane ghosts. These studies provided

evidence that this Mg^{2+}-ATPase has properties in common with the H^{+}-pumps of yeast vacuoles, plant vacuolysosomes, secretory granules, and clathrin-coated vesicles (Forgac *et al.* 1983), thought to play a role in endocytosis, endosomes and chromaffin granules (Moriyama and Nelson 1987).

The lysosomal proton pump was reconstituted into proteoliposomes using *Escherichia coli* phospholipids (D'Souza *et al.* 1987) and finally purified from rat liver lysosomes (Arai *et al.* 1993) and identified as a vacuolar (v)-type pump.

1.3.3.2 Lysosomal cystine transport.

The lysosomal cystine transport gene codes for 367 amino acids and has six or seven putative transmembrane spanning domains. The sequence also revealed the glycine-tyrosine (GY) dipeptide five amino acids from the C-terminus (Town *et al.* 1998), thought to be the targeting motif for lysosomal membrane proteins (Honing *et al.* 1996). The cystine transporter allows the passage of cystine from the lysosome to the cytoplasm.

The consequence of cystine storage in lysosomes and hence storage in cells, is the disease cystinosis (Gahl 1992). Cystinosis presents itself either as an infantile nephropathic type, an adolescent nephropathic type, or less frequently, as a benign or adult non-nephropathic type. Schneider (1967) found the heterozygote parent's leucocytes had approximately six-times the normal levels of free cystine. The heterozygote leucocyte referring to one normal copy and one dysfunctional copy of the cystine transporter. Gahl *et al.* (1984) measured cystine counter-transport in leucocyte lysosomes of heterozygotes to be approximately half of that observed in non-cystinotics. These data suggested that cystinosis was a cystine transport disease. This autosomal recessive disorder has a varying severity that correlates with elevated

levels of cystine. The clinical symptoms range from photophobia due to cystine crystals in the cornea, to kidney malabsorption of essential nutrients, electrolytes and water. The renal tubular Fanconi syndrome causes retarded growth. Further disease progression includes a requirement for dialysis, kidney and thyroid replacement, endocrine insufficiency, difficulty swallowing, and blindness (Gahl 1992).

Patients are treated with cysteamine, which acts by converting cystine to cysteine and cysteine-cysteamine. These products are then able to leave the cystinotic lysosome, the latter via the lysine transporter (Pisoni *et al.* 1985). Treatment of these patients with cysteamine to reduce storage has been successful (Gahl *et al.* 1987) and the earlier the commencement of treatment the better the prognosis (Markello *et al.* 1993). This disease has been studied for over thirty years, and only recently has the gene for this transporter was found (Town *et al.* 1998). This is the first lysosomal transport gene identified, excluding the ubiquitous proton pump.

1.3.3.3 Lysosomal sialic acid transport.

Mancini *et al.* (1989, 1991) demonstrated a sialic acid carrier in human lysosomal membranes. This transporter showed a wide substrate specificity for acidic monosaccharides including glucuronic acid. Co-transport was stimulated with a proton gradient (K_t of 0.24 mM), and inhibited by diisothiocyanatostilbene disulphonic acid (DIDS). The transporter also exhibited counter-transport.

The failure of the lysosomal egress of sialic acid is responsible for infantile free sialic acid disease (Tietze *et al.* 1989), and Salla disease, the adult type (Renlund *et al.* 1983). The

transporter has been successfully reconstituted into artificial proteoliposomes (Mancini *et al.* 1992), and has now been cloned (Verheijen *et al.* 1999).

1.3.3.4 Lysosomal cobalamin transport.

A specific lysosomal transporter for cobalamin (vitamin B12) was recognised using cultured fibroblasts (Rosenblatt *et al.* 1985). The metabolism of this vitamin is complex, and involves extracellular and intracellular steps (Sillaots and Rosenblatt 1992). Cobalamin provides cofactors required for the conversion of methyl-malonyl-coenzyme A to succinyl-coenzyme A, and the formation of methionine from homocysteine.

An individual found with abnormalities in the metabolism of methyl-malonate and homocysteine had lysosomal storage of free cobalamin (Rosenblatt *et al.* 1985). This transporter was found to be pH-dependent with a K_t of 3.5 mM, and exhibited counter-transport (Idriss and Jonas 1991). Purification or isolation of this transporter has not yet been achieved.

1.3.3.5 Lysosomal sulphate transport.

Lysosomal sulphate transport has been characterised using rat liver by Jonas and Jobe (1990). Lysosomes were isolated after treatment with methionine methyl ester, which caused their swelling and rupture. The transport of sulphate across the lysosomal membrane is via a saturable carrier. The direction of ion transport through a carrier is dictated by the electrochemical gradient (*Section 1.1.4*). If the concentration of sulphate is higher outside a lysosome, the net transport will therefore be an influx of the ion into the vesicle. Conversely, if the concentration of sulphate is higher inside a vesicle (an outward gradient), sulphate will efflux from the vesicles into the surrounding environment. A relatively recent family of

sulphate transporters with similar characteristics to the lysosomal one has been found (*Section 1.5.2*). Although no disease has been described due to failure of the lysosomal sulphate transporter, such failure may contribute to pathology of an unexplained lysosomal storage disease.

1.3.4 Consequences of lysosomal dysfunction.

The lysosome's functions are to isolate an intracellular space for its activities and to degrade various intracellular and extracellular components into monomeric subunits. The interruption of these conceptually simple tasks of the lysosome has wide-ranging, and serious implications. A number of bacterial organisms that infect humans do so by avoiding lysosomal degradation. *Mycobacterium tuberculosis* prevents the phagosome enclosing it from fusing with the lysosome, and *Listeria monocytogenes* a meningitis causing bacteria, produces a phospholipase which destroys the integrity of the lysosomal membrane (Karp 1999).

As alluded to earlier, lysosomal dysfunction is also caused by genetic anomalies that affect the function of the lysosomal hydrolytic enzymes (*Figure 1.5* and *Table 1.2*) and transporters (*Section 1.3.3.2*), resulting in lysosomal storage disorders (LSD). Understanding the biological basis of these disorders has and still does present a considerable task. LSD have been reported in many species including emu (Kim *et al.* 1996) and kangaroo (Rothwell *et al.* 1990). It is in the human however, where they have been well characterised and catalogued (Applegarth *et al.* 1997). These disorders have been divided into six groups: the glycogenosis, glycolipidosis, mucopolysaccharidoses, oligosaccharidoses, transport and other disorders. The failure to degrade the sulphated glycosaminoglycans heparan sulphate, dermatan sulphate, keratan sulphate and chondroitin sulphate, collectively make up the group

of LSD known as mucopolysaccharidoses (MPS) disorders (Hopwood and Brooks 1997; Hopwood and Morris 1990). Twelve enzymes are involved in the breakdown of these sulphated glycosaminoglycans (*Table 1.5*). Although only seven of these enzymes are sulphatases due to the stepwise exo-degradative process (*Section 1.3.1.1*), any defective enzyme activity of the other five would similarly result in storage of sulphated glycosaminoglycans.

The storage products of hydrolysis that result from a defective transporter can cause LSD. Known lysosomal transporter disorders (*Table 1.6*) include the storage of cystine and sialic acid (Gahl *et al.* 1998) and cobalamin (Rosenblatt *et al.* 1985) (*Sections 1.3.3.2, 1.3.3.4*).

Table 1.5 Mucopolysaccharidoses.

(*Sulphatase enzymes.)

MPS type	Eponym	Enzyme deficiency	Stored substrate
I	Hurler / Scheie	α-L-iduronidase (E.C. 3.2.1.76)	HS, DS
II	Hunter	*iduronate-2-sulphatase (E.C. 3.1.6.13)	HS, DS
IIIA	Sanfilippo	*sulphamidase (E.C. 3.10.1.1)	HS
IIIB	Sanfilippo	α-*N*-acetylglucosaminidase (E.C. 3.2.1.50)	HS
IIIC	Sanfilippo	acetyl-CoA:α-glucosaminidase *N*-acetyltransferase (E.C. 2.3.1.3)	HS
IIID	Sanfilippo	*glucosamine-6-sulphatase (E.C 3.1.6.14)	HS, GlcNAc6S
IVA	Morquio	*galactose-6-sulphatase (E.C. 3.1.6.4)	KS, CS, GalNAc6S
IVB	Morquio	β-D-galactosidase (E.C. 3.2.1.23)	KS
VI	Maroteaux-Lamy	**N*-acetylgalactosamine-4-sulphatase (E.C. 3.1.6.1)	DS, CS, GalNAc4S, GalNAc4,6diS
VII	Sly	β-D-glucuronidase (E.C. 3.2.1.31)	CS, HS, DS
?		*glucuronate-2-sulphatase (E.C. 3.1.6.18)	HS, CS
?		*glucosamine-3-sulphatase (E.C. 3.1.6.15)	HS

Abbreviations: heparan sulphate (HS), dermatan sulphate (DS), chondroitin sulphate (CS), keratan sulphate (KS), *N*-acetylglucosamine-6-sulphate (GlcNAc6S), *N*-acetylgalactosamine-4-sulphate (GalNAc4S), *N*-acetylgalactosamine-4,6-disulphate (GalNAc4,6diS).

Table 1.6 Storage disorders due to transport defects.

Disease name	Enzyme defect	Substance stored
Lysosomal Enzyme Transport Disorders		
Mucolipidosis II/III (I-cell disease/ pseudo-Hurler polydystrophy)	*N*-acetylglucosamine-1-phosphotransferase	multiple substrates
Lysosomal Membrane Transport Disorders		
Cystinosis	cystine transporter	free cystine
Salla	sialic acid / glucuronic acid transporter	free sialic acid and glucuronic acid
cblF	cobalamin transporter	cobalamin

1.4 Non-lysosomal anion exchangers.

There have been a number of non-lysosomal transporters described which are functionally similar and may be homologous in sequence or structure. Among these are a number of transporters with similar characteristics to the lysosomal sulphate transporter. These similarities include the ions they transport, the inhibitors to which they are sensitive and their mechanisms of action. The anion exchanger (AE) in red blood cells (known as Band 3) and other members of this family (AE2 and AE3) demonstrate a range of transporter functions (*Section 1.4.1.1*).

1.4.1 Functions of the chloride / bicarbonate transporters.

Other members of the Band 3 anion exchanger family reviewed by Alper (1991) are expressed in the renal proximal tubule, heart, brain and white blood cells. The non-erythroid Cl^-/HCO_3 exchangers function in concert with other plasma membrane transporters to regulate cell volume, pH and chloride concentration. The functions of each transporter depend on other transporters with which they are combined. The Cl^-/HCO_3^- exchanger acidifies the interior of the cell which, when coupled with a Na^+/H^+ acid extruder, regulates intercellular pH (Tanner 1993). Other acid extruders that can work in concert include the H^+/lactate co-transporter, the H^+/K^+-ATPase, and the vacuolar H^+-ATPase (Alper 1991).

1.4.1.1 The erythrocyte anion transporter.

The anion transporter in red blood cells comprises 25% of the membrane proteins and is also known as Band 3 or capnophorin (Jennings and Al Rhaiyel 1988). Band 3 increases the capacity of blood to carry CO_2 as HCO_3^- from tissues to lungs (Tanner 1996) as bicarbonate is more soluble than carbon dioxide. The hydration of CO_2 occurs in the erythrocyte, which is then exchanged by Band 3 for plasma Cl^-. This equilibration of HCO_3^- allows the entire

volume of blood to be used for its transport (Tanner 1993). There are many aspects to Band 3, this review however, only includes aspects that may increase an understanding of anion transporters such as the lysosomal sulphate transporter.

Hereditary spherocytosis, due to a deficiency of Band 3 protein, causes haemolytic anaemia with varying degrees of haemolysis. The occurrence of pincered (transformed shape) erythrocytes and their reduced ability to pass through narrow pores leads to a requirement for a splenectomy which removes the narrowest filter in the body. The shape transformation may be due to the cytoskeletal anchoring functions of Band 3 (Reinhart *et al.* 1994).

1.4.1.2 Structure and stability of Band 3.

The fourteen membrane-spanning domains of thirteen members of the anion exchanger family are highly conserved. Mostly conserved amino acid substitutions were found in the transmembrane domains compared with the more frequent random substitutions in the interconnecting extra-membranous loops (Wood 1992).

The integral membrane and anion transport domains of Band 3 were delipidated then reconstituted to see what influence different lipid environments had on stability (Maneri and Low 1988). Stability of the membrane domain was found to be exquisitely sensitive to the acyl chain length of its phospholipid environment, increasing almost linearly in dimyristoleylphosphatidylcholine (C14:1) to dinervonylphosphatidylcholine (C24:1). The integral domain was also found to be stabilised by increasing the degree of saturation of the fatty acyl chains and by elevating the cholesterol content of the membrane. Even though Band 3 was native in all reconstituted lipid systems, the protein's stability was clearly much greater in phosphatidylethanolamine and phosphatidylcholine than phosphatidylserine and

phosphatidylglycerol (Maneri and Low 1988). Numerous studies have found Band 3 functions as a dimer (Casey and Reithmeier 1991; Cuppoletti *et al.* 1985; Wang *et al.* 1993).

1.4.1.3 Transport properties of Band 3.

Sulphonic acids, including 4,4'-diacetamido stilbene-2,2'-disulphonic acid (DAS) and 2-(4'-amino phenyl)-6-methylbenzene thiazol-3',7-disulphonic acid (APMB) produce a reversible inhibition of sulphate equilibrium exchange in human red cells. A study of the sidedness of action, of a number of these sulphonic acids, in red cell ghosts revealed that some, like DAS inhibit only at the outer membrane surface while others, such as APMB, inhibit at either surface. This finding suggests that at least two different types of membrane sites are involved in the control of anion permeability (Zaki *et al.* 1975).

Evidence supports a mechanism with a single proton-binding site that can alternatively have access to the cytoplasmic and extracellular solutions. The proton binding and transport site could be coupled to the single anion transport site for co-transport, but the two sites could be on opposite sides of the membrane at the same time and thus can be asynchronously transported by conformational changes of Band 3 (Milanick and Gunn 1986).

1.4.1.4 Transport of sulphate by Band 3.

Milanick and Gunn (1984) investigated the sulphate transport capacity of Band 3. Sulphate influx into human red blood cells was measured at 0 and 22°C at several fixed external pH values between 3 and 10. Sulphate transport observed Michaelis-Menten kinetics at each pH. Sulphate influx was stimulated 100-fold by a proton gradient. The flux was stilbene-sensitive

even in valinomycin-treated* cells and hence independent of membrane potential. The proton-activated influx appears to be proton-sulphate co-transport. At high pH there was a proton-independent flux that was membrane-potential and stilbene-sensitive. The proton-insensitive flux appeared to be a SO_4^{2-}/Cl^- exchange or a net sulphate influx (Milanick and Gunn 1984).

1.4.1.5 Common properties of Band 3 and the lysosomal sulphate transporters.

Scheuring *et al.* (1986) developed a method that reconstituted Band 3 into spherical phospholipid bilayers following solubilisation and purification with Triton X-100. Sulphate transport, very similar to that in erythrocytes, was measured in these proteoliposomes and inhibited by 4,4'-diisothiocyanodihydrostilbene-2, 2'-disulphonic acid (H_2DIDS) and flufenamate. Scheuring *et al.* (1988) found at 37°C, pH 7.2, and 10 mM sulphate that one reconstituted Band 3 molecule could exchange approximately 590 sulphate ions per minute.

Similarities between Band 3 and the lysosomal sulphate transporter have been shown using transport inhibitors (Koetters *et al.* 1995a). Both transporters were sensitive to DIDS, acetamido isothiocyanatostilbene disulphonic acid (SITS) and phenylglyoxal, which affect critical lysine and arginine residues. Band 3 and the lysosomal sulphate transporter show pH-dependent anion transport, exhibit counter-transport of sulphate and were sensitive to membrane potential at neutral pH. However, these two transporters are not identical because the potent Band 3 inhibitor dipyridamole had no effect on lysosomal sulphate transport. Although Band 3 shows increased proton-sulphate co-transport at low pH, at higher pH

* Valinomycin depolarises any potential difference across a phospholipid membrane

monovalent anion-like bicarbonate become the preferred anion, which does not occur with the lysosomal sulphate transporter.

1.4.2 Mitochondrial anion transport.

A specific mechanism for sulphate uptake in the mitochondria against a concentration gradient was observed with an external pH optimum of 5.5 (Winters *et al.* 1962). The parathyroid hormone stimulates the uptake of sulphate into cartilage, soft tissue, and its urinary excretion. This hormone promoted mitochondrial-competitive accumulation of sulphate, arsenate and phosphate (Rasmussen *et al.* 1964). Crompton *et al.* (1974, 1975) experimented with sulphate transport in rat liver mitochondria and suggested it was transported by the dicarboxylate carrier, as sulphate elicited an intra-mitochondrial inhibitable efflux of phosphate, malate, succinate and malonate. In addition to this route of sulphate flux Saris (1980) found sulphate was transported by a H^+ symporter in the mitochondria. The dicarboxylate carrier had a lower K_m suggesting the symporter is more important at higher sulphate concentrations.

The dicarboxylate carrier is located in the inner mitochondrial membrane. In an electroneutral exchange this carrier transports malate, succinate and other dicarboxylates in exchange for phosphate, sulphate and thiosulphate. The nuclear encoded sequence of the dicarboxylate carrier was partly determined (Iacobazzi *et al.* 1992) and more recently completed along with its gene structure. The gene encodes a 287 amino acid protein that is highly expressed in liver and kidney (Fiermonte *et al.* 1999).

1.5 Mammalian sulphate specific transporters.

1.5.1 Sodium-dependent sulphate transporter.

Studies with brush border membranes from rat renal cortex by Pritchard (1987) demonstrated that both a sodium / sulphate co-transporter and a sulphate / anion exchanger were present in the same membranes. David *et al.* (1992) compared the substrate specificity of these two renal sulphate transporters, the sodium-dependent and sulphate exchanger. The sodium-dependent luminal transporter had a K_m of 0.8 mM while the contraluminal exchanger had a K_m of 1.4 mM. These transporters work in concert in the proximal renal tubule to reabsorbed filtered electrolytes (*Figure 1.6*). The sodium / sulphate symporter is in the luminal (apical) membrane transporting sulphate from the lumen into the proximal cell, and the sulphate / oxalate antiporter in the contraluminal (basolateral) membrane transports sulphate from the proximal cell to the interstitium (connective tissue) (Ullrich 1994).

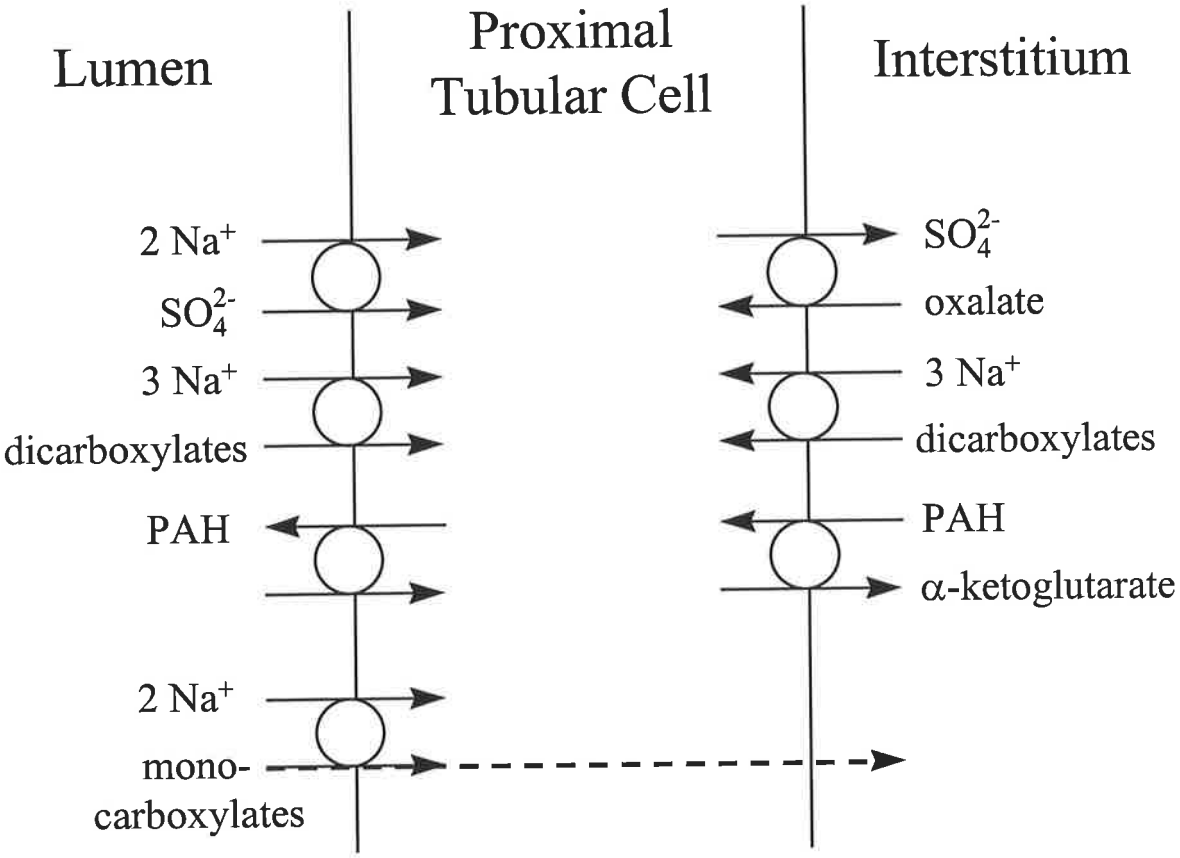

Figure 1.6 Organic anion transporters in the proximal renal tubule.

The proximal luminal cell has specific transporters in the luminal and contraluminal cell membranes. The luminal membrane exchanges between the lumen and the tubular cells, while the contraluminal membrane transporters exchange between the tubular cell and the interstitium. Abbreviation: *para*-aminohippurate (PAH). This diagram was reproduced from Ullrich (1994).

The first mammalian sulphate-specific anion transporter was cloned by functional expression from rat kidney cortex (Markovich *et al.* 1993). This kidney sulphate transporter's character, contrasts sharply with that of the lysosome. The kidney transporter contrasts in being sodium-dependent, hence its abbreviated name NaSi-1, and is unaffected by 1 mM DIDS*, an anion-exchange inhibitor of sodium-independent anion transporters. Markovich (1993) also reported the tissue distribution of NaSi-1 as determined by Northern blots shown in *Table 1.7*. Part of this tissue distribution however, was in no doubt contributed to by NaSi-2. This second Na^+/SO_4^{2-} co-transporter's cDNA has almost 500 bp more than NaSi-1, although it codes for the identical 595 amino acids as NaSi-1 (Norbis *et al.* 1994).

In current-clamped oocytes, NaSi-1 was expressed and subject to electrophysiological analysis. The Na^+/sulphate co-transporter had a half-maximal inward current at about 0.1 mM sulphate and 70 mM sodium. Oxyanions thiosulphate and selenate created similar currents as sulphate with similar K_m values (Busch *et al.* 1994). These and other observations show that NaSi-1 was electrogenic and carried positive charge into the cell. The lack of pH dependence of inward current led Busch *et al.* (1994) to propose that the co-transport of sulphate and Na^+ had a stoichiometry of 1:3. More recently the immunolocalisation of NaSi-1 has been determined to be restricted to the apical membrane of the proximal tubules (Lotscher *et al.* 1996).

* 4,4'-Diisothiocyanatostilbene-2,2'-disulphonate

Table 1.7 Tissue distribution of NaSi-1 in rat.

The expression of NaSi-1 was determined by Western blot analysis (Markovich *et al.* 1993).

Tissue	NaSi-1
kidney cortex (rat)	✓✓✓
kidney medulla/papila	✓
duodenum and jejunum	✓
ileum	✓✓
proximal colon	×
lung	×
liver	×
brain	×
heart	×
skeletal muscle	×

1.5.2 The sodium independent sulphate anion transporter family.

More recently the first cloned Na^+-independent sulphate transporter was reported (Bissig *et al.* 1994). This saturable (K_m ~0.14 mM) sulphate anion transporter (SAT-1) was cloned by functional expression from rat liver. This transporter has several common properties with the lysosomal sulphate transporter. Both are sodium-independent and sulphate specific, and can be inhibited by DIDS. The SAT-1 protein is characteristically more similar to the lysosomal sulphate transporter than to Band 3. The SAT-1 protein had no significant homology to any other proteins in the database when it was first identified.

Oocyte expression studies (Markovich *et al.* 1994) of the transporters involved in renal proximal tubular sulphate reabsorption identified the transporters as NaSi-1 and SAT-1. This study also contrasted the difference in the two transporter's characteristics.

1.5.2.1 Distribution and gene location of SAT-1.

Bissig *et al.* (1994) looked at the tissue distribution of SAT-1 in rat (*Table 1.8*). Liver and kidney showed strong signals, with brain and muscle showing weaker signals. However, the SAT-1 transporter was found to be essential for the uptake of extracellular sulphate required for glycosaminoglycan sulphation in chondrocytes (Morcuende *et al.* 1996). This suggests that SAT-1 may be expressed in other tissues not screened by Bissig *et al.* (1994). Northern blot analysis was also performed using liver from a number of species. No signal was found in human, rabbit, chicken, turtle, frog or skate. The only species beside rat, in which a signal was found was the mouse (Bissig *et al.* 1994).

Table 1.8 Tissue distribution of SAT-1 in rat.

Distribution of SAT-1 was determined by Northern blot analysis (Bissig *et al.* 1994).

Tissue	SAT-1
liver	✓✓
kidney	✓✓
muscle	✓
brain	✓
duodenum	×
ileum	×
proximal and distal colon	×
heart	×
lung	×

1.5.2.1.1 SAT-1 and α-L-iduronidase genes overlap.

Clarke *et al.* (1994) isolated the murine lysosomal α-L-iduronidase (IDUA) gene responsible for MPS I and found that the second exon of IDUA overlapped with the 3' untranslated region of SAT-1. Further studies (Clarke *et al.* 1997) found both the human and murine SAT-1 genes reside within the second intron of IDUA. The SAT-1 and IDUA genes are transcribed from opposite DNA strands.

There are very few reported mammalian genes that overlap. Whether SAT-1 is any more likely to be lysosomal due to it overlapping a known lysosomal gene becomes an interesting question. More objective questions such as the effects of the known mutations in the overlapping IDUA exon on the SAT-1 gene could be asked.

1.5.2.2 Diastrophic dysplasia sulphate transporter.

Another sulphate transporter was cloned which is responsible for the well-characterised human osteochondrodysplasia known as diastrophic dysplasia (DTDST) (Hastbacka *et al.* 1994). The predicted DTDST amino acid sequence showed 48% identity to the rat SAT-1 gene. The tissue distribution of the DTDST, as determined by Northern blot analysis, was found it to be widely expressed. All tissues screened expressed DTDST, and included liver, thymus, small intestine, testis, kidney, brain, colon, ovary, lung, spleen, prostate, leucocytes, heart, skeletal muscle and placenta.

The clinical features of this chondrodysplasia, first characterised by Lamy and Maroteaux in 1960, include short-limbed stature, generalised dysplasia of the joints, peculiar flexion limitation of the finger joints, 'hitchhiker' thumbs and a cleft palate. Positional cloning by disequilibrium mapping identified the affected gene DTDST. The only other disease gene

mapped this way prior to DTDST, based on point mutations and not deletions, or translocations for example, was that of cystic fibrosis (Hastbacka *et al.* 1994).

Since the cloning of the DTDST gene, it has been found to be the cause of two other chondrodysplasias, both caused by mutations in the DTDST gene. Achondrogenesis type IB is the most severe chondrodysplasia of the three (Superti-Furga 1994; Superti-Furga *et al.* 1995), and atelosteogenesis type II which is more severe than diastrophic dysplasia and less than achondrogenesis type IB (Hastbacka *et al.* 1996).

1.5.2.3 A sulphate transporter 'Down Regulated in Adenoma'.

The gene DRA was so coined as it was found to be down-regulated in colon adenomas and adenocarcinomas (Schweinfest *et al.* 1993). Initially DRA was thought to be a transcription factor based on weak homologies to a nuclear localisation signal, an acidic-activating domain and a homeobox motif, as there was no homology to any other gene. The DTDST protein was reported to have 33% and 48% identity with DRA and SAT-1 respectively (Hastbacka *et al.* 1994). These three proteins SAT-1, DRA and DTDST were the start of a new protein family, and had no significant homology to any other known sequences. The tissue distribution of DRA in normal human tissues appeared to be even more tissue-specific than SAT-1. Of the twelve cell lines (*Table 1.9*) and tissues screened for DRA expression only in normal colon tissue was there any detected. It could not be detected in lung, heart, placenta, spleen, brain, liver, pancreas, bone marrow, peripheral blood leucocytes, testis or ovary.

Table 1.9 ***Tissue distribution of DRA in human cell lines analysed by Northern blots (Schweinfest et al. 1993).***

Tissue	Cell line	DRA
colon, epithelial-like	CCD841CoN	×
colon fibroblasts	CCD18Co	×
colon	CCD33	×
colon fibroblasts	CCD112CoN	×
intestinal smooth muscle	HISM	×
lymphoblasts	RPMI 7666	×
thymus	HS67	×
bladder	FHS738.B1	×
lung	WI-38	×
skin	Detroit 55	×
breast epithelia	HBL-100	×
testis	Hs1.Tes	×

Later studies however, have found DRA to be expressed in the intestinal tract (Byeon *et al.* 1996) and prostate (Hoglund *et al.* 1996). The latter study also found that mutations in the DRA gene were responsible for congenital chloride diarrhoea disease. The clinical presentation of chloride diarrhoea disease is a lifetime, potentially fatal diarrhoea with a high chloride content. The failure of this transporter in contributing to the maintenance of a proper osmotic balance results in disease.

1.5.2.4 Pendrin, a thyroid-specific sulphate transporter.

The most recent sulphate transporter found (Everett *et al.* 1997) belonging to the SAT-1 family is pendrin. This transporter is named after Pendred syndrome, which was described a century ago and is characterised by congenital deafness and goitre. The gene was found by positional cloning using three large consanguineous families.

The percent amino acid sequence identities between pendrin and DRA, DTDST and SAT-1 are 45, 32 and 29% respectively. Northern blot analysis of thyroid, pancreas, adrenal medulla, testis, thymus, small intestine, stomach, heart, brain, placenta, lung, liver, skeletal muscle, pancreas and kidney, only found expression in the thyroid. During the mapping of pendrin it was found that DRA, which has most homology with pendrin, has a similar intron-exon gene structure suggesting a distant gene duplication. These two genes are coded in opposite directions and although not coinciding there is only about 48 kb between the 3' ends (Everett *et al.* 1997). The number of mammalian SAT-1 proteins in the family now stands at four, ranging from 29 to 48% in homology (*Table 1.10*).

Table 1.10 Percent amino acid identity between members of the SAT-1 family.

All sequences in this table are human except SAT-1, which is rat. Identities were determined by the Bestfit program run on ANGIS* using the local homology algorithm of Smith and Waterman (Rechid *et al.* 1989).

	DTDST	DRA	Pendrin
SAT-1	48	33	29
DTDST		33	32
DRA			45

* Australian National Genomic Information Service, University of Sydney, http://www.angis.org.au

1.6 Other sulphate-specific transporters.

A number of sulphate-specific transporters with homology to the SAT-1 family have been found in other species. A H^+/sulphate co-transporter was isolated from *Brassica napus L.* (oilseed rape) root membranes (Hawkesford *et al.* 1993). Three plant sulphate transporters from *Stylosanthes hamata* (forage legume) have been cloned. All three are H^+/sulphate co-transporters, of which two are high affinity and one is a low affinity transporter (Smith *et al.* 1995a). Two high affinity sulphate transporters have also been cloned from *Saccharomyces cerevisiae* (Cherest *et al.* 1997).

1.7 A chronological perspective of this study.

At the inception of this study the protein that resembled most closely, the lysosomal sulphate transporter was Band 3. The initial strategies used to identify the lysosomal sulphate transporter therefore revolved around Band 3. During this study the SAT-1 family of proteins emerged, which resemble more closely the lysosomal sulphate transporter. This family of proteins remains the only mammalian family that is sulphate-specific and sodium-independent. Strategies of this study were accordingly changed to focus on a SAT-1-like lysosomal sulphate transporter.

2. Materials and General Methods.

2.1 Materials.

2.1.1 Biological materials (Tissues, cells and serum).

Human placenta. Ethics approval no. 18/95 and RECW738/07/98	Women's and Children's Hospital Adelaide, Australia.
Animal Ethics approval AE66 and AE234/3/98	Women's and Children's Hospital Adelaide, Australia.
New Zealand White rabbit	Institute of Medical and Veterinary Science (IMVS), Adelaide, South Australia.
Semilop rabbit	IMVS, Adelaide, South Australia.
Skin fibroblast cell lines 1229 and 3125, 4620.	National Referral Laboratory cell bank held in the Department Chemical Pathology, Women's and Children's Hospital, Adelaide, Australia.

2.1.2 Tissue culture media and enzyme.

Foetal calf serum (FCS)	CSL Ltd., Parkville, Victoria, Australia.
Ham's F12	Gibco BRL, Life Technologies, Grand Island, NY, USA.
Basal Medium Eagle (BME)	Gibco BRL, Life Technologies, Grand Island, NY, USA.
Trypsin/versine	CSL Ltd., Parkville, Victoria, Australia.
Recombinant iduronidase (8965 nmol/min/mg)	Department Chemical Pathology, Women's and Children's Hospital, Adelaide, Australia.
Six-well plates (3.5 cm diameter wells)	Corning®, New York, USA.
75 cm^2 flasks	Corning®, New York, USA.

2.1.3 Radiochemicals.

Glucosamine D-[1-^{3}H] GlcN HCl (2.3 Ci [85.1 TBq] /mmol)	Amersham™ Life Science, Buckinghamshire England
[^{3}H]-Heparan sulphate (6.1 µCi [226 kBq] /mL)	Department Chemical Pathology, Women's and Children's Hospital, Adelaide, Australia
Phenylglyoxal [7-^{14}C] (888 MBq/mmol, 6.59 MBq/mg).	Amersham™ Life Science, Buckinghamshire England. Cat. No. CFA.700
Sodium [^{32}P]-phosphate (3000 mCi [111 TBq] / mmol)	NEN® Research Products DuPont®, Wilmington DE, USA.
Sucrose [^{14}C(U)] (0.18 GBq/mmol, 4.78 mCi/mmol).	NEN® Research Products DuPont®, Wilmington DE, USA. Cat. No. NEC-100
Sodium [^{35}S]-sulphate (550 mCi [20.4 TBq] /mmol, 2 mCi [74 MBq] /mL).	NEN® Research Products DuPont®, Wilmington DE, USA. Cat. No. NEX-041

2.1.4 Immunological materials, reagents and peptides.

Freund's Complete Adjuvant	GIBCO, Grand Island, NY, USA Cat # 660-5721AD
Freund's Incomplete Adjuvant	Sigma Chemical Co. St. Louis, MO, USA.
Sheep anti-rabbit immunoglobulin, affinity isolated, HRP conjugate	Silenus Laboratories, Hawthorn, Australia. Cat. No. RAH
4-Chloro-1-naphthol	Bio-Rad Laboratories, Hercules, CA, USA
Sheep anti-rabbit FITC conjugate	Silenus Laboratories, Hawthorn, Australia.
Western blot enhanced chemiluminescence reagents	NEN® Research Products DuPont®, Wilmington DE, USA. Cat. No. NEL102
Diphtheria toxoid	Chiron Mimotopes Pty Ltd, Clayton, Victoria, Australia
Synthetic peptides coupled to diphtheria toxoid	Chiron Mimotopes Pty Ltd, Clayton, Victoria, Australia
Synthetic peptides coupled to Thiopropyl-Sepharose 6B	Chiron Mimotopes Pty Ltd, Clayton, Victoria, Australia
96-Well vinyl plates	Costar®, Cambridge, MA, USA. Cat. No. 2595

2,2'-Azino *bis* (3-ethylbenzothiazoline-6-sulphonic acid) diammonium (ABTS)	©Pierce Chemical Company, Rockford, IL, USA. Cat. No. 34026.
Lab-Tek® 2 Well Chamber Slide™	Nunc, Naperville, IL, USA. Cat. No. 178565

2.1.5 Electron microscopy and photographic materials

Immunoglobulin free bovine serum albumin	Sigma Chemical Co. St. Louis, MO, USA. Cat. No. A-7638
Protein A-gold conjugate (10 nm)	Biocell Research Laboratories, LA, USA. Batch 9537.
Cold water fish gelatine	Sigma Chemical Co. St. Louis, MO, USA. Cat. No. G-7765
Low acid glycol methacrylate (LA-GMA) resin	Structure Probe Inc, West Chester, Pennsylvania, USA
Multigrade Developer and Fixative	ILFORD Imaging Australia Pty Ltd, Mt. Waverley, Victoria, Australia
Formvar coated 200 mesh square nickel grids	Guilder Grids, Grantham, England
Spurr's low viscosity epoxy resin	TAAB, Berkshire, England

2.1.6 Chromatographic and other media.

Ion Exchange	
Amberlite XAD-2	Fluka Chemie AG, CH-9471, Buch S, Switzerland
Biobeads SM-2	Bio-Rad Laboratories, Hercules, CA, USA (Cat. No. 152-3920)
Dowex AG1-X8	Bio-Rad Laboratories, Hercules, CA, USA
Econo-Pac 1 mL anion Q cartridge	Bio-Rad Laboratories, Hercules, CA, USA

Affinity	
Concanavalin A-Sepharose	Pharmacia AB, Uppsala, Sweden
Red Dye No. 78	Centre for Protein and Enzyme Technology, La Trobe University, Australia
Affi-Gel® 15	Bio-Rad Laboratories, Hercules, CA, USA
Gel Filtration	
Bio-Gel P2	Bio-Rad Laboratories, Hercules, CA, USA (Cat. No. 150-4114)
Sephadex G-10	Pharmacia AB, Uppsala, Sweden
Sephadex G-50	Pharmacia AB, Uppsala, Sweden

2.1.7 Chemicals.

Acridine orange	Eastman Kodak Company, Rochester NY, USA
acrylamide, 40% (w/v), bis : acrylamide (37.5:1)	Gradipore Ltd., NSW, Australia
adenosine triphosphate	Sigma Chemical Co. St. Louis, MO, USA.
ammonium persulphate (AMPS)	Ajax Chemicals, Auburn 2144, Australia
albumin, crude chicken dried egg white	Sigma Chemical Co. St. Louis, MO, USA. Cat. no. A-5253
amplify™ (fluorographic reagents)	Amersham International plc, Buckinghamshire England.
bicinchoninic acid (BCA)	Sigma Chemical Co. St. Louis, MO, USA.
brilliant blue G-colloidal concentrate	Sigma Chemical Co. St. Louis, MO, USA. Catalogue no. B-2025
butan-1-ol	Ajax Chemicals, Auburn 2144, Australia
carbonyl cyanide m-chlorophenylhydrazone (CCCP)	Sigma Chemical Co. St. Louis, MO, USA.
cytochrome-C	Sigma Chemical Co. St. Louis, MO, USA.

3,3-dimethyl glutaric acid (DMG)	Sigma Chemical Co. St. Louis, MO, USA.
dimethylsulphoxide (DMSO)	Ajax Chemicals, Auburn 2144, Australia
ethylenediaminetetra acetic acid (EDTA)	Ajax Chemicals, Auburn 2144, Australia
ethanol	Ajax Chemicals, Auburn 2144, Australia
25% formaldehyde	BDH Ltd, Poole, England.
glycine	BDH Ltd, Poole, England.
HEPES (*N*-2-hydroxyethylpiperazine-*N*'-2-ethanesulphonic acid)	Sigma Chemical Co. St. Louis, MO, USA.
heparin, sodium salt	Sigma Chemical Co. St. Louis, MO, USA.
hydrochloric acid (11.6 M)	Ajax Chemicals, Auburn 2144, Australia
30% hydrogen peroxide	Ajax Chemicals, Auburn 2144, Australia, Cat. no. 260
4-methylumbelliferyl-2-acetamido-2-deoxy-β-D-glucopyranoside	Koch-Light Ltd. Suffolk, England
methyl α-D-glucopyranoside	Sigma Chemical Co. St. Louis, MO, USA. Cat. no. M-9376
methyl α-D-mannopyranoside	Sigma Chemical Co. St. Louis, MO, USA. Cat. no. M-6882
3-mercaptopropanoic acid	BDH Ltd, Poole, England. Cat. # 44143
methanol	Ajax Chemicals, Auburn 2144, Australia
nonylphenoxy polyethoxy ethanol (NP40)	Fluka Chemie AG, CH-9471, Buch S, Switzerland. Cat. number 74385
Optiphase 'HiSafe' 3 liquid scintillation cocktail	Cat. no. SC/9205/21 Wallac UK, Milton Keynes, England
Percoll®	Pharmacia AB, Uppsala, Sweden
L-α-phosphatidylcholine Type XVIE from fresh egg yolk.	Sigma Chemical Co. St. Louis, MO, USA. Cat. no. P-3556, Lot 53H83531
phosphoric acid (14.7 M)	Ajax Chemicals, Auburn 2144, Australia
potassium chloride	Ajax Chemicals, Auburn 2144, Australia

Sigmacote® (silicanising reagent)	Sigma Chemical Co. St. Louis, MO, USA. Cat. SL-2
silver nitrate	Calbiochem, San Diego, CA, USA
sodium dodecyl sulphate (SDS)	BDH Ltd, Poole, England. Cat. 444464T
sodium azide	Sigma Chemical Co. St. Louis, MO, USA. Cat. S-8032
sodium bicarbonate	BDH, Merck Pty Ltd, Kilsyth 3137, Australia.
sodium chloride	Ajax Chemicals, Auburn 2144, Australia
sodium dithionite (sodium hydrosulphite)	Ajax Chemicals, Auburn 2144, Australia. Cat. 481
sodium gluconate	Ajax Chemicals, Auburn 2144, Australia
sodium hydroxide	Ajax Chemicals, Auburn 2144, Australia
sucrose	Ajax Chemicals, Auburn 2144, Australia
N,*N*,*N*',*N*'-tetramethyl ethylenediamine (TEMED)	Bio-Rad Laboratories, Hercules, CA, USA
Tris(hydroxymethyl)aminomethane (Tris)	Boehringer Mannheim Corp., Boehringer, Germany
Tris (Ultra pure)	ICN, Aurora, Ohio, USA. Cat. 103133
Thesit® (polyoxethylene 9 laural ether)	Boehringer Mannheim Corp., Boehringer, Germany
Triton X-100	Ajax Chemicals, Auburn 2144, Australia
Tween 20	BDH Ltd, Poole, England. Cat. # 44143
valinomycin	Sigma Chemical Co. St. Louis, MO, USA.

2.1.8 Equipment.

Beckman Airfuge™.	Beckman Instruments, Inc., Palo Alto, CA, USA
Beckman J2-M1 centrifuge JA-10, JA-20 rotors	Beckman Instruments, Inc., Palo Alto, CA, USA
Beckman L-90 ultra centrifuge Ti-70 rotors	Beckman Instruments, Inc., Palo Alto, CA, USA
Econo System Low pressure chromatography	Bio-Rad Laboratories, Hercules, CA, USA
High voltage electrophoresis, Model L24	Shandon Southern, Midrand, South Africa
KitchenAid model K45 mincer	The Hobart MFG. Co. Troy Ohio, USA
Moulinex hand mincer No. 2	Moulinex, Paris, France
Perkin-Elmer λ5 spectrophotometer and Luminescence spectrophotometer LS50B	Perkin-Elmer, Norwalk, Connecticut, USA
Pharmacia 3500XL power supply	Pharmacia AB, Uppsala, Sweden
3 mL Potter-Elvehjem (glass tube & teflon pestle) homogeniser	Wheaton Science Products, Millville NJ, USA
Protean II Xi vertical electrophoresis cell	Bio-Rad Laboratories, Hercules, CA, USA
Steel luer for glass syringes	Portland Surgical, Portland, Victoria Australia
Titertek Multiskan plate reader Bio-Tek EL900, Ceres plate reader	MCC Flow Laboratories, U.K. Bio-Tek Instruments , Inc., Winooski, USA
Wallac 1409 liquid scintillation counter	Wallac Oy, Turku, Finland

2.1.9 Miscellaneous materials.

XOMAT XK-1 autoradiography film	Eastman Kodak Company, Rochester NY, USA
PVDF membrane	Bio-Rad Laboratories, Hercules, CA, USA
Density marker beads	Pharmacia AB, Uppsala, Sweden

2.2 Methods.

2.2.1 Preparation and collection of placentae.

Human placenta was chosen as a source of lysosomes for two main reasons. Placenta was a readily available source of human tissue and the quantity of tissue used, approximately 0.5 kg per placenta enabled milligrams of highly enriched lysosomal membrane proteins to be isolated. Placentae obtained were from either full-term normal vaginal delivery or near full-term caesarean deliveries. The tissue was transported to the laboratory on ice within one hour of a caesarean delivery, or stored on ice for less than three hours before collection, after a normal vaginal delivery.

Only normal placentae were collected. Placentae from premature births, twins, with single artery umbilical cords or any abnormal pathology were not collected. Only one placenta was prepared on any one day. The placenta was placed with the basal surface consisting of maternal cotyledons down with the apical or foetal surface in view. The umbilical cord, placental membranes (amnion and chorion laeve that enclosed the foetus) and any significant fibrinoid deposits were removed.

2.2.2 Preparation of cytoplasmic organelles from human placentae.

All solutions and tissue were kept ice-cold unless otherwise stated. Up to 0.5 kg of trimmed placenta was cut into approximately two centimetre cubed pieces, and washed three times to remove blood, by gently stirring in 0.5 L of sucrose buffer (0.25 M sucrose, 1 mM EDTA, pH 7). The tissue was minced by a KitchenAid model K45 mincer, then passed through a Moulinex hand mincer No. 2 using 1 L of sucrose buffer. This homogenate was processed through both mincers a second time prior to centrifugation at 750 ***g*** in a Beckman JA-10 rotor for 10 min at 4°C. The supernatant (cellular contents) were aspirated, filtered through two

layers of cotton gauze (Johnston™) and kept on ice while the pellets were processed through the mincing, centrifugation and supernatant filtering a second time. The pooled supernatants were centrifuged in a JA-10 rotor at 8000 ***g*** for 20 min at 4°C. The supernatant (microsomal) was aspirated and the pelleted granular fraction was resuspended in approximately 50 mL of the sucrose buffer. The granular fraction was layered on two 10 mL isotonic 50% Percoll® cushions and centrifuged at 1000 ***g*** for 10 min at 4°C in a bench-top centrifuge to sediment contaminating erythrocytes. The granular fraction on top of the Percoll® was removed and diluted to 320 mL with sucrose buffer containing 25% Percoll®, and centrifuged in eight 40 mL tubes in a JA-20 rotor at 31000 ***g*** for 60 min at 4°C. The density gradients were fractionated and the densest 10 mL (lysosomal-rich) from the bottom of each tube was pooled and a second gradient formed by centrifugation under the same conditions. If mitochondria were to be further enriched the next densest 10 mL of each tube was pooled and a mitochondrial-rich third gradient formed. The second and third Percoll® gradients were fractionated and either washed free of Percoll® to obtain intact cytoplasmic organelles (*Section 3.3.1.1*) or salt-washed to isolate membranes and associated integral proteins (*Section 2.2.4.1*).

2.2.3 Protein quantification and enzyme assays.

The degree of cytoplasmic organelle enrichment in various fractions was determined by measuring and comparing the activity of various marker enzymes.

2.2.3.1 Protein quantification.

Protein determinations were performed using bicinchoninic acid (BCA) by the method of Smith *et al.* (1985) using bovine serum albumin (BSA) as a standard.

2.2.3.2 Determination of β-*N*-acetylhexosaminidase (EC 3.2.1.52) activity.

β-*N*-Acetylhexosaminidase also known as *N*-acetyl-β-glucosaminidase, or more commonly as β-hexosaminidase is a soluble luminal lysosomal protein. This enzyme was measured fluorometrically using the 4-methylumbelliferyl substrate as described by Leaback and Walker (1961).

2.2.3.3 Assaying acetyl-coenzyme A α-glucosaminide *N*-acetyltransferase (EC 2.3.1.78) activity.

Heparan-α-glucosaminide *N*-acetyltransferase or acetyl-CoA:α-glucosaminide *N*-acetyltransferase (GNAT), is a lysosomal biosynthetic membrane enzyme and was assayed as previously described by Meikle *et al.* (1995) using 5 μM [^{3}H]-GlcN as the substrate. This assay was used to determine the level of enrichment of lysosomal membranes.

2.2.3.4 Determination of cytochrome-*C* oxidase (EC 1.9.3.1) activity.

Cytochrome-*C* oxidase is a mitochondrial inner membrane protein. Activity was determined based on the method of Cooperstein and Lazarow (1951) using a Perkin-Elmer λ5 spectrophotometer. A reduced cytochrome-*C* solution (0.21 mg/mL) was freshly prepared by shaking for several minutes in 30 mM sodium phosphate, pH 7.4, and 4 mM sodium hydrosulphite. Ten to twenty microlitres of sample was added to 1 mL of reduced cytochrome-*C* solution and the absorbance was recorded over the following 5 min at 550 nm. The rate of cytochrome-*C* oxidation was determined by the change in A_{550} with time.

2.2.3.5 Determination of monoamine oxidase (EC 1.4.3.4) activity.

Monoamine oxidase (tyramine oxidase) is a mitochondrial outer membrane enzyme used as a marker for enrichment of mitochondria or the membranes of mitochondria. The assay was performed as described by Singh and Poulos (1995).

2.2.4 Preparation of proteins from organelles.

2.2.4.1 Isolation of organelle membranes and associated proteins.

Membrane proteins were separated from matrix proteins by freezing and thawing three times in 1M NaCl followed by centrifugation in a Beckman Ti 70 rotor at 100,000 ***g*** for 1 h at 4°C. The sedimented membranes and association proteins were then resuspended and subject to a second round of freezing and thawing in 1M NaCl and centrifugation at 100,000 ***g*** to reduce the amount of soluble matrix proteins in the sedimented membrane protein pellets.

2.2.4.2 Solubilisation of membrane proteins for SDS-PAGE.

The stock solution from which solubilisation solution was prepared was: 5x loading solution with dye: 50% (w/v) sucrose, 10% (w/v) SDS and 0.01% (w/v) bromophenol blue; and 10 M urea. Unless the sample was in a small volume before solubilisation it was freeze-dried. Solubilisation solution contained 7.5 M urea, 1x loading solution and 5% (v/v) β-mercaptoethanol or 10 mM dithiothreitol (DTT). Samples were incubated in 20 µL of solubilisation solution for mini gels or 50 µL for large gels at 37°C for 1 h, or overnight at room temperature. These low temperature incubations are required when urea is present; the normal procedure is to boil for 3 min.

2.2.4.3 Extraction of phospholipid from membrane proteins.

Membrane proteins (50-500 µg) were freeze-dried before the addition of 1 mL of $CHCl_3$: methanol (2:1) and then vortexed for 10 s. The samples were microfuged (13,000 ***g***) for 10 min at 25°C, the supernatant removed and the remaining pellet air dried. The pellet was then solubilised in the appropriate solution for SDS-PAGE, 2-DE or storage.

2.2.5 Chromatography used to fractionate proteins.

Concanavalin A-Sepharose (Con A-Sepharose) was used for the enrichment of lysosomal proteins because it binds many glycosylated proteins. Polyoxethylene 9-laural ether (Thesit®) which does not interfere with absorbance at 280 nm, was used to extract membrane proteins from phospholipid membranes. Con A-Sepharose columns were used on a Bio-Rad Laboratories low pressure chromatography system (Econo-System) at 25°C. This chromatography system had a UV detector (280 nm) and a conductivity meter, allowing protein concentrations and buffers to be monitored respectively.

2.2.5.1 Preparation of protein samples for chromatographic fractionation.

Membrane proteins prepared by salt washes (*Section 2.2.4.1*) were extracted before fractionation with Con A-Sepharose. Membrane proteins at 2 mg/mL were extracted from their phospholipid membranes by stirring overnight at 4°C with an equal volume of a 2x extraction buffer (2% (w/v) Thesit®, 300 mM NaCl, 20% (w/v) glycerol, 0.1 mM EDTA, 100 mM MOPS, pH 7). The extracted proteins were clarified at 100,000 ***g*** for 1 h at 4°C.

2.2.5.2 Preparation and use of Con A-Sepharose to fractionate proteins.

Con A-Sepharose was cross-linked and packed into a 1 x 10 cm column. Fresh Con A-Sepharose was centrifuged at 175 ***g*** for 2 min in a bench top centrifuge and the supernatant (20% ethanol) discarded. The slurry was swollen in PBS for 1 h, centrifuged at 175 ***g*** for 2 min and the supernatant removed. The Con A-Sepharose was cross-linked with 0.2% (v/v) glutaraldehyde during which it was mixed by occasional inversion for 2 h. After the preparation of a Con A-Sepharose column and before its first use the column was equilibrated with 1x extraction buffer containing 3 mM $MgCl_2$ and 3 mM $CaCl_2$.followed by a mock elution with 20% (w/v) methyl α-D-mannopyranoside in 1x extraction buffer.

Extracted membrane protein samples were loaded onto the Con A-Sepharose column at 0.5 mL/min after the addition of $MgCl_2$ and $CaCl_2$ to give final concentrations of 3 mM each. Sample that did not bind to Con A-Sepharose was washed through the column with 1x extraction buffer. Proteins were eluted from the column with 20% (w/v) methyl α-D-mannopyranoside in 1x extraction buffer with 3 mM $MgCl_2$ and 3 mM $CaCl_2$. The Con A-Sepharose columns after each use were washed, with four column volumes of regeneration buffer (1% (w/v) Triton X-100, 20% (w/v) glucopyranoside, 1 M NaCl) and stored in PBS containing 0.02% (w/v) NaN_3 at 4°C.

2.2.5.3 Preparation and use of Red Dye to fractionate proteins.

Red Dye No. 78 was used to further fractionate the Con A Sepharose flow through fraction. The Red Dye matrix was prepared and generated with 5 M urea, then equilibrated in the elution buffer (20% (w/v) methyl α-D-mannopyranoside in 1x extraction buffer with 3 mM $MgCl_2$ and 3 mM $CaCl_2$) applied to Con A Sepharose (*Section 2.2.5.2*). The protein fraction that bound to the Red Dye, and was eluted with 2 M NaCl contained an enrichment of GNAT.

2.2.6 Polyacrylamide gel electrophoresis.

Polyacrylamide gel electrophoresis (PAGE) was used to separate proteins by molecular mass and by isoelectric focus point (pI). Denaturing SDS-PAGE was used to separate proteins on the basis of molecular mass, and isoelectric focusing tube-gels separated proteins on the basis of pI. Combining these two methods of separation by following isoelectric focusing with SDS-PAGE results in two-dimensional electrophoresis (2-DE).

2.2.6.1 SDS-PAGE.

The method of Laemmli (1970) was used to resolve proteins on SDS-PAGE gels. Resolving gels contained 0.375 M Tris-HCl, pH 8.8, 10 or 12.5% (w/v) polyacrylamide (30:0.8 acrylamide : bis-acryl), 0.1% SDS, 0.1% (w/v) ammonium persulphate (AMPS), 0.05% (v/v) TEMED. Stacking gels contained 0.125 M Tris-HCl, pH 6.8, 3.75% (w/v) polyacrylamide, 0.5% (w/v) AMPS and 0.075% (v/v) TEMED. The polyacrylamide gel solutions were degassed before the addition of SDS or cross-linking catalysts. Water-saturated butan-1-ol (0.2 mL) was carefully overlayed on each resolving gel until polymerisation. Resolving gels were left to polymerise for 1 h to overnight; stacking gels were also allowed to set for at least 1 h. A ten toothed comb was used to form wells in the stacking gel of approximately 20 µL.

Mini-gels (82 mm wide by 73 mm long) for SDS-PAGE was performed using the Hoeffer Mighty Small Electrophoresis units multi-castor. Large-gels were cast using a Bio-Rad Laboratories system (16 x 20 cm), which had 50 µL sample (0.75 mm thick gels) wells. 1-D gels were 0.75 mm, while 2-DE gels were 1.5 mm thick. The reservoir buffer contained 25 mM Tris-HCl, 192 mM glycine, 0.1% (w/v) SDS, at pH 8.3. Electrophoresis was

conducted at a constant current of 20 mA per 0.75 mm gel, 30 mA per 1.5 mm gel, or at a constant voltage of 200 V for either thickness gel.

2.2.6.2 Two-dimensional gel electrophoresis.

Two-dimensional electrophoresis was a modification of the method by O'Farrell (1975). The first dimension (isoelectric focusing) was performed using a Bio-Rad Laboratories model 175 tube system with the second dimension (resolution by relative molecular mass) run as described in *Section 2.2.6.1*, with the exception that the tube gel was overlaid onto the resolving gel and set with 1% (w/v) low melting point agarose dissolved in 0.125 M Tris-HCl, pH 6.8 and 0.1% (w/v) SDS. The second dimension (SDS-PAGE) was pre-electrophoresed with 1 mM thioglycolic acid added to the reservoir buffer, prior to overlaying the tube gel if the sample was to be used for *N*-terminal sequencing.

Samples were dialysed, freeze-dried and resuspended in 10 µL of 8 M urea, 1% (w/v) SDS, 1% (w/v) DTT and then incubated at 37°C for 1 h. To this was added 20 µL of a second solubilisation solution (8 M urea, 4% (w/v) CHAPS, 5% (v/v) Biolytes® and 0.0025% (w/v) bromophenol blue which was then incubated for a further 30°min at 37°C. The solubilised proteins were then centrifuged in an airfuge at 100,000 ***g*** for 15 min. The clarified supernatant was then applied to the top of a 14 cm (1.5 mm thick) tube gel containing 8 M urea, 4% (w/v) polymerised acrylamide, 0.4% (w/v) CHAPS and 5% (v/v) Biolytes®, pH 3-10. Between use the glass tubes were chromic acid washed and silanised with Sigmacote®.

The electrophoretic conditions for the tube gels were 0-300 V over 30 min, 300 V for 12 h, 300-1500 V over 30 min, 1500 V for 2 h, 1500-100 V over 1 h and 100 V for 2 h. This

voltage was applied using a Pharmacia 3500XL power supply. The top (anode) reservoir contained 20 mM NaOH and the cathode reservoir 6 mM phosphoric acid. pI markers (Bio-Rad) were subject to isoelectric focusing in one of the same batch of tube gels used to focus samples so as to calibrate 2-DE gels in the pI dimension.

The acrylamide gels were expelled from the glass tubes and incubated in 5 mL of equilibration buffer (0.5 M Tris-HCl, pH 6.8, 2% (w/v) SDS, 7.2 g urea, 6 mL glycerol) with 12.5 mg DTT for 10 min at 25°C while rocking. The tube gels were then incubated in 5 mL of equilibration buffer containing 225 mg idoacetamide and 0.0025% (w/v) bromophenol blue for 10 min at 25°C. Idoacetamide which improves resolution, was omitted if the sample was used for *N*-terminal sequencing, as it prevents *N*-terminal blocking.

2.2.7 Visualisation of proteins resolved by electrophoresis.

2.2.7.1 Brilliant blue G-colloidal stain.

Acrylamide gels were fixed overnight with 7% (v/v) glacial acetic acid, 40% (v/v) methanol. Four parts (40 mL) Brilliant blue G-colloidal concentrate was mixed with one part (10 mL) methanol and vortexed for 30 sec and immediately used to stain gels for 2 h. The gels were rinsed in 25% (v/v) methanol for 60 sec, then destained for approximately 20 sec in 10% (v/v) glacial acetic acid, 25% (v/v) methanol. Gels were rinsed again in 25% (v/v) methanol then destained in 25% (v/v) methanol for up to 24 h.

2.2.7.2 Silver stain.

All steps were performed at room temperature with gentle shaking. Polyacrylamide gels were fixed for 30 min to overnight with 40% (v/v) ethanol and 10% (v/v) acetic acid. Fixative was poured off and 250 mL of incubation solution containing 30% (v/v) ethanol, 0.5 M sodium

acetate, 8 mM sodium thiosulphate, and 0.13% (w/v) glutaraldehyde was added for 30 min to overnight. Three washes in water for 5 min each for gels 0.75 mm thick and 10 min for gels 1.5 mm thick was performed. Silver solution (250 mL) was added for 40 min containing 0.1% (w/v) silver nitrate and 25 µL of 25% (v/v) formaldehyde. The gels were rinsed very briefly in water and developed in 250 mL of 2.5% (w/v) sodium carbonate containing 25 µL of 25% (v/v) formaldehyde. Development was stopped with 40 mM EDTA (Chataway and Barritt 1995).

2.2.8 Drying polyacrylamide gels.

Gels that were to be autoradiographed, were dried under vacuum while sandwiched between a sheet of cellophane and a sheet of Whatman 3MM filter paper at 50°C for 1-2 h. Stained gels were dried overnight on a Hoeffer drying frame between two sheets of cellophane.

2.2.9 Electro-blotting of samples from polyacrylamide gels to membrane filters.

Two methods were used to transfer SDS-PAGE resolved protein samples to an inert membrane. The first method was the widely used Towbin (1979) method where the transfer occurs in a Tris-buffered glycine solution (192 mM glycine, 20% (v/v) methanol, 25 mM Tris-HCl, pH 8.3). This method was used to transfer samples from large gels (10 x 14 cm) to nitrocellulose membrane filters.

A second method (Ploug *et al.* 1989) was used to specifically transfer membrane proteins to PVDF membranes in a 3-cyclohexylamino-1-propanesulphonic acid (CAPS) buffer (10 mM CAPS-NaOH, pH 11, 20% methanol). The PVDF membranes were pre-wet in 100% methanol and then equilibrated in transfer buffer. After samples were resolved by

SDS-PAGE the polyacrylamide gels were washed for 10 min in CAPS buffer before being placed adjacent to the PVDF membrane, which was then sandwiched between Whatman 3MM paper. The sandwich was assembled after each layer was pre-wet in transfer buffer and air bubbles removed.

The current used to transfer depended on the size of the polyacrylamide gel. The large gels were transferred at 0.5 A for 1 h, or 0.15 A for 16 h at 4°C. The transfer of mini-gels (82 x 73 mm) was conducted at 250 mA for 1 h on ice in a mini Hoeffer system.

2.2.10 Immunological methods.

2.2.10.1 Polyclonal antibody production.

Rabbits were kept and bled by Julie Goldfinch and Lisa Prestwood in the Animal House, Women's and Children's Hospital, Adelaide, Australia.

2.2.10.1.1 Immunisation regime.

Polyclonal antibodies were raised in New Zealand White rabbits, by administration of antigens subcutaneously near the rear legs or at four sites on the back of the neck with a 21G needle. The first inoculation included Complete Freund's Adjuvant, the second and third booster inoculations were with Freund's Incomplete Adjuvant and the remaining antigen boosts were in PBS alone. Inoculations were administered four weeks apart. Each inoculation contained either 100 μg of protein or 100 nmoles of peptide in a final volume of 1 mL (split between a number of sites). Adjuvants were emulsified with PBS in a ratio of 2:1.

Peptide conjugates were purchased from Chiron Mimotopes Pty. Ltd. Peptides were conjugated to the carrier protein diphtheria toxoid, with the bifunctional coupling reagent 6-maleimido caproic acyl *N*-hydroxy succinimide ester (MCS).

2.2.10.1.2 Preparation of polyclonal antibody from serum.

Test bleeds (10 mL) were collected from the rabbit's ear prior to immunisation. After the immunisation regime was completed, serum was collected by a heart puncture. Serum was left at room temperature for 1 h followed by 4°C overnight to clot. The clotted blood was centrifuged at 6238 ***g*** and 4°C for 10 min. The supernatant was recovered and microfuged for 10 min at 10,000 ***g*** and 4°C to further clarify. The supernatant was collected, NaN_3 added to a final concentration of 0.02% and stored at -20°C in aliquots.

2.2.10.1.3 Enzyme linked immuno-sorbant assay (ELISA).

The volume of antibody incubations and colour development reactions per well were 100 µL. Vinyl 96-well plates were coated with antigen samples in 100 µL 0.1 M $NaHCO_3$ at 4°C overnight. Plates were washed three times with Tris-buffered saline (TBS), 0.25 M NaCl, 20 mM Tris-HCl, pH 7. Primary antibodies were serial diluted in TBS with 1% (w/v) bovine serum albumin (BSA) starting at 1:1000 in the left side of the plate and continuing across the plate to a final dilution of $1:2.048x10^6$. Plates were covered with parafilm and incubated at room temperature for 2 h. Plates were washed three times in TBS and incubated for 1 h at room temperature with a secondary sheep anti-rabbit antibody diluted 1:1000 in TBS containing 1% (w/v) BSA. After a further three washes colour development substrate (10 mL 50 mM citrate, pH 4, 0.2 mL ABTS (10 mg tablet dissolved in 0.6 mL) and 10 µL 30% H_2O_2) was added and the optical density of each sample-well read at 414 nm after 15 min.

2.2.10.2 Detection of protein on Western blots.

2.2.10.2.1 General Western blot method.

Blotted membrane filters were blocked with 1% (w/v) dry defatted milk in TBS for 1 h at room temperature. The filters were washed in TBS for 10 min and the primary and secondary antibodies were diluted with 1% (w/v) BSA in TBS. The primary antibodies were incubated for 3 h at room temperature or 16 h at 4°C, and the secondary antibody was incubated for 1 h at room temperature. Membrane filters were washed between and after antibody incubations with TBS for 10 min, followed by two 20 min washes in TBS containing 0.05% (v/v) NP-40 and then another 10 min wash in TBS. The secondary antibody was then detected by colour development with 4-chloro-1-napthol (*Section 2.2.10.3*).

2.2.10.2.2 Modified Cetus® Western blot method.

This method is a modification of the instructions in an antibody detection kit supplied with an anti-ras p21 monoclonal antibody from Cetus Corporation©, Emeryville, CA 94608, USA. All incubation steps were performed with agitation either by rocking or rotation. Membrane blots were blocked in 1 M glycine, 5% (w/v) non-fat dry milk, 1% (w/v) crude ovalbumin, and 5% (w/v) expired foetal calf serum (FCS) for 1 h at room temperature. Membranes were washed three times for 5 min in 0.1% (w/v) dry non-fat milk, 0.1% (w/v) crude ovalbumin, 1% (v/v) expired FCS and 0.1% (v/v) Tween-20 in PBS (wash solution). The primary antibody was diluted (1 in 1000) into wash solution and incubated with the membrane at 4°C overnight (approximately 16 h). Membrane blots were then washed three times for 5 min, the secondary antibody diluted (1 in 1000) in wash solution and incubated for 1 h at room temperature. Membrane blots were washed again three times for 5 min and then a final wash in TBS for 5 min before the secondary antibody was detected as described (*Section 2.2.10.3*).

2.2.10.3 Visualisation of a secondary antibody.

Detection of the secondary antibody was achieved by colour development using 4-chloro-1-napthol, or by the more sensitive enhanced chemiluminescence (ECL) detection, which was recorded on photographic film. The secondary antibody used was a sheep anti-rabbit immunoglobulin conjugated to horse radish peroxidase (Silenus Laboratories).

Membrane blots subject to colour development for secondary antibody detection were incubated in a peroxidase substrate. The substrate was freshly prepared by dissolving 60 mg 4-chloro-1-napthol in 20 mL of ice-cold methanol before adding 100 mL of TBS and 60 µL of 30% (v/v) hydrogen peroxide. The substrate was added to membrane blots at room temperature until the purple-coloured signal was clear or the background began to rise (approximately 1 to 5 min). Colour development was stopped by rinsing the filter in water after which it was dried. More sensitive detection of secondary antibody was by ECL (*see Section 2.2.11*).

2.2.11 Western blot analysis visualised by Enhanced Chemiluminescence.

Western blot analysis was performed as described in *Section 2.2.10.2* until the addition of colour development substrate. After the blot was washed in TBS, equal parts of ECL reagents A and B (NEN® Research Products DuPont®, Wilmington, USA) were added for 1 min, the excess reagent blotted off and the membrane sealed in plastic. The sealed membrane was placed on Kodak XK-1 film for 1 min or more and processed by hand in developer for approximately 1 min, fixed for several minutes, rinsed in water and dried.

3. Characterisation and Partial Purification of the Lysosomal Sulphate Transporter.

3.1 Introduction.

The human lysosomal sulphate transporter has potential clinical significance as reviewed in *Section 1.3.2.3*. Studying the lysosomal sulphate transporter in human tissue could shed light on some of the unresolved human lysosomal disorders, where some patients show lysosomal storage but not a known enzyme deficiency. The homology between the human lysosomal sulphate transporter and other species is unknown, hence the use of human tissue was preferable, avoiding the need to repeat purifications or isolations in multiple species.

Previous characterisation studies of the lysosomal sulphate transporter were performed using lysosomes isolated from rat liver. Ohkuma *et al.* (1982) found the preparation of normal (unmodified) lysosomes in a pure state difficult without previous treatment of animals with reagents such as Triton WR-1339. The resulting preparation of Triton-modified lysosomes (tritosomes) had an increased density, which facilitated an otherwise difficult isolation.

Turning lysosomes into tritosomes changed the behaviour of the lysosomal proton pump. Ohkuma *et al.* (1982) found activity of the lysosomal proton pump resistant to inhibition by *N,N'*-dicyclohexylcarbodiimide (DCCD) and azide in normal lysosomes but highly sensitive to these in tritosomes. The validity of tritosomes as a model for studying lysosomal sulphate transport could be questioned considering such changes.

Treatment of animals with Triton WR-1339 also causes a change in lipid composition of lysosomes. There is a substantial increase in the lysosomal phospholipids bis (monoacylglycerol) phosphate and acylphosphatidylglycerol a related lipid, and an

increase in sphingomyelin. Phosphatidylinositol however, showed a significant decrease in the lysosomal membrane (Matsuzawa and Hostetler 1980) (Hayashi *et al.* 1981).

This study focused on the human lysosomal sulphate transporter, which precluded the use of Triton WR-1339 and required the development of a specific purification procedure. Placenta was used as a source of human lysosomes as this was the only human tissue readily available in large amounts. A large amount of tissue is required to purify what is potentially a very low abundant protein.

The isolation of lysosomes involves a number of steps that have been extended and refined with time. Most isolations have been from rat liver; firstly the cells are gently broken so as to keep the cytoplasmic organelles intact, then a crude lysosomal fraction is obtained by differential centrifugation which is subjected to a self-generating gradient composed of modified colloidal silica (Percoll®) (Pertoft *et al.* 1978). Percoll® consists of silica particles (15-30 nm diameter) coated with polyvinylpyrrolidone, which can form gradients within the density range of 1.0-1.3 g/mL, and remains iso-osmotic throughout this range. Others have used two successive Percoll® gradients, swelling and bursting the rat liver lysosomes between gradients with methionine methyl ester (Symons and Jonas 1987).

As sulphate transporters are present in numerous cellular membranes such as mitochondria (*Section 1.4.2*) and plasma membrane (*Section 1.5.1*), it was crucial to prepare lysosomes that contained little contamination from other cellular components. In addition, the purified lysosomes need their phospholipid membrane integrity to be maintained to preserve activity of the sulphate transporter.

The activity of a transporter cannot be determined, in the majority of cases, by the classical enzyme substrate to product conversion measurements. To measure transport of ions across the membranes of isolated cytoplasmic organelles there are several requirements. Simply, the molecules or ions not transported have to be separated from the transported molecules. More specifically, this requires the transport protein to be in a phospholipid membrane, which forms an intact vesicle. The enclosed space or lumen can then hold ions either transported into the vesicle, or those to be transported out of the vesicle. Transported molecules can then be separated from non-transported molecules by separating the vesicles from the surrounding medium.

One approach to the purification of membrane transporters has been through reconstitution of solubilised proteins into proteoliposomes (*Section 3.4.5*). Membrane proteins extracted from phospholipid membranes, separated chromatographically and then reconstituted into artificial phospholipid vesicles will enable sulphate transport to be assayed. The production of such proteoliposomes could assist in the purification of other lysosomal transporters as well as the sulphate transporter.

3.2 Experimental Aims.

The primary objectives of this section of work were to:

- produce highly enriched preparations of lysosomes from human placenta;
- characterise the sulphate transporter in lysosomes in comparison to other cytoplasmic organelles; and
- solubilise and reconstitute the sulphate transporter into artificial proteoliposomes to facilitate its purification.

The achievement of these objectives required the development of a lysosomal purification procedure for human placenta. Before sulphate transport could be measured, the integrity of the lysosomes was determined by the measurement of H^+-ATPase activity (acidification). Suitable methods for the measurement of sulphate transport in both isolated lysosomes and reconstituted proteoliposomes were developed. This is the first comparative study of subcellular sulphate transporters in isolated human cytoplasmic organelles.

3.3 Methods.

3.3.1 Lysosomal proton pump assay.

The vacuolar or v-type proton pump has formally been named the H^+-transporting ATPase synthase (EC 3.6.1.34), although it is more commonly known as the v-type H^+-ATPase. This H^+-ATPase can be assayed in organelles using a pH-sensitive dye. This assay was performed to ascertain lysosomal phospholipid membrane integrity. The isolated organelles were washed free of Percoll® before H^+-ATPase activity could be assayed. Percoll® interfered with this assay as it fluoresced under the same excitation and emission wavelengths required for the pH-sensitive dye, acridine orange.

3.3.1.1 Washing and buffering of intact cytoplasmic organelles.

Lysosomal-rich fractions (7-10, of ten fractions) from the second Percoll® gradient (*Section 3.4.1*) were pooled and diluted ten to twenty times in 0.25 M sucrose, with 1 mM EDTA, pH 7, or 20 mM 3,3-dimethyl glutaric acid (DMG), pH 7 and centrifuged at 10,000 ***g*** for 30 min at 4°C in a Beckman JA-10 rotor. The supernatant was aspirated, taking care not to aspirate any of the loose pellet. The pellet was gently resuspended and re-pelleted in approximately 450 mL of sucrose solution resulting in a tighter pellet free of Percoll®. The pellet was resuspended in the DMG-buffered sucrose solution and organelles allowed to equilibrate. The molarity of DMG was varied in some experiments as stated.

3.3.1.2 Proton pump (H^+-ATPase) measurements.

The pH change (organelle acidification) resulting from the H^+-ATPase was observed using a Perkin Elmer Luminescence spectrophotometer LS50B. Excitation and emission were set at 492 nm and 540 nm respectively, with slit widths of 5.0 and the neutral density filter removed. The time drive protocol was set at 0.1 sec intervals with a response of 0.5 sec and a

temperature of 37°C. The intact washed lysosomes were stirred in 2 mL of acidification medium containing 0.25 M sucrose, 1 μM valinomycin (500 μM stock solubilised in ethanol), 10 μM acridine orange, 2 mM $MgCl_2$, 100 mM KCl, and 10 to 20 mM DMG, pH 7.0, depending on the DMG concentration in the cytoplasmic organelles. Acidification was started with 10 μM ATP and the ethanol-soluble protonophore carbonyl cyanide *m*-chlorophenylhydrazone (CCCP) was used at 10 μM to release the proton gradient.

3.3.2 Electron microscopy.

Electron microscopy was performed by Richard C. A. Davey, Department of Chemical Pathology, Women's and Children's Hospital, North Adelaide, South Australia.

3.3.2.1 Negative staining of liposomes.

Proteoliposomes were diluted to obtain a monolayer coating. One drop of liposome solution was placed on formvar-coated 200 mesh square nickel grids and allowed a few seconds for the liposomes to settle. Excess fluid was drained from the grid by touching the side of the grid with Whatman No. 1 filter paper.

Negative staining was employed to visualise the specimen by placing one drop of 1% (w/v) aqueous uranyl acetate onto the grid and again draining the excess from the side, allowing several seconds to dry before examination with a Hitachi H-7000 transmission electron microscope (Hitachi, Tokyo, Japan), operating at an accelerating voltage of 75 kV.

3.3.2.2 Fixation and section preparation of placental tissues.

Placenta was fixed in 2% (v/v) formaldehyde, 2% (v/v) glutaraldehyde in 0.1 M cacodylate buffer, pH 7.2, with 5 mM calcium chloride for 2-3 h, followed by post-fixation with 1% (w/v) osmium tetroxide in 0.1 M cacodylate buffer, pH 7.2, with 5 mM calcium chloride.

Specimens were dehydrated in a graded series of ethanol concentrations and embedded in Spurr's low viscosity epoxy resin.

Semithin (1 μm) survey sections were obtained using an Ultracut ultramicrotome (Leica, Vienna, Austria) and stained with 1% (w/v) toluidine blue in 1% (w/v) di-sodium tetraborate. For each block a correctly orientated area for sectioning was selected. Ultrathin sections with silver-gold interference colour (60-90 nm thick) were cut and mounted on formvar-coated 200 mesh square nickel grids. Sections were stained with 4% (w/v) uranyl acetate, followed by Reynolds lead citrate, and examined with a Hitachi H-7000 transmission electron microscope, operating at an accelerating voltage of 75 kV.

3.3.2.3 Processing tissue for immunohistochemistry.

Tissue was fixed in freshly prepared 4% (w/v) formaldehyde, 0.5% (v/v) glutaraldehyde in 0.1 M PBS, pH 7.4 (Tokuyasu 1984) for 1 h, followed by a 5 min wash in 0.1 M PBS, pH 7.4 to remove excess aldehyde. Specimens were dehydrated in a graded series of aqueous ethanol solutions before being embedded in low acid glycol methacrylate (LA-GMA) resin (Stirling *et al.* 1990).

3.3.2.4 Immunogold labelling.

Ultrathin sections 60-90 nm thick with silver-gold interface were cut from LA-GMA resin-embedded tissue. Sections were mounted on formvar-coated 200 mesh square nickel grids and labelled by the method of Stirling and Graff (1995). Grids were pre-incubated with 0.01 M PBS, pH 7.4 containing 1% (w/v) immunoglobulin-free BSA. Grids were incubated with anti-SAT-1 polyclonal antibody diluted one hundred times in PBS containing 1% (w/v) BSA and 1% (v/v) polyoxyethylenesorbitan monolaurate (Tween-20) overnight at 4°C. Grids

were washed with PBS (3 x 5 min), then with PBS containing 1% (w/v) BSA for 5 min. The grids were then incubated with Protein A-gold conjugate (10 nm) diluted in PBS containing 1% (w/v) BSA and 1% (v/v) Tween-20 and 0.1% (v/v) cold water fish gelatine for 1 h at 20°C. Grids were then washed with three changes of deionised water for 5 min each.

Negative controls were performed on subsequent serial sections by substituting the primary antibody with pre-immune serum at dilutions that matched the anti-SAT-1 primary antibody concentrations. All controls were performed under the same conditions. Sections were stained with 4% (w/v) aqueous uranyl acetate followed by Reynolds lead citrate, and examined with a Hitachi H-7000 transmission electron microscope (Hitachi, Tokyo, Japan) operating at an accelerating voltage of 75 kV.

3.3.3 Sulphate transport.

To measure sulphate transport in enriched lysosomal fractions the free external sulphate must be removed at nominated time points. Transport of sulphate can be either into the organelle (influx) or out of the organelle (efflux). A number of methods were employed to quickly separate organelles containing labelled sulphate from the external sulphate containing medium. The amount of sulphate within the organelles was then determined by liquid scintillation counting.

Organelles were concentrated if necessary, by microfuging (10,000 ***g***) at room temperature for 5 min and a calculated amount of supernatant discarded. The amount of organelles used was based on a BCA protein determination (*Section 2.2.3.1*), and typically 100 µg of organelles were used per time point.

3.3.3.1 Sulphate influx into cytoplasmic organelles by a sulphate concentration gradient.

Enough lysosomal or mitochondrial sample for a number of time points was incubated in 0.25 M sucrose, 100 μM $Na_2{}^{35}SO_4$, and 20 mM HEPES, pH 7, at room temperature for 1 h. At each time point a 50 μL (100 μg protein) aliquot was taken and the sulphate transport was stopped (*Section 3.3.3.5*), the organelles separated by filtration from the external sulphate, and quantitated by scintillation counting. The separation of organelles was achieved by vacuum filtering for isolated organelles, or column chromatography for reconstituted vesicles (*Section 3.3.3.5*). Non-specific binding of [^{35}S]-sulphate was determined after 1 μL of Triton X-100 was added to the mixture to disrupt the organelles, remaining in the influx solution, and a 50 μL aliquot assayed for sulphate influx as were the other aliquots.

3.3.3.2 Sulphate influx into and efflux from cytoplasmic organelles, by counter transport and *trans*-stimulation with sulphate.

Cytoplasmic organelles were incubated at room temperature with 1 M sodium sulphate for 30 min allowing the sulphate to equilibrate. The samples were diluted ten fold into a solution containing 100 μM $Na_2{}^{35}SO_4$, 0.25 M sucrose and 20 mM HEPES, pH 7. Aliquots of 50 μL were taken at various time points and the amounts of sulphate transported determined by filtration followed by scintillation counting. This protocol was also used to measure sulphate efflux, where the organelles were first equilibrated with labelled sulphate. Efflux was initiated by diluting the organelles (20 fold) in label free buffer (0.25 M sucrose, 20 mM HEPES, pH 7) containing 1 mM of either sulphate or a counter ion.

3.3.3.3 Sulphate influx into cytoplasmic organelles by co-transport or *cis*-stimulation with a pH gradient.

Influx with a pH gradient was essentially the same as that described in *Section 3.3.3.1*. The sample was buffered at pH 7 and the radio-labelled sulphate solution introduced buffered by titrated amounts of MES, pH 5, and MES free acid to a final concentration of 20 mM MES, pH 5.

3.3.3.4 Sulphate influx into proteoliposomes with a pH gradient.

Proteoliposomes were incubated in 30 µL of 100 µM $Na_2{}^{35}SO_4$, 10 µM valinomycin, 30 mM MES, pH 5.5. Sulphate transport was stopped by the addition of 70 µL ice-cold buffer (100 mM KCl, 20 HEPES, pH 7.4). This mixture was then separated into free sulphate and vesicle by either size exclusion (*Section 3.3.3.5.2*) or anion exchange (*Section 3.3.3.5.3*), and the sulphate retained with the vesicle quantitated by liquid scintillation counting.

3.3.3.5 Stopping sulphate transport.

Sulphate transport was arrested by a number of methods. The method used to stop the transport of sulphate depended on the organelle or vesicles being assayed (discussed in *Sections 3.4.4 and 3.4.6*).

3.3.3.5.1 Amicon vacuum manifold.

An Amicon vacuum manifold apparatus was kindly lent by Prof. Greg Barritt, Department of Biochemistry, School of Medicine, Flinders Medical Centre, Bedford Park, South Australia.

Sulphate transport was stopped at the required time points by dilution of the reaction volume 50 times into 1 mL of ice-cold isotonic buffer. The diluted samples were poured onto glass fibre or nitrocellulose filters, each fitted into a vacuum manifold where 2 x 20 mL of buffer was added to wash through any free sulphate. The filters were removed, air dried and subject

to scintillation counting in 10 mL of Optiphase 'HiSafe' 3 liquid scintillation cocktail fluid with a Wallac 1409 liquid scintillation counter.

3.3.3.5.2 Size exclusion

Sulphate transport in vesicles or organelles stopped by the addition of an ice-cold buffer were applied to a small Sephadex G50 column. This mixture was filtered through a 4mm x 5 cm column of Sephadex G50 (prepared in a glass wool plugged Pasteur pipette). The sample was washed through the column by the addition of 0.9 mL of ice-cold buffer. The sulphate in the proteoliposomes was excluded from the column and passed through in the void volume. The sulphate in the proteoliposome eluate was determined by liquid scintillation counting after the adding of 4 mL of HiSafe™.

3.3.3.5.3 Anion exchange.

Sulphate transport in vesicles or organelles stopped by the addition of an ice cold-buffer were applied to 1 mL Dowex AG1-X4 (mesh 100-200) columns and washed with 1.25 mL of ice cold buffer. The columns were prepared in 1 mL syringes, using Dowex in the ionic formate form and pre-treated with 2.5 mg of BSA in 0.8 mL.

3.3.4 Proteoliposome formation.

Membranes were concentrated at 10,000 ***g*** for 5 min, or diluted with 20mM HEPES, pH7.4, to obtain 1.3 mg protein in 150 µl. An equal volume of extraction solution (6% (v/v) Triton-X100, 200 mM KCl, 2 mM DTT and 20 mM HEPES, pH 7.4) was added and the mixture placed on ice for 10 min. The mixture was airfuged™ for 20 min at 150,000 ***g*** (30 psi) at 4°C.

Of the extracted membrane protein, 200 μL was added to a reconstitution solution (60 μL 10% Triton-X100 (peroxide free), 100 μL (10 mg) sonicated L-α-phosphatidylcholine (type XVIE from fresh egg yolk), and 320 μL KCl buffer (119 mM KCl, 24 mM HEPES, pH 7.4). This mixture was passed fifteen times over a 0.5 x 3.6 cm column of Amberlite XAD-2 (Fluka) or Biobeads SM-2 (BioRad) at 1 mL/min (Mancini *et al.* 1992).

The Amberlite XAD-2 and Biobeads SM-2 were initially washed in five volumes of 100% (v/v) methanol, washed with water and equilibrated in 100 mM KCl, and 20 mM HEPES, pH 7.4. The phosphatidylcholine (100 mg) was initially dissolved in 1 mL of 20 mM HEPES, pH 7.4, sonicated on ice with an Ultrasonics (W225) for 1 h (30-50% duty, output 3) and 200 μL aliquots were stored under nitrogen at -20°C.

3.4 Results and Discussion.

3.4.1 Isolation of lysosomes from human placenta.

Placentae were obtained either from full-term normal vaginal deliveries or near full-term caesarean deliveries (*Section 2.2.1*). Lysosomes were isolated by tissue and cell disruption, differential centrifugation and density gradient centrifugation on Percoll® self-forming density gradients (*Section 2.2.2*). Percoll® density gradients were used to sediment particles to their isopycnic position. The densities of subcellular particles in Percoll® have been reported in many studies. The apparent buoyant densities vary depending upon the source of cytoplasmic organelles, the gradient media and the effects of osmolarity. At physiological osmolarity (0.25 M sucrose) subcellular particles separate in Percoll® gradients from the buoyant to the dense in the following order, plasma membrane, Golgi, ER, peroxisomes, mitochondria, endosomes and finally lysosomes (Batt and Mann 1983; Forsbeck *et al.* 1986; Kornilova *et al.* 1987; Meikle *et al.* 1995; Miskimins and Shimizu 1982; Nauseef and Clark 1986; Normann and Flatmark 1982; Norseth *et al.* 1982).

In brief, the final purification procedure was as follows. A placenta was homogenised and fractionated by differential centrifugation, producing a granular fraction containing the more dense cytoplasmic organelles. These were subject to fractionation on a Percoll® density gradient (*Section 2.2.2*). The lower quarter (10 mL) of each tube contained nearly all of the lysosomal activity but also half of the mitochondrial activity, and was subject to a second round of centrifugation. The bottom fractions (second gradient) containing most of the lysosomal activity with minimal mitochondrial contamination were pooled, and used for further experiments. For preparation of mitochondria, the third quarter of the first gradient was collected, re-centrifuged, and mitochondria isolated from the middle region of this

secondary gradient, which was relatively free of lysosomal contamination. This procedure was validated by enzyme marker assays.

Enzyme marker assays were performed to determine cytoplasmic organelle distribution (*Section 2.2.3*). The granular fraction resulted in enrichment of lysosomes (β-hexosaminidase, GNAT and acid phosphatase), mitochondria (cytochrome-*C* oxidase) and plasma membrane (5' nucleotidase) (*Table 3.1*) with only minor contamination from ER (glucose-6-phosphatase), Golgi (galactosyltransferase) and peroxisomes (catalase).

Table 3.1 Enzyme marker analysis of placental cellular fractions.

Specific activities are expressed as nmol.min^{-1}.mg^{-1}*, pmol.min^{-1}.mg^{-1}† or μmol.min^{-1}.mg^{-1}‡. The data shown here from this laboratory has been published (Meikle *et al.* 1995).

Marker enzymes	Cell homogenate	Cell contents	Cell content supernatant	Granular fraction	Lysosomes
β-Hexosaminidase*	36	15	11	85	1164
GNAT†	2	1	0.7	6	53
Acid phosphatase*	49	49	36	210	672
Cytochrome-C oxidase*	17	13	3	149	11
5' nucleotidase*	57	111	101	386	21
Glucose-6-phosphatase*	9	16	19	22	11
Catalase‡	254	207	203	60	9
Galactosyltransferase†	96	128	89	176	5

When the granular fraction was separated on the first Percoll® gradient most of the lysosomal activity was found in the lower or densest fractions, peaking in fraction ten. Marker enzymes for ER, plasma membrane, Golgi and peroxisomes migrated to the top region of the gradient. Mitochondria presented a broader profile extending into the lower region of the gradient and represented the only significant contamination in the lysosomal fractions (*Table 3.2*).

Table 3.2 Enzyme marker analysis of primary Percoll® density gradient.

The data expressed as a percent of total activity (mol.min^{-1}.mL^{-1}) from this laboratory has been published (Meikle *et al.* 1995).

Fraction	1	2	3	4	5	6	7	8	9	10
β-Hexosaminidase	6	4	4	4	4	4	5	8	19	42
GNAT	20	7	3	3	4	7	3	5	15	33
Acid phosphatase	25	20	11	4	4	4	5	6	11	10
Cytochrome-*C* oxidase	18	24	12	12	9	8	6	6	3	2
5' nucleotidase	46	35	8	3	2	1	2	1	1	1
Glucose-6-phosphatase	43	30	8	3	3	2	2	2	3	4
Catalase	40	31	16	6	2	1	1	1	1	1
Galactosyltransferase	21	18	11	14	13	10	7	3	2	1

Figure 3.1 illustrates the density gradient profile of a granular fraction in the primary Percoll® gradient. For clarity of presentation only the mitochondrial and lysosomal enzyme markers are shown. The lower 10 mL from each of the first gradient tubes which contained approximately half the mitochondrial activity, and over seventy percent of the lysosomal activity were pooled. This pool was used to generate a second Percoll® gradient. In this second gradient (*Figure 3.2A*), the mitochondria migrated into the more buoyant top half, while most of the lysosomes migrated to the denser region of the gradient, peaking in fraction nine. A heterogeneous population of lysosomes was observed with some lysosomes co-migrating with the mitochondria in the upper region of the gradient. Lysosomes isolated from fractions seven, eight and nine of the secondary gradients had minimal mitochondrial contamination and were used for subsequent lysosomal transport studies. Enrichment of mitochondria was achieved by pooling the third quarter (fractions 6-7.5) from each tube of the

first gradient and forming another secondary gradient (*Figure 3.2B*). Fractions in the middle region of this gradient rich in mitochondria with minimal lysosomal contamination were used in subsequent studies on mitochondria.

The Percoll® gradients depicted in *Figure 3.1* and *Figure 3.2* are representative of results from over twenty different placental preparations, although variations in the density of both mitochondria and lysosomes were observed.

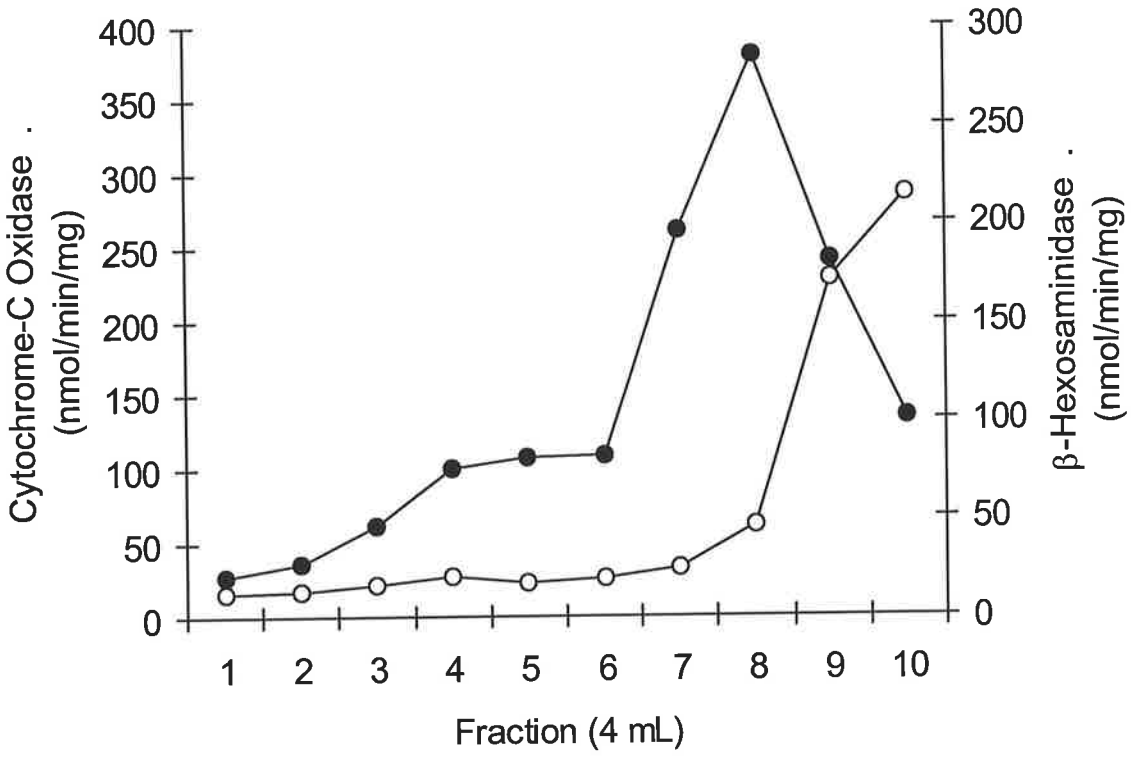

Figure 3.1 Percoll® density gradient centrifugation (primary) of the granular fraction from human placenta.

The granular fraction from a human placenta (prepared as described *Section 2.2.2*) was resuspended in 25% Percoll®, 0.25 M sucrose, 1 mM EDTA, pH 7.0 (320 mL). The sample was centrifuged in a Beckman JA-20 rotor (8 x 40 mL tubes) at 31000 ***g*** for 1 h at 4°C. Fractions were assayed for cytochrome-*C* oxidase (●) and β-hexosaminidase (○). This is a representative result from over twenty different placental preparations.

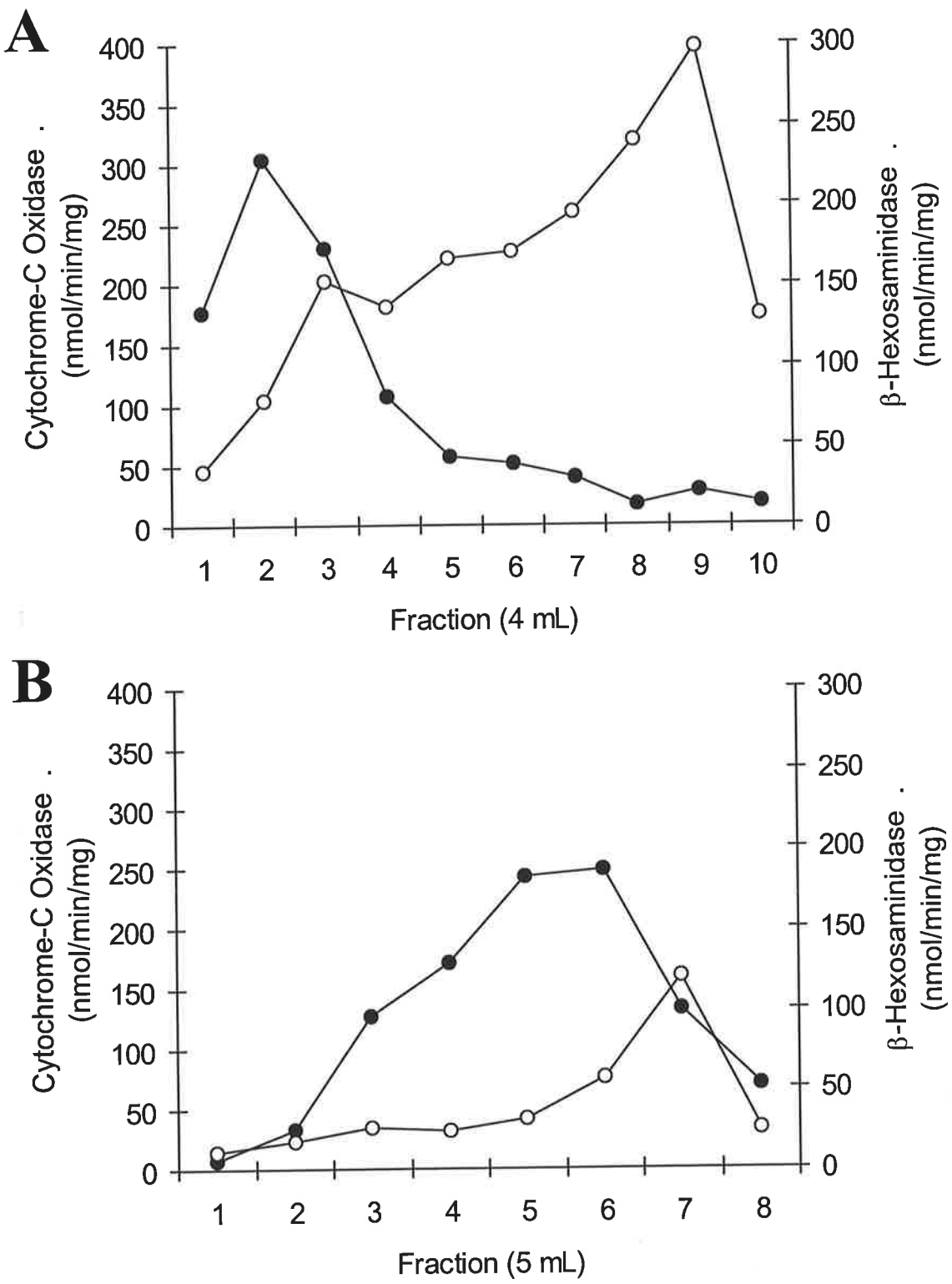

Figure 3.2 Percoll® density gradient centrifugation (secondary) of the granular fraction from human placenta.

The primary Percoll® gradient shown in *Figure 3.1* was fractionated and the most dense 10 mL from each of eight tubes (panel A), and the second most dense 10 mL (panel B), were pooled and centrifuged in a Beckman JA-20 rotor (2 x 40 mL tubes) at 31000 ***g*** for 1 h at 4°C to form secondary Percoll® gradients. Fractions were assayed for cytochrome-*C* oxidase (●) and β-hexosaminidase (○). These were representative results from over twenty different placental preparations.

3.4.1.1 Density of placental cytoplasmic organelles separated in a Percoll® density gradient.

Density marker beads were separated at the same time, on equivalent Percoll© density gradients, as cytoplasmic organelles from a placental granular fraction. The positions of the beads were used to construct a map of the density gradient (*Figure 3.3B*) from which the densities of cytoplasmic organelle fractions were determined. Lysosomal enrichment was measured by β-hexosaminidase activity, while monoamine oxidase activity reflected that of mitochondrial enrichment. The mitochondrial density fell between 1.055 and 1.07 $g.mL^{-1}$, and lysosomes predominantly between 1.07 and 1.133 $g.mL^{-1}$ (*Figure 3.3A*). Monoamine oxidase is an outer mitochondrial membrane while cytochrome-*C* oxidase is an inner mitochondrial membrane enzyme. The comparison of these two enzyme markers (data not shown) indicated the same level of mitochondrial enrichment. If the scanning spectrophotometer (Perkin Elmer, LS50B) required for cytochrome-*C* oxidase was in use, monoamine oxidase was assayed using a fluorimeter (Perkin-Elmer LS-5 luminescence spectrometer).

Mitochondria are the closest organelle in density to lysosomes, which are found to be the densest organelle when isolated by the method described (*Section 2.2.2*). The assays of the Percoll® density gradients for the lysosomal and mitochondrial marker enzymes therefore illustrate that the lysosomal fractions are free of other contaminating organelles.

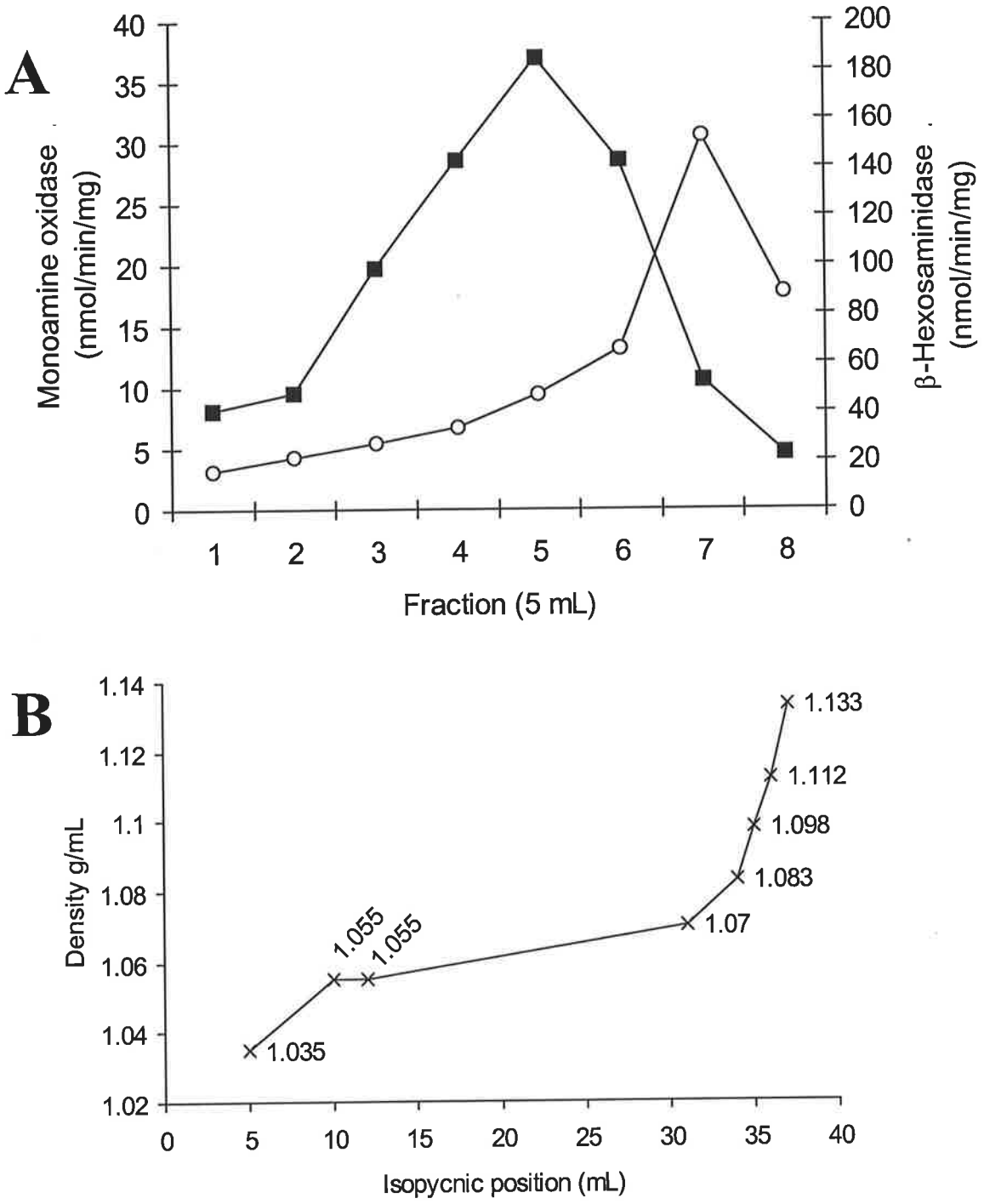

Figure 3.3 The density profile of a primary Percoll® gradient as measured with density marker beads.

A granular fraction isolated from human placenta (panel A) and density marker beads (Pharmacia) (panel B) were suspended in 25% Percoll®, 0.25 M sucrose, 1 mM EDTA, pH 7.0 (40 mL). The samples were centrifuged at the same time in a Beckman JA-20 rotor (8 x 40 mL tubes) at 31000 ***g*** for 1 h at 4°C. The granular fractions were assayed for monoamine oxidase (■) and β-hexosaminidase (○). The positions of the density marker beads (×) were determined by measuring their distance from the top of the Percoll® gradient.

3.4.2 Determination of lysosomal integrity by H^+-ATPase activity.

The measurement of ion transport across the lysosomal membrane relies on the transporter residing in an intact organelle membrane. The lumen of intact lysosomes (lysosol) can be acidified in the presence of ATP. Lysosomal integrity therefore, can be verified by acidification before assaying the sulphate transport. Proton transport or H^+-ATPase activity (*Section 1.3.3.1*) in lysosomes has been identified and characterised in rat liver lysosomes (Ohkuma *et al.* 1982). This proton pump was later purified and identified as an anion-sensitive v-type H^+-ATPase (Arai *et al.* 1993). The v-type denotes it as a vacuolar pump. The H^+-ATPase transporters of other cellular membranes also needed to be considered when using H^+-ATPase activity as an indicator of lysosomal integrity.

Acridine orange has been used in biology to indicate pH and measure transmembrane proton fluxes in various vesicles. The main advantage of optical probes such as acridine orange is that transport activity can be monitored continuously as a function of time (Palmgren 1991). Acridine orange, a fluorescent weak base is mostly protonated at physiological pH. The neutral amine (free base) form of acridine orange is the only membrane-permeable species. When an intravesicular pH is more acidic than the external medium (caused by an outward directed proton gradient), acridine orange re-equilibrates, accumulating in the acidic intravesicular compartment. At sufficiently high concentrations the fluorescence of acridine orange is self-quenched. Acridine orange consists only of monomers when dilute, and forms aggregation dimers, trimers and oligomers at higher concentrations which are responsible for the self-quenching.

Concentration and self-quenching of acridine orange fluorescence within the vesicles decreases acridine orange fluorescence measured in the external medium. Conversely, as the intravesicular proton gradient dissipates, internal acridine orange returns to the extravesicular space resulting in a time-dependent increase in fluorescence measured in the external medium (Holmberg *et al.* 1989; Ramaswamy *et al.* 1989). The release of a proton gradient (alkalisation) on addition of membrane-permeablising agents (proton-ionophores) clearly verifies a proton gradient was generated. If only the conditions being tested are altered, the comparative rates of proton transport can be measured using this technique.

Lysosomes were gently isolated under osmotic conditions (*Section 2.2.2*) to minimise rupturing. They were washed free of Percoll® *(Section 3.3.1.1)* and assayed for H^+-ATPase activity to determine the integrity of their membranes *(Section 3.3.1.2)*. The H^+-ATPase activity was measured on the same day as the subcellular fractionation due to its rapid inactivation, also reported by others (Andersson *et al.* 1989). Acidification by proton pumping could not be demonstrated in lysosomes isolated from four different placentae collected after normal vaginal delivery. Acidification and alkalisation were demonstrated however, in five lysosomal preparations from placentae delivered by caesarean section. *Figure 3.4* depicts a representative trace of acidification and alkalisation of a lysosomal sample. In lysosomal preparations that could be not acidified, neither could transport of sulphate be demonstrated *(Section 3.4.4)*. The addition of ATP causes a large increase in fluorescence before its biological effect of acidification, which quenches fluorescence. The decrease in relative fluorescence following the addition of ATP indicates the rate of acidification. The protonophore CCCP has a small quenching effect before it dissipates the proton gradient causing an increased in fluorescence.

After demonstrating that the protocol used to isolate lysosomes delivered them intact, it was assumed the more robust, double-membraned mitochondria were also unbroken. Mitochondrial outward proton pumping is the reverse of that in lysosomes, therefore any proton pumping activity would not be seen in an acidification assay.

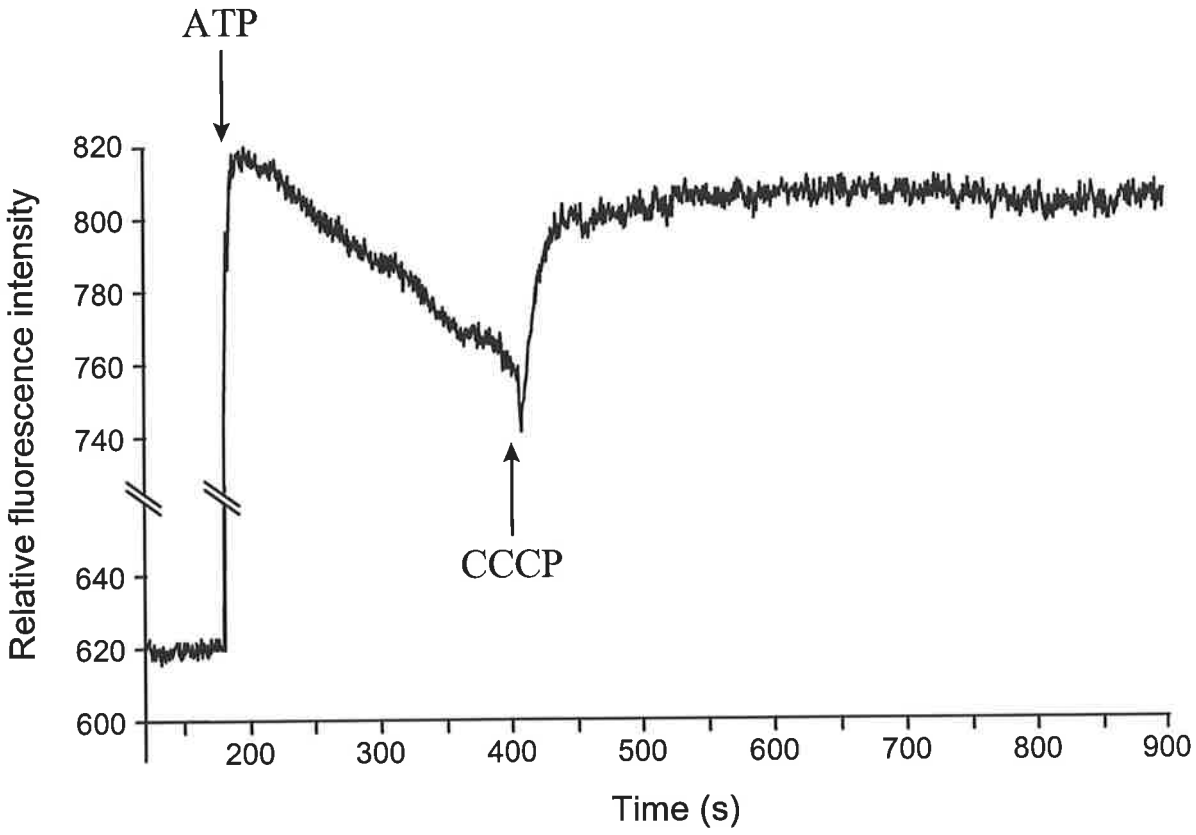

Figure 3.4 Lysosomal acidification measured with the fluorescent dye acridine orange.

Intact washed lysosomes (200 μg) were stirred in 2 mL of acidification medium (0.25 M sucrose, 1 μM valinomycin, 10 μM acridine orange, 2 mM $MgCl_2$, 100 mM KCl, 12 mM DMG, pH 7.0). ATP-dependent acidification was initiated at 190 s by 10 μM ATP. At 400 s the proton gradient was dissipated by 10 μM of the protonophore CCCP. The time course of acridine orange fluorescence at 540 nM was monitored at 0.1 s intervals with excitation at 492 nM with 5 nM slits on both monochromators.

3.4.2.1 Assay conditions that effect proton pumping.

The addition of KCl to the acidification medium enhanced the pumping of protons into the lysosomes (*Figure 3.5*). Trace A, assayed in the presence of 100 mM KCl, shows strong acidification with a slope of 0.290 (fluorescence intensity was relative with time in seconds), and almost complete dissipation of the pH gradient with the addition of the protonophore CCCP. Trace B assayed in the absence of KCl shows a lower rate of acidification with a slope of 0.194 and almost no dissipation of the gradient with the addition of the protonophore CCCP. This suggests genuine acidification is greater in the presence of KCl. Other studies (Andersson *et al.* 1989) have also found the omission of KCl greatly reduces lysosomal H^+-ATPase activity. The addition of the washed lysosomes to the acidification medium caused an initial decrease in acridine orange fluorescence. This decrease in fluorescence is most likely due to increased turbidity in the acidification medium.

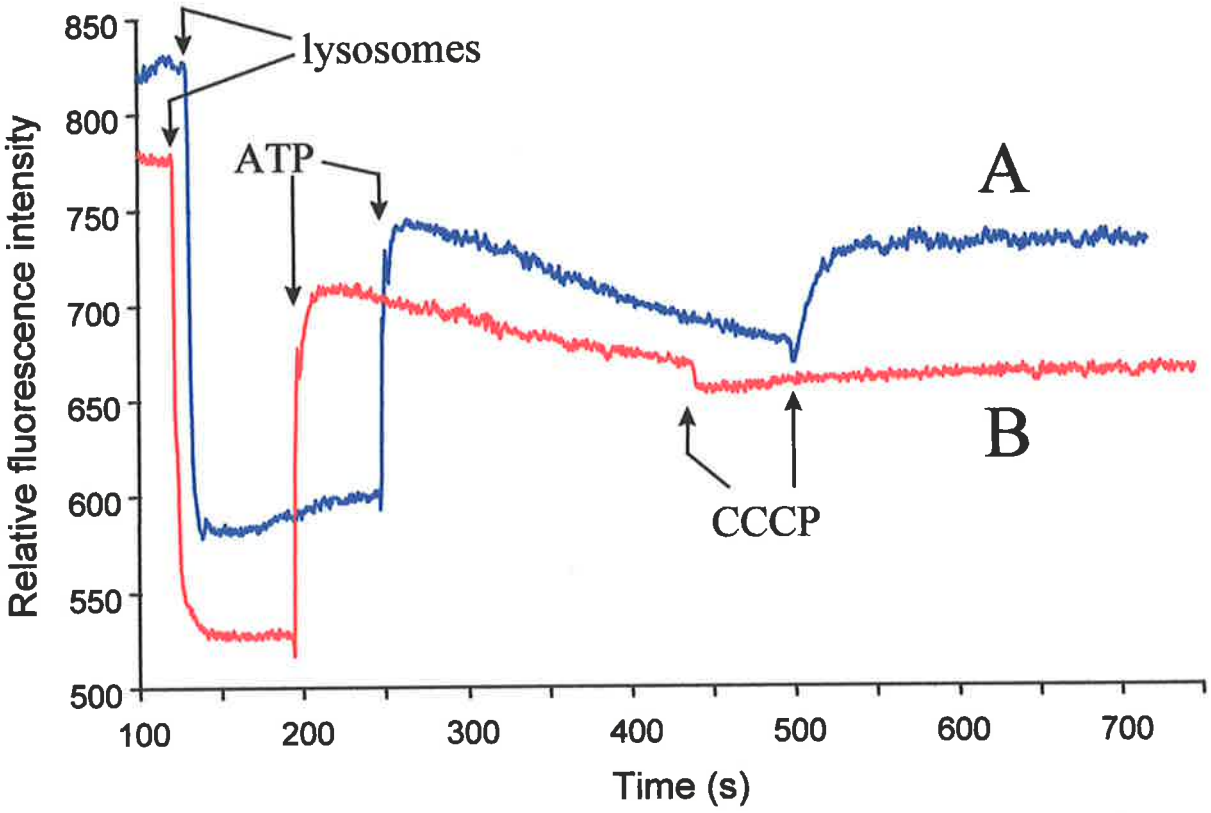

Figure 3.5 Effect of chloride on the acidification of lysosomes.

The acidification mediums (0.25 M sucrose, 1 µM valinomycin, 10 µM acridine orange, 2 mM $MgCl_2$, 100 mM KCl, 12 mM DMG, pH 7.0) (A), and without KCl (B), were put in the cuvettes at t=0. Intact washed lysosomes (200 µg) were added to stirred acidification mediums (2 mL) with KCl (A) and without KCl (B) at 131 and 120 s respectively. Acidification of the two conditions was initiated with 10 µM ATP at 248 and 194 s, followed by alkalisation with 10 µM of protonophore CCCP added at 500 and 438 s respectively. The time course of acridine orange fluorescence at 540 nM was monitored at 0.1 s intervals with an excitation set at 492 nM with 5 nM slits on both monochromators.

The buffer gradient across the lysosomal membrane was found to be critical for efficient acidification (*Figure 3.6*). The effect of buffer gradient was demonstrated by varying the external concentration when the internal buffer concentration was kept at 12 mM DMG (*Section 3.3.1.1*). Effective acidification occurred only when the internal and external buffer concentrations were equal. Changing the concentration of DMG in the acidification medium to either 6 or 20 mM prevented acidification by the lysosomal H^+-ATPase.

The effect of freezing lysosomal preparations on their ability to acidify was investigated to determine if samples could be stored before use. Samples frozen, thawed and then assayed for H^+-ATPase activity showed a reduction in acidification. Subsequent freezing and thawing further reduced measurable acidification. A reduction in sulphate transport activity after cycles of freezing and thawing was also found *(Section 3.4.4.2)*.

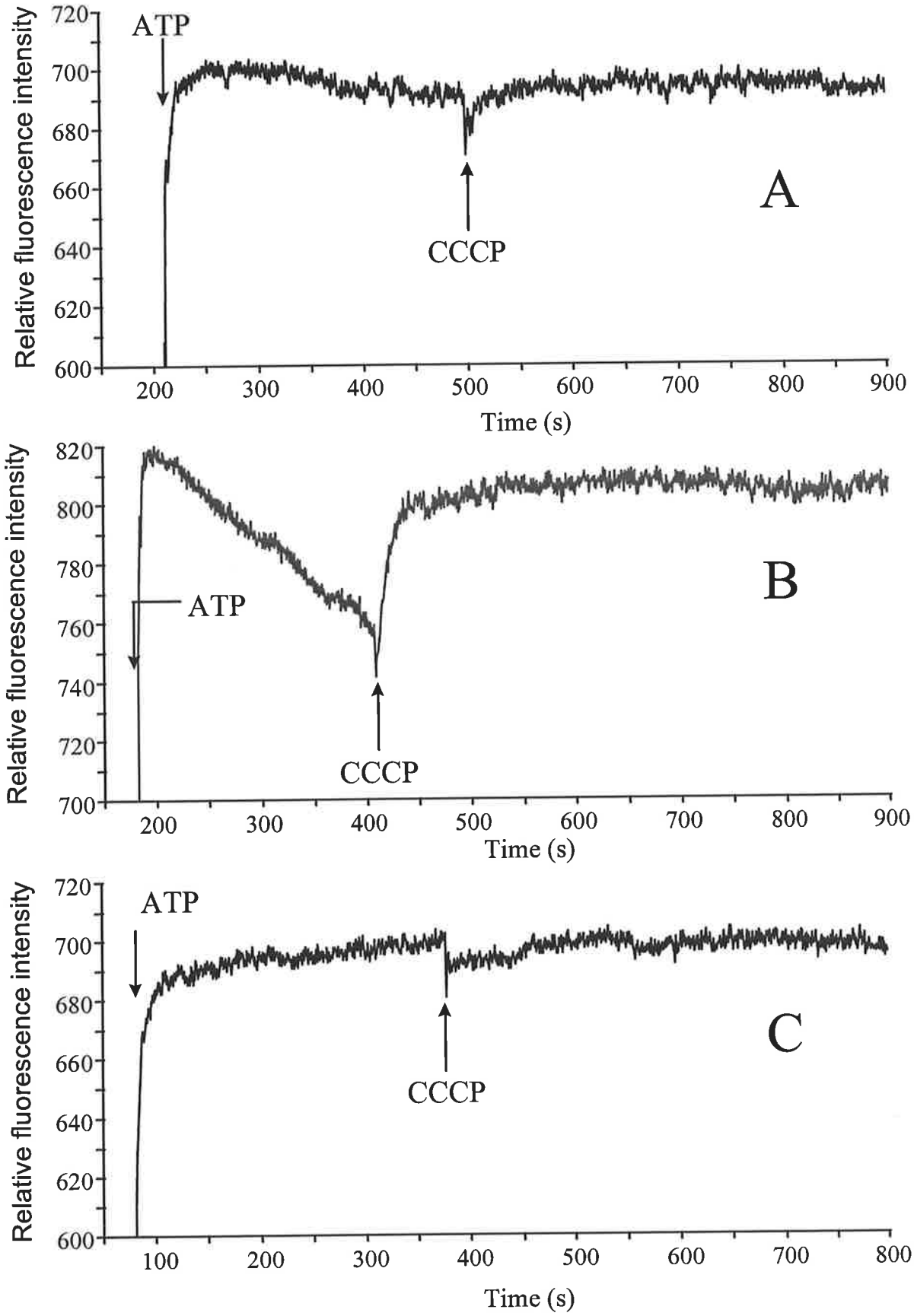

Figure 3.6 Effect of a buffer gradient on lysosomal acidification.

Lysosomal samples buffered with 12 mM DMG, pH 7 were mixed in acidification medium as described in *Figure 3.4* with varying concentrations of DMG. The various concentrations of DMG in the acidification media were 6, 12 and 20 mM shown in panels A, B and C respectively.

3.4.2.2 Determination of acidification rates for different cytoplasmic organelle fractions separated in a Percoll® gradient.

To determine whether or not contaminating organelles in lysosomal preparations effected acidification rates, and hence the estimation of lysosomal integrity, the rates of acidification for different Percoll® gradient fractions were determined and correlated with enzyme markers for lysosomes and mitochondria. The fractions were assayed for GNAT and cytochrome C-oxidase activities and combined into four pools A, B, C and D *(Figure 3.7)*. Pool A had the greatest mitochondrial cytochrome-*C* oxidase activity, and pool C had the greatest lysosomal GNAT activity. These pooled fractions were assayed for H^+-ATPase driven acidification, by acridine orange fluorescence (*Figure 3.8*). Comparison of *Figure 3.7* with *Figure 3.8* demonstrates that acidification rates show a strong correlation with the lysosomal enzyme marker GNAT, while no effect from mitochondria (the nearest organelle in density) could be seen on the rate of acidification. The rates at which different fractions could acidify were proportional to, or reflected the amount of lysosomal enrichment. This supports that the H^+-ATPase activity measured was lysosomal.

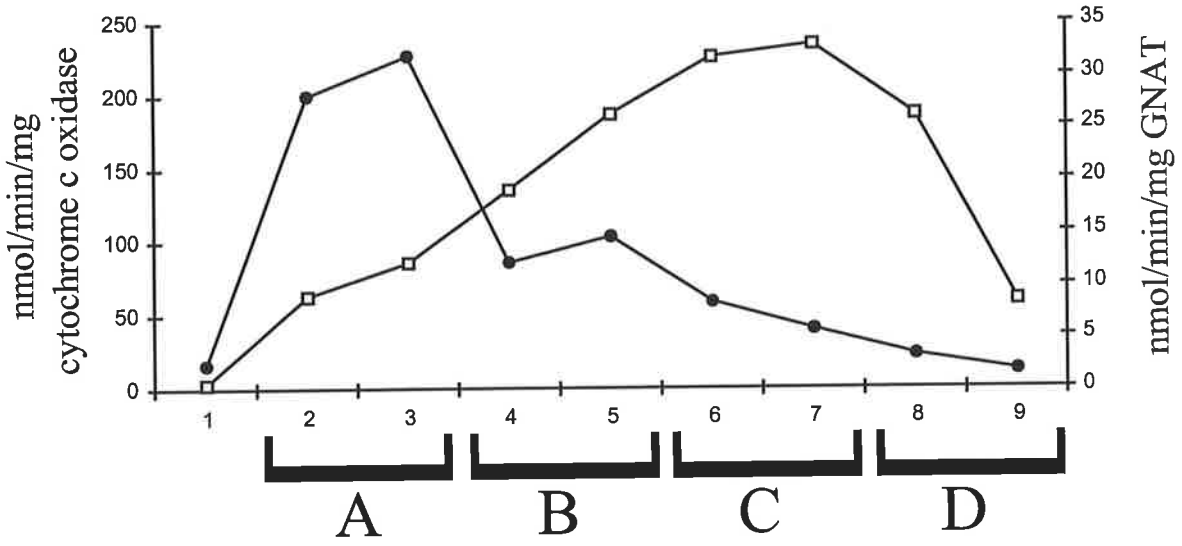

Figure 3.7 Lysosomal and mitochondrial enzyme activities of fractions pooled and assayed for acidification by H^+-ATPase.

A placental granular fraction was separated on two consecutive Percoll® gradients. The lysosomal-rich fractions from the primary gradient (*Figure 3.1*) were separated on a second gradient and assayed for cytochrome-*C* oxidase (●) and GNAT (□). Fractions 2 and 3, 4 and 5, 6 and 7, 8 and 9 were pooled, labelled A, B, C and D, and assayed for acidification and alkalisation rates (*Figure 3.8*).

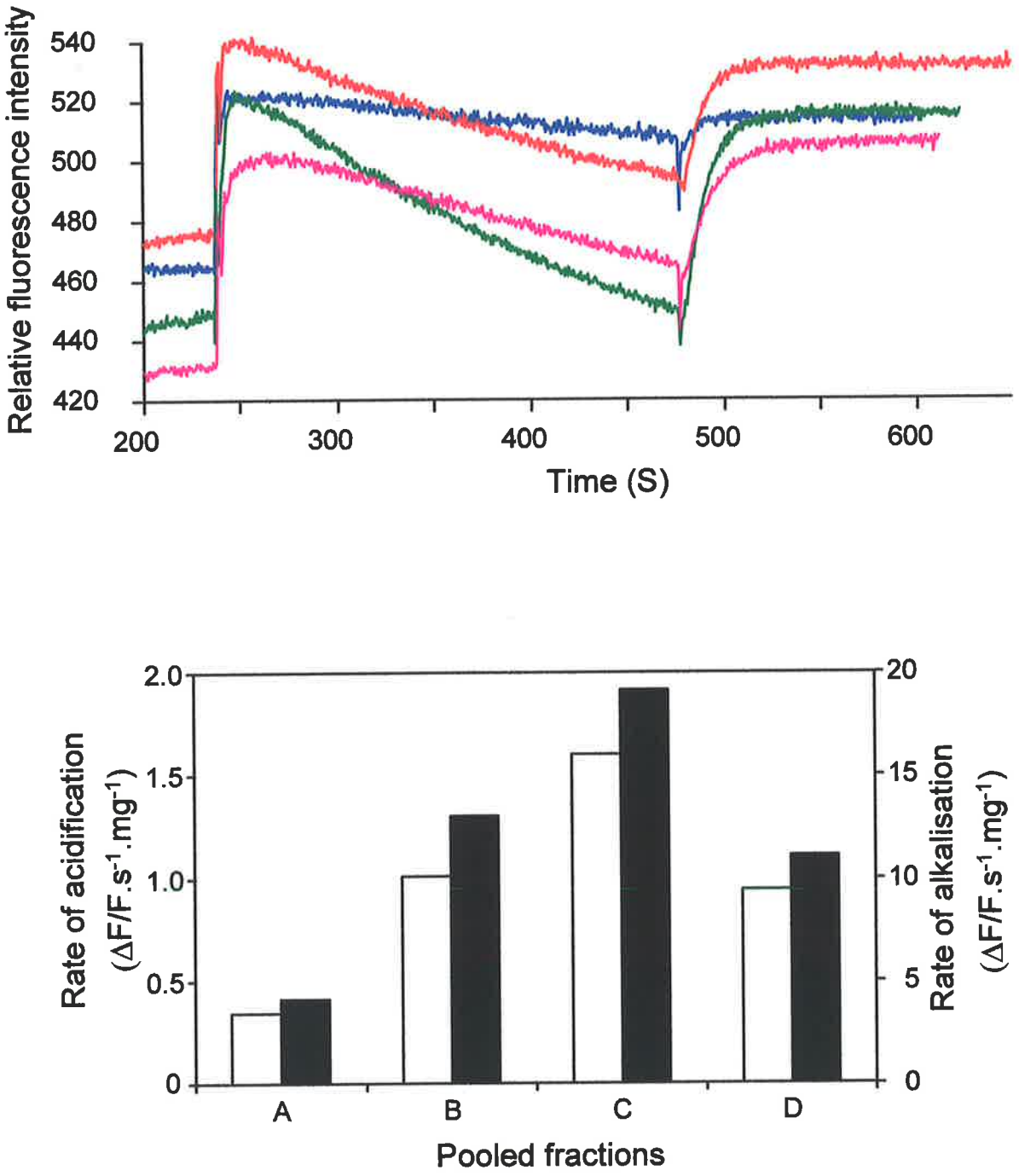

Figure 3.8 H^+-ATPase activity of lysosomal and non-lysosomal cytoplasmic organelles.

Granular fractions isolated down a Percoll® gradient (*Figure 3.7*) were assayed for the ability of cytoplasmic organelles to be acidified as described in *Figure 3.4*. Traces of the time course of acridine orange fluorescence of pooled fractions A (blue trace), B (red), C (green) and D (pink) are overlayed (panel A). Acidification initiated with 10 μM ATP was at 238 s and 10 μM CCCP was added at 475 s. The rates of acidification (open columns) and alkalisation (filled columns) were calculated from 300 to 450 s and 480 to 490 s respectively (panel B).

3.4.3 Morphology of placenta.

Electron microscopy was performed by Richard C. A. Davey, Department of Chemical Pathology, Women's and Children's Hospital, North Adelaide, South Australia.

To investigate why acidification could not be measured in lysosomes isolated from full-term placentae, electron microscopy studies were performed. Electron micrographs showing cellular morphology of both vaginal and caesarean delivered placental chorionic villus are shown in *Figure 3.9*.

The histological section shown from a full-term placenta (panel A) was fixed one hour after delivery (of child). The contrasting section from caesarean acquired tissue (panel B) was fixed within 30 min of delivery. The full-term placental tissue displays a breakdown of microvilli and membranes along the trophoblastic margin compared with equivalent sections from a caesarean delivery. There were swollen vacuoles with the appearance of lysosomes, presumably because of apoptosis. The best cellular morphology, in terms of clear intact phospholipid membranes can be seen in the tissue from caesarean sections.

Four other placentae delivered by caesarean section with variable delays in processing, supported this trend of increased disruption of cellular structure, with increasing time between delivery and fixation (data not shown). The lysosomal H^+-ATPase may not have been able to acidify lysosomes isolated from full-term placentae due to the loss of either activity or phospholipid membrane integrity. The observed decrease in phospholipid membrane integrity supports the latter as a plausible explanation. The phospholipid membranes in full-term placentae may have been more fragile and sustained further damage during isolation of organelles, rendering them not suitable for transport assays.

Figure 3.9 Electron micrographs of placental chorionic villus from caesarean and vaginal deliveries.

Human placental tissue sections were fixed (*Section 3.3.2.2*) within 1 h of a normal vaginal delivery (panels A and B), and within 30 min of a delivery by caesarean section (panels C and D). Electron micrographs show high magnification of 13,500 with the scale bar representing 1 μm (panels A and C), and low magnification of 2,800 times with the scale bar equal to 5 μm. The 60-90 μm thick sections of chorionic villus show microvilli (M), syncytiotrophoblast (S), erythrocytes (E) and cytoplasmic vacuoles (V).

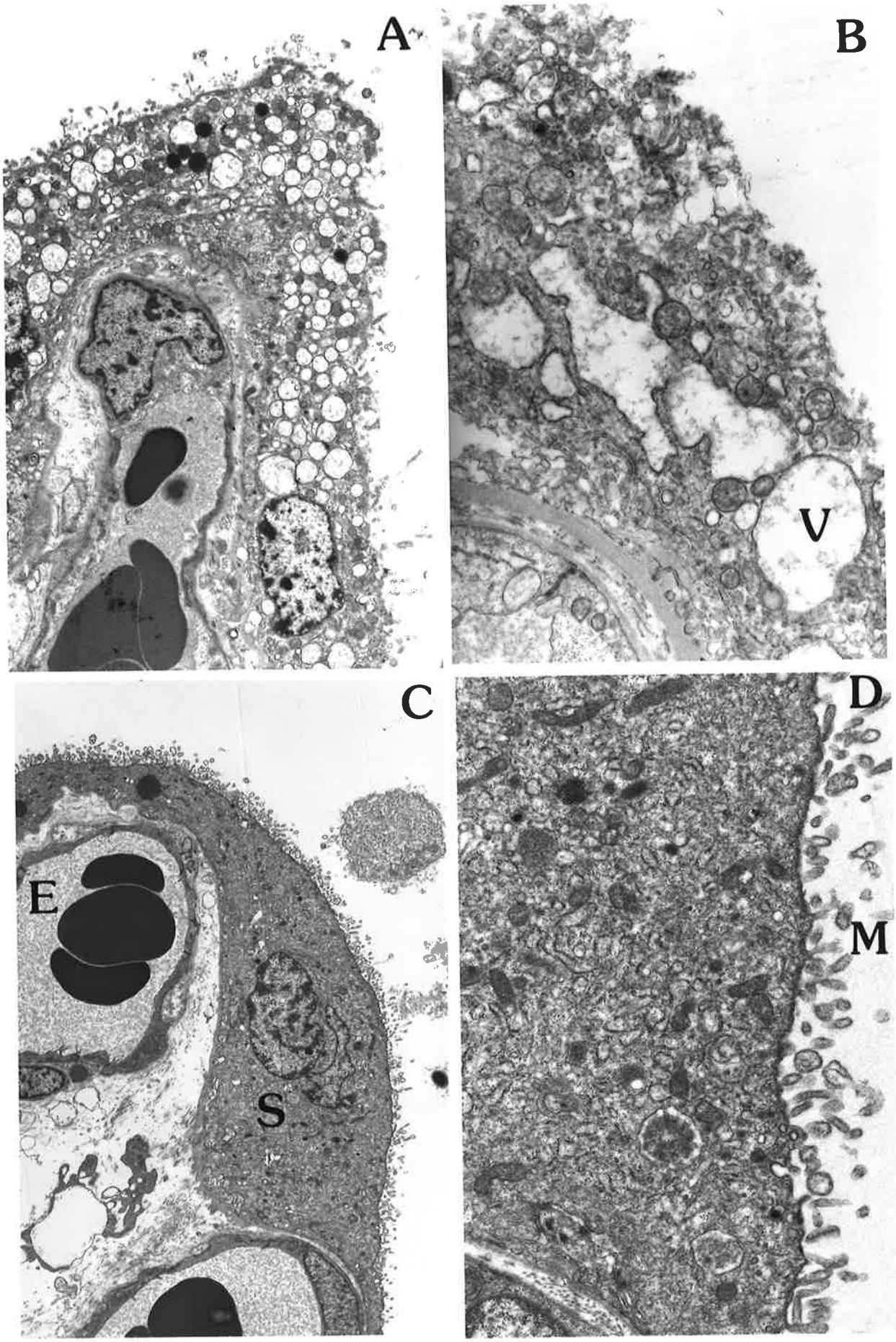
A
B
V
C
E
S
D
M
5μm
1μm

3.4.4 Sulphate transport in lysosomes and mitochondria.

After establishing a protocol that yielded intact cytoplasmic organelles, sulphate transport could be performed using enriched organelles. Preliminary studies showed mitochondria were also able to transport sulphate. With mitochondria being the largest contaminant in the lysosomal preparations, the mitochondrial sulphate transporter was characterised and compared with the lysosomal sulphate transporter.

As was found with proton transport (*Section 3.4.2*), sulphate transport could not be measured in lysosomes isolated from placenta of a normal vaginal delivery. All further sulphate transport studies with isolated lysosomes or isolated lysosomal proteins were performed using lysosomes isolated from caesarean-delivered placenta. Lysosomal membrane proteins were extracted and reconstituted into artificial phospholipid vesicles. The transport of sulphate across these proteolipid membranes was measured.

3.4.4.1 Development of sulphate transport assays.

A prerequisite for the measurement of ion transport is the separation of transported ions from untransported ions. Transport of sulphate can be either into the organelle (influx) or out of the organelle (efflux). Radio-labelled sulphate ($Na_2{}^{35}SO_4$) was used to quantify transported sulphate. Influx or uptake of sulphate into cytoplasmic organelles was performed by incubation in an isotonic uptake solution containing radio-labelled sulphate (*Section 3.3.3.1*). Efflux or egress of sulphate was performed by firstly loading the organelles with labelled sulphate, and then efflux started by incubating the organelles in a large volume free of labelled sulphate. Organelles were loaded by equilibration in a solution containing radio-labelled sulphate (*Section 3.3.3.2*). Aliquots of organelles were taken at various time

points during sulphate transport and separated from either the influx or the efflux solutions (*Section 3.3.3.5*).

A number of methods were evaluated to enable the separation of lysosomes from their incubation solutions that contained labelled sulphate. These included vacuum filtering, ion exchange and gel filtration (*Section 3.3.3.5*). Filtering through a membrane under vacuum was found to be the most appropriate for intact lysosomes and mitochondria; it was rapid, all samples could be filtered under the same conditions, and an excess of wash buffer could be used.

A number of steps were found to increase reproducibility and reduce non-specific binding of sulphate to filters with the vacuum filtering technique. These included wetting filters in wash buffer before the separation of cytoplasmic organelles from uptake or efflux solutions, and diluting the sample into ice-cold isotonic buffer before filtering. Filtered samples that were washed with buffered 0.25 M sucrose solution were more reproducible than those washed with PBS. The pore size of the filters used had a significant effect, with GF/F (0.7 μM) filters retaining more organelles than GF/A (1.6 μM) filters. Nitrocellulose filters (0.45 μM) showed no significant improvement over the GF/F filters.

3.4.4.2 Sulphate uptake into lysosomes and mitochondria.

Sulphate uptake into lysosomes was performed with a pH of 7.0 inside and out. A typical result of a sulphate uptake experiment is illustrated in *Figure 3.10*. Equilibration of radio-labelled sulphate inside and out by a simple sulphate gradient occurred within one hour, with the initial linear uptake lasting approximately ten minutes. After the last timed point, detergent was added to disrupt the organelles (*Section 3.3.3.1*), and another aliquot was

subjected to filtration. This allowed the background sulphate bound to the organelles, and not simply that which was enclosed within, to be determined. Sulphate uptake was also performed with isolated mitochondria and a typical result is illustrated in *Figure 3.11*. Mitochondrial sulphate uptake with a simple sulphate gradient (no pH gradient) also showed an initial linear rate in the first ten minutes. Mitochondrial uptake was four- to five-fold greater than that of lysosomal sulphate uptake. Samples stored at -20°C overnight prior to transport measurements showed a reduction in sulphate transport by approximately fifty percent. This reduction in transport continued with each successive freezing and thawing. When samples of either lysosomes or mitochondria were salt-washed (*Section 2.2.4.1*) to lyse the organelles for the removal of soluble and membrane-associated proteins, sulphate transport could not be measured.

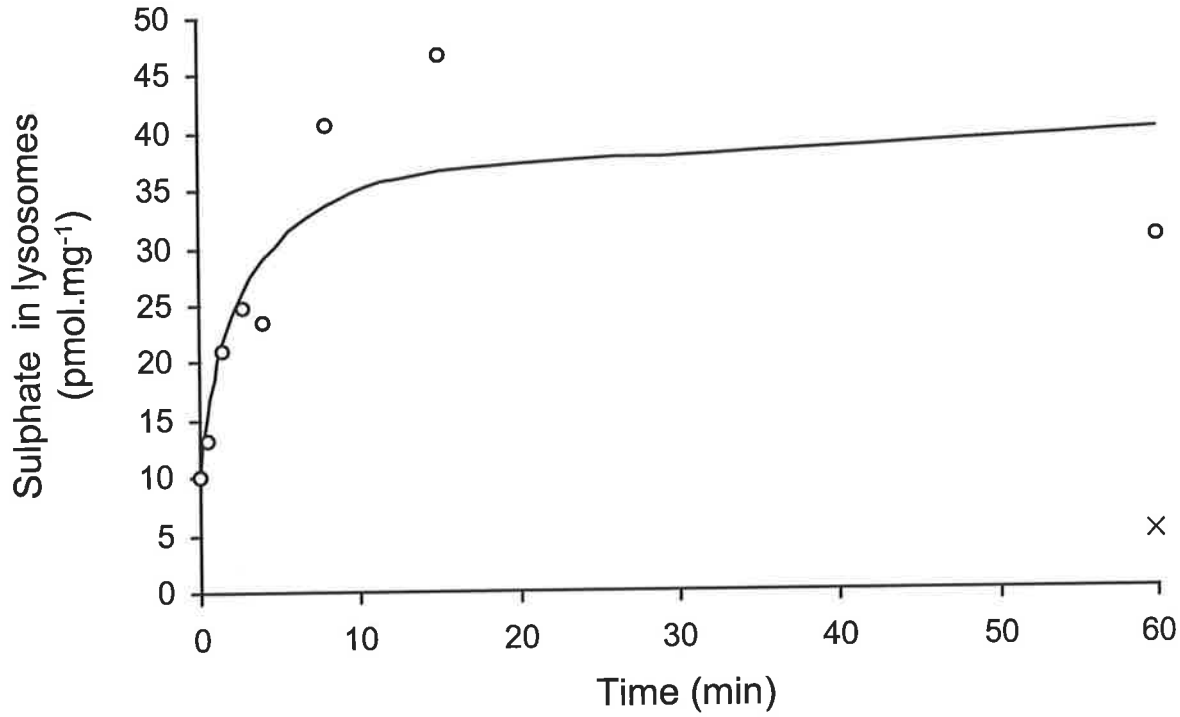

Figure 3.10 Time course of sulphate uptake into intact lysosomes.

A lysosomal-rich sample buffered with 0.25 mM sucrose, 20 mM DMG, pH 7.0, was incubated in the same buffer with a final concentration of 136 μM $Na_2{}^{35}SO_4$ added. At each time point 50 μL (100 μg protein) of the reaction was stopped by dilution into 1 mL ice-cold buffer and washed on a GF/F filter (0.7 μM) under vacuum. The filters were dried and radioactivity determined by liquid scintillation counting. Non-specific sulphate binding (×) was determined as described in *Section 3.3.3.1*.

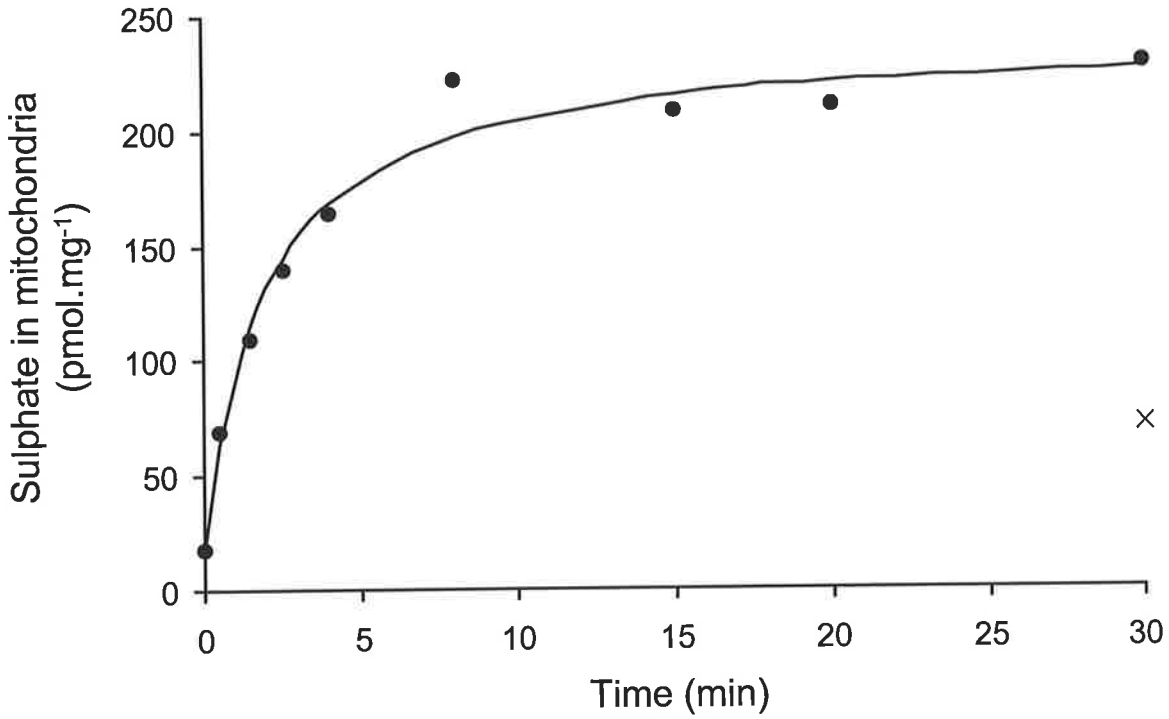

Figure 3.11 Time course of sulphate uptake into human placental intact mitochondria.

A mitochondrial-rich sample buffered with 0.25 mM sucrose, 20 mM DMG, pH 7.0, was incubated in the same buffer with a final concentration of 130 μM $Na_2{}^{35}SO_4$ added. At each time point 50 μL (200 μg determined by BCA protein assay) of the reaction was stopped by dilution into 1 mL of ice-cold buffer and washed on a GF/F filter (0.7 μM) under vacuum. The filters were dried and radioactivity determined by liquid scintillation counting. Non-specific sulphate binding (×) was determined as described in *Section 3.3.3.1.*

3.4.4.3 Sulphate egress from lysosomes and mitochondria.

An intact (not salt-washed) lysosomal sample was loaded with 100 μM sulphate (*Section 3.3.3.2*). Sulphate efflux was then measured over approximately 30 minutes (*Figure 3.12*). Like sulphate uptake, a linear rate of efflux occurs during the first ten minutes. When lysosomal ghosts from this sample of lysosomes were produced by salt-washing, sulphate egress could not be demonstrated. Mitochondrial and lysosomal sulphate efflux were compared. This was performed by loading 100 μg (protein) of organelles from mitochondrial and lysosomal-rich fractions (*Figure 3.13*) and measuring sulphate egress over ten minutes. Mitochondria had a greater rate of sulphate egress than lysosomes.

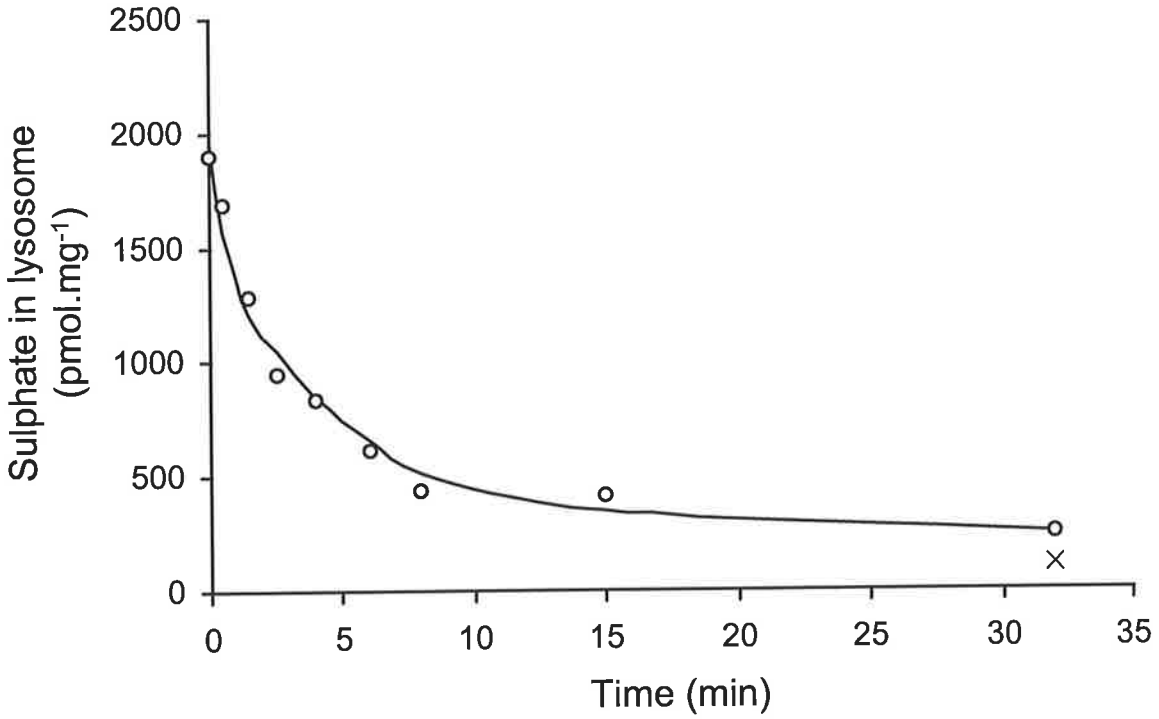

Figure 3.12 Time course of sulphate efflux from human placental intact lysosomes.

An intact lysosomal sample in 0.25 M sucrose, 12 mM DMG, pH 7.0, was concentrated and equilibrated for thirty minutes with 300 μM labelled sulphate. Efflux was initiated by a ten-fold dilution of the sample. At each time point 77 μL (200 μg protein) of the reaction was stopped by mixing with 0.9 mL of ice cold-buffer and washed on a GF/F filter (0.7 μM) under vacuum. The filters were dried and the amount of sulphate retained within the lysosomes was determined by liquid scintillation counting. Non-specific sulphate binding (×) was determined as described in *Section 3.3.3.1.*

Figure 3.13 Comparison of mitochondrial and lysosomal sulphate egress.

A placental granular fraction was separated on two consecutive Percoll® density gradients as described in *Figure 3.1* and *Figure 3.2*. The second gradient (A) assayed for mitochondrial (●) and lysosomal (○) enzymic markers, was pooled into five consecutive eight mL fractions. The samples varied from the mitochondrial-richest to the lysosomal-richest (■▲□△◇).

Samples were loaded with 1 M of labelled sodium sulphate in 0.25 M sucrose, 10 mM DMG, pH 7, for 30 min. A zero minute time point was determined by mixing 5 µL (100 µg protein) aliquots of sulphate-loaded organelles with 0.9 mL ice-cold buffer and filtering immediately. The 1, 3 and 10 min time points were determined by a ten fold dilution of loaded organelles into buffered sucrose at room temperature, before egress was stopped by dilution into ice-cold buffer (0.25 mM sucrose, 10 mM DMG, pH 7) and vacuum filtering through a Whatman GF/F filter. The sulphate retained by filtered organelles was quantitated by liquid scintillation (B).

A

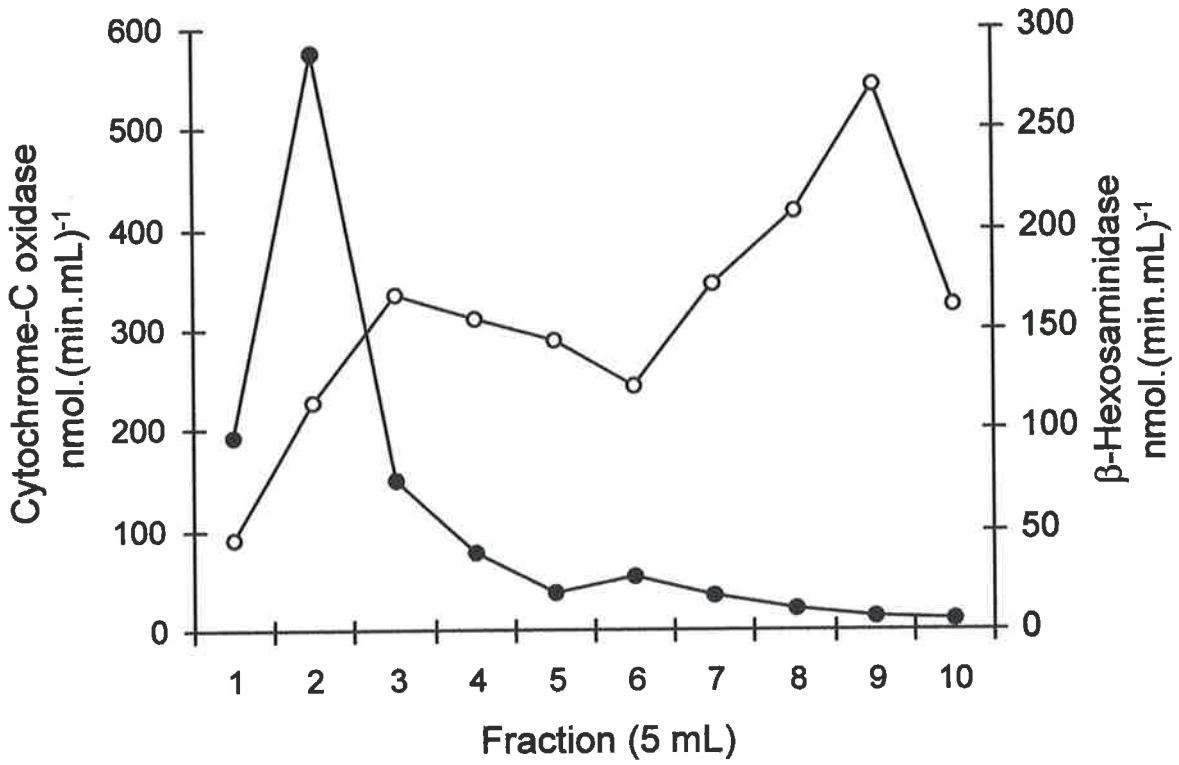
Cytochrome-C oxidase
nmol.(min.mL)-1
β-Hexosaminidase
nmol.(min.mL)-1
600
500
400
300
200
100
0
300
250
200
150
100
50
0
1 2 3 4 5 6 7 8 9 10
Fraction (5 mL)

B

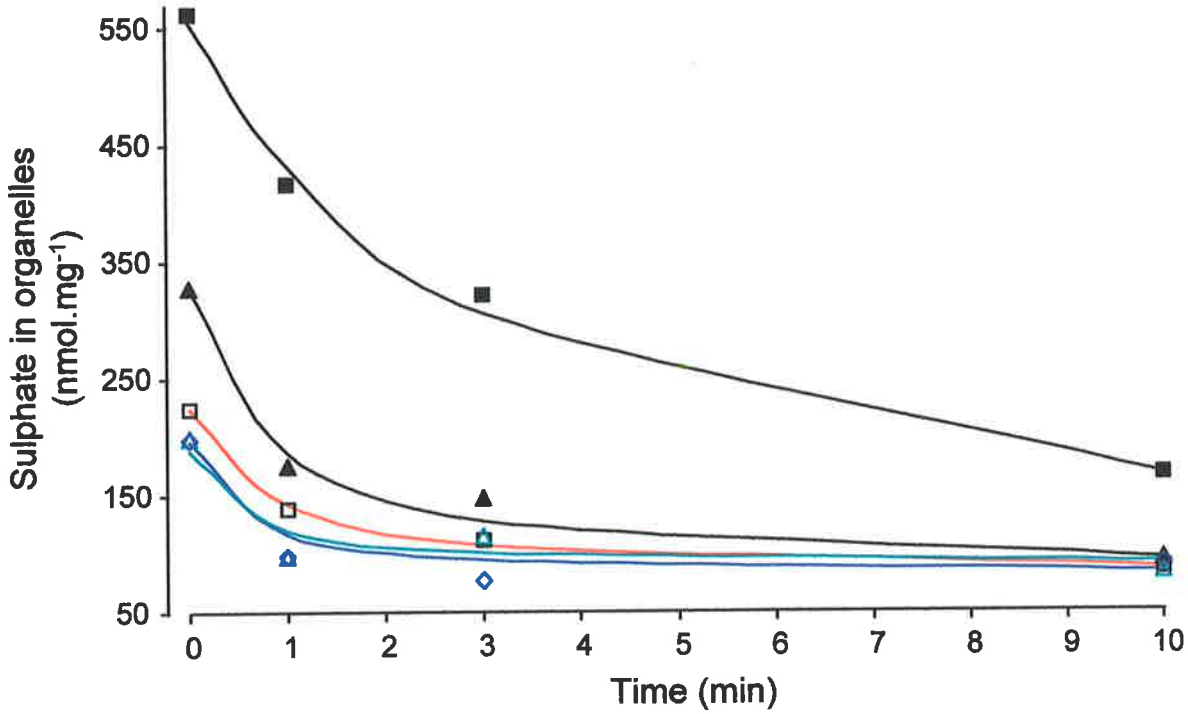
Sulphate in organelles
(nmol.mg-1)
550
450
350
250
150
50
0 1 2 3 4 5 6 7 8 9 10
Time (min)

The quantities of sulphate mitochondria were able to hold per mg (protein) of sample was larger than that of lysosomes as observed during the rates of sulphate flux experiments (*Figure 3.13*). Whether this was because mitochondria were more numerous or larger was not known. To determine the relative capacities of these two organelles to contain sulphate, their total volumes per mg (protein) were compared (*Table 3.3*). The mitochondrial-rich fraction had an approximate three-fold larger volume per mg of protein than the lysosomal-rich fraction.

Table 3.3 Comparative internal volumes of mitochondria and lysosomes.

The internal volumes of mitochondrial- and lysosomal-rich fractions were determined using pooled fractions of the Percoll® density gradient shown in *Figure 3.13*. Comparative volumes were determined by loading 100 µg (protein) samples with 1 M sulphate and calculating the internal sulphate concentration.

Fraction	Volume ($\mu L.mg^{-1}$)
A	9.9
B	5.8
C	3.5
D	2.9
E	2.7

3.4.4.4 Co-transport and counter-transport in lysosomes and mitochondria.

Radio-labelled sulphate was transported into lysosomes, by either co-transport with a *cis* acting proton gradient (*cis*-stimulation) or counter-transported by pre-loading lysosomes with 1 M Na_2SO_4. Loading organelles with a concentration of a counter-transport ion higher than the labelled external ion (used to quantify ion uptake) causes *trans*-stimulation of ion transport. Sulphate transport into lysosomes was compared under these conditions with

uptake by a simple sulphate gradient, and using lysosomal membrane ghosts (*Figure 3.14*). Salt-washed lysosomal membrane ghosts transported very little or no sulphate compared with intact lysosomes. *Trans*-stimulation by sulphate loading of intact cytoplasmic organelles increased uptake four-fold above that of simple uptake. *Cis*-stimulation with a pH gradient increased uptake still further. Similar transport was observed when mitochondria were used for sulphate uptake (*Figure 3.15*). The uptake of sulphate under conditions of a pH gradient however, did not equilibrate to the same level as either a sulphate gradient alone or a counter-sulphate gradient. This suggests that a pH gradient-mediated co-transport may increase non-specific binding of inorganic sulphate to the organelles during sulphate transport.

Thus far, sulphate transport has been compared with and without a pH gradient, where the lysosomes have an intravesicular pH of 7 (pH_i 7) and are incubated in an isotonic, inorganic sulphate-containing solution buffered at pH 7 or pH 5. When the lysosomal intravesicular pH is 5, and they are incubated without a pH gradient by incubation in a sulphate uptake solution, also buffered at pH 5 (pH_o 5), the apparent sulphate transport is much higher than expected. The lack of a proton gradient by pH_i 7 and pH 7 out (pH_o 7) is the same as pH_i 5 and pH_o 5, however, the labelled sulphate associated with the organelles is higher in the latter than that assayed for sulphate transport with a gradient (pH_i 7 and pH_o 5). The explanation could be that either transport was greater at the lower pH, or sulphate was non-specifically binding to molecules associated with the organelles such as protein or lipid. All three conditions (pH_i 7, pH_o 7 and pH_i 7, pH_o 5 and pH_i 5, pH_o 5) were treated with detergent to quantify the non-specific binding of sulphate (*Section 3.3.3.1*). All three had a similar low level of non-specific sulphate binding.

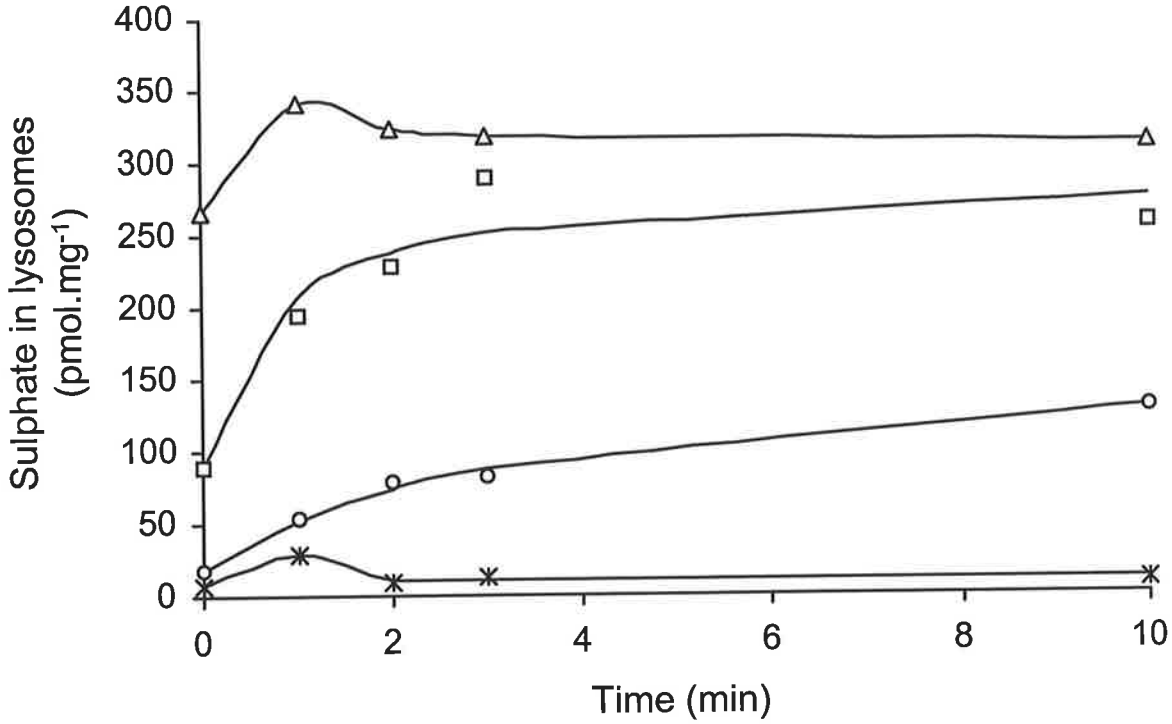

Figure 3.14 Time course of sulphate uptake in salt-washed lysosomes and intact lysosomes, either with or without stimulation of sulphate uptake.

Lysosomes were incubated in 100 μM radio-labelled sulphate with 10 mM DMG, pH 7.0, inside and out, unless indicated otherwise. At each time point 100 μg (protein) of vesicles from the reaction was stopped by mixing with 0.9 mL of ice-cold buffer and washed on a 0.45 μM nitrocellulose filter under vacuum. The filters were dried and sulphate retained within the lysosomes was determined by liquid scintillation counting. The conditions of sulphate uptake were: influx with salt washed lysosomal membranes (✳); influx with intact lysosomal vesicles (○); *trans*-stimulation of intact lysosomes by pre-loading with 1 M unlabelled sulphate (□); *cis*-stimulation of intact lysosomes by incubation in 10 mM DMG, pH 5 (△).

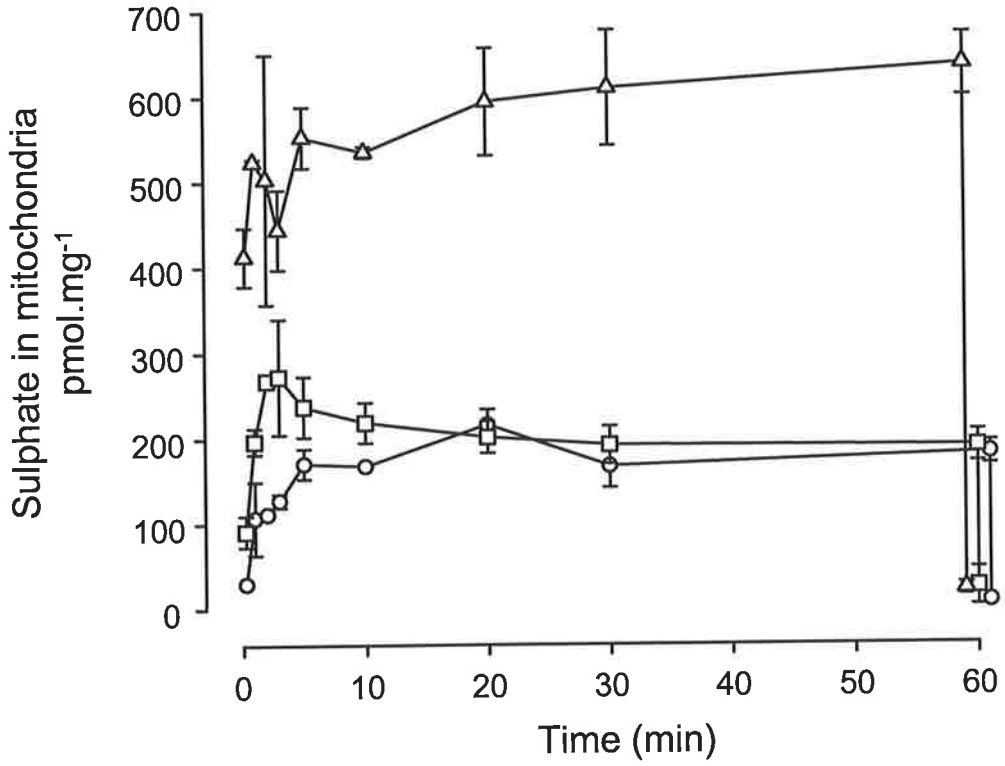

Figure 3.15 Time course of sulphate uptake into mitochondria by cis- and trans-stimulation.

Intact mitochondria were incubated in 100 μM radio-labelled sulphate with 10 mM DMG, pH 7.0, inside and out (○), unless indicated otherwise. At each time point 100 μg (protein) of sample from the reaction was stopped by mixing with 0.9 mL of ice-cold buffer and then washed on a 0.45 μM nitrocellulose filter under vacuum. The filters were dried and sulphate retained within the lysosomes was determined by liquid scintillation counting. *Trans*-stimulation was performed by pre-loading with 1 M unlabelled sulphate (□), and *cis*-stimulation by incubation in 10 mM DMG, pH 5 (△).

3.4.4.5 *Trans*-stimulation of sulphate transport with substrate analogues.

Lysosomes and mitochondria were pre-loaded with 10 mM potential counter-transport ions and assayed for the uptake of 100 µM labelled sulphate. Lysosomes were *trans*-stimulated by molybdate, sulphate and thiosulphate (*Table 3.4*). Mitochondria were *trans*-stimulated by molybdate, sulphate, thiosulphate and taurine (*Table 3.5*). Chloride, bicarbonate and phosphate did not act as counter-transport ions for the uptake of sulphate in either lysosomes or mitochondria.

Table 3.4 Rates of sulphate transport into lysosomes pre-loaded with different anions.

Lysosomes were preloaded by a 30 min incubation with 10 mM of selected anion in 0.25 M sucrose and 20 mM HEPES, pH 7. The control sample was mock-loaded in the same buffered sucrose solution. After 0.5 and 1.0 min incubations with 100 µM $Na_2{}^{35}SO_4$ at 72 MBq.nmol^{-1} (2 mCi.nmol^{-1}) in buffered isotonic sucrose, 100 µL (100 µg protein) aliquots were washed on a filter (0.45 µm nitrocellulose) placed in a vacuum manifold (*Section 3.3.3.5.1*). The rates of sulphate transport into the lysosomes were determined using these two time points. Values are the mean ± S.D. and $n = 3$. Statistical analysis was performed using the Student's t test, with each anion compared against the control. Only p-values of less than 0.05 are shown.

Anion	pmol.min^{-1}.mg^{-1}	± standard deviation	p
Control	13.0	0.5	
Molybdate	30.4	13.4	<0.05
Taurine	12.2	1.7	
Sulphate	25.3	9.7	<0.05
Bicarbonate	13.1	3.7	
Thiosulphate	19.7	4.5	<0.05
Phosphate	13.0	0.7	
Chloride	13.5	5.3	

Table 3.5 Rates of sulphate transport into mitochondria pre-loaded with different anions.

Mitochondrial were preloaded by a 30 min incubation with 10 mM of selected anion in 0.25 M sucrose and 20 mM HEPES, pH 7. The control sample was mock-loaded in the same buffered sucrose solution. After 0.5 and 1.0 min incubations with 100 µM $Na_2{}^{35}SO_4$ at 72 MBq.nmol^{-1} (2 mCi.nmol^{-1}) in buffered isotonic sucrose, 100 µL (100 µg protein) aliquots were washed on a filter (0.45 µm nitrocellulose) placed in a vacuum manifold (*Section 3.3.3.5.1*). The rates of sulphate transport into the mitochondria were determined using these two time points. Values are the mean ± S.D. and $n = 3$. Statistical analysis was performed using the Student's t test, with each anion compared against the control. Only p-values of less than 0.05 are shown.

Anion	pmol.min^{-1}.mg^{-1}	± standard deviation	p
Control	13.3	2.7	
Chloride	20.4	0.8	
Thiosulphate	97.1	4.9	<0.005
Sulphate	77.1	2.9	<0.002
Bicarbonate	21.4	0.7	
Taurine	40.3	3.4	<0.003
Molybdate	85.3	3.1	<0.002

3.4.4.6 Inhibition of sulphate transport with anion exchange inhibitors.

Sulphate transport was inhibited by the sulphonic acid stilbene derivatives DIDS* and SITS†, and by phenylglyoxal (*Table 3.6*). Whether the inhibitor was pre-incubated with the sample, introduced when the radio-labelled sulphate uptake started or both, inhibition was similar (*Figure 3.16*).

Table 3.6 Percent inhibition of sulphate transport by anion exchange inhibitors.

Inhibitor	Lysosomes	Mitochondria
DIDS (1 mM)	74	49
SITS (5 mM)	70	27
Phenylglyoxal (50 mM)	57	42

After 20 min incubation with the respective inhibitors, sulphate uptake into organelles was determined in the presence of a proton gradient (pH 7.0 in, pH 5.0 out) using 100 µM $Na_2{}^{35}SO_4$ and the inhibitor. Sulphate transport was assayed at 0.5 and 1.0 min. Control organelles were assayed under the same conditions in the absence of inhibitors.

* diisothiocyanatostilbene disulphonic acid
† acetamido isothiocyanatostilbene disulphonic acid

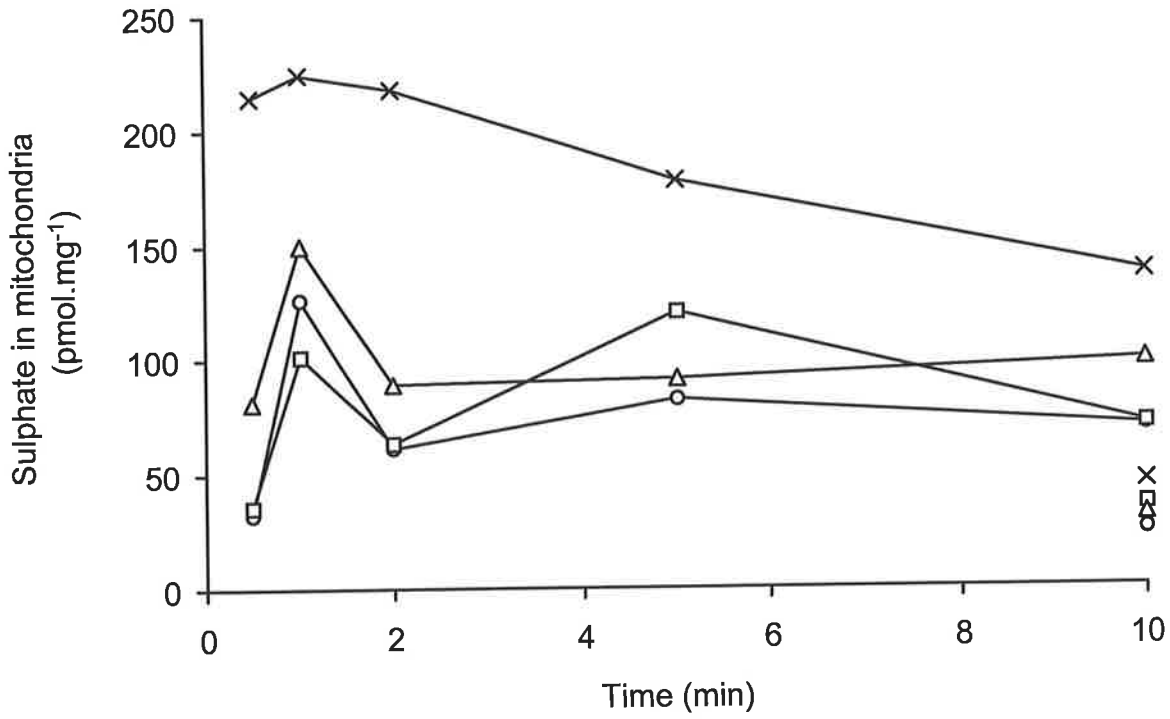

Figure 3.16 Inhibition of sulphate transport by phenylglyoxal.

Mitochondria stored at -20°C in 0.25 M sucrose, 20 mM HEPES, pH 7, were thawed and assayed for sulphate transport in the presence of a proton gradient (0.25 M sucrose, 20 mM MES, pH 5, 100 μM $Na_2{}^{35}SO_4$). Phenylglyoxal (5 mM) was added to mitochondria (100 μg protein) 20 min before and during sulphate transport (○); before but not during the assay (□); only during the assay (△); or not used (×). The group of unjoined points at 10 min illustrate the non-specific binding of sulphate (*Section 3.3.3.1*) for each set of conditions.

3.4.4.7 Differences and similarities between lysosomal and mitochondrial sulphate transporters.

Sulphate transport in lysosomes and mitochondria showed fundamental similarities. They were both resulted from secondary active transport mechanisms, they had specificities for counter-transport ions and were inhibited with the same anion exchange inhibitors (DIDS, SITS and phenylglyoxal). There were significant differences however, mitochondria showed greater sulphate uptake and egress than did lysosomes. Mitochondria demonstrated a larger volume per milligram (protein) of sample that could be loaded with sulphate. Taurine counter-transported with sulphate in mitochondria but not in lysosomes. Sulphate uptake was affected more by the sulphonic stilbene derivatives DIDS and SITS in lysosomes than in mitochondria. The lysosomal and mitochondrial sulphate transporters therefore, could be distinguished if they were successfully assayed during their purification.

3.4.5 Reconstitution of lysosomal membrane proteins into phospholipid vesicles.

The lysosomal proton pump has been characterised after reconstitution into artificial membrane vesicles also known as proteoliposomes (Okamoto *et al.* 1996). If purification of the lysosomal sulphate transporter were to be by chromatographic methods, reconstitution of the lysosomal membrane proteins would also be required to assay the transporter. Membrane proteins were extracted with three percent Triton X-100 mixed with phospholipid in a buffered salt solution and passed over an Amberlite XAD-2 column fifteen times to remove the detergent. The detergent was removed to allow the protein to return to its native state within a phospholipid bilayer that would form a vesicle. The vesicles could then be assayed for sulphate transport.

The ability to reconstitute a protein is not always guaranteed. Commercial non-ionic detergents such as Triton X-100 have been reported to oxidise the functional sulphydryl groups of integral membrane transport proteins (Chang and Bock 1980). The formation of oxidising agents such as peroxide in aqueous solutions is initiated by light and oxygen. Precautions were taken to prevent phospholipid oxidation by adding the anti-oxidant butylated hydroxy-toluene to freshly prepared phospholipids.

3.4.5.1 Electron micrograph of proteoliposomes.

Electron microscopy was performed by Richard C. A. Davey, Department of Chemical Pathology, Women's and Children's Hospital, North Adelaide, South Australia.

Proteoliposomes were formed by the method of Mancini *et al.* (1992) (see *Section 3.3.4*). Briefly, membrane proteins (1.3 mg) were extracted on ice for 10 min in 300 µL containing 3% (v/v) Triton X-100, 100 mM KCl, 1 mM DTT and 10 mM HEPES, pH 7.4. The soluble supernatant was collected after centrifugation at 150,000 ***g*** (30 psi), for 20 min in a Beckman Airfuge™ at 4°C. The extracted protein (200 µL) was added to 60 µL of 10% (v/v) Triton X-100, 100 µL (10 mg) sonicated phosphatidyl choline liposomes and 320 µL of 24 mM HEPES, pH 7.4 and 119 mM KCl. The detergent was removed by fifteen passages over a 0.5 x 3.6 cm column of Amberlite XAD-2. The proteoliposomes formed were unilamelar vesicles with diameters ranging between 30 and 200 nM (*Figure 3.17*).

Figure 3.17 Electron micrograph of proteoliposomes.

Proteoliposomes were formed by reconstituting detergent solubilised membrane proteins into phospholipid vesicles. The proteoliposomes were negative stained with uranyl acetate and examined with a transmission electron microscope (*Section 3.3.2.1*). The final magnification is 23,600 times with the bar representing 1 μm.

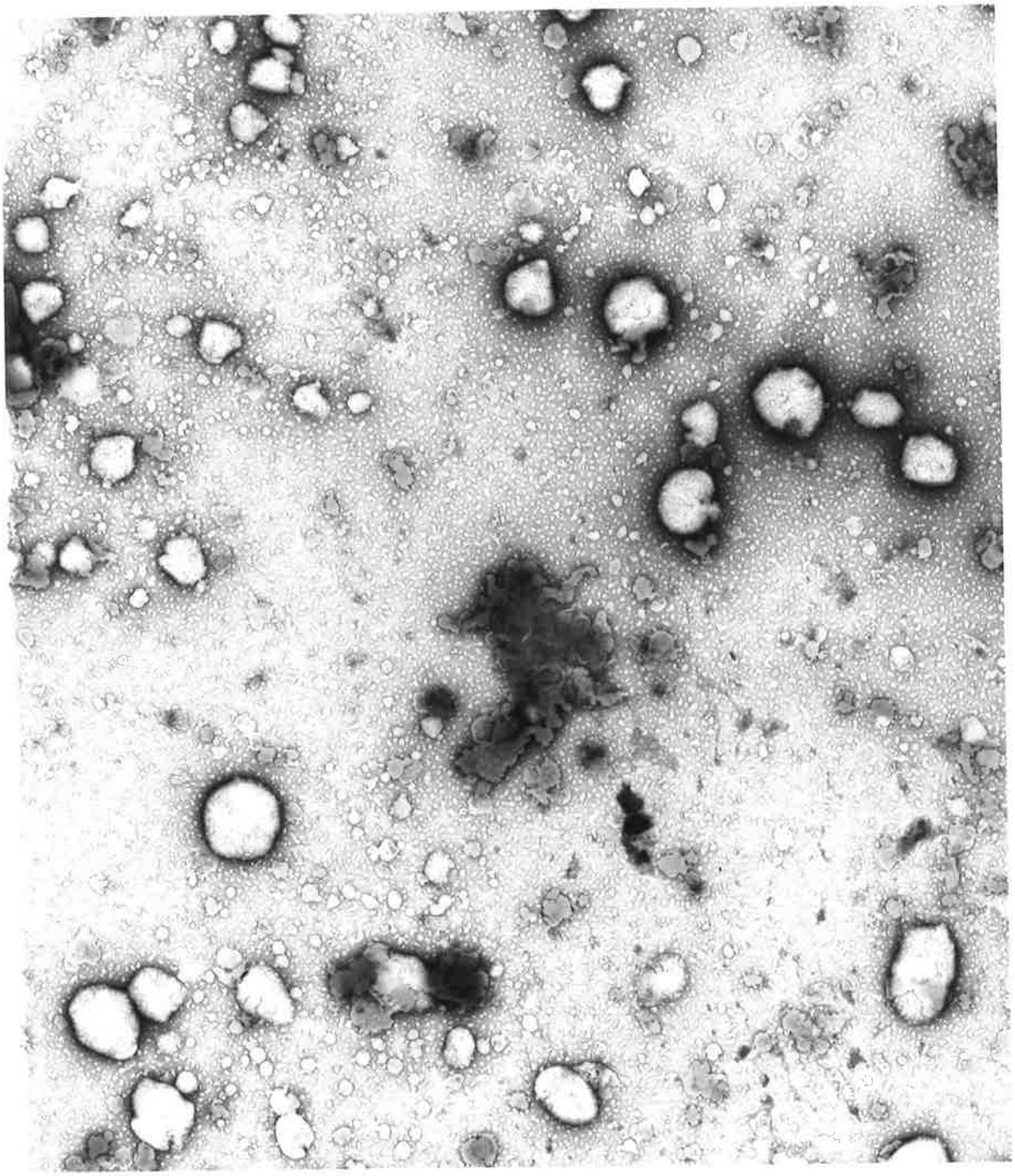

1μm

3.4.5.2 Development of reconstitution methodology.

In the method of Mancini *et al.* (1992) proteoliposomes were passaged fifteen times over Amberlite XAD-2. The number of passages for detergent removal was varied to determine how critical passage number was and what effect this number had on vesicle formation and diameter. This was performed by cycling the proteoliposome mixture over an Amberlite XAD-2 column, taking seven aliquots from 12 to 38 passages and viewing them by electron microscopy. *Table 3.7* shows the resulting sizes with increasing passage number of the vesicle populations formed. Higher passage numbers had an increased heterogeneity of diameters of the vesicles formed.

Table 3.7 Effect of vesicle diameter with passages over Amberlite XAD-2.

Volume of reconstitution mixture cycled over Amberlite XAD-2 was 0.68 mL. Amberlite XAD-2 adsorbed the Triton X-100 from the reconstitution mixture to form proteoliposomes. The diameters of the dominant populations of vesicles were measured from electron micrographs.

Number of passages	Average size of largest population
12	550 nM
16	180 nM
21	160 nM
25	120 nM
29	240 nM
34	180 nM
38	180 nM

3.4.6 Sulphate transport in proteoliposomes.

Sulphate transport was performed on proteoliposomes as with intact lysosomes. A number of different methods were employed to separate the vesicles from external sulphate to measure the amount of sulphate uptake during transport. Proteoliposomes were not as robust and required methods gentler than vacuum filtering.

Vacuum filtering to separate sulphate external to proteoliposomes was performed as described for intact lysosomes (*Section 3.4.4.1*). This method of filtering the vesicles (out of the sulphate transport solution) however, was not able to demonstrate sulphate transport using a sulphate gradient in proteoliposomes. Pre-loading the proteoliposome vesicles with sulphate to stimulate counter-transport did however, show an apparent increase in the amount of radio-labelled sulphate taken up.

The problem of vacuum filtering to remove free sulphate was most probably physical harshness on these vesicles. A physically gentler method of removing sulphate not contained within the proteoliposome was performed with Sephadex G50. In this filtration method, the excluded vesicles passed through the Sephadex gel before the external sulphate. Sulphate uptake with a pH gradient was measured in proteoliposomes using Sephadex G50 instead of vacuum filtering (*Figure 3.18*).

After finding that apparent sulphate transport in proteoliposomes could be measured by gel filtration using Sephadex G50, but not by vacuum filtration, sulphate transport was measured in salt-washed lysosomal ghosts with the gentler method. *Figure 3.19* shows that sulphate uptake into lysosomal ghosts can be measured when free external sulphate was separated by Sephadex G50 rather than through a membranous filter.

To determine whether significant amounts of sulphate leaked from proteoliposomes during the Sephadex G50 filtration step of the transport assay, their volumes were measured. Proteoliposomes were formed in the presence of labelled sulphate, which is transportable, and in the presence of labelled sucrose, which is not transportable. The proteoliposome volumes were calculated after unincorporated label was separated by Sephadex G50: 0.58 μL proteoliposome volume per 100 μL (or 0.58 %) proteoliposome mixture was produced, as calculated from sucrose incorporation. Formation of proteoliposomes in the presence of radio-labelled sulphate included 0.2% volume of sulphate. This was less than half the volume of sucrose contained during proteoliposome formation, suggesting some sulphate was transported out of the vesicle during the separation of proteoliposomes from the surrounding solution by filtration with Sephadex G50.

To reduce the time taken to separate sulphate external to vesicles, Dowex AG1-X8 was used. This method of ion exchange to remove external sulphate was much faster than filtration. This reduces the time in which sulphate can leak out of the lysosome while being assayed. Dowex reduced variation between replicates as Sephadex G50 had some variation between the void volumes of mini-columns. Dowex AG1-X8 with 20-50 mesh flowed too fast to exchange sulphate where as the 100-200 mesh flowed faster than Sephadex G50 and efficiently exchanged the free labelled sulphate. Both the chloride and format forms of Dowex efficiently exchanged sulphate. Better results were observed when the Dowex was pre-blocked with BSA. The use of Dowex in future transport studies could reduce the number of replicates required, and save time as it is an easier media to handle and pack into columns.

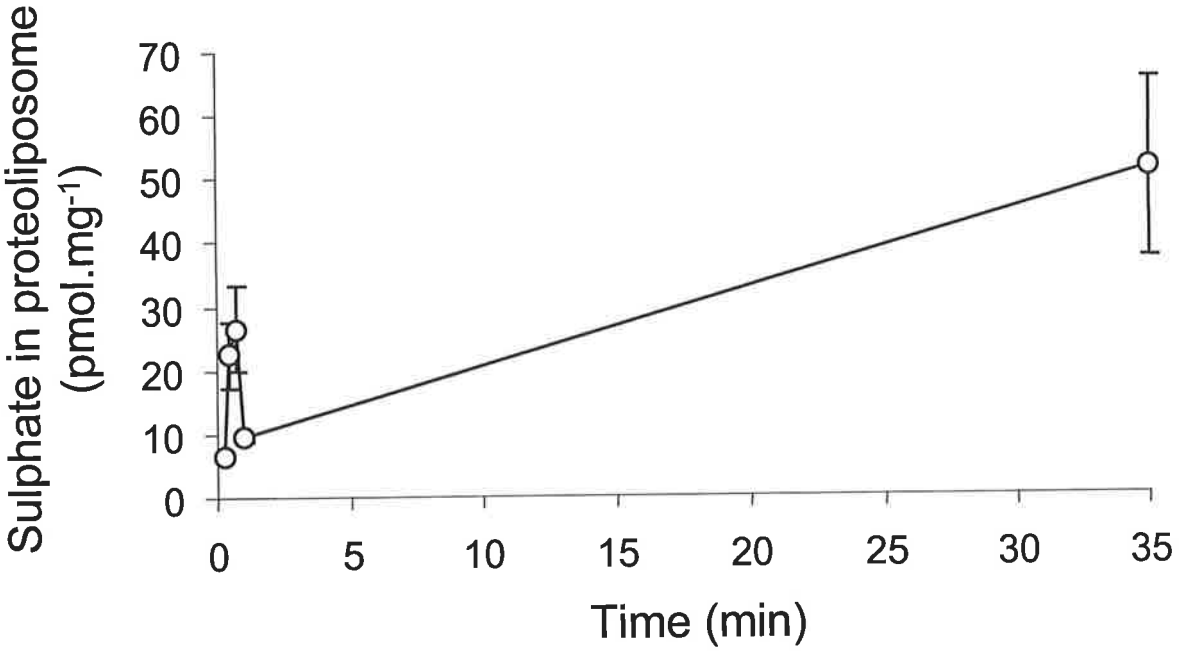

Figure 3.18 Proteoliposome uptake of sulphate with a pH gradient.

Proteoliposomes were incubated in 30 µL of 100 µM $Na_2{}^{35}SO_4$, 10 µM valinomycin, 30 mM MES, pH 5.5. At the indicated times sulphate transport was stopped by the addition of 70 µL ice-cold (100 mM KCl, 20 HEPES, pH 7.4) buffer. This mixture was applied to a 0.4 x 5 cm column of Sephadex G50, which was washed through the column by the addition of 0.9 mL of ice-cold buffer. The sulphate in the proteoliposome eluate was determined by liquid scintillation counting. Standard deviations are illustrated for each time point.

Figure 3.19 Sulphate transport into salt-washed lysosomal ghosts.

Salt-washed lysosomal ghosts were assayed for sulphate uptake without a proton gradient (panel A) and with a proton gradient (panel B). Uptake was initiated by adding 25 μL (22 μg protein) of lysosomal ghosts to 5 μL of uptake solution at 25°C. Transport was assayed by washing the lysosomal ghosts through 1 mL of Sephadex G50 with 0.9 mL 100 mM KCl, 20 mM HEPES, pH 7.4, at 4°C. The excluded or eluted ghosts were counted by liquid scintillation. Sulphate uptake solution without a pH gradient contained 60 μM valinomycin, 600 μM sulphate and 120 mM HEPES, pH 7.4, while that with a pH gradient consisted of 60 μM valinomycin, 600 μM sulphate, 240 mM MES free acid.

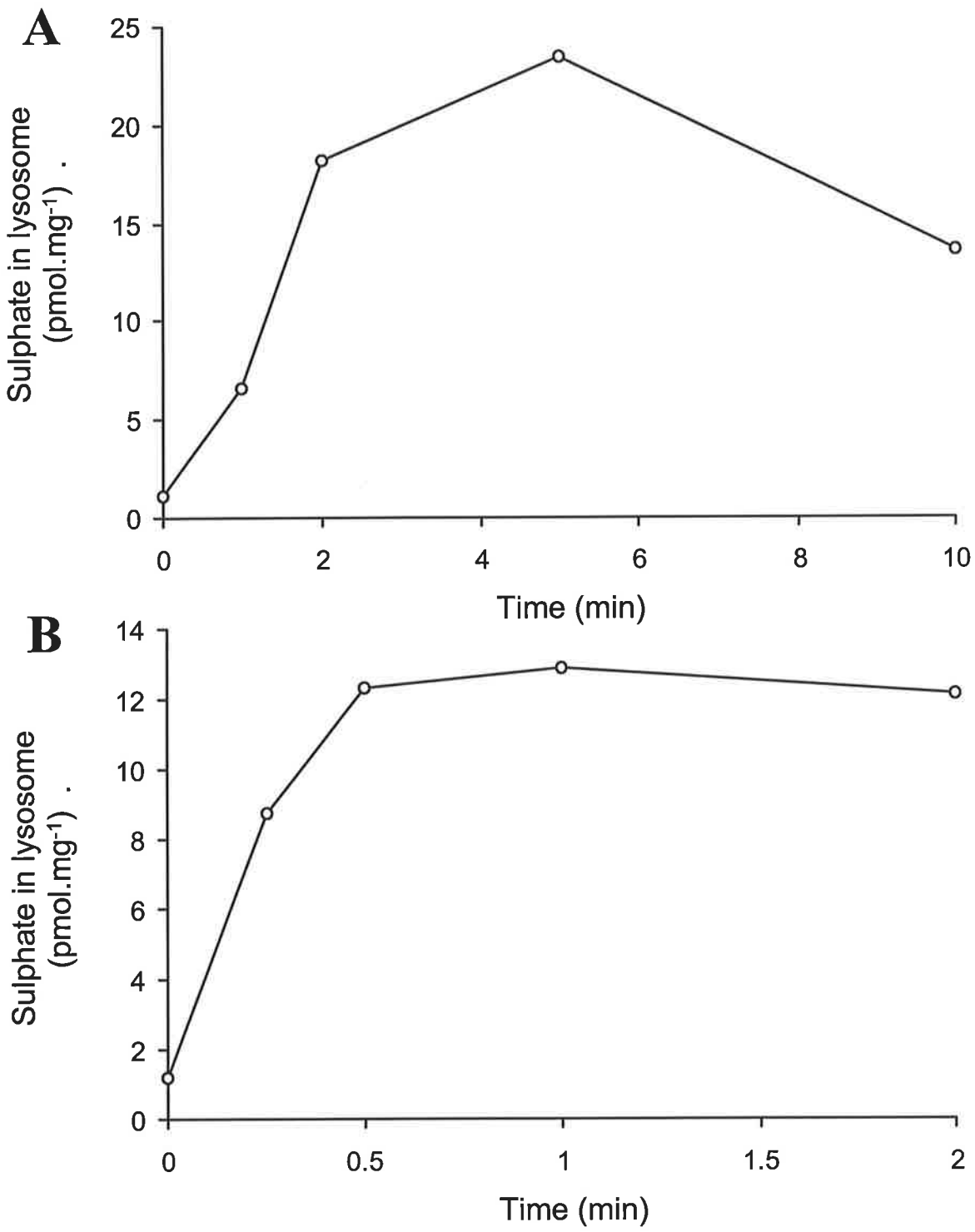
A
Sulphate in lysosome (pmol.mg-1) .
25
20
15
10
5
0
0
2
4
6
8
10
Time (min)
B
Sulphate in lysosome (pmol.mg-1) .
14
12
10
8
6
4
2
0
0
0.5
1
1.5
2
Time (min)

3.4.7 Sulphate transports differently in proteoliposomes than lysosomes.

If sulphate influx could not be measured with intact lysosomes neither could it be by counter or co-transport. Yet, in proteoliposomes counter-transport was apparently measured, when influx by a simple sulphate gradient could not be measured. To determine the background noise of sulphate transport phospholipid vesicles were formed in the absence of membrane proteins. When these vesicles were assayed, apparent sulphate transport could be measured. Interaction of sulphate with proteoliposomes was further investigated by phospholipid sulphate binding experiments.

3.4.7.1 Sulphate interaction with phospholipid.

As reconstitution was performed with a phospholipid different to that of the lysosome, the affinity of sulphate with this phosphatidylcholine from fresh egg yolk (Sigma Chemical Co., St. Louis, MO, USA) was examined. Sulphate was found to bind phosphatidylcholine (PC) in a concentration-dependent manner, and phosphate was unable to reduce this interaction. Sulphate did not bind to PC dipalmitoyl however, which is a saturated synthetic lipid. Nor did sulphate bind in a time-dependent manner to phospholipid of isolated lysosomes. This was observed when transport studies on lysosomes from full-term placentae were performed.

3.4.7.2 Thin layer chromatography of phosphatidylcholine.

The egg yolk PC used for reconstitution was tested for purity by TLC. *Figure 3.20* shows that that egg yolk PC used contained a very polar contaminant. This contaminant was most likely lyso-PC, which is positively charged and may have contributed to the time-dependent, non-specific binding of sulphate.

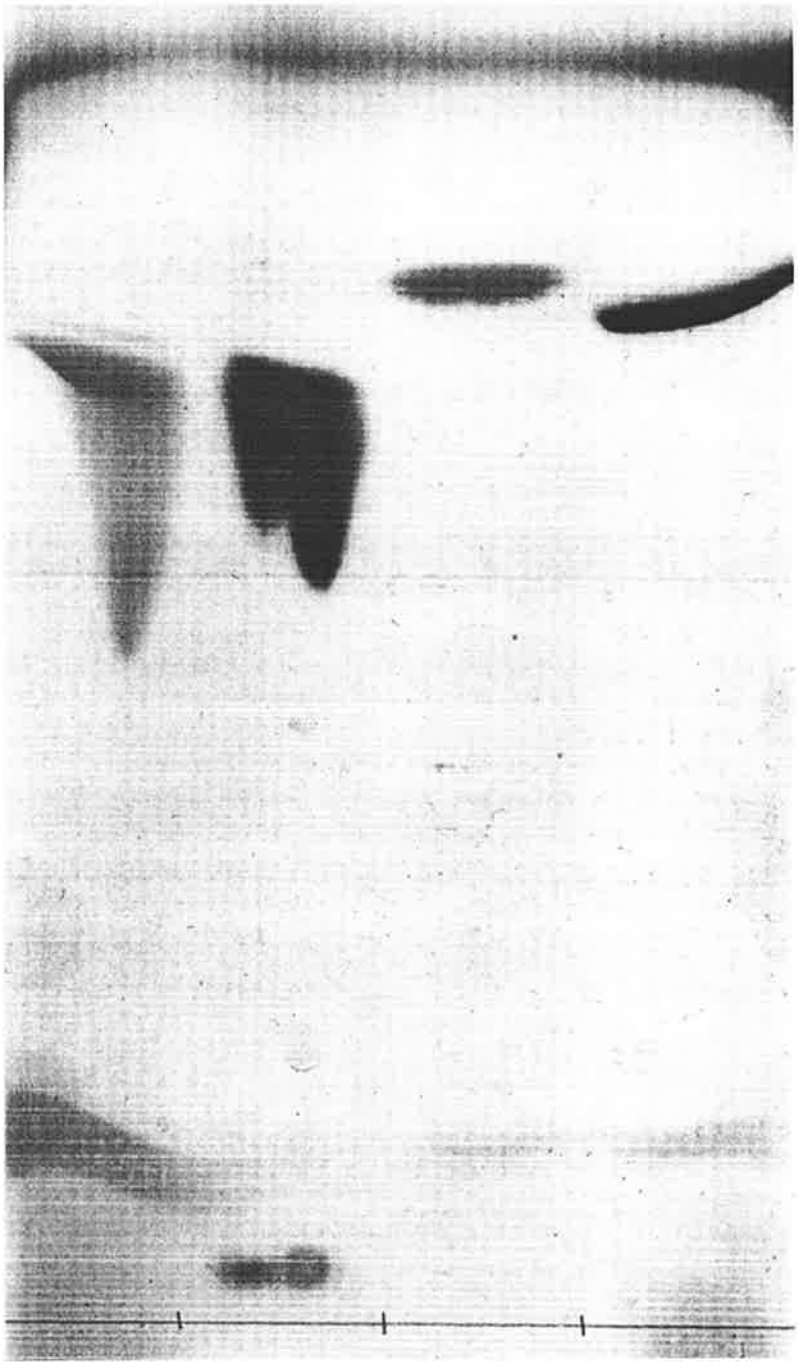

Figure 3.20 Thin layer chromatography of reconstituted phosphatidylcholine.

Lanes:1) dipalmitoyl phosphatidylcholine; 2) egg phosphatidylcholine; 3) phosphatidyl ethanolamine 4); cardiolipin (diphosphatidyl glycerol). The ratio of solvents used to separate the lipids was chloroform/methanol/water (65:25:4, by vol.). Lipids were visualised by iodine vapour.

3.5 General Discussion.

Highly enriched unbroken lysosomes and mitochondria were prepared from human placenta. Acidification of lysosomes isolated from caesarean-derived placentae was successful, but not from placentae delivered by normal vaginal delivery. Placentae obtained from caesarean births had the lysosomes isolated with less delay than lysosomes from a full-term delivered placenta. A child is delivered by caesarean in approximately twenty minutes with the placenta soon following. The vaginal delivery of child and placenta, on average, takes considerably longer and is highly variable. The collection of placenta from unpredictable normal vaginal deliveries resulted in delays between the delivery and lysosomal isolation, requiring placentae to be kept on ice prior to their preparation.

Activity of marker enzymes could be measured from placenta of either method of delivery. This suggests that, not protein but, perhaps phospholipid membrane integrity was compromised in vaginally-delivered placentae that prevented acidification. A decline in cellular membrane morphology was confirmed by electron micrographs. The deterioration was particularly evident at the trophoblastic membranes and microvilli. Preparation of lysosomes from placenta for further transport studies was only from caesarean births. This decision resulted in collection and use of fresher placental tissue as experiments could more easily be organised around elective caesarean sections.

When acidification was measured in lysosomes, the presence of KCl increased the rate of acidification. Ohkuma *et al.* (1982) demonstrated chloride was the most effective membrane-permeant anion required for Mg-ATP-driven acidification of lysosomes. The reduction in acidification of samples frozen and thawed most likely resulted from the rupture,

reduced size or the turning inside-out of a portion of the lysosomes. Altering the buffer concentration external to the lysosome, relative to that of the lumen, prevented proton pumping. These three changes in assay conditions demonstrate that in addition to ATP, organelles required a membrane-permeant anion, minimal breaking and resealing of membranes and isotonic buffer concentrations so as not to affect proton transport.

When correlated with enzyme markers no cytoplasmic organelles other than lysosomes were acidified. This supports the argument that lysosomal organelles were intact and that the acidification was not an artefact of some other contaminating cytoplasmic organelle present in the density gradients.

3.5.1 Sulphate transport

Like proton pumping, sulphate transport was only measurable in lysosomes from placentae of caesarean births. The flux (uptake or egress) of sulphate could be measured in either lysosomes or mitochondria. Sulphate uptake in mitochondria was higher than that observed in lysosomes. This higher rate may have reflected either the larger volume per mg of protein or the involvement of different transporters. Sulphate transport in lysosomal and mitochondrial samples could be stimulated by either counter-transport with a specific ion or co-transported with a pH gradient. The *trans*-stimulation of sulphate transport in both lysosomes and mitochondria is evidence that the transport is carrier-mediated.

Sulphate transport was inhibited in lysosomes and mitochondria by the stilbene derivatives (DIDS and SITS) and phenylglyoxal. The stilbene derivatives were more effective inhibitors of lysosomal sulphate transport than that of mitochondria. This supports the concept that the transport of sulphate in lysosomes and mitochondria is facilitated by different transporters.

Reconstitution of lysosomal membrane proteins into unilamelar phospholipid vesicles was achieved. Apparent sulphate transport in these proteoliposomes was measured when sulphate external to the vesicles was gently and quickly separated by gel filtration. Sulphate however, was shown to bind to the egg phospholipid used in the reconstitution of membrane proteins. As apparent sulphate transport was observed when *trans-stimulated* using unlabelled sulphate, at least part of the apparent transport observed was real, due to the excess of sulphate present in pre-loading the vesicles before transport.

The non-specific binding of sulphate to the egg phosphatidyl-choline could not be blocked with phosphate. The egg phospholipid contained a very polar compound, possibly lyso-PC, which may have contributed to binding of sulphate. The endeavour to find a satisfactory phospholipid that does not oxidise or leak, and supports the activity of transporters, is another study in its self.

If the apparent sulphate transport measured in proteoliposomes, is a combination of sulphate transport and binding of sulphate to phosphatidyl-choline, then difficulties may arise in knowing which transporter is being assayed. A more certain approach therefore, was required to identify the lysosomal sulphate transporter.

4. Identification of proteins involved in lysosomal sulphate transport.

4.1 Introduction.

During the characterisation of the lysosomal sulphate transporter, a search for the proteins involved was initiated. To date few lysosomal membrane proteins have been isolated (*Section 1.3.2.3*). The first lysosomal transporter isolated was the ubiquitous vacuolar H^+-ATPase. This vacuolar proton pump was the only known lysosomal transporter during this study. The isolation of other lysosomal membrane or transporter proteins would provide further valuable insight for future strategies in the isolation and characterisation of other lysosomal membrane proteins. Since the completion of this study, two lysosomal transporters have been cloned. The cystine transporter gene was mapped to 17p13 (Town *et al.* 1998) after thirty years of interest in the disease cystinosis, which results from defective lysosomal transport of cystine (*Section 1.3.3.2*); and more recently the sialic acid transporter gene was mapped to 6q14-q15 (Verheijen *et al.* 1999).

The approaches used to identify proteins involved in lysosomal sulphate transport exploited the function of the transporter. The first approach involved affinity labelling of membrane proteins with anion exchange inhibitors. The second approach employed polyclonal antibodies generated against a functionally related protein. The related protein used in these endeavours was the erythrocyte anion transporter (*Section 1.4.1.1*), also known as Band 3. The antibodies were then used to identify related proteins by cross-reactivity. This approach has been successfully used to identify anion transporters in plasma membrane, Golgi and mitochondria (*See Section 4.4.2.1*).

4.2 Experimental Aims.

The objectives of this section of work were to fractionate the lysosomal membrane proteins, and then to identify and enrich those involved in sulphate transport. The fractions enriched with the lysosomal sulphate transporter had to be determined. The proteins in these fractions then needed to be isolated, identified and their cellular location confirmed. Other abundant lysosomal membrane proteins found in the course of these studies were also investigated.

4.3 Methods.

4.3.1 Fluorography.

SDS-PAGE gels were fixed in 25% (v/v) isopropanol and 10% (v/v) acetic acid for 30 min while rocking at room temperature. The fixative solution was poured off and the gel was soaked in Amplify™ for 30 min while rocking. Gels were placed on 3MM paper, covered with a piece of cellophane and dried under vacuum at 60°C for 2 h. Gels were then exposed to Kodak XAR film at -80°C.

4.3.2 Preparation of a polyclonal antibody against the human erythrocyte anion exchanger protein.

Human erythrocyte anion exchanger protein was kindly donated by Dr. Rob McPherson in Dr. Leann M. Tilley's laboratory, Department of Biochemistry, La Trobe University, Bundoora, Victoria, Australia.

Erythrocyte ghost membranes were prepared from whole blood by two washes in 5 mM sodium phosphate, 0.16 mM NaCl, pH 7.4, at 4°C. After each sedimentation at 2200 ***g*** for 5 min the thin layer of white cells was aspirated. Erythrocytes were then washed three times in 5 mM sodium phosphate, pH 8, at 4°C. Haemoglobin was aspirated until a white pellet of membranes (approximately one-fifth of total volume) remained, after centrifugation at

17,000 ***g*** for 12 min at 4°C. Peripheral proteins were then removed by incubation in 1 mM CAPS-NaOH, pH 12, leaving Band 3 intact in the plasma membranes. Band 3 constituted approximately 95% of the remaining protein.

Band 3 antibodies were raised in New Zealand White rabbits. Antigen was injected subcutaneously with a 21G needle in the rear haunches. Prepared Band 3 protein (2 mg) was resuspended in 1 mL of phosphate buffered saline (PBS) with a hand-held 3 mL homogeniser. The immunisation regime is described in *Section 2.2.10.1.1* used 100 µg of Band 3 protein for each inoculation.

4.4 Results.

4.4.1 Characterisation of lysosomal membrane proteins by SDS-PAGE.

4.4.1.1 Distribution and abundance of membrane proteins in a Percoll® density gradient.

Cytoplasmic organelles from a placental granular fraction were separated (*Section 2.2.2*) on a Percoll® density gradient (*Figure 4.1*). Over 88% of mitochondria, determined by cytochrome-*C* oxidase activity, were contained within the first two fractions, while the lysosomal distribution, determined by β-hexosaminidase and GNAT activities, peaked in fraction seven.

The Percoll® gradient can therefore, be divided into two fractions: a relatively pure 'lysosomal fraction' and a 'mitochondrial-enriched fraction' that contains some lysosomes. There are two ways of identifying candidate lysosomal proteins from their distribution. The protein concentration will increase with increasing lysosomal enrichment, which could mean that it is present throughout the gradient and in increasing amounts, or that it is seen at the

lysosomal end of the gradient only. A protein that is only seen at the start of the gradient can only be mitochondrial.

The membrane proteins isolated (*Section 2.2.4.1*) from these eight fractions were compared by SDS-PAGE (*Section 2.2.6.1*) (*Figure 4.2*). A prominent protein of 49 kDa in apparent molecular mass, increased in abundance with increasing lysosomal enrichment.

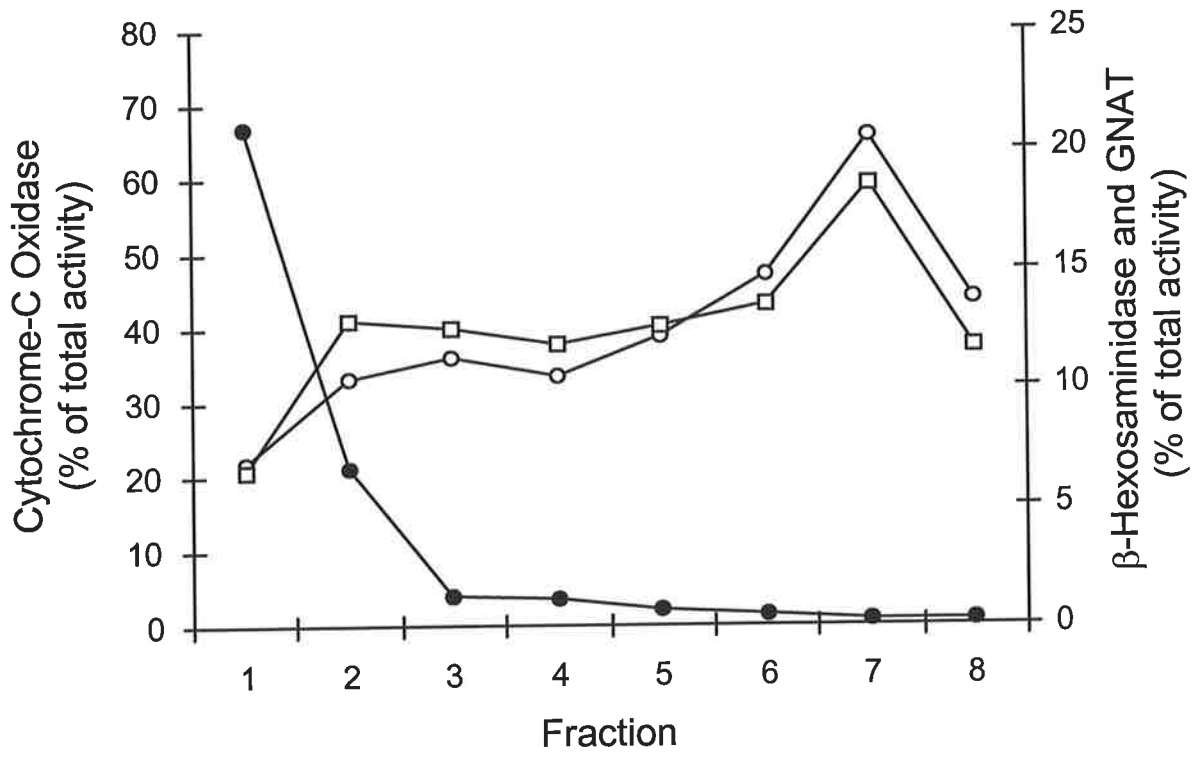

Figure 4.1 Fractionation of lysosomes and mitochondria by Percoll® density gradient centrifugation.

A placental granular fraction was fractionated on two consecutive Percoll® density gradients as described in *Section 2.2.2*. The second gradient was fractionated and the eight 5 mL fractions were assayed for cytochrome-*C* oxidase (●), β-hexosaminidase (○) and acetyl-CoA: α-glucosaminide *N*-acetyltransferase (GNAT) (□).

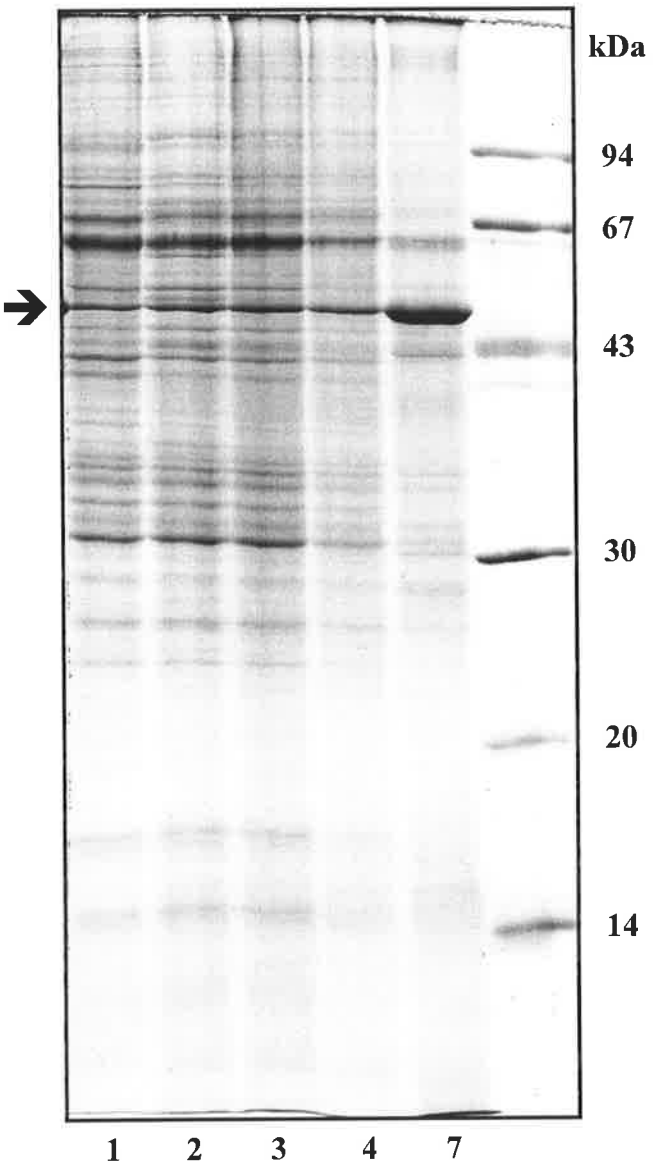

Figure 4.2 Distribution of a major membrane protein in a Percoll® density gradient.

Membrane proteins from the Percoll® density gradient of cytoplasmic organelles in a placental granular fraction (*Figure 4.1*) were separated by SDS-PAGE. The lane numbers indicate the corresponding fractions of the Percoll® density gradient. Samples (50 µg) were resolved for 4 h at 400 V on a 16x20 cm 12.5% polyacrylamide gel and stained with Coomassie Brilliant Blue G-Colloidal. A prominent protein of 49 kDa in relative molecular mass is indicated by the arrow.

4.4.1.2 Identification of a major protein isolated from lysosomal preparations.

The identity of the 49 kDa protein was determined by *N*-terminal sequencing (*Table 4.1*) to be cholesterol desmolase. The 19 *N*-terminal residues sequenced were identical to the *N*-terminus of mature human cholesterol desmolase (Morohashi *et al.* 1987) of approximately 56 kDa (Morohashi *et al.* 1984). The extent of the accumulation of this protein in the lysosomal fraction varied between preparations. Cholesterol desmolase is also known as the cytochrome P450 side-chain-cleaving enzyme (P450scc).

Table 4.1 N-terminal sequence of an abundant protein from a lysosomal membrane preparation.

The lysosomal protein fraction containing cholesterol desmolase was separated by SDS-PAGE, transferred to PVDF, and the Coomassie blue stained band cut out for *N*-terminal sequencing. Sequencing was performed at CSL Ltd., Parkville, Victoria, Australia.

***N*-terminal sequenced**	**Protein identified**
ISTRSPRPFNEIPSPGDNG	Human Cholesterol Desmolase

4.4.1.3 Western blot analysis of cholesterol desmolase in Percoll® fractions.

Western blots were kindly probed with anti-cholesterol desmolase antibodies in Dr. Ray Rodgers' laboratory, Department of Medicine, Flinders University of South Australia.

Western blot analysis of cholesterol desmolase was performed (Rodgers *et al.* 1988) on placental granular fractions separated on a secondary Percoll® density gradient (*Figure 4.3*). Cholesterol desmolase was detected at an apparent relative molecular mass of 54 kDa in all of the Percoll® fractions (lanes 1-8). Bovine corpus luteum loaded as a positive control contained P450scc at a molecular mass of 58 kDa. This particular preparation of organelles did not show the same distribution of this major protein as was seen in *Figure 4.2*; this protein was not obviously raised in any fraction (data not shown). It did show however, several

additional proteins of 42, 38, 25 and 22 kDa in the densest or lysosomal-richest fraction (lane 8). These additional lower molecular mass proteins were detected on the Western blot, which suggested that some of the cholesterol desmolase had been partly degraded in the lysosome. A large smear of cholesterol desmolase was also detected in this fraction which migrated only a small distance into the resolving gel.

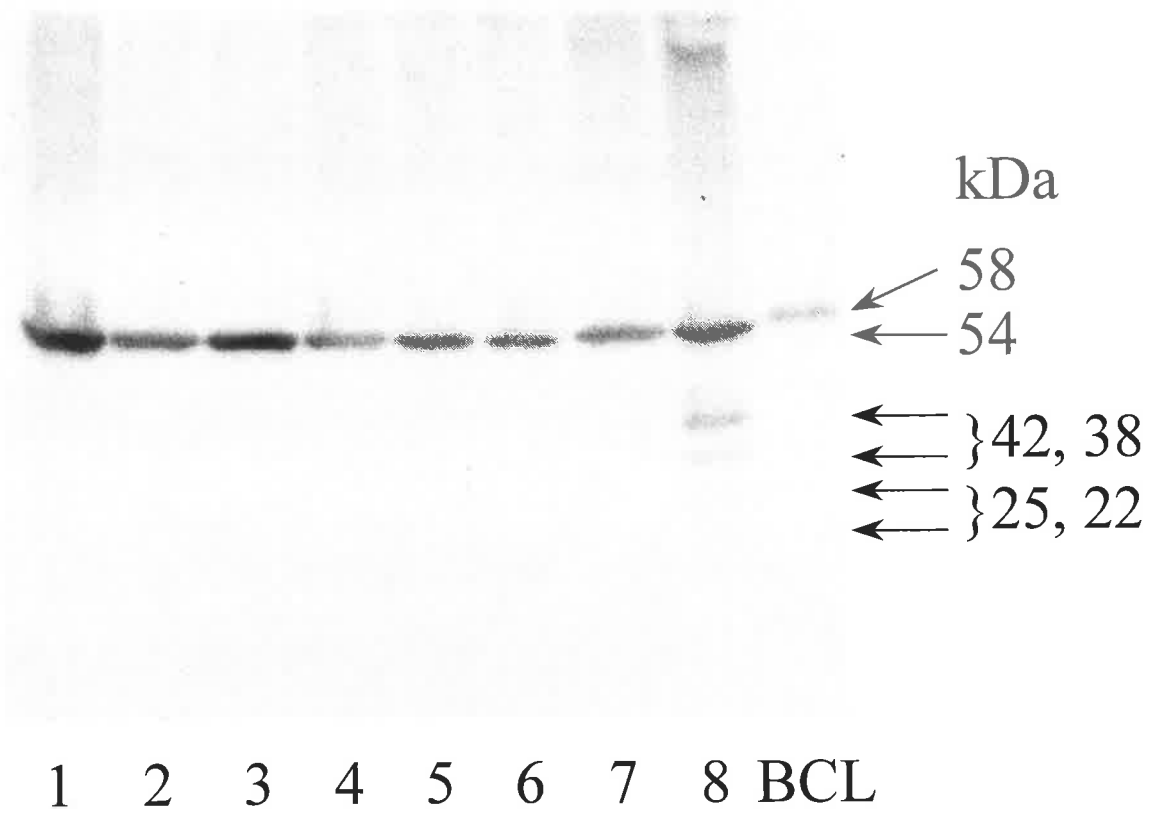

Figure 4.3 Western blot analysis of fractions from a secondary Percoll® density gradient with an anti-cholesterol desmolase monoclonal antibody.

Membrane proteins (100 μg) from a Percoll® density gradient of cytoplasmic organelles were separated by SDS-PAGE. The lane numbers correspond to the fractions of a Percoll® gradient like those illustrated in *Figure 4.1*. A bovine corpus luteum (BCL) sample (10 μg) was similarly subject to SDS-PAGE. The samples were resolved on a mini gel (10% polyacrylamide) at 200 V and transferred to PVDF membrane in CAPS buffer (20% methanol, 10 mM CAPS-NaOH, pH 11) at 250 mA for 1 h. The blotted PVDF membrane was probed with an anti-cholesterol desmolase monoclonal antibody, which was detected with an iodinated goat-anti-rabbit antibody. The immunoblot was autoradiographed and developed using Kodak XAR film.

4.4.1.4 Affinity labelling of anion transporters.

A strategy used for identifying proteins is to label the proteins of interest with a compound that has a specific affinity for those proteins. A number of membrane proteins have been identified with such a strategy. The glucose transporter in rat adipocytes was identified and characterised by cross-linking to cytochalasin B (Horuk *et al.* 1983). In chloroplasts the anion transport inhibitor DIDS, only bound to the phosphate translocator proteins on the inner membrane of the chloroplast envelope (Rumpho and Sack 1989).

Anion exchange inhibitors have been shown to bind to specific amino acid residues of anion transporters, for example the disulphonic stilbene derivative H_2DIDS reacts with lysine residues to form a covalent bond (Okubo *et al.* 1994). The lysosomal sulphate transporter can also be inhibited by anion exchanger inhibitors (*Section 3.4.4.6*). More specifically the sulphate transporter in placental lysosomes was sensitive to the anion exchange inhibitors phenylglyoxal, DIDS and SITS (*Section 3.4.4.6*).

Membrane proteins from selected Percoll® gradient fractions were incubated with radio-labelled anion exchange inhibitors, separated by SDS-PAGE and detected by fluorography. Membrane proteins incubated with [^{14}C]-phenylglyoxal, resolved by SDS-PAGE and subject to fluorography are shown in *Figure 4.4*. Many proteins appear to be labelled non-specifically by phenylglyoxal. The quantities of proteins labelled at the various molecular masses appeared to reflect the quantities of proteins stained by Coomassie blue at those molecular masses (data not shown). Coomassie blue staining did not quench the signal detected on autoradiographic film. Membrane proteins labelled with [$^{3}H_2$]-DIDS showed a pattern of labelling similar to that seen with phenylglyoxal.

To increase the specificity of labelling with [$^3H_2$]-DIDS, membrane proteins were labelled in two stages. In the first stage membrane proteins were labelled in the presence of sulphate with unlabelled DIDS. The rationale for this approach was that the sulphate would protect the proteins of interest from being labelled and the DIDS would block the non-specific proteins. The proteins were then washed to remove the sulphate and the unbound DIDS. In the second stage the washed proteins were incubated with [$^3H_2$]-DIDS to label the proteins formerly protected by sulphate. The population of proteins labelled under these conditions again did not appear to be specific. The non-specific binding of the anion exchangers identified too many proteins to enable the detection of the sulphate transporter. The sulphate transport proteins needed to be identified with a more specific tool such as an antibody.

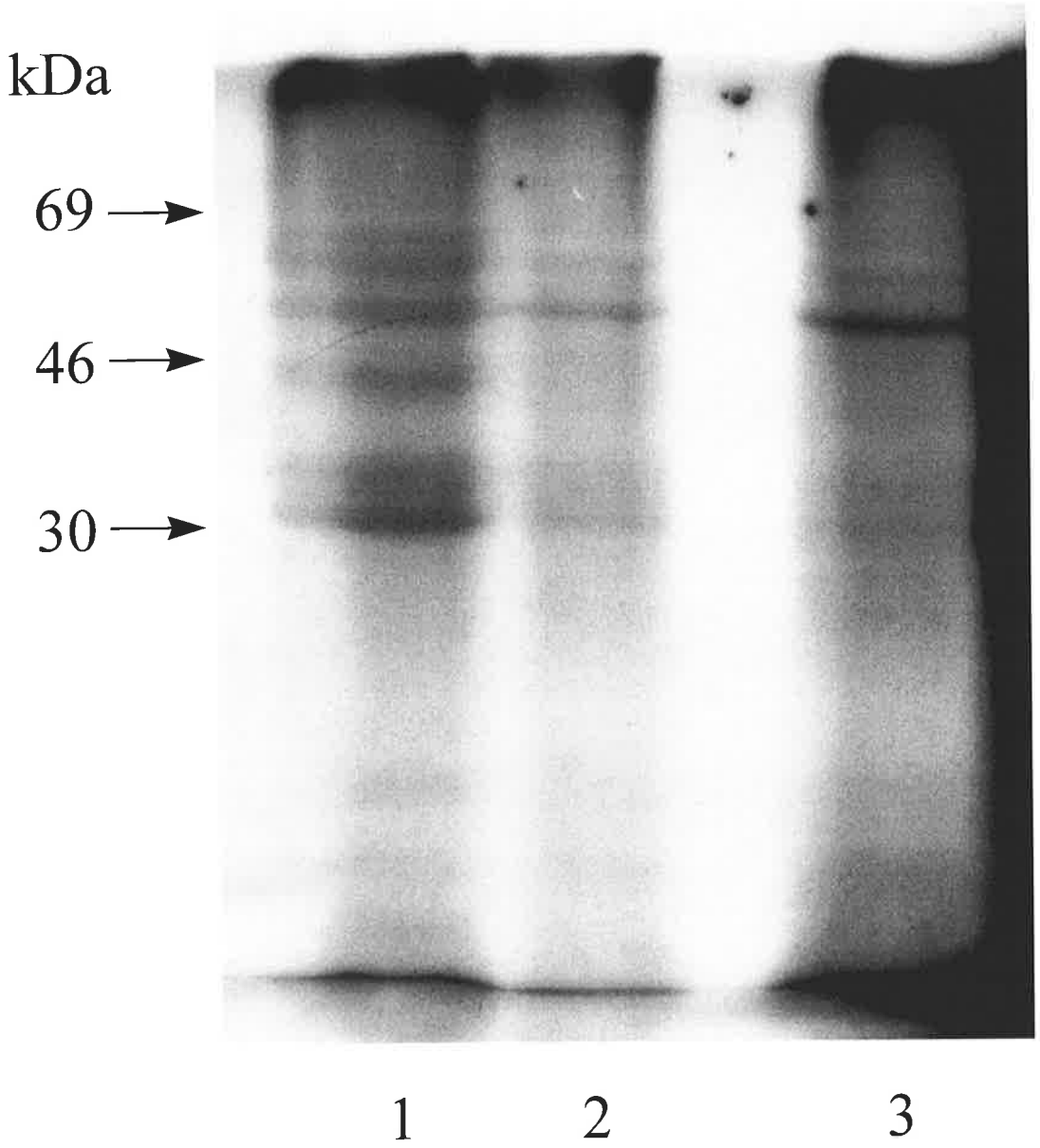

Figure 4.4 Membrane proteins labelled with [^{14}C]-phenylglyoxal.

Membrane proteins (100 µg) from fractions 1, 4 and 6 of the Percoll® gradient shown in *Figure 4.1* were labelled with phenylglyoxal ($C_6H_5{}^{14}COCHO$). Proteins were labelled by incubation in 0.5 mM [^{14}C]-phenylglyoxal (888 MBq.mmol^{-1}, 24 mCi.mmol^{-1}), 20 mM HEPES, pH 7, at 37°C for 2 h. The three labelled fractions (Lanes 1, 2 and 3 respectively) were separated by SDS-PAGE (large 10% polyacrylamide gel), at 30 mA. The gel was fixed, incubated in Amplify™, dried under vacuum at 70°C, and fluorography was performed at -80°C for 20 h on Kodak XAR film (*Section 4.3.1*).

4.4.2 Immunological search for the lysosomal anion exchanger.

4.4.2.1 Production of a polyclonal antibody against the anion exchanger Band 3.

Band 3 protein was kindly donated by Dr. Rob McPherson in Dr. Leann M. Tilley's laboratory, Department of Biochemistry, La Trobe University, Bundoora, Victoria, Australia.

At this stage in the project the protein most related to the lysosomal sulphate transporter was thought to be the erythrocyte anion exchanger, also known as Band 3 (*See Section 1.4.1.1).* It had been demonstrated that Band 3 is able to transport sulphate and is sensitive to the same anion exchange inhibitors as the lysosomal sulphate transporter (Gartner *et al.* 1997; Jennings and Al Rhaiyel 1988; Koetters *et al.* 1995a; Scheuring *et al.* 1986, 1988).

Antibodies against membrane transporters are commonly employed for their identification. The tonoplast sucrose carrier in sugarcane is an example (Getz *et al.* 1994). Antibodies to Band 3 have identified an immunoreactive anion transporter in rat kidney. More specifically, localisation was to the basolateral plasma membrane of intercalated cells of the distal tubule and collecting ducts (Drenckhahn *et al.* 1985). Kellokumpu *et al.* (1988) identified a protein with antibodies to Band 3 in Golgi membranes, and speculated that it was involved in sulphate transport. Ostedgaard *et al.* (1991) identified a protein antigenically related to Band 3 expressed in mitochondria. The variable tissue expression of this protein was strongest in kidney mitochondrial intercalated cells of the collecting duct. The detected protein was again thought to play a role in anion transport. The cross-reactivity of proteins to Band 3 antibodies was encouraging, particularly as two of these findings were in cytoplasmic organelles. It was therefore decided to look for cross-reactivity between antibodies to Band 3 and the lysosomal membrane proteins.

Band 3 antigen was prepared by treating erythrocyte ghost membranes, which contain 25% Band 3 protein, with 1 mM CAPS-NaOH, pH 12, to remove peripheral proteins. The

resulting antigen preparation contained 95% Band 3 and was used to raise polyclonal antibodies in rabbit. Polyclonal antibodies to the Band 3 protein were prepared as described in *Section 4.3.2*. The anti-Band 3 serum had a titre of greater than 1 in $1x10^4$ against the Band 3 antigen, 1 in $1.28x10^4$ against the Band 3 membrane domain (prepared by a trypsin digest), and 1 in 200 against BSA. Antibody titres reported are the dilution that gave a signal two standard deviations above background in a direct enzyme-linked immuno-sorbant assay (ELISA). Background ELISA readings were those taken in the absence of the anti-Band 3 antibody.

4.4.2.2 Inhibition of transport by antibody interaction.

To test whether the Band 3 antibody was binding to the sulphate transporter, its effect on lysosomal sulphate transport rates was examined. The antibodies diluted one hundred fold were incubated with lysosomes under conditions of sulphate uptake, without stimulation, and with *trans* and *cis* stimulation (*Section 3.4.4.4*). Incubation with the polyclonal antibody increased the amount of sulphate retained when lysosomes were filtered from the incubation mixture. Transport inhibition could not be measured as the sulphate appeared to bind the polyclonal serum, which then bound to the filter used to separate the incubation solution from the lysosomes. The Band 3 polyclonal antibody was therefore employed to identify proteins by Western blot analysis.

4.4.2.3 Fractionation and preparation of lysosomal membrane proteins.

Western blot analysis was initially performed on either membrane proteins from single fractions of a Percoll® density gradient, or pooled Percoll® density gradient fractions that underwent chromatographic fractionation. The single membrane protein fractions were selected to be the most enriched in either lysosomes or mitochondria. The pooled fractions

were the mitochondria-enriched from the top of the secondary Percoll® gradient or the lysosomal fraction from the bottom or less buoyant part of the secondary Percoll® gradient. The comparison of lysosomal and mitochondrial-enriched fractions in Western blot analysis further clarified whether the detected proteins were lysosomal or mitochondrial.

Chromatographic separation of pooled fractions is summarised in *Figure 4.5*. The membrane proteins were separated from the luminal or matrix proteins by repeated freezing and thawing in high salt and then the sedimentation of either lysosomal or mitochondrial-enriched membranes (*Section 2.2.4.1*). Membrane proteins were extracted from the membrane and solubilised with Thesit® (*Section 2.2.5.1*), the detergent-soluble proteins were separated into two fractions, those that bound to Concanavalin A-Sepharose (Con A-Sepharose), and those that flowed through or did not bind (*Section 2.2.5.2*). The protein that bound to Con A-Sepharose was then separated into those that bound to the Red Dye matrix and those that did not (*Section 2.2.5.3*). Approximately half of the membrane proteins were soluble in Thesit®, and of the soluble fraction, approximately 20% bound to Con A-Sepharose. Approximately 30% of the protein that bound to Con A-Sepharose also bound to the Red Dye matrix.

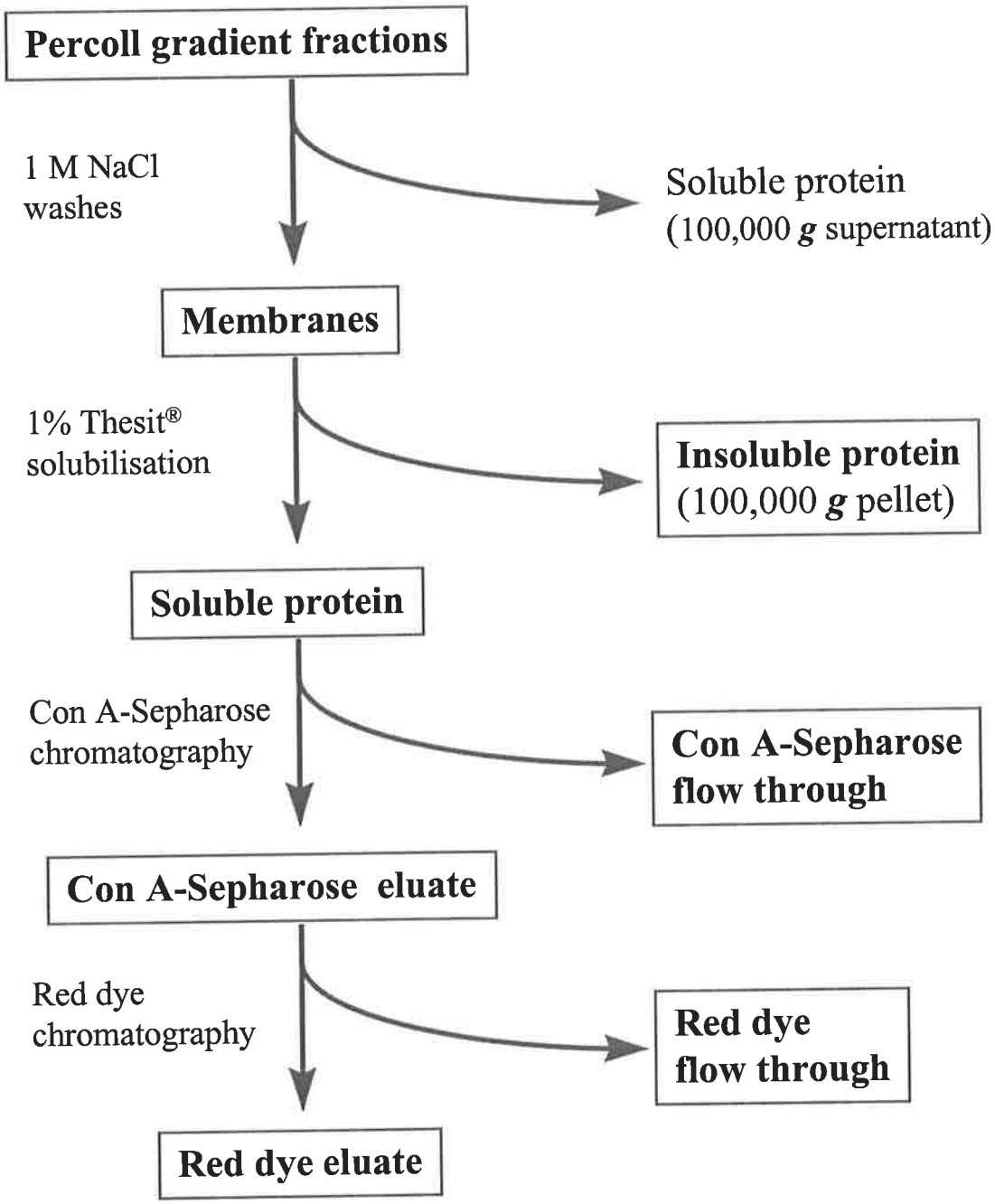

Figure 4.5 Flow chart of membrane protein fractionation.

Selected fractions from a Percoll® density gradient were pooled and the soluble proteins were separated from the membrane proteins by two successive salt washes, followed by sedimentation. The soluble supernatant proteins were discarded and the membrane pellet retained. The membrane pellet was stirred overnight in extraction buffer (1% (w/v) Thesit®, 10% (w/v) glycerol, 150 mM NaCl, 50 μM EDTA, 50 mM MOPS, pH 7) at 4°C. The Thesit® insoluble fraction was pelleted (100,000 ***g***, 1 h) and the soluble fraction was fractionated into a Con A-Sepharose flow through and a Con A-Sepharose elution (eluted with 10% methyl α-D-mannopyranoside). The fraction eluted from Con A-Sepharose was then fractionated into Red dye flow through and that eluted with 2 M NaCl (*See Sections 2.2.4.1 and 2.2.5 for detailed methods*).

4.4.3 Western blot analysis of membrane fractions with an anti-Band 3 polyclonal antibody.

4.4.3.1 Identification of Band 3 cross-reactive membrane proteins by SDS-PAGE and Western blot analysis.

Western blot analysis of lysosomal membrane proteins, mitochondrial-enriched membrane proteins and Band 3 protein was performed with the anti-Band 3 polyclonal antibody (*Figure 4.6*). The lysosomal- and mitochondrial-enriched membrane proteins were from single fractions, richest in the respective organelles from a secondary Percoll® density gradient (*See Section 3.4.1*). The apparent molecular masses of the proteins detected with the anti-Band 3 polyclonal antibody are listed in *Table 4.2*. Two proteins were detected in a sample of Band 3 antigen used to raise the anti-Band 3 antibodies, one of 95 kDa and the other 46 kDa. The 46 kDa protein represents the membrane domain of Band 3. In the lysosomal sample a 46 and a 44 kDa protein were detected. As Band 3 is degraded in the lysosome (Hare and Huston 1985; Madsen *et al.* 1992; Turrini *et al.* 1991) the proteins common to the lysosomal and Band 3 samples, were most probably Band 3. Ostedgaard *et al.* (1991) reported a 45 kDa protein antigenically related to Band 3 however, which was located in the kidney mitochondria. In both the lysosomal- and mitochondrial-enriched samples a 28 kDa protein was detected although it was more abundant in the mitochondrial-enriched sample. Three candidate proteins with approximate molecular masses of 86, 80 and 77 kDa (candidates 1, 2 and 3, respectively) were only detected in the lysosomal sample. In both the mitochondrial-enriched and lysosomal fractions a 58 kDa protein (candidate 4) was also detected, although a stronger signal was seen in the lysosomal sample.

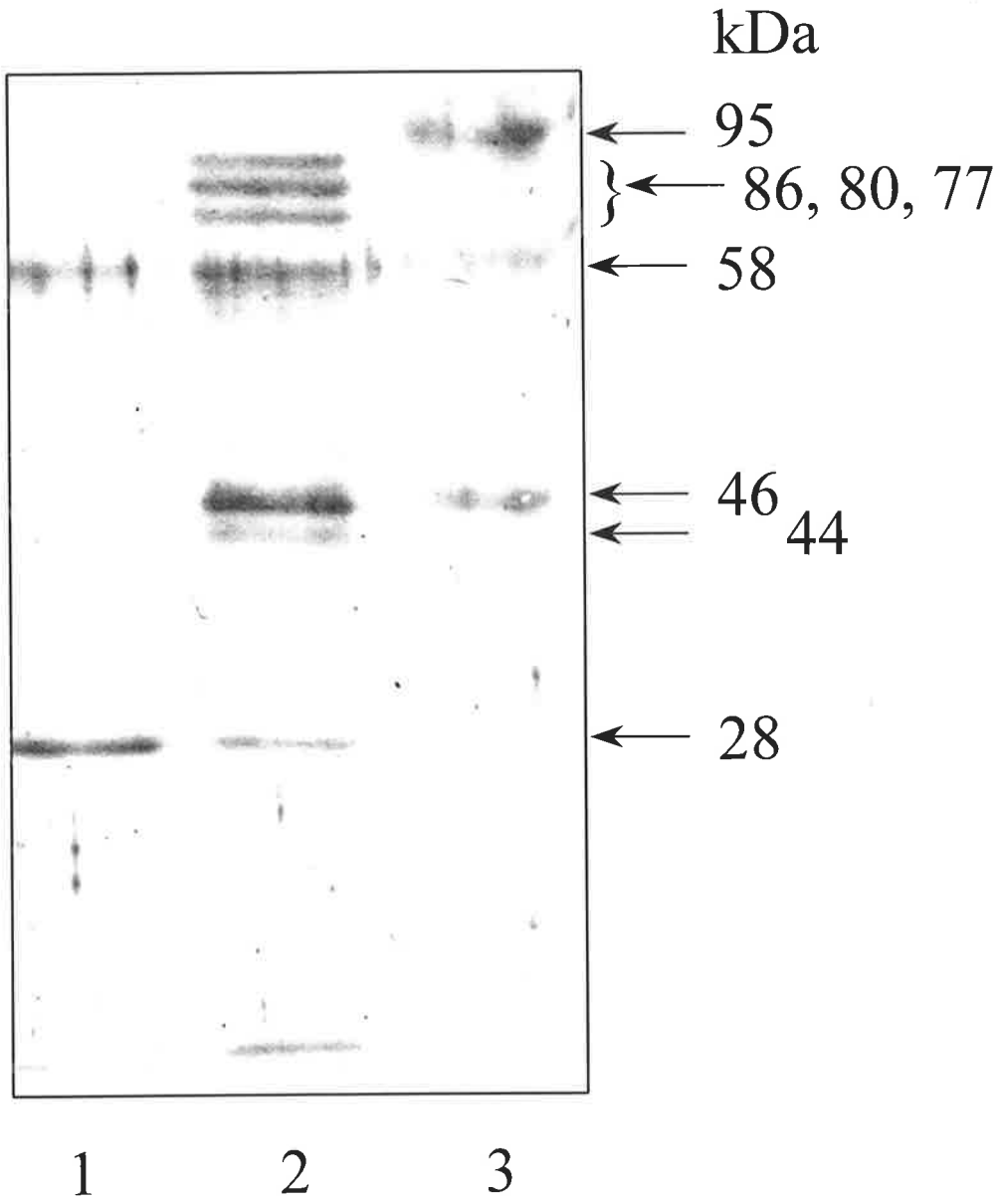

Figure 4.6 Western blot analysis of mitochondrial-enriched and lysosomal membrane proteins with an anti-Band 3 polyclonal antibody.

Membrane proteins were separated by SDS-PAGE on a mini gel (10% acrylamide) at 20 mA per gel, and transferred to PVDF in CAPS buffer at 150 mA for 2 h. Mitochondrial-enriched (1) and lysosomal (2) membrane proteins (50 µg), and 5 µg of Band 3 (3) protein were loaded. Western blot analysis was performed as described in *Section 2.2.10.2.1*. The anti-Band 3 polyclonal serum was used at a one hundred fold dilution and incubated for 90 min at room temperature. The secondary sheep anti-rabbit immunoglobulin antibody (conjugated to HRP) was used at a one hundred fold dilution, and later visualised with chloro-1-napthol (*Section 2.2.10.3*).

Table 4.2 Band 3 cross-reactive proteins.

Relative molecular masses of cross-reactive proteins detected from the Western blot analysis (*Figure 4.6*) of mitochondrial-enriched and lysosomal membrane proteins. Whole Band 3 protein was used as a positive control.

kDa	Mitochondrial	Lysosomal	Band 3
95			✓
86		✓	
80		✓	
77		✓	
58	✓	✓	✓
46		✓	✓
44		✓	
28	✓	✓	

Lysosomal luminal proteins are all glycosylated (*Section 1.3.2.3*) and it is thought that most lysosomal membrane proteins will also be glycosylated. Mitochondrial membrane proteins however, are not trafficked through the endoplasmic reticulum and Golgi apparatus and therefore, do not contain complex *N*-linked glycosylation, although *O*-linked glycosylation can occur in the cytoplasm. To enrich lysosomal membrane proteins and remove contaminating mitochondrial proteins, lysosomal membrane proteins were divided into Con A-Sepharose binding and non-binding fractions. Proteins that bind to Con A-Sepharose are glycosylated and are therefore less likely to be mitochondrial.

Membrane proteins were solubilised with Thesit® before they were loaded onto a Con A-Sepharose column. Not all membrane proteins were soluble in Thesit®, and so it was necessary to establish whether the Band 3 cross-reactive proteins were Thesit® soluble or insoluble. Hence, a Western blot analysis using Band 3 polyclonal antibodies was repeated on the same highly mitochondrial-enriched and lysosomal samples alongside Thesit® soluble

and insoluble fractions of these samples (*Figure 4.7*). As no proteins of interest were detected in the lysosomal Thesit® insoluble fraction, detection of Band 3 cross-reactive proteins could be looked for in the Thesit® soluble Con A-Sepharose fractions.

Additional proteins were detected in the soluble fractions (*Figure 4.7*), as a longer development time was allowed during the detection (by colour development) of the secondary antibody. The 77, 86, and 80 kDa proteins (candidates 1, 2 and 3) previously detected in the lysosomal membrane fraction (*Figure 4.6*) were again detected. The abundance of these proteins in the mitochondrial-enriched fraction was very small compared with the lysosomal fraction. The 28 kDa protein was not seen in either the mitochondrial Thesit® insoluble or Thesit® soluble fraction that did not bind Con A-Sepharose.

Western blot analysis with anti-Band 3 antibody was then performed on samples further enriched by Con A-Sepharose to narrow the field of candidate anion exchange proteins. *Figure 4.8* displays such an analysis, with only one major cross-reactive protein of 58 kDa (candidate 4) seen. The 58 kDa protein was seen however, in both the mitochondrial-enriched and lysosomal, Con A-Sepharose flow through and eluate fractions.

Proteins cross-reactive with anti-Band 3 antibodies, that appeared to be lysosomal and not mitochondrial, were the 86, 80, 77, 46, and 44 kDa in size. No lysosomal candidate proteins were detected in the Thesit® insoluble fraction. The 58 kDa candidate protein does not appear to separate with the lysosomal fractions; and the 28 kDa candidate protein was detected in the mitochondrial fractions, and is found in the Con A Sepharose flow through.

Figure 4.7 Anti-Band 3 Western blot analysis of membrane proteins.

Membrane proteins were separated by SDS-PAGE (10% polyacrylamide mini gel) at 20 mA per gel. Approximately 3 μg of each sample has been silver stained (A), and 50 μg transferred (150 mA, 1 h) to a PVDF membrane (*Section 2.2.6.1*) for Western blot analysis (B). Samples analysed from a Percoll® gradient were: mitochondrial-enriched membrane proteins (1); lysosomal membrane proteins (2); mitochondrial-enriched Con A-Sepharose non-binding membrane proteins (3); Thesit® insoluble lysosomal membrane proteins (4); Thesit® insoluble mitochondrial-enriched membrane proteins (5); and molecular weight markers (6). The anti-Band 3 polyclonal serum and the secondary sheep anti-rabbit antibody were used at a one hundred fold dilution, and visualised with chloro-1-napthol (*Section 2.2.10.2.1*).

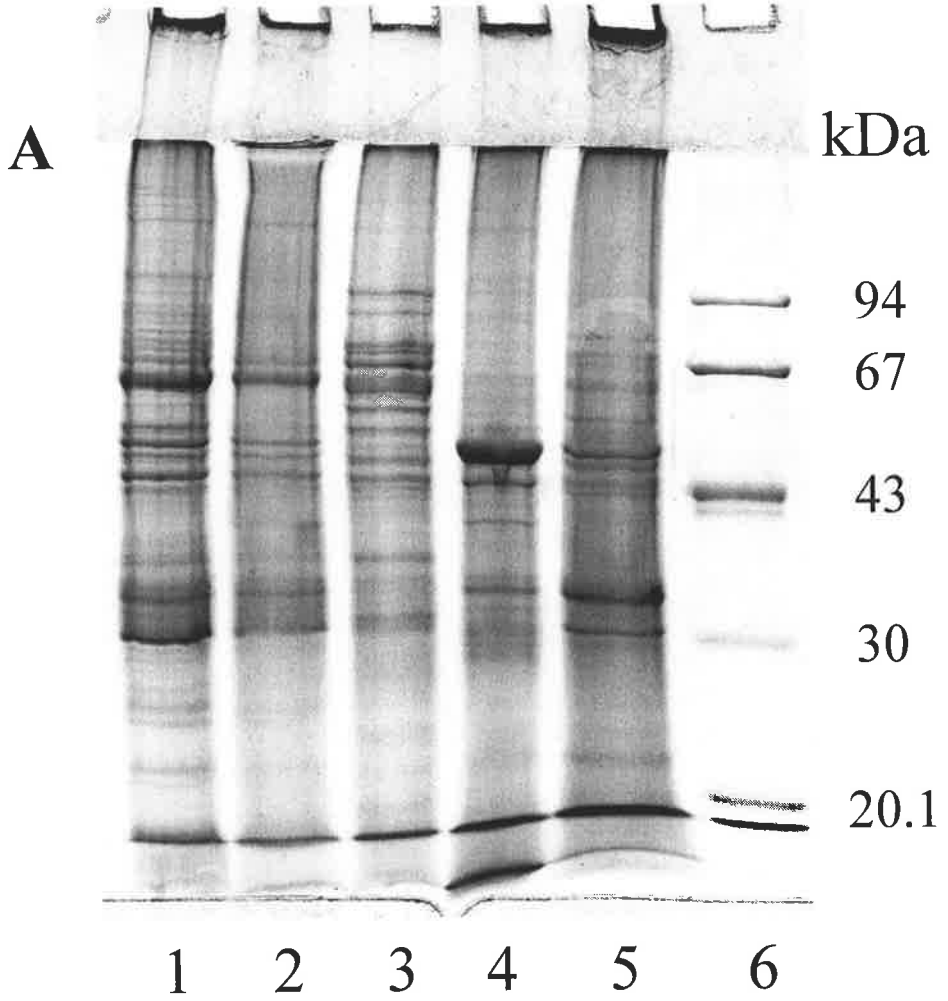
A
kDa
94
67
43
30
20.1
1 2 3 4 5 6
B
kDa
80
53
37
28
86
58
47
43
26
20
1 2 3 4 5

Figure 4.8 Anti-Band 3 Western blot analysis of membrane proteins divided by Con A-Sepharose.

Mitochondrial-enriched (2-4), and lysosomal (5-8) samples were separated by SDS-PAGE (10% polyacrylamide, mini gel) at 20 mA per gel. Approximately 3 μg of each sample has been silver stained (A), and 50 μg transferred (150 mA, 1 h) to a PVDF membrane (*Section 2.2.6.1*) for Western blot analysis (B). The samples were fractionated into those that did not bind to Con A-Sepharose (2 and 5) and those that were eluted from Con A-Sepharose with 10% (w/v) methyl α-D-mannopyranoside (3, 4, 6, 7) or 20% (w/v) methyl α-D-glucopyranoside (8). Lanes 3 and 4, and 6 and 7 are duplicates. The anti-Band 3 polyclonal serum and the secondary sheep anti-rabbit antibody were used at a one hundred fold dilution, and visualised with chloro-1-napthol (*Section 2.2.10.2.1*).

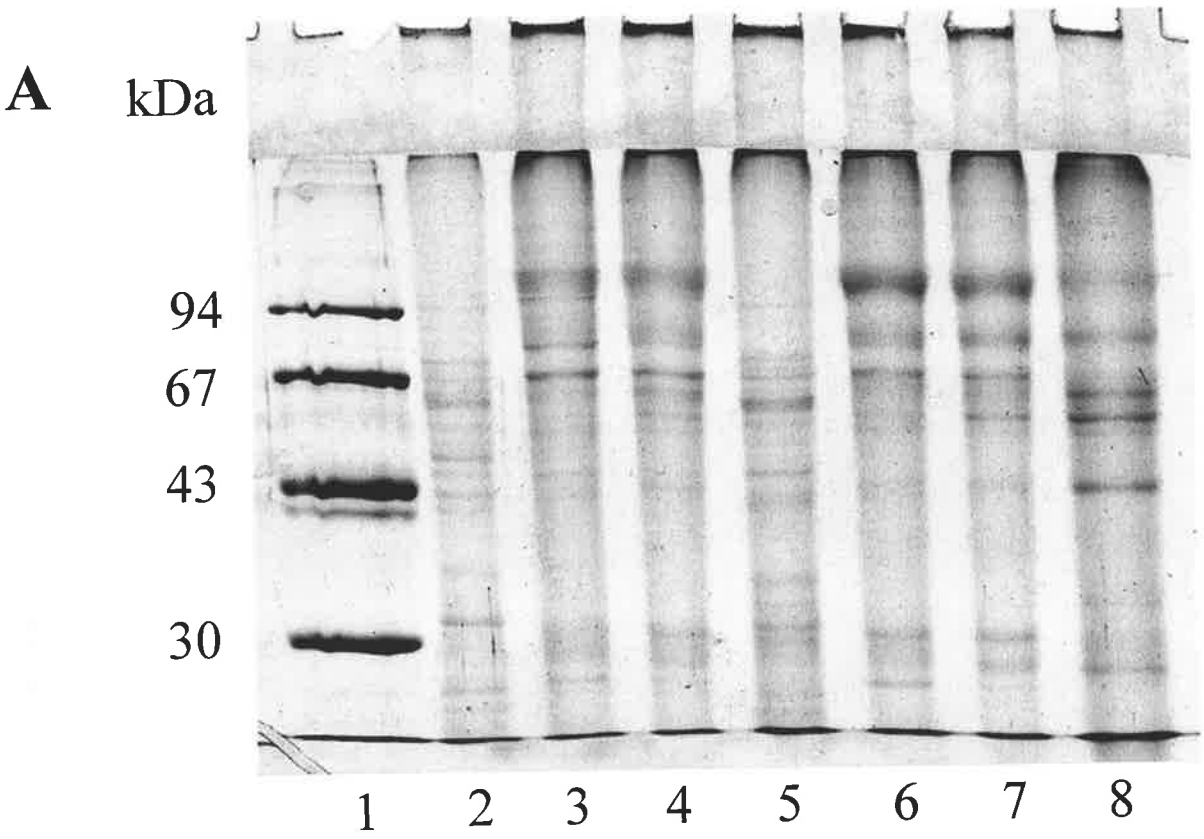
A
kDa
94
67
43
30
1 2 3 4 5 6 7 8

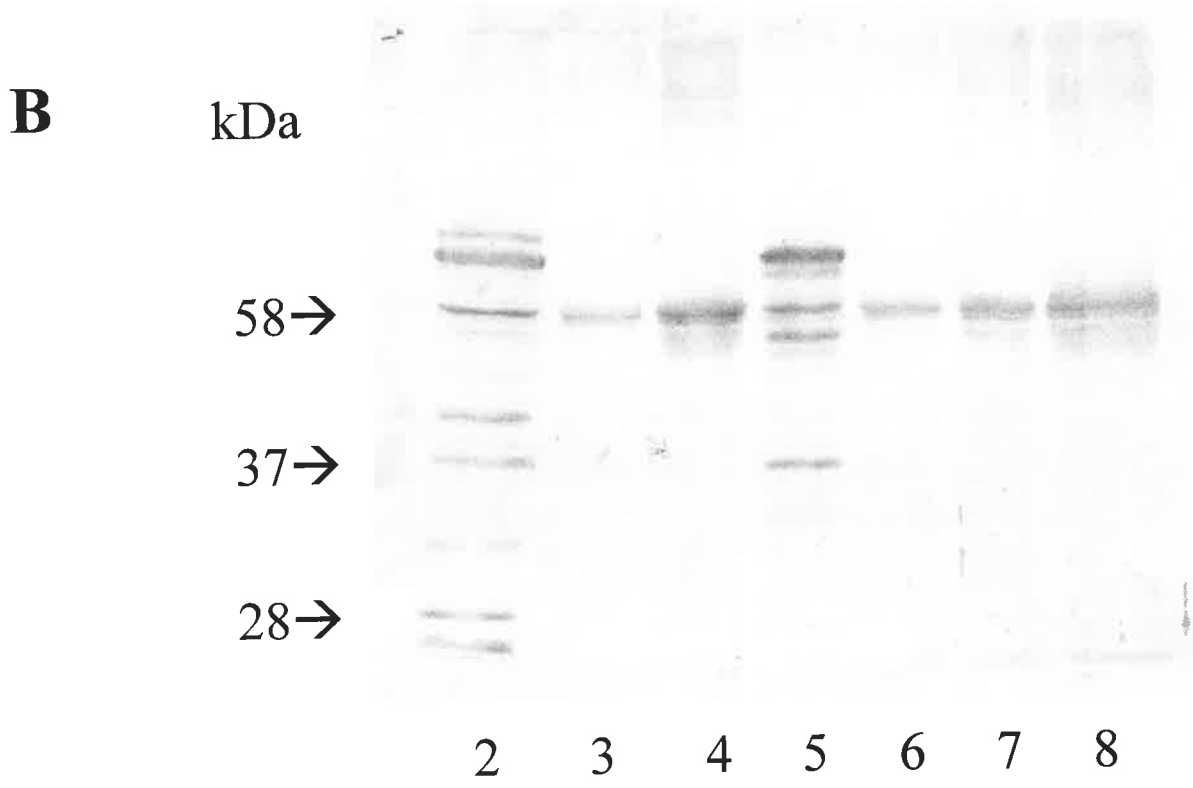
B
kDa
58→
37→
28→
2 3 4 5 6 7 8

4.4.3.2 Western blot analysis of lysosomal membrane proteins.

To further clarify the picture seen with Western analyses of SDS-PAGE separated samples, Western blot analyses of samples separated by 2-DE (*Section 2.2.6.2*) were performed. The advantage of 2-DE over SDS-PAGE is the ability to determine the number of proteins seen at a particular molecular mass due to each protein's distinct isoelectric point(s). Proteins were separated in isoelectric focusing gels (primary dimension) followed by a SDS-PAGE separation (secondary dimension).

4.4.3.2.1 Western blot analysis of lysosomal Con A-Sepharose eluate.

Lysosomal membrane proteins that bound Con A-Sepharose were analysed by Western blot analysis after separation by 2-DE (*Figure 4.9*). Three closely grouped discrete spots were observed on the Western blot, one of which was smeared a short distance in the pI dimension. These cross-reactive proteins all had the same molecular mass of 58 kDa (candidate 4). The pI values determined for these proteins were from 5.2 to 5.3. The corresponding proteins on the silver stained gel were located by molecular mass, pI and comparison of the 2-D patterns.

Figure 4.9 Anti-Band 3 Western blot analysis of Con A-Sepharose eluate separated by 2-DE.

Thesit® soluble lysosomal membrane proteins that were bound to Con A-Sepharose were separated by 2-DE (*Section 2.2.6.2*) and transferred in a CAPS buffer at 250 mA for 1 h to PVDF. Silver stained proteins (A) labelled 1, 2 and 3, cross-reacted with anti-Band 3 polyclonal antibodies (B). The isoelectric focusing gel contained 5% (v/v) 5-8 and 5% (v/v) 3-10 ampholytes. The second dimension (SDS-PAGE) mini gels (10% polyacrylamide) were electrophoresed at 20 mA per gel. The anti-Band 3 polyclonal serum and the secondary sheep anti-rabbit antibody were used at a one hundred fold dilution, and visualised with chloro-1-napthol (*Section 2.2.10.2.1*).

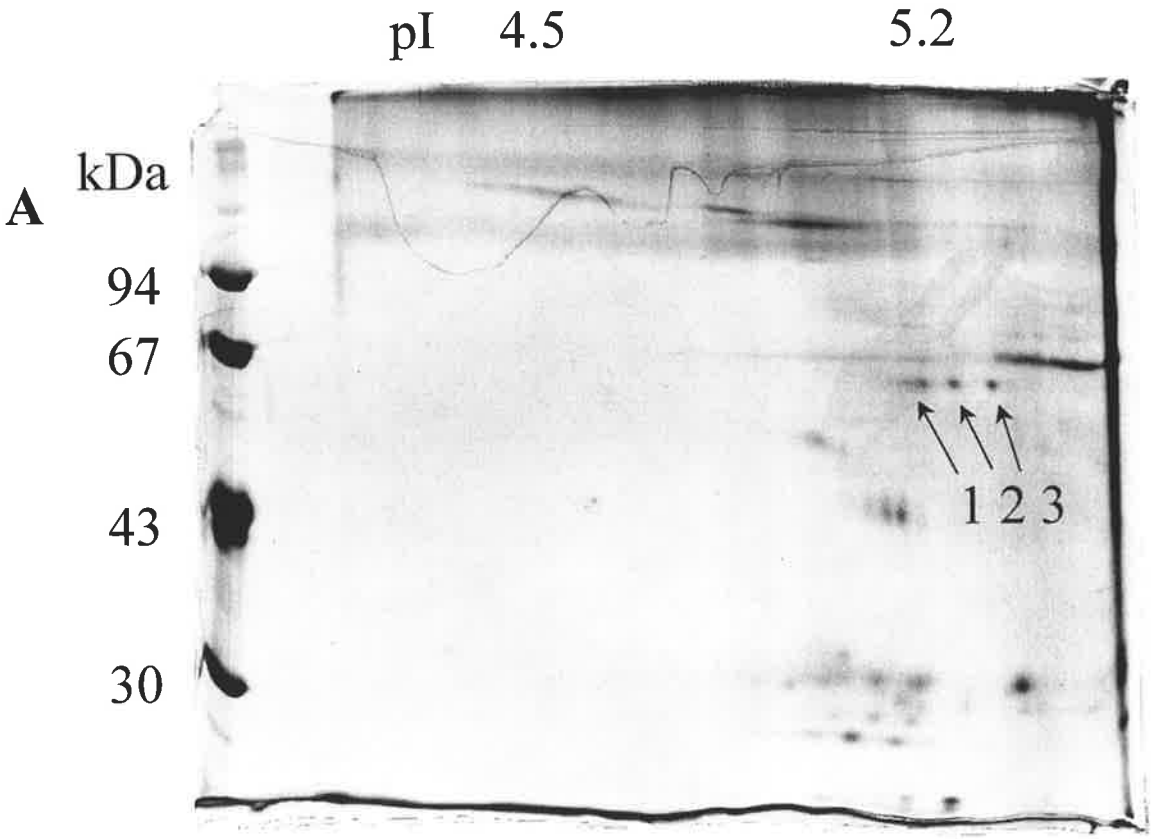
pI 4.5
5.2
A
kDa
94
67
43
30
1 2 3

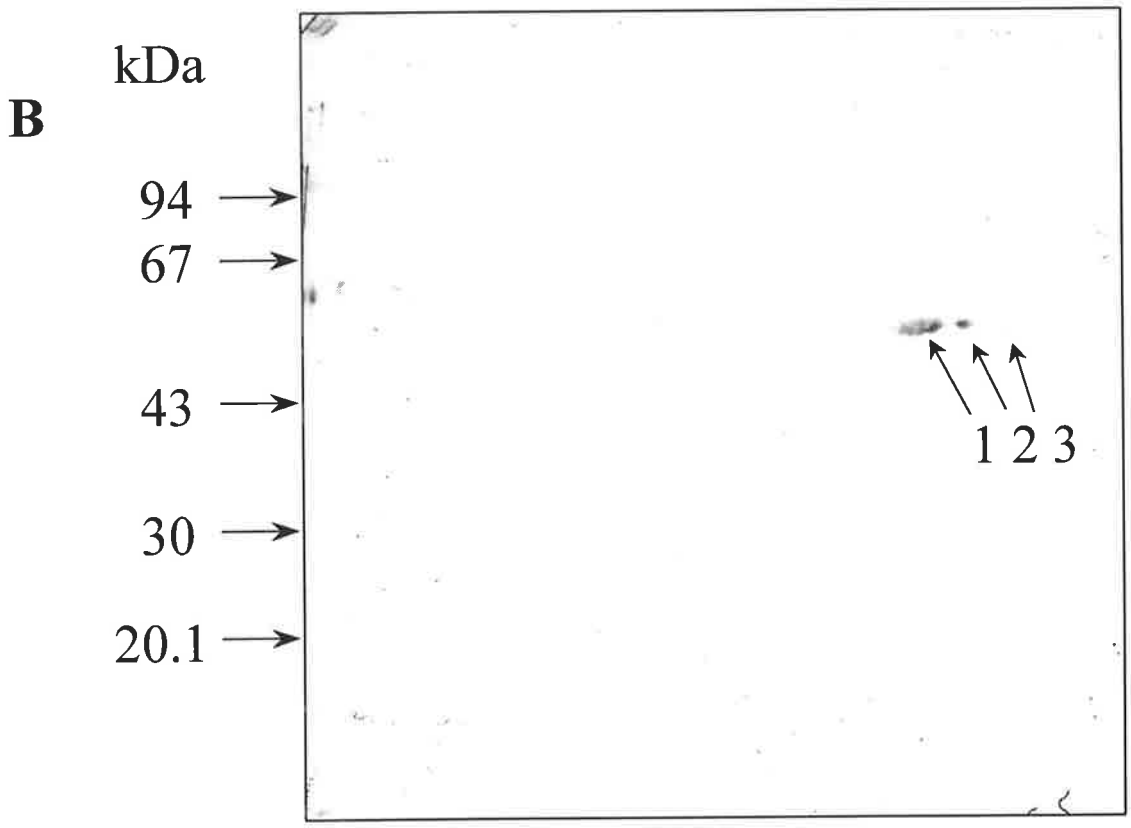
B
kDa
94
67
43
30
20.1
1 2 3

4.4.3.2.2 Investigation of Western blot analysis to increase sensitivity.

Some proteins detected by the chloro-1-napthol colour development (method described in *Section 2.2.10.3*) were faint and difficult to see on the Western blotted PVDF membrane. The proteins identified were easily visible if observed under UV light (Domingo and Marco 1989). Although this technique of viewing Western blots developed with chloro-1-napthol was significantly more sensitive, the image could not be recorded. A method recommended in a Western blot analysis kit by Cetus® Corporation (*Section 2.2.10.2.2*) was evaluated to increase the sensitivity of this colour development when viewed under normal white light. The essential difference between the methods is that the Cetus method uses more complex and concentrated blocking solution (1 M glycine, 5% milk, 5% FCS and 1% ovalbumin) and washing solution (0.1% milk, 0.1% ovalbumin and % FCS). The more general method blocked with 1% BSA in TBS, and washed with TBS. Antibody incubations in both methods were in their respective wash solutions. The Cetus® method unequivocally resulted in a stronger, clearer detection when developed with chloro-1-napthol and viewed under visible white light (*Figure 4.10*).

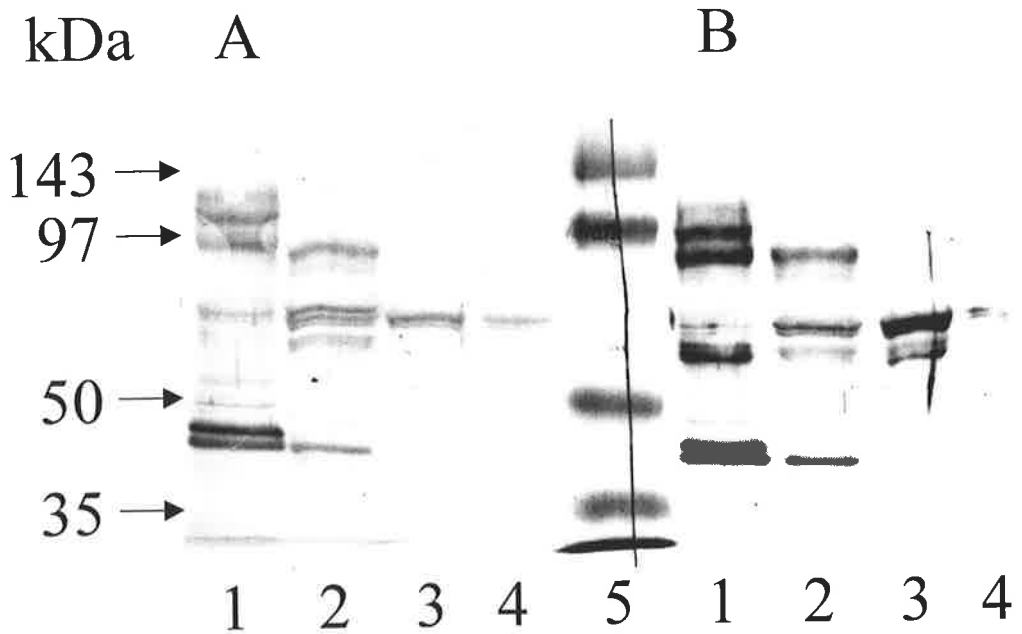

Figure 4.10 Comparison of two blocking methods in Western blots.

Duplicate samples of lysosomal membrane proteins (1); Con A-Sepharose non-binding (2); Con A-Sepharose binding (3); and Red Dye non-binding (4), were resolved by SDS-PAGE (10% polyacrylamide) at 30 mA per gel. After the transfer of samples to PVDF, the membrane was cut down the middle of the pre-stained molecular weight markers (5). Samples on one half (A) were blocked with 1% BSA in TBS for 1 h then washed three times for 10 min in TBS. Samples on the other half (B) were blocked with 1 M glycine, 5% (w/v) dried low fat milk, 5% (v/v) FCS and 1% (w/v) ovalbumin for 1 h, followed by three 5 min washes in PBS containing 0.1% (w/v) dried low fat milk, 1% (v/v) FCS, and 0.1% (w/v) ovalbumin. The primary anti-Band 3 antibody was diluted one hundred fold in the respective wash solutions and the membranes were incubated for 5 h at 25°C, followed by three 5 min washes. Both membrane halves (A and B) were incubated for 1 h at 25°C in the secondary antibody (sheep anti-rabbit) diluted one hundred fold in the respective wash solutions. Three 5 min washes in their respective wash solutions were followed by a 5 min wash in TBS. PVDF membranes were then developed with the 4-chloro-1-napthol colour reagent as described in *Section 2.2.10.2*.

4.4.3.2.3 2-D Western blot analysis of Red Dye matrix flow through proteins.

Experience in this laboratory has found that Red Dye No. 78 (*Section 2.2.5.3*) could sub-fractionate enriched lysosomal membrane proteins that bound Con A-Sepharose (*personal communication, Alison M. Whittle*). This resulted in two pools of further enriched lysosomal proteins (*See Figure 4.5 for chromatography flow chart*). The Red Dye flow through fraction, when analysed with anti-Band 3 antibody by Western blot analysis (one dimensional) revealed a 58 kDa protein (*Figure 4.10*). A Western blot analysis by 2-DE of the Red Dye flow through was therefore performed (*Figure 4.11*). A number of proteins were detected which could be located on a silver stain of a duplicate sample electrophoresed at the same time under the same conditions. As Western blot analysis can be more sensitive at detecting proteins than silver staining, a number of identified proteins low in abundance could not be located when silver stained. These low abundance proteins of approximately 80 kDa (candidate 2) were detected within the region shown by the triangle in *Figure 4.11* panel A. Two proteins (indicated by 1 and 2) were weakly detected by anti-Band 3 antibody, these however, could easily be seen by silver stain.

The 58 kDa protein detected by the anti-Band 3 polyclonal antibody was found to have three isoelectric points (5.2 to 5.3) in the lysosomal Con A Sepharose; however, it was not seen in the Red Dye flow through when resolved by 2-DE. The 80 kDa protein detected in a Red Dye flow through was too low in abundance to be by visualised by silver staining. The variation in the level of protein immuno-detection depends on: the method used for detection; the preparation of lysosomal membrane proteins, which would vary in abundance from individual to individual; and the method of resolution (SDS-PAGE or 2-DE).

Visualisation of secondary antibody with chloro-1-napthol was stronger when using a method (Cetus®) that employs blocking and washing solutions, which contain a larger concentration and variety of proteins.

Figure 4.11 Anti-Band 3 Western blot analysis of Red Dye flow through protein separated by 2-DE.

A sample (50 μg) of lysosomal membrane proteins that bound to Con A-Sepharose but did not bind to Red Dye were separated by 2-DE. The sample was silver stained (A) and subject to Western blot analysis (B). An IEF-gel containing ampholytes 5-8 (5%) and 3-10 (5%) was electrophoresed as described in *Section 2.2.6.2*. The proteins focused by the IEF-gel were separated in the second dimension by SDS-PAGE (10% polyacrylamide) at 30 mA per gel and transferred for 1.5 h at 250 mA in CAPS buffer to PVDF membrane. Western blot analysis was performed as described in *Section 2.2.10.2.2*. The anti-Band 3 antibody diluted one hundred fold was incubated at 25°C for 5 h. The secondary sheep anti-rabbit antibody was diluted one hundred fold and incubated for 1 h, prior to being visualised with 4-chloro-1-napthol colour reagent (*Section 2.2.10.2*). The triangle in panel A corresponds to the region of antibody clearly detected in panel B. The proteins indicated by 1 and 2 correspond to proteins weakly detected in panel B.

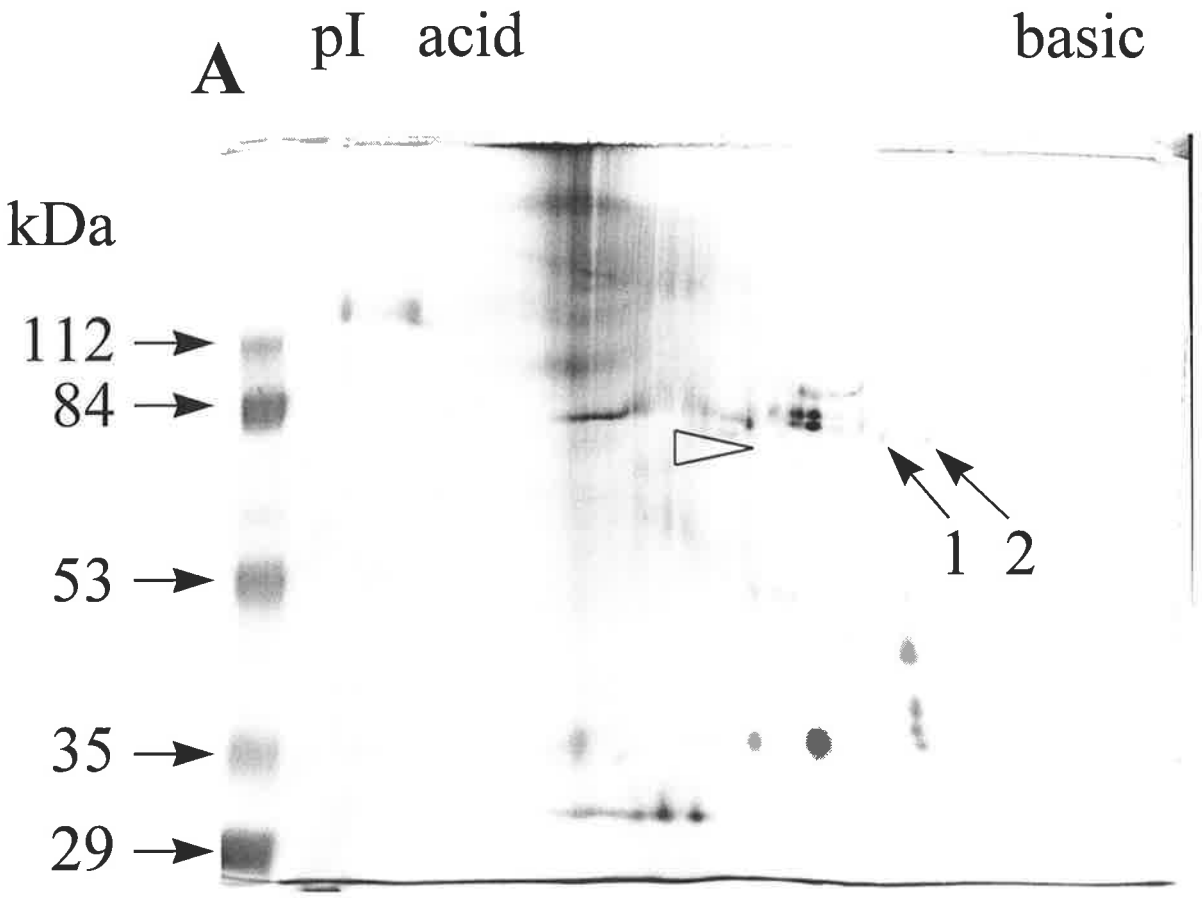
A
pI acid
basic
kDa
112
84
53
35
29
1 2

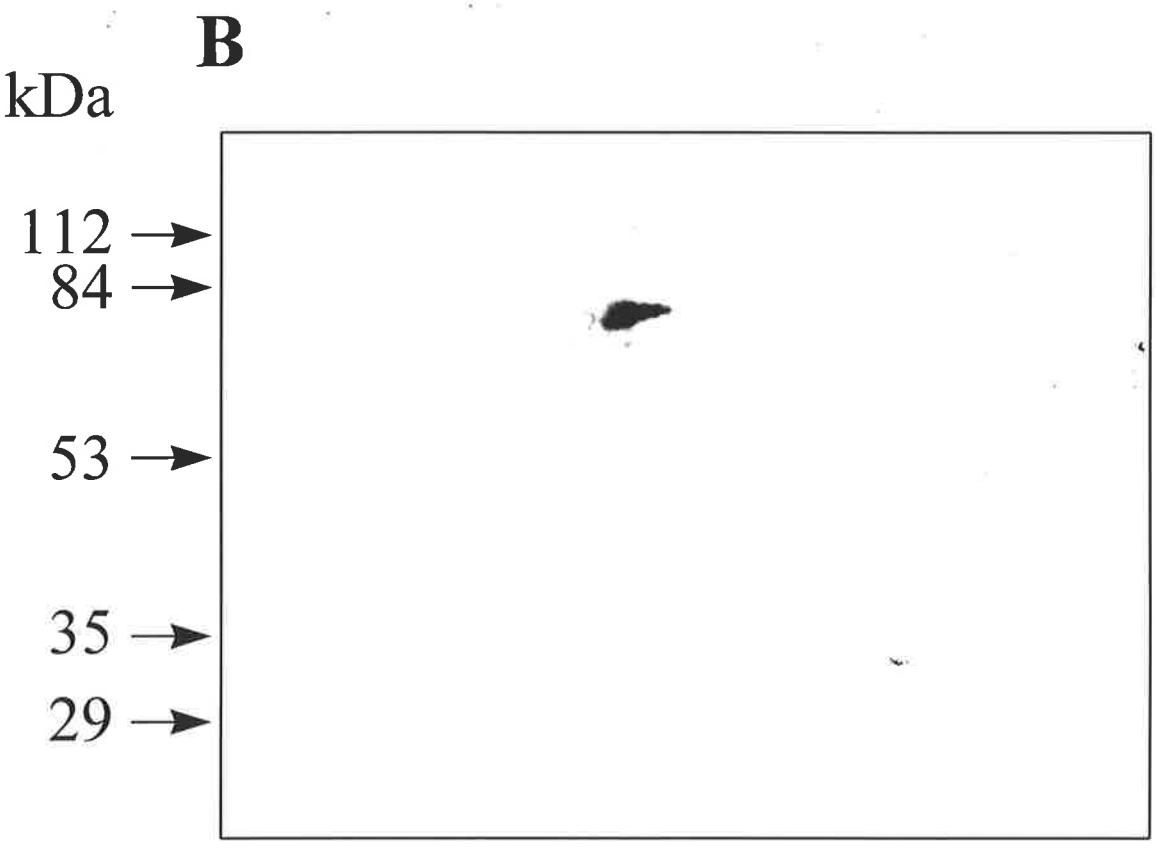
B
kDa
112
84
53
35
29

4.4.4 Separation of membrane proteins by 2-DE for *N*-terminal sequencing.

4.4.4.1 Development of methods to increase quantity of protein resolved by 2-DE.

Relatively small quantities (fmoles) of protein are required for Western blot analysis compared to that required (pmoles) for *N*-terminal sequencing. When larger amounts of membrane proteins were separated by 2-DE, problems of solubility and resolution arose. Ways of overcoming these problems were investigated.

A major problem with membrane proteins is their relative insolubility, resulting in poor resolution by 2-DE. The effect of removing membrane phospholipid by solvent extraction (*Section 2.2.4.3*) was investigated. There was no difference in separation of the proteins by 2-DE. Some protein was lost during the extractions, although this seemed not to be selective for any particular molecular mass proteins, but appeared as if less sample was electrophoresed (*Figure 4.12A and B*).

4.4.4.1.1 Determination of the level of SDS tolerated in an isoelectric focusing gel.

Solubilisation of integral membrane proteins with SDS is very effective as demonstrated by SDS-PAGE. The isoelectric focusing step of 2-DE (the first dimension) does not include SDS however, as ionic detergents affects protein migration. Both urea and CHAPS were present to maintain solubility instead. During isolation, fractionation and storage of membrane proteins it was important to prevent samples from becoming insoluble. Several conditions in particular caused samples to become insoluble. After solvent extraction of phospholipid from membrane proteins, if the sample was stored dry, or drying was accelerated by vacuum, then proteins became less soluble. Alternatively, if membrane

proteins were freeze dried to reduce sample volume, solubility was also a problem. Adding SDS to a sample before drying or storage at -20°C greatly increased protein solubility (data not shown).

The effect of SDS on isoelectric focusing (IEF) was determined by separation of 2-DE molecular weight protein standards with increasing amounts of SDS present in the IEF-gel. This was achieved by mixing the sample containing SDS with the IEF-gel before polymerisation. The concentrations of SDS in the gels were 0, 3.3, 6.7 and 13.3 mg/mL (data not shown). It was observed that the white precipitates formed in the basic end (anode) of the IEF tube-gel were proportional in size to the amount of SDS present. The sample with 3.3 mg/mL of SDS showed slight streaking in the pI dimension and a narrowing of the pI range; 6.7 mg/mL of SDS caused further streaking and a reduction of the resulting pI range; the highest SDS level (13.3 mg/mL) resulted in all proteins being smeared the length of the pI dimension. Small amounts of SDS in samples to maintain solubility therefore, were not detrimental, provided the protein of interest did not streak or become lost due to it falling outside the reduced pI range of separation. Proteins outside the pI range were not retained in the isoelectric focusing gel but migrated into either the anode or cathode buffers.

4.4.4.1.2 Alternative introduction of samples to IEF-PAGE.

In these studies, a number of cross-reactive proteins were detected by SDS-PAGE but not by 2-DE. This may have been the result of certain proteins not entering the IEF-gel. Samples to date had been loaded on top of the IEF-gel at the basic end (anode). Mitochondrial samples due to there relative abundance, were used to demonstrate the difference between loading a sample of membrane proteins onto the basic end of an IEF-gel (*Figure 4.12C*) and adding the a sample to the IEF-gel before polymerisation (*Figure 4.12A and B*). When samples were

loaded at the basic end, the proteins were more tightly focused, and the ampholyte pI gradient formed was expanded at the acid end (*Figure 4.12C*). The basic end of the gradient was contracted in comparison with a large number of proteins concentrated at this end. Proteins of samples mixed with the IEF-gel before polymerisation did not focus as well as those loaded onto the IEF-gel.

When samples were loaded onto the basic end of IEF tube-gels, many proteins were concentrated at the alkaline end (anode) of the gel, resulting in their poor resolution. Protein samples were therefore loaded onto the acid end of the IEF-gel to test if the proteins detected by 1-D Western blot analysis, and not 2-D Western blot analysis could be detected. An acidic loading was also intended to test whether proteins would migrate into the IEF-gel with improved resolution at the alkaline end. This approach however, was not successful as many proteins did not enter the IEF-gel and many that did were not well resolved (data not shown).

The protocol used for preparative IEF therefore, did not include methanol chloroform extraction unless the sample required the removal of Thesit®. Samples were routinely stored in 0.1% (w/v) SDS to enhance solubility. Samples were loaded on top of the gel (anode) and were not applied to IEF-gels by pre-mixing with the gel before polymerisation.

Figure 4.12 Comparison of pre-treatment and the introduction of samples to isoelectric focusing gels.

A sample (100 μg) of mitochondrial-enriched membrane proteins that did not bind to Con A-Sepharose was separated by 2-DE. The sample was either mixed with the focusing gel before polymerisation (A and B) or loaded on to the basic end of the IEF-gel (C). The sample was also either subject to a $CHCl_3$: methanol extraction (A) prior to focusing (*described in Section 2.2.4.3*) or focused without prior extraction (B and C). The IEF-gels (7.5 cm) contained ampholytes 5-8 (5%) and 3-10 (5%) and were electrophoresed as described in *Section 2.2.6.2*. The IEF-focused samples were separated in the second dimension by mini SDS-PAGE (12.5% polyacrylamide) at 30 mA per gel.

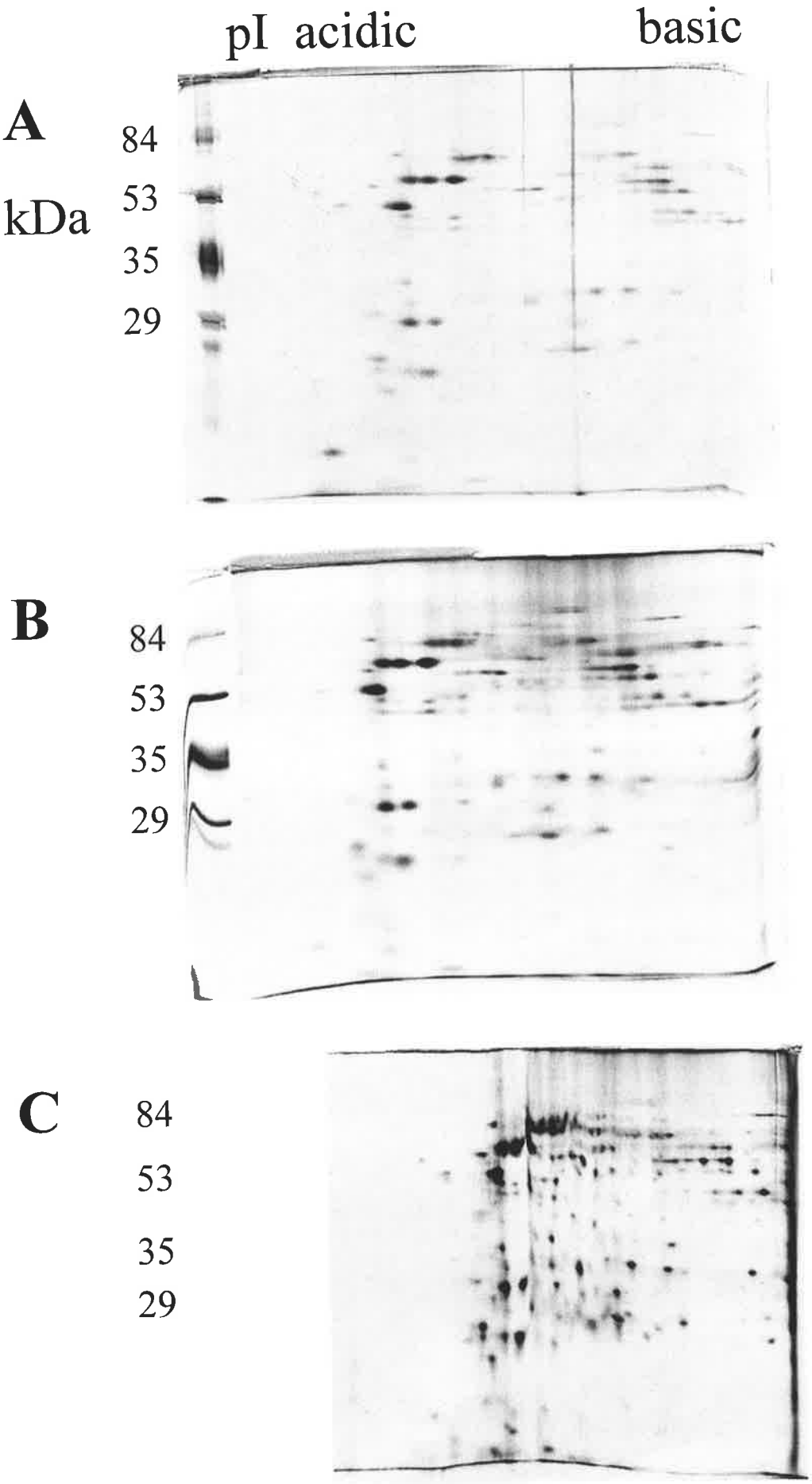
pI acidic
basic
A
kDa
84
53
35
29
B
84
53
35
29
C
84
53
35
29

4.4.4.2 Identification of proteins by amino acid *N*-terminal sequencing.

A comparison of the mitochondrial-enriched (*Figure 4.13*) and lysosomal (*Figure 4.14*) Con A Sepharose flow through samples, by 2-DE Western blot analysis and silver staining, illustrates the presence of a 58 kDa protein (candidate 4) with a pI of 5.2 in both samples (*labelled 1 in Figure 4.13 and Figure 4.14*), and which cross-reacts with anti-Band 3 antibodies. The protein appeared to be more abundant in the lysosomal sample as seen by the silver stained 2-D gels. The 58 kDa protein was seen in both the Con A Sepharose flow through and eluate when analysed by a 1-D Western blot (*Figure 4.8*). As isolated lysosomal fractions have only small amounts of mitochondrial protein, relative to the amount of lysosomal protein in isolated mitochondrial fractions, as determined by enzyme assays, the protein was assumed to be lysosomal. The amount of lysosomal protein isolated was only adequate for analytical purposes, which required the identified protein to be *N*-terminally sequenced from the more abundant mitochondrial-enriched fraction that also contained lysosomal proteins. *N*-terminal sequencing of the candidate 4 protein identified it as the mitochondrial matrix protein P1 (Jindal *et al.* 1989; Venner *et al.* 1990). Several other abundant proteins in the lysosomal Con A-Sepharose flow through were also identified, on the basis of pI and molecular mass in the mitochondrial fractions, then sequenced (*Table 4.3*). Two of these were identified as the peptide binding protein 74 (Domanico *et al.* 1993). The mitochondrial matrix protein P1, and the peptide binding protein 74, were represented multiple times when separated by 2-DE, which varied slightly in pI. This variation is typically seen due to differences in post-translational modification.

The application of membrane protein samples to an IEF-gel resulted in better resolution when applied at the basic end of the gel and not mix into the gel prior to polymerisation. Lipid extraction of membrane proteins did not affect resolution of the proteins on an IEF-gel.

Candidate lysosomal proteins identified on the basis of relative abundance in the purer lysosomal fractions (determined by enzyme assays), were *N*-terminally sequenced from the mitochondrial fractions. Two proteins were identified: the first protein which cross-reacted with anti-Band 3 antibodies was the mitochondrial heat shock protein 60 (HSP 60); and the second protein which did not cross-react with anti-Band 3 antibodies was the peptide binding protein 74 (PBP 74), also reported to have a mitochondrial location (Bhattacharyya *et al.* 1995). The cellular location of PBP 74 by other workers however, was reported to be localised to cytoplasmic vesicles and not mitochondria ((Kellokumpu *et al.* 1988). The PBP 74 is also thought to play a role in antigen presentation with the MHC class II molecules (VanBuskirk *et al.* 1991). The mitochondrial proteins *N*-terminally sequenced, were also present in the pure lysosomal fractions. These fractions had very little mitochondrial contamination, which was determined by mitochondrial enzyme assays. The abundance of enriched-mitochondrial fractions also contained lysosomal proteins.

Figure 4.13 Anti-Band 3 Western blot analysis of mitochondrial Con A-Sepharose flow through membrane proteins by 2-DE.

Mitochondrial-enriched membrane proteins that did not bind to Con A-Sepharose (100 μg) were separated by 2-DE. Duplicate gels were either silver stained (A) or subject to Western blot analysis (B). The IEF tube-gels (7.5 cm) contained ampholytes 5-8 (5%) and 3-10 (5%) and were electrophoresed as described in *Section 2.2.6.2*. The focused tube-gels were separated in the second dimension by 1.5 mm thick mini SDS-PAGE (12.5% polyacrylamide) electrophoresed at 30 mA per gel. The anti-Band 3 polyclonal serum was diluted 150-fold and incubated at 25°C for 4 h. The secondary sheep anti-rabbit antibody was diluted 100-fold before visualisation by chloro-1-napthol as described in *Section 2.2.10.2*. The proteins numbered 1-6 were *N*-terminally sequenced (*See Table 4.3*).

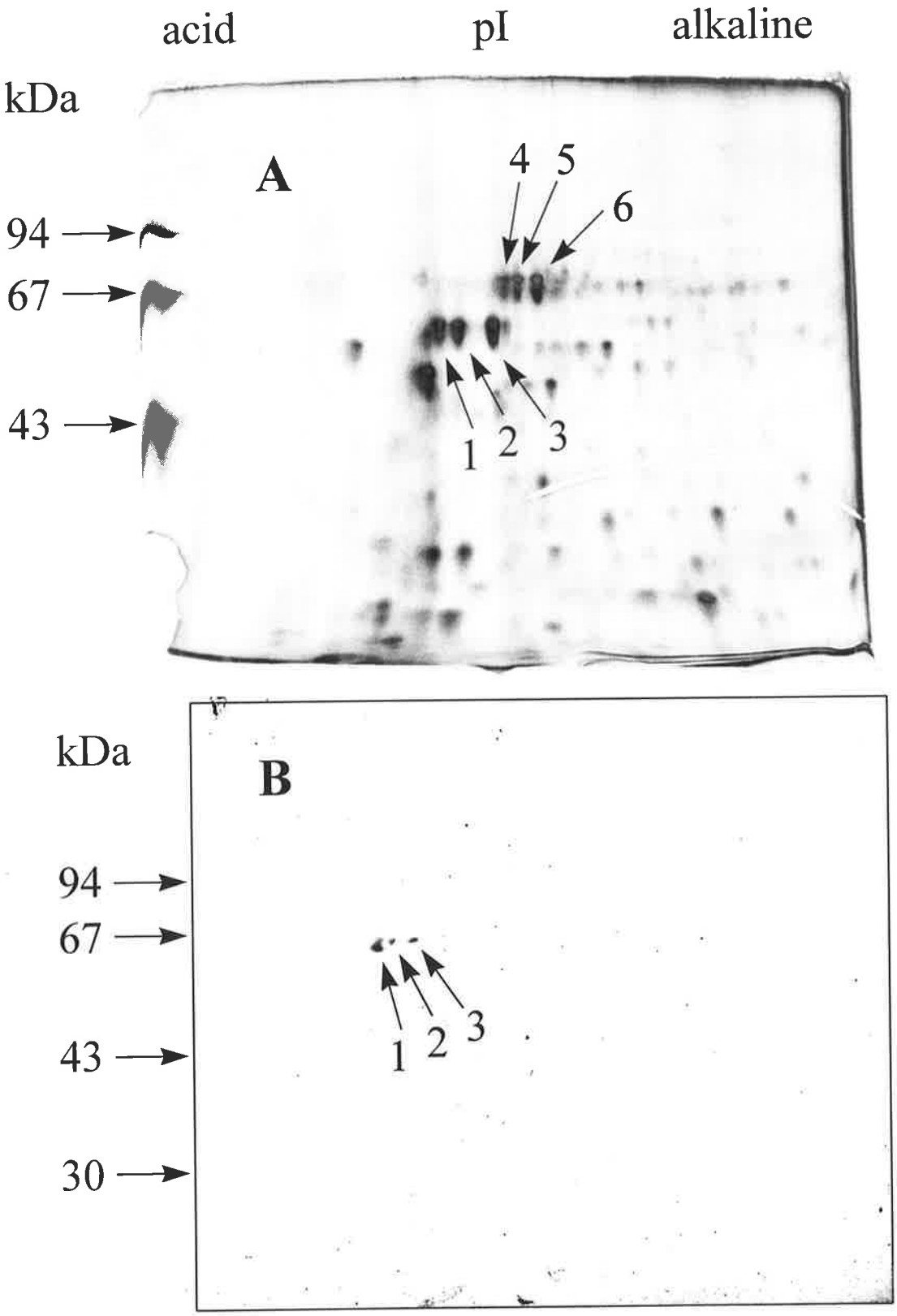
acid
pI
alkaline
kDa
A
94
67
43
4
5
6
1
2
3
kDa
B
94
67
43
30
1
2
3

Figure 4.14 Anti-Band 3 Western blot analysis of lysosomal Con A-Sepharose flow through membrane proteins by 2-DE.

Lysosomal-enriched membrane proteins that did not bind to Con A-Sepharose (100 μg) were separated by 2-DE. Duplicate gels were either silver stained (A) or subject to Western blot analysis (B). The IEF tube-gels (7.5 cm) contained ampholytes 5-8 (5%) and 3-10 (5%) and were electrophoresed as described in *Section 2.2.6.2*. The focused IEF tube-gels were separated in the second dimension by 1.5 mm thick mini SDS-PAGE (12.5% polyacrylamide) electrophoresed at 30 mA per gel. The anti-Band 3 polyclonal was diluted 150-fold and incubated at 25°C for 4 h. The secondary sheep anti-rabbit antibody was diluted 100-fold before visualisation by chloro-1-napthol as described in *Section 2.2.10.2*. The proteins numbered 1-6 were *N*-terminally sequenced (*See Table 4.3*).

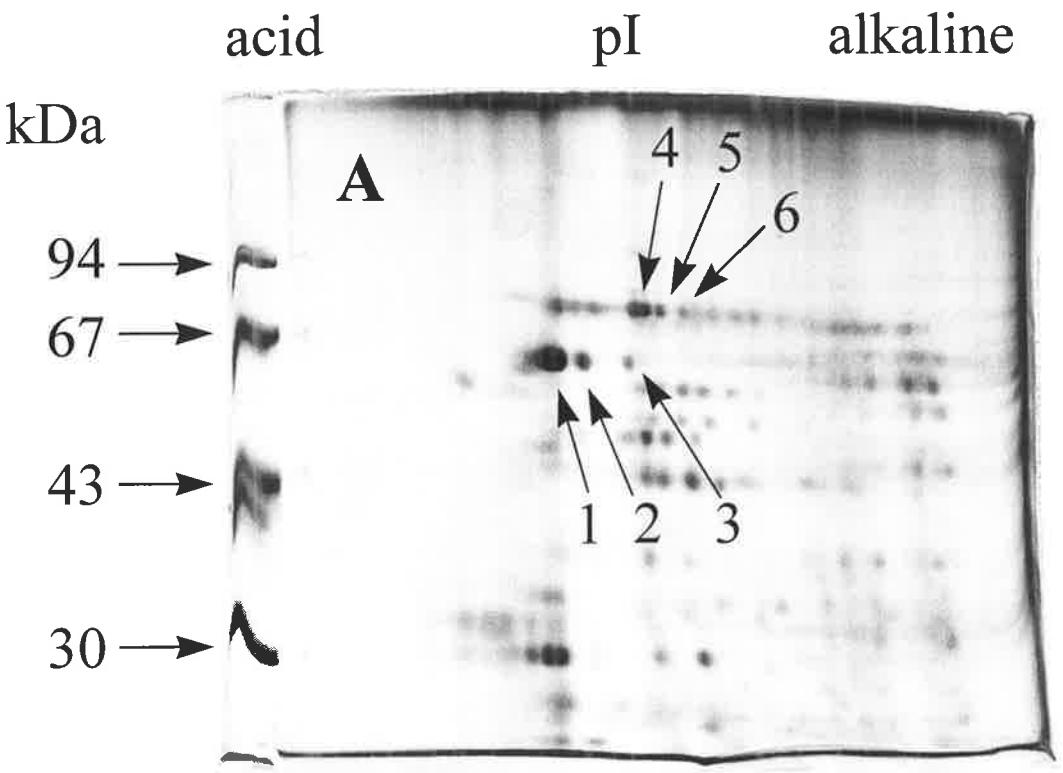
acid
pI
alkaline
kDa
A
94
67
43
30
4
5
6
1
2
3

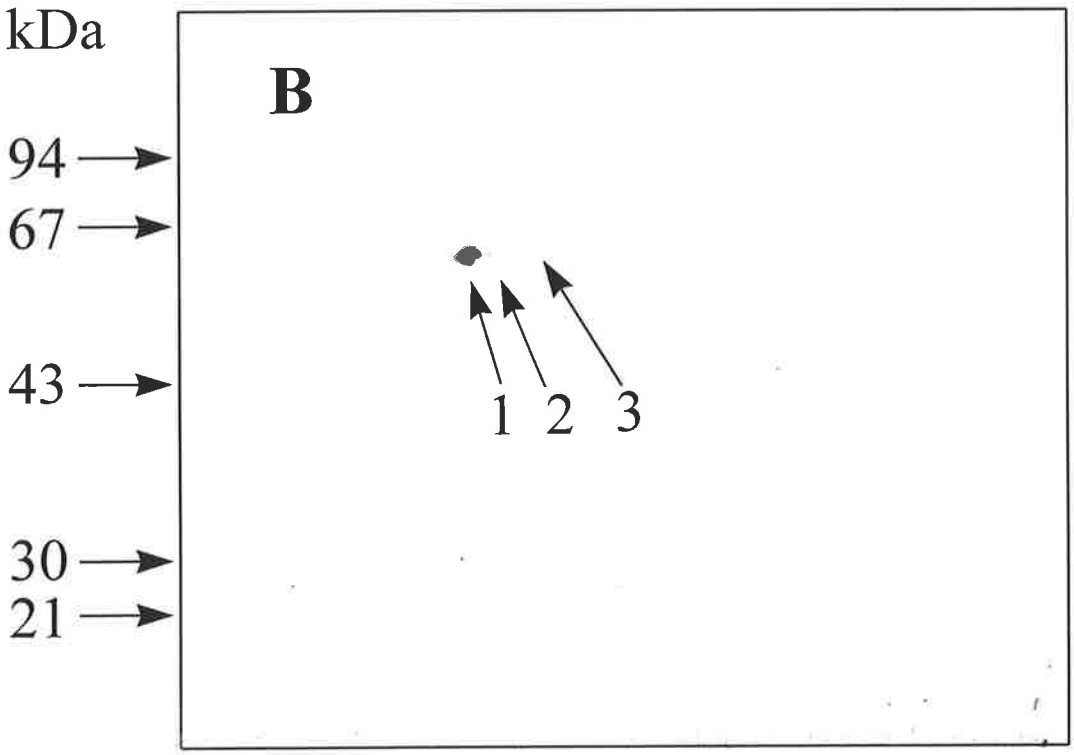
kDa
B
94
67
43
30
21
1
2
3

Table 4.3 N-terminal sequence of Con A-Sepharose non-binding lysosomal-enriched membrane proteins.

Sequencing was performed by Edman degradation in Dr. R.J. Simpson's laboratory, Joint Protein Structure Laboratory, Ludwig Institute for cancer Research and the Walter and Eliza Hall Institute of Medical Research, Parkville, Victoria, Australia. The protein identification (ID) numbers correspond to those labelled in *Figure 4.13* and *Figure 4.14*.

ID	kDa	pI	Candidate	N-terminal sequenced	Protein identified	Swiss-Prot Entry Name
1	58	5.2	4	AKDVKFGADARALMLQGVDL LADAVAVTMGPKGXTVIIEQ…	Mitochondrial matrix protein P1 (nuclear encoded)	P60_Human
2	58	5.3	4	AKDVKFGADARALML	Mitochondrial matrix protein P1	P60_Human
3	58	5.3	4	AKDVKFGADARALML	Mitochondrial matrix protein P1	P60_Human
4	76	5.4		XSEAIKXAVVXIDXXT…	PBP-74	GR75_Human
5	76	5.5		No sequence obtained		
6	76	5.6		AXEAI…	PBP-74	GR75_Human

4.5 General Discussion.

The discovery of a single dominant protein in the lysosomal membrane preparation that contributed up to fifty percent of total protein in some preparations was intriguing. This protein was isolated, sequenced and identified unexpectedly as cholesterol desmolase. Cholesterol desmolase converts cholesterol to pregnenolone and is the rate-limiting step of steroid hormone synthesis (Chung *et al.* 1986). This protein is known by several names including cytochrome P-450scc*. The cytochrome P450 super-family is a group of heme-thiolate monooxygenases that oxidise compounds including xenobiotics, fatty acids and steroids and requires electron transfer proteins. P-450ssc is expressed in steroidogenic tissues or endocrine organs including adrenal cortex, testis, ovary and placenta (Young *et al.* 1995).

Cholesterol desmolase is required in placenta to produce the steroid hormone progesterone, which supports pregnancy in eutherian mammals. Progesterone early in pregnancy is secreted by the ovarian corpus luteum. The placenta later produces progesterone in much larger amounts to maintain pregnancy (Rodgers 1990; Young *et al.* 1995). Although the human P-450scc gene is mostly expressed in the placenta in early- and mid-gestation, Chung *et al.* (1986) found P-450scc mRNA accumulates in response to cAMP. This second messenger (cAMP) has a very wide range of functions including the enhanced degradation of glycogen and lipids. Parturition of a placenta may cause such an increase in glycogen and lipid degradation.

* Cholesterol Monooxygenase (Side-Chain Cleaving) (EC 1.14.15.6), Cholesterol Side-Chain Cleavage Enzyme; Cytochrome P-450(SCC); Cytochrome P450, subfamily XIA1; CYP11A1; Cholesterol, reduced-adrenal-ferrodoxin: oxidoreductase (Side-Chain-Cleaving).

The P-450 enzymes involved in the metabolism of xenobiotics are targeted to the ER by an *N*-terminal sequence and receive electrons from specific donors. Cholesterol desmolase however, has been localised to mitochondrial cistae in bovine placentome and corpus luteum by electron microscopy (Ben David and Shemesh 1990). Mitochondrial P-450 enzymes use a different group of electron donors and are targeted to the space between the inner and outer membrane before translocation to the inner membrane (Black *et al.* 1994). Black *et al* (1994) also found P-450scc could not function if targeted to the ER by the microsomal *N*-terminal leader sequence, further confirming it as a mitochondrial protein.

The discovery of the mature-length cholesterol desmolase protein, a mitochondrial inner membrane protein, enriched with the placental lysosomes, suggests that proteins without lysosome function can be contained within or be associated with the lysosome. It was not due to mitochondrial contamination as determined by the enzyme marker cytochrome *C* oxidase (*Section 2.2.3.4*). The cause of apparent cholesterol desmolase accumulation in the lysosome can only be speculated upon. P-450scc may be more resistant to lysosomal proteolysis resulting in its accumulation. The incomplete degradation of mitochondria and other cellular components by the lysosome, therefore may have resulted in the presence of P-450scc and other non-lysosomal proteins within the lysosome.

The use of anion exchange inhibitors to recognise the lysosomal sulphate transporter identified a number of proteins. These chemical probes were not found to be specific enough, when labelling highly enriched lysosomal membrane proteins using a sulphate binding protection strategy. Antibodies to the erythrocyte anion exchanger (Band 3) were then employed to search for functionally related proteins in lysosomal preparations. The protein preparations were further enriched by sub-fractionation of samples chromatographically. Western blot analysis was then performed on samples separated by SDS-PAGE.

Anti-Band 3 antibodies detected a 46 kDa protein in both the Band 3 antigen preparation and in the lysosomal membrane preparation. These are possibly the same proteins, as a consequence of Band 3 being degraded within the lysosome (Hare and Huston 1985; Madsen *et al.* 1992; Turrini *et al.* 1991). Anti-Band 3 antibodies detected a 28 kDa protein in both lysosomal and mitochondrial preparations. Whether this protein functioned in both organelles or only one was not known.

To identify the proteins detected, Western blot analysis was performed after their separation by 2-DE. A number of proteins separated by 2-DE cross-reacted with Band 3 antibodies. One of these, identified in the Con A-Sepharose flow through, was the mitochondrial matrix protein P1, which like cholesterol desmolase is not a lysosomal protein. This protein is more commonly known as a member of the heat shock protein 60 (HSP-60)* chaperonin family. It became apparent that some mitochondrial proteins were enriched in the lysosomal membrane protein-rich fractions. This however, did not seem to be the case with the soluble proteins that were separated from the membrane proteins after organelle enrichment. Using similar methods fourteen different soluble proteins were identified from the lysosomal fraction although none of them were mitochondrial (Chataway *et al.* 1998). The presence of non-lysosomal proteins enriched in lysosomal membrane fractions appeared to result from incompletely degraded tissue-specific proteins, which were further enriched chromatographically. The reason HSP-60 cross-reacted with the anti-Band 3 antibody is probably due to the large range of homologies it has with a large number of proteins, including the mannose-6-phosphate receptor (Jones *et al.* 1993).

---

* This protein has a number of descriptions including: mitochondrial matrix protein P1 precursor; P60 lymphocyte protein; 60 kDa chaperonin; heat shock protein 60 (HSP-60); protein cpn60; groel protein; and hucha60.

To identify proteins by *N*-terminal sequencing, larger amounts of protein needed to be separated by 2-DE. Separating large amounts of membrane proteins by electrophoresis presented solubility problems. The method of applying samples to IEF-gels was investigated, and it was found that storage and drying of membrane protein samples to be separated by 2-DE can contain a small amount of SDS to maintain solubility without unduly affecting pI focusing. Sensitivity of Western blot analysis with anti-Band 3 antibody was increased by a method that blocked more thoroughly before the primary antibody, and during the primary and secondary antibody incubations and washing steps.

At this point in the study the sulphate transporter had not been identified. The selective inhibitors identified many bands, and it is quite possible one of these was the lysosomal sulphate transporter. The Band 3 protein most probably did not have enough homology with the lysosomal sulphate transporter for the anti-Band 3 antibody to clearly identify the transporter. The use of this antibody ceased with the emergence of a new family of sulphate transporters more characteristic of the lysosomal transporter. The next chapter continues with the identification of the lysosomal sulphate transporter using information from this new group of proteins.

5. The relationship between a sulphate anion transporter family and the lysosomal sulphate transporter.

5.1 Introduction.

In late 1994 the first described sodium-independent sulphate-specific transporter was cloned from rat liver (Bissig *et al.* 1994). Prior to this, the only other sulphate transporters reported were sodium-dependent and unaffected by the anion exchange inhibitors DIDS and SITS. The new rat sulphate anion transporter (SAT-1), however, was sensitive to inhibition by DIDS and SITS which is characteristic of the lysosomal (sodium-independent) sulphate transporter. Bissig *et al.* (1994) searched and found no significant homology to SAT-1 with previously identified membrane transport proteins. This SAT-1 transporter therefore, greatly influenced the continuation of this study.

The publication of this rat sulphate anion transporter (SAT-1) provided a new avenue of investigation into the lysosomal sulphate transporter. Sequence information from SAT-1 or antibodies to the rat SAT-1 protein could be used to search for the lysosomal sulphate transporter. This chapter continues the search for the lysosomal sulphate transporter, with the additional information gained from the new sulphate anion transporter family. This new family of sulphate transporters is reviewed in *Section 1.5.2.*

5.2 Experimental Aims.

The rat sulphate anion transporter (SAT-1) was the first of the new family of proteins described as sulphate transporters (Bissig *et al.* 1994). It had similar characteristics as the human lysosomal sulphate transporter. The initial objective was to determine if SAT-1 could be detected in humans. The next aim was to determine if the lysosomal sulphate transporter could be located by immunological cross-reactivity to part of the SAT-1 protein sequence.

5.3 Methods

5.3.1 Molecular biology.

5.3.1.1 Oligonucleotide cleavage and deprotection.

Columns upon which oligonucleotides were synthesised were filled with concentrated NH_4OH by fitting two 1 mL syringes to each end of the column. A total of 1 mL of NH_4OH was pushed back and forth through the column. The columns were left for 1 h at room temperature, the NH_4OH recovered and the procedure repeated with a fresh 1 mL of NH_4OH. The NH_4OH solutions were incubated at 55°C overnight. Oligonucleotides were precipitated by the addition of 1 mL n-butanol to each 100 µL of NH_4OH. The solutions were vortexed for 15 sec, microfuged (10,000 ***g***, 5 min), the butanol was removed and the pellets resuspended in 100 µL H_2O. The resuspended pellets were precipitated again with n-butanol, washed with 70% ethanol and dried. Pellets were then resuspended in 40 µL H_2O, combined and quantitated spectrophotometrically at 260 nM (1.0 A_{260} = 33 µg/mL).

5.3.1.2 Oligonucleotide dot blots.

Approximately 10 ng DNA quantities were spotted onto dry Genescreen filters and allowed to air dry. Filters were wet in 2 M NaCl, 0.1 M NaOH and again allowed to air dry. Oligonucleotides were end-labelled in a total volume of 10 µL containing 2 µL γ-[^{32}P]-ATP (10 mCi/mL), 100 ng oligonucleotide, 1 µL 1mM spermidine, and 0.5 µL polynucleotide kinase, in 10 mM Tris-HCl, pH 8, 10 mM $MgCl_2$, 5 mM DTT for 30 min at 37°C. Filters were pre-hybridised for two hours followed by an overnight hybridisation in 6xSSC, 0.1% SDS at 42°C.

5.3.1.3 RNA extraction.

The method for RNA extraction from tissue was based on that published by Chomczynski and Sacchi (1987). Fresh tissue (0.5-1.0 g) was placed in 2 mL of 4 M guanidinium thiocyanate, 25 mM sodium citrate, pH 7, 0.5% sarcosyl, 0.1 M β-mercaptoethanol (solution D), and homogenised for 30 sec with an Omni mix set on three, in a 10 mL tube. To 1 mL of this homogenate in a polypropylene tube, 0.1 mL 2 M sodium acetate, pH 4, 1 mL water-saturated phenol, and 0.2 mL $CHCl_3$: iso-amyl alcohol (49:1) was added. This mixture was vortexed and placed on ice for 15 min, and microfuged (10,000 ***g***) for 20 min at 4°C. The aqueous phase was transferred to another tube and mixed with 1 mL of isopropanol and placed at -20°C for 2 h. After centrifugation at 10,000 ***g*** for 20 min at 4°C, the supernatant was aspirated and the pelleted RNA was solubilised with 300 µL of solution D. The RNA was precipitated with 300 µL (1 volume) of isopropanol at -20°C for 1 h. The RNA pellet was sedimented by centrifugation for 10 min at 10,000 ***g*** at 4°C, then washed with 5 x 1 mL aliquots of 75% ethanol followed by centrifugation for 2.5 min (10,000 ***g***) at 4°C. The pellets were vacuum dried for 30 min and solubilised in 500 µL of diethyl pyrocarbonate treated water.

5.3.1.4 cDNA synthesis.

Synthesis of cDNA was performed in a total volume of 50 µL of Gibco BRL buffer containing; 100 µM DTT, 3 µg total RNA, 1 µL RNAsin (200 U/µL), 1 µL 10 µM (300 ng/µL) nonomers, 3 µL RTase (200 U) and 1 µL 25 mM dNTPs. The RNA mixture was denatured at 65°C for 3 min and placed on ice. The RTase and dNTPs were mixed separately on ice then added to the reaction mixture, which was then incubated at 37°C for 30 min. Following the addition of 5 µL 3M NaOH the reaction was incubation at 37°C for a further 30 min. The cDNA was precipitated by the addition of 1.25 µL 32% HCl, 6 µL 3 M sodium

acetate, pH 5.5 and 190 µL 95% ethanol then pelleted by centrifugation (10,000 ***g*** for 15 min at 4°C). The pelleted cDNA was washed with 70% ethanol, dried and resuspended in 50 µL water.

5.3.1.5 Polymerase chain reaction.

Each polymerase chain reaction (PCR) was performed in a total volume of 100 µL in a 0.5 mL tube. The reactions consisted of 1x Gibco BRL Taq polymerase buffer, 2.5 mM $MgCl_2$, 400 µM dNTP, 200 ng of each primer, and 1 unit of Taq polymerase. In optimising the conditions of each new PCR, reactions were performed with and without 10% (v/v) dimethylsulphoxide (DMSO). The target nucleic acid was added last and the reaction overlayed with 25 µL of mineral oil. The cyclic incubation protocol was denaturation (94°C), annealing (temperature calculated for each pair of primers) and extension (72°C) each for 20 s unless otherwise stated. After the desired number of cycles, a 3 min extension step was used to complete newly primed unfinished products. PCR products were electrophoresed in 8 mL 3% (w/v) new sieve and 1% (w/v) agarose gels on glass cover slips (45 x 60 mm) in TAE at 100 V for 20 min, followed by ethidium bromide staining which was visualised with UV (300 nm).

5.3.2 Antibody production

5.3.2.1 Production of polyclonal antibodies to synthetic peptides.

Peptide-conjugates were used to raise two polyclonal antibodies in rabbits as described in *Section 2.2.10.1.1.* The first was an eighteen residue peptide conserved in the SAT-1 family (*See Section 5.4.2.1*), H-FATSAALAKSLVKTATGC*-NH_2 4.6 mg (83% pure as determined by mass spectrometer analysis) which was coupled to 6.8 mg of diphtheria toxoid-MCS. A second peptide (*See Section 5.4.3.1*) of twelve residues unique to a member of the SAT-1 family (with a cysteine added to the C-terminus required for coupling), H-FDPSQDGLQPGAC-NH_2 (2 mg) was coupled to 9.3 mg diphtheria toxoid-MCS.

5.3.2.2 Purification of antibodies.

5.3.2.2.1 Adsorption against diphtheria toxoid.

Diphtheria toxoid (26 mg) was coupled to Affi-Gel® 15 (5 mL) in 0.1 M HEPES, pH 7.5 at 4°C overnight as described by the manufacturer's instructions. The coupled Affi-Gel® 15 was put in a column (1 x 6 cm) and washed with PBS. The diphtheria toxoid attached to the Affi-Gel® 15 was denatured with a 0-4 M gradient of urea over 10 min at 0.5 mL/min, then 4 M urea for 10 min, before a 30 min wash with PBS. Antibodies (0.5 mL serum) were adsorbed by mixing with the Affi-Gel® 15-diphtheria toxoid slurry overnight at 4°C. The non-adsorbed antibodies were washed from the slurry with PBS and the antibodies that bound to the Affi-Gel® 15-diphtheria toxoid column were eluted with 0.1 M sodium phosphate, pH 2.5 and 0.1 M triethylamine, pH 11.5 with a PBS wash in between.

---

* The single letter amino acid code used for peptides. A is alanine, C is cysteine, D is aspartic acid, E is glutamic acid, F is phenylalanine, G is glycine, H is histidine, I is isoleucine, K is lysine, L is leucine, M is methionine, N is asparagine, P is proline, Q is glutamine, R is arginine, S is serine, T is threonine, V is valine, W is tryptophan and Y is tyrosine.

5.3.2.2.2 Affinity purification of antibodies raised to peptides.

Peptides coupled to thiopropyl-Sepharose 6B gel were purchased from Chiron Mimotopes Pty. Ltd. and used for affinity purification of antibodies. Approximately 916 nmoles (1.6 mg) of the peptide (83% pure) conserved in the SAT-1 family H-FATSAALAKSLVKTATGC-NH_2 (Mr 1739) was coupled to approximately 2.1 mL of packed thiopropyl-Sepharose 6B gel. The unique SAT-1 peptide, H-FDPSQDGLQPGAC-NH_2 (Mr 1333) was also coupled with 1306 nmoles (1.7 mg) of the 76% pure peptide conjugated to approximately 2.1 mL of packed thiopropyl-Sepharose 6B gel.

Peptide-specific antibodies were purified from serum according to the manufacturer's instructions. Serum (5 mL) was mixed with the peptide immunogen coupled to thiopropyl-Sepharose 6B gel and 3 mL PBS overnight at 4°C. Serum was collected and the gel washed five times with PBS, and then three times with 0.15 M NaCl. The gel was mixed with 10 mL 0.1 M glycine, pH 2.5 for 10 min at room temperature. The eluted antibody was collected and neutralised with 0.1 M NaOH. The gel was rinsed with 15 mL PBS which was then pooled with the eluate.

5.4 Results.

The cloning of a number of specific sulphate transporters whose characteristics were similar to those of the lysosomal sulphate transporter has provided new leads in pursuit of the lysosomal transporter. The rat SAT-1 sequence, which was the first available, was used to search for the human sulphate anion transporter in the lysosome. Other proteins with significant homology to rat SAT-1 appeared during this work, forming a new family. The degree of uniqueness or conservation of regions of the SAT-1 sequence, compared to other members of the sulphate transporter family, was then used to identify peptide sequences for the production of antibodies.

5.4.1 Search for the human SAT-1 cDNA sequence.

Dr. Hamish Scott, Department of Chemical Pathology, Women's and Children's Hospital, North Adelaide, South Australia, kindly gave advice on the design of primers for iduronidase and SAT-1 amplification.

If the murine gene organisation is similar to human and canine then the human SAT-1 gene lies within the second intron of the iduronidase gene (Clarke *et al.* 1994). The coincidence of two genes overlapping on opposite strands of DNA in the human genome is a rare occurrence. Whether this increased the likelihood that SAT-1 was also a lysosomal protein required investigation. To test whether the human SAT-1 gene could be detected, oligonucleotides were synthesised to rat SAT-1 cDNA (*See Table 5.1*).

Table 5.1 SAT-1 rat oligonucleotides.

	cDNA bp*	Oligonucleotide sequence
SAT-1-1	544-567	5' GCTGCCCCAGTACCGCCTTAA(GA)GA 3'
SAT-1-2	988-965	5' CACGAAGCCCAGCCGGAGGATNCC 3'
SAT-1-3	2018-2047	5' TACTATGCCAACAAGGATTTCTTCCTTCGG 3'

5.4.1.1 Dot blot experiments with rat oligonucleotides.

Homology of the rat SAT-1 gene to the human iduronidase gene was initially tested by dot blot experiments using the oligonucleotides in *Table 5.1*. A cosmid clone A157.1 containing the human iduronidase gene was used to test for this homology. The clone A157.1 has been described by Pohl *et al.* (1988) and MacDonald *et al.* (1989). *Figure 5.1* shows that oligonucleotides 2 and 3 hybridise with high stringency, although oligonucleotide 1 showed binding only at lower stringency.

* Bases pair numbers refer to the EMBL Data Bank sequence with accession number L23413.

Figure 5.1 Hybridisation of rat SAT-1 oligonucleotides to A157.1.

Six samples of DNA were arranged (A) onto each of three Genescreen nylon filters. The DNA samples blotted were 0.5 µg SPP/Eco RI (1); 0.5 µg pUC19 (2); 1 µg cosmid A157.1 (3 and 4); and 0.5 µg lambda DNA (5 and 6). The six DNA samples were hybridised with the SAT-1 oligonucleotides (1, 2 and 3) described in *Table 5.1.* The oligonucleotides were end-labelled and hybridised to the filters (*Section 5.3.1.2*). The three filters were washed for 10 min in 6xSSC and 0.1% SDS at 42°C (B); the same filters were washed for a further 10 min in 2xSSC and 0.1% SDS at 42°C (C); these filters were then washed again for 10 min in 1xSSC and 0.1% SDS at 55°C (D). Hybridisation to filters was visualised by autoradiography.

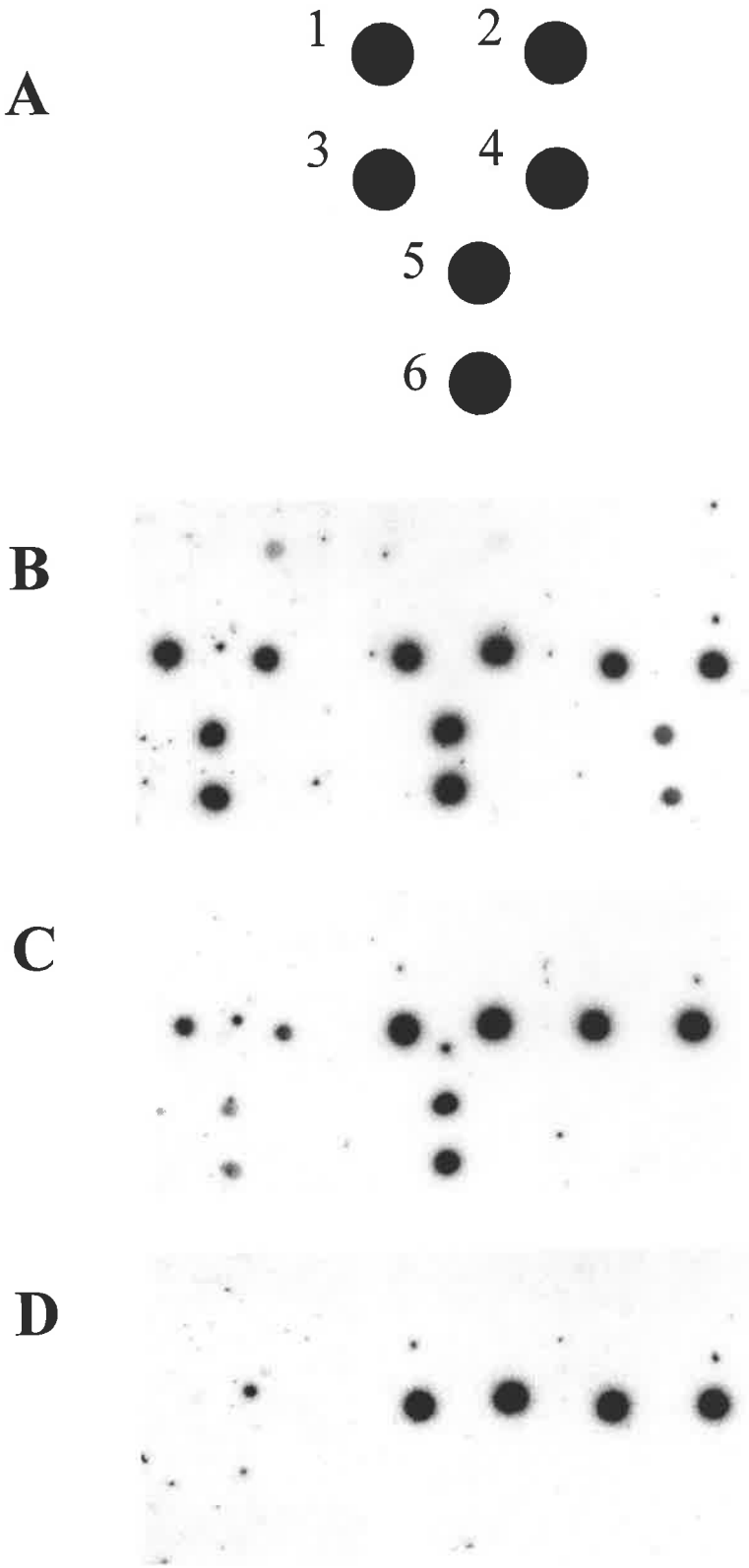
A
1
2
3
4
5
6
B
C
D
SAT1-1
-2
-3

5.4.1.2 PCR of rat and human tissues with rat SAT-1 primers.

Oligonucleotides 1 and 2, or 2 and 3, could be used as primer pairs. Oligonucleotide 2 was designed to hybridise to the nucleotide strand opposite that of oligonucleotides 1 and 3. Oligonucleotides 1 and 2 were used for polymerase chain reaction (PCR), firstly on rat liver cDNA. The expected product of 444 bp resulted under a wide range of conditions tested (*Figure 5.2A*). Human skin fibroblast cDNA was synthesised and tested by PCR using primers for iduronidase. The iduronidase-containing cosmid A157.1 was used as the positive control template. Both the fibroblast and cosmid DNA samples produced a 225 bp product (*Figure 5.2B*). The fibroblast DNA produced an additional 84 bp product resultant from alternative splicing. The SAT-1 PCR was repeated using rat liver, human kidney and skin fibroblasts (*Figure 5.2C*). A lot of product was produced from the rat cDNA but very little was produced from the human cDNA. As the SAT-1 primers produced PCR products in rat tissues but not in human tissues, a difference exists in either the sequences of the primer annealing sites or the structure of the genes. It was decided at this point to approach the search for human SAT-1 with immunological techniques.

Figure 5.2 Polymerase chain reactions performed: on rat and human cDNA with rat SAT-1 primers; and on human cDNA with iduronidase primers.

All 50 µL PCR reaction mixtures contained 1x buffer (Gibco-BRL), 2.5 mM Mg^{2+}, 400 µM dNTP, 2 ng/µL of oligonucleotides, 0.2 U/100 µL of Taq and 10% DMSO unless stated otherwise. Forty cycles were performed with 15 sec denaturation, 15 sec annealing, and 30 sec extension (described in *Section 5.3.1.5*) unless stated otherwise. The molecular weight markers used were pUC cut with Hpa II.

A Rat liver cDNA subject to polymerase chain reaction with SAT-1 primers under an array of conditions.

Oligonucleotides 1 and 2 (described in *Table 5.1*) were used to generate a 444 bp product. Reactions were annealed at 50°C (1-4), 57°C (5-8), or 65°C (9-12). During thermo-cycling reaction mixtures contained 10% DMSO (2, 6 and 10), 10% DMSO and 5 mM Mg^{2+} (3, 7 and 11), or 5 mM Mg^{2+} without DMSO (4, 8 and 12). PCR products, negative controls (13 & 14) and molecular weight markers (15) were electrophoresed as described in *Section 5.3.1.5*.

B Human cDNA and A157.1 subject to polymerase chain reaction with iduronidase primers.

Polymerase chain reactions were performed using primers (annealed at 58°C) that generate a 225 bp iduronidase product. The target cDNAs were the cosmid clone A157.1 that contained the human iduronidase gene (2), and human fibroblast cDNAs (3-5) from three different syntheses. The PCR products, molecular weight markers (1) and a negative control (6) were electrophoresed as described in *Section 5.3.1.5*.

C Rat SAT-1 primers used for polymerase chain reaction with rat and human cDNA.

Polymerase chain reactions were performed as described above (A). Target cDNA from rat liver (1), human kidney (2), human fibroblast (3), and a negative control (4), were subject to PCR amplification. The resultant products and molecular weight markers (5) were electrophoresed as described in *Section 5.3.1.5*.

A

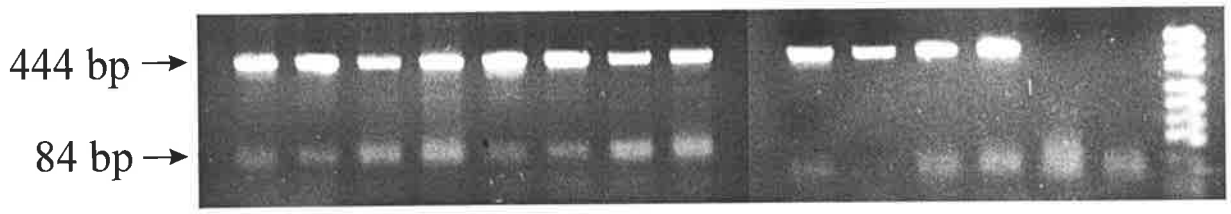

B

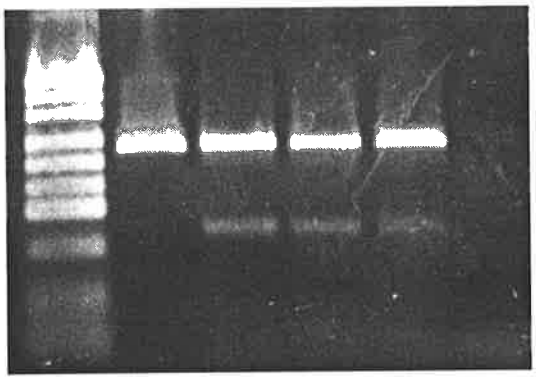

C

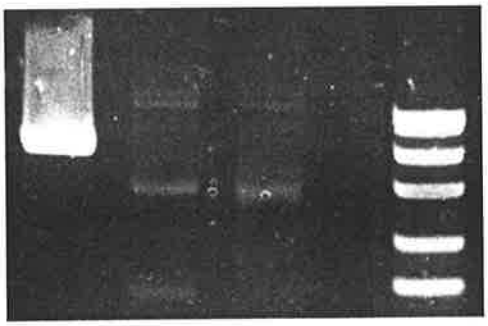

5.4.2 Search for the lysosomal sulphate transporter and the human SAT-1 protein using a conserved region of the sulphate transporter family.

Protein sequences are more conserved across species than DNA, due to the wobble in the nucleotide triplet code. The search for human SAT-1 therefore continued at the protein level by raising antibodies to a region of the rat SAT-1 sequence that was conserved . Two new members of the SAT-1 family had become evident at this stage. The first of these was gene down regulated in adenoma (DRA) of human colon (Schweinfest *et al.* 1993), which was recognised as a sulphate transporter due to a 31% amino acid identity with SAT-1 from rat. The second was the diastrophic dysplasia (DTD) sulphate transporter in human (Hastbacka *et al.* 1994) with 48% identity to the rat SAT-1 protein. With three members of the family known, a conserved region of the SAT-1 sequence was determined.

5.4.2.1 Design of a conserved peptide antigen to SAT-1 and production of polyclonal antibody.

The rat SAT-1 (SAT1_RAT), human DRA (DRA_HUMAN), and human DTDST (DTD_HUMAN) peptides were aligned and the trans-membrane structure predicted (Hastbacka *et al.* 1994). The entry names (shown in parenthesis) used by the Swiss Protein Database (Bairoch and Apweiler 2000) were used where possible, when referring to specific proteins of this sulphate transporter family. From this alignment a conserved sequence of eighteen residues on the fifth of six extra-membranous loops was chosen (*Figure 5.3*), as it was more antigenic. A synthetic peptide of this sequence was coupled to diphtheria toxoid and used to raise antibodies in rabbit as described in *Section 5.3.2.1*. The titres of this polyclonal antibody after four immunisations with the coupled peptide were 1:8,000 against BSA, 1:1,024,000 against diphtheria toxoid (DT), and greater than 1:4,096,000 against the conserved SAT-1 peptide coupled to DT.

Figure 5.3 Synthetic peptide of the rat SAT-1 sequence from a conserved region of the known sulphate transporter family.

The amino acid sequences of three sulphate transporters were aligned: the rat anion transporter (SAT1_RAT), the human diastrophic dysplasia (DTD_HUMAN) and that which is down regulated in human colon adenoma (DRA_HUMAN). The alignment was performed with the GCG* program Pileup, with an open gap penalty of 3.0, a gap extension penalty of 0.1 using the Blosum 62 scoring matrix. The eighteen residues shown of the alignment correspond to the residues of Swiss-Prot protein sequence database entries; 397-414 of SAT1_RAT, 434-451 of DTD_HUMAN and 391-408 of DRA_HUMAN. The program GenDoc (Version 2.0.004 by Karl B. Nicholas) was used to present this part of the alignment.

* Genetics Computer Group, Inc. WISCONSIN PACKAGE, Version 8.1-UNIX, August 1995 and the EGCG extensions to the WISCONSIN PACKAGE, Version 8.1.0, March 1996.

5.4.2.2 Comparison of Band 3 and conserved SAT-1 cross-reactive proteins.

To determine whether common proteins cross-react with both anti-Band 3 and anti-SAT-1 polyclonal antibodies, a range of samples were separated by SDS-PAGE at the same time, under the same conditions (see *Sections 2.2.4.2* and *2.2.6.1* for description of sample preparation). Western analyses were performed using either anti-Band 3 or anti-SAT-1 polyclonal antibody as described in *Section 2.2.10.2*. The relative molecular masses of the proteins recognised by the antibodies were determined (*Table 5.2*), showing Band 3 and SAT-1 polyclonal antibodies do not identify a common set of proteins. Although many proteins were detected by anti-SAT-1 polyclonal antibodies, a few proteins demonstrated very strong cross-reactivity. These were a 45 kDa protein in whole membranes, a 67 kDa protein in mitochondrial membranes, a 61 kDa protein in Con A-Sepharose flow through and a 34 kDa protein in Con A-Sepharose eluate of lysosomal proteins. There were many more SAT-1 cross-reactive proteins with a weak signal detected in the Red Dye non-binding fraction not included in *Table 5.2*.

Table 5.2 Proteins which cross reacted with anti-Band 3 and anti-SAT-1 (conserved peptide) antibodies.

Sample	M_r of anti-Band 3 reactive proteins	M_r of anti-SAT-1 reactive proteins
whole placental membrane protein	90	82
	86	65
	74	60
	63	45 *
	39	34
	35	29
		28
mitochondrial membrane proteins	90	67 *
	86	60
	74	55
	63	28
	41	
	39	
	24	
lysosomal membrane protein	90	66
	83	28
	48	27
	43	
	42	
Con A-Sepharose non-binding protein	76	61 *
	72	34
	63	32
	57	29
	40	
	38	
	36	
	35	
Con A-Sepharose binding protein	63	34 *
	57	28
lysosomal Red-Dye non-binding protein	36	28
	35	
	33	

* SAT-1 detected proteins that were strongly cross-reactive.

5.4.2.3 Western blot analysis of placental subcellular fractions with the anti-SAT-1 conserved sequence polyclonal antibody.

A number of SAT-1 cross-reactive proteins detected in whole placental membrane proteins were not seen in any of the other fractions examined. One protein of 82 kDa that gave a strong signal in the placental homogenate was found to be enriched in the cell content fraction. The cell content fraction was divided into a granular and a microsomal fraction. The microsomal fraction showed further enrichment of the 82 kDa protein. This protein was separated by 2-DE and a pI of 5.9 determined. When a range of larger quantities of microsomal samples were separated by 2-DE in order to obtain *N*-terminal sequence, solubility became a problem. The microsomal membrane proteins did not focus well in the first dimension or transfer well from the first to the second dimension. Although this protein was of interest because it was detected by anti-SAT-1 antibodies, it was not a lysosomal protein and, was not pursued further.

5.4.2.4 Western blot analysis of lysosomal protein with the polyclonal antibody.

A 28 kDa protein was detected with the anti-SAT-1 antibody in the lysosomal and mitochondrial protein fractions that bound to Con A-Sepharose (*Figure 5.4*). The signal detected by Western blot analysis was clearly stronger in the lysosomal fraction compared to the mitochondrial fraction. The mitochondrial fraction contains some lysosomal protein, which explains why it was also detected in the mitochondrial fraction. When detected with anti-Band 3 antibody (*Figure 4.7*) however, a stronger signal against the 28 kDa protein was found in the mitochondrial-enriched membrane fraction, although these were not Con A-Sepharose enriched fractions. This protein was not detected in the fractions that did not bind Con A-Sepharose. The Red Dye flow through protein sample also contained the 28 kDa cross-reactive protein (data not shown). Prior to the enrichment of proteins by

Con A-Sepharose chromatography, those proteins that were not soluble in Thesit® were removed (*See Section 2.2.5*). The 28 kDa protein detected in the Con A-Sepharose-enriched lysosomal and mitochondrial fractions was more abundant in the Thesit® insoluble fractions than the soluble fractions (*Figure 5.5*). Con A-Sepharose without a protein sample was also eluted with and without Thesit® extraction buffer and analysed by Western blot with anti-SAT-1 antibodies. This found Con A-Sepharose did not contribute to the 28 kDa protein detected (*Figure 5.5*).

In summary, the 28 kDa protein membrane protein was more abundant in: the mitochondrial-enriched fraction then the lysosomal fraction when detected with anti-Band 3 antibody; the lysosomal fraction compared with the mitochondrial-enriched Thesit® soluble Con A-Sepharose bound fraction when detected with anti-SAT-1 antibody. This protein was most abundant and comparable in the lysosomal and mitochondrial Thesit® insoluble fractions, although some was detected in the lysosomal Thesit® soluble fraction, resulting in it being more abundant in the lysosomal Con A-Sepharose bound fraction.

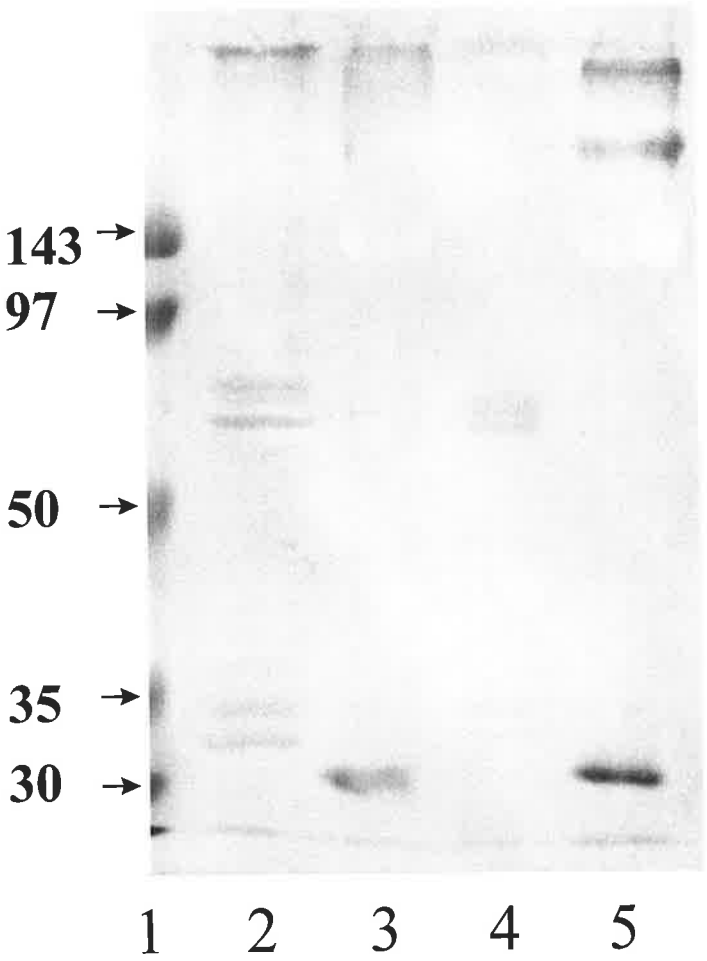

Figure 5.4 Western blot analysis of samples separated with Con A-Sepharose using anti-SAT-1 conserved sequence antibody.

Membrane proteins (50 µg) were separated by SDS-PAGE (10% acrylamide mini-gels) as described in *Section 2.2.6.1.* Molecular weight markers (1), mitochondrial-enriched (2-3), lysosomal-rich (4-5), Con A-Sepharose non-binding proteins (2 and 4), and Con A-Sepharose binding proteins (3 and 5) were then transferred to a PVDF membrane. Western blot analysis was performed as described in *Section 2.2.10.2.2* with a one hundred fold dilution of primary antibody.

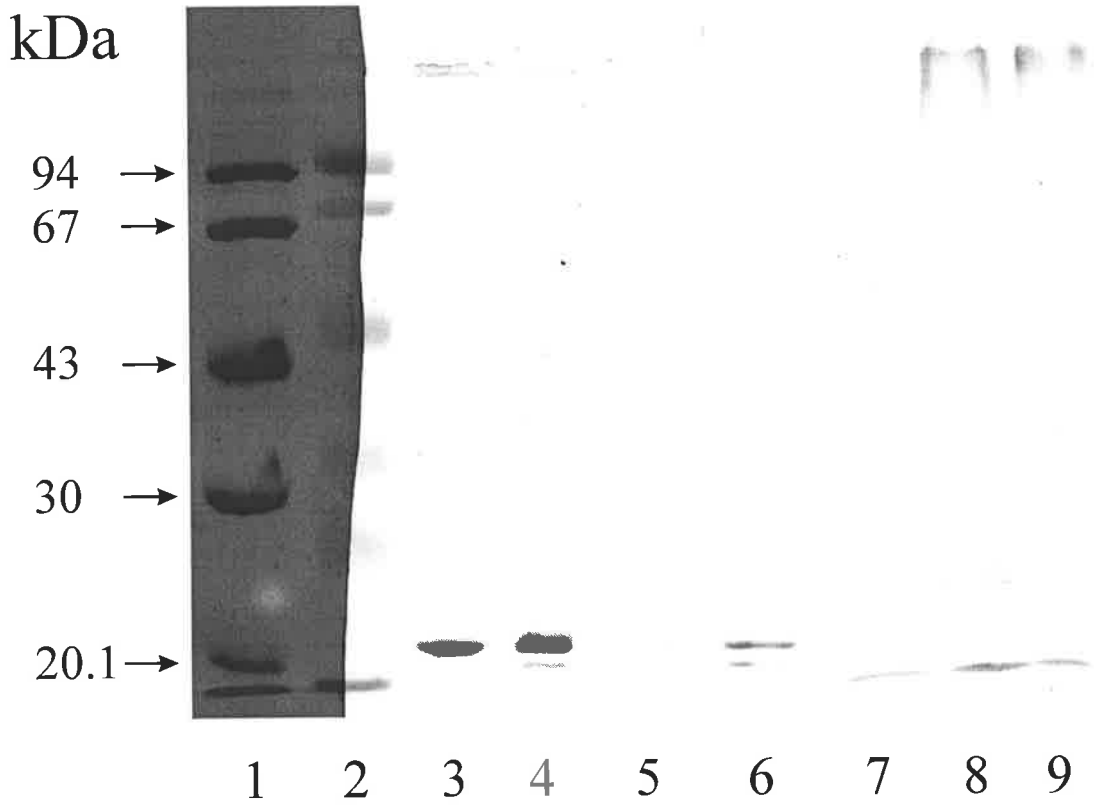

Figure 5.5 Western blot analysis of Thesit® insoluble and soluble membrane proteins with the anti-SAT-1 (conserved peptide) antibody.

Samples (20 μg) were separated by mini SDS-PAGE (12.5% acrylamide) at 30 mA per gel. Molecular weight markers (1), pre-stained molecular weight markers (2), mitochondrial-enriched (3 and 5), lysosomal (4 and 5), Thesit® insoluble mitochondrial and lysosomal (3 and 4), Thesit® soluble mitochondrial and lysosomal (5 and 6), uncross-linked Con A-Sepharose (7), elution of Con A-Sepharose that was not loaded with a sample (8), and extraction of Con A-Sepharose without sample treated with Thesit® protein extraction buffer (9).

5.4.2.5 Western blot analysis of Thesit® insoluble and Red Dye flow through lysosomal membrane proteins.

Thesit® insoluble and Red Dye flow through protein fractions were good candidate fractions from which to obtain *N*-terminal sequence. There were significant amounts of Thesit® insoluble material, and the Red Dye flow through fractions containing fewer proteins as they had been very highly enriched, also contained *N*-glycosylated proteins as they were also Con A-Sepharose binding.

2-D Western blot analyses of Thesit® insoluble lysosomal membrane proteins detected a number of cross-reactive proteins, with both anti-Band 3 and anti-conserved SAT-1 sequence polyclonal antibodies (Western blots not shown). The proteins detected in the Thesit® insoluble sample are indicated on a silver stained 2-DE gel (*Figure 5.6*) at 60 kDa (pI~5.7), 80 kDa (pI~5.9) and 75 kDa (pI~6.5). The latter two proteins were not clearly seen by silver stain, indicating their low level of abundance.

Western blot analysis of the Red Dye flow through proteins after separation by 2-DE detected SAT-1 cross-reactive proteins (Western blot not shown). The proteins that showed cross-reactivity are indicated on a silver stained duplicate gel (*Figure 5.7*). The 43 kDa proteins detected at a pI of approximately 4.5 and indicated by (1) were too low in abundance to be seen by silver staining. The other proteins detected at approximately 70 kDa and 80 kDa (5 and 5.8 in pI respectively) were visible with silver staining.

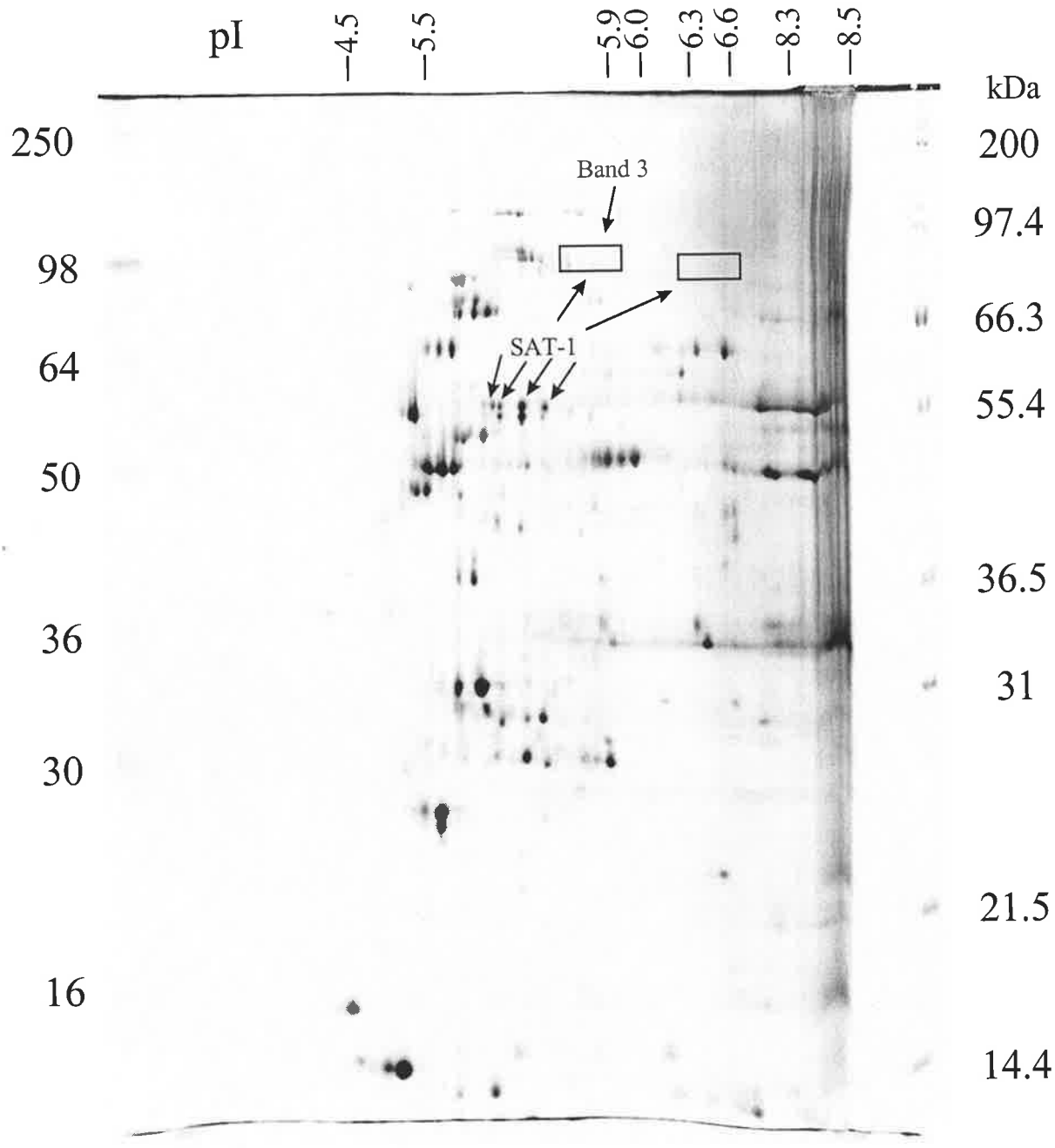

Figure 5.6 Silver stained Thesit® insoluble lysosomal membrane proteins separated by 2-DE, with Band 3 and SAT-1 cross-reactive proteins indicated.

Thesit® insoluble membrane proteins (150 μg) were focused with 5% 3-10 ampholytes in a 7.5 cm long gel as described in *Section 2.2.6.2*. The second dimension (SDS-PAGE) was resolved on a large 12.5% polyacrylamide gel at 200 V (*Section 2.2.6.1*). The proteins and regions identified by Western blot analysis are indicated by either arrows or an open box, respectively. The pI range was determined by separating standards under the same conditions on an identical 2-DE gel (not shown).

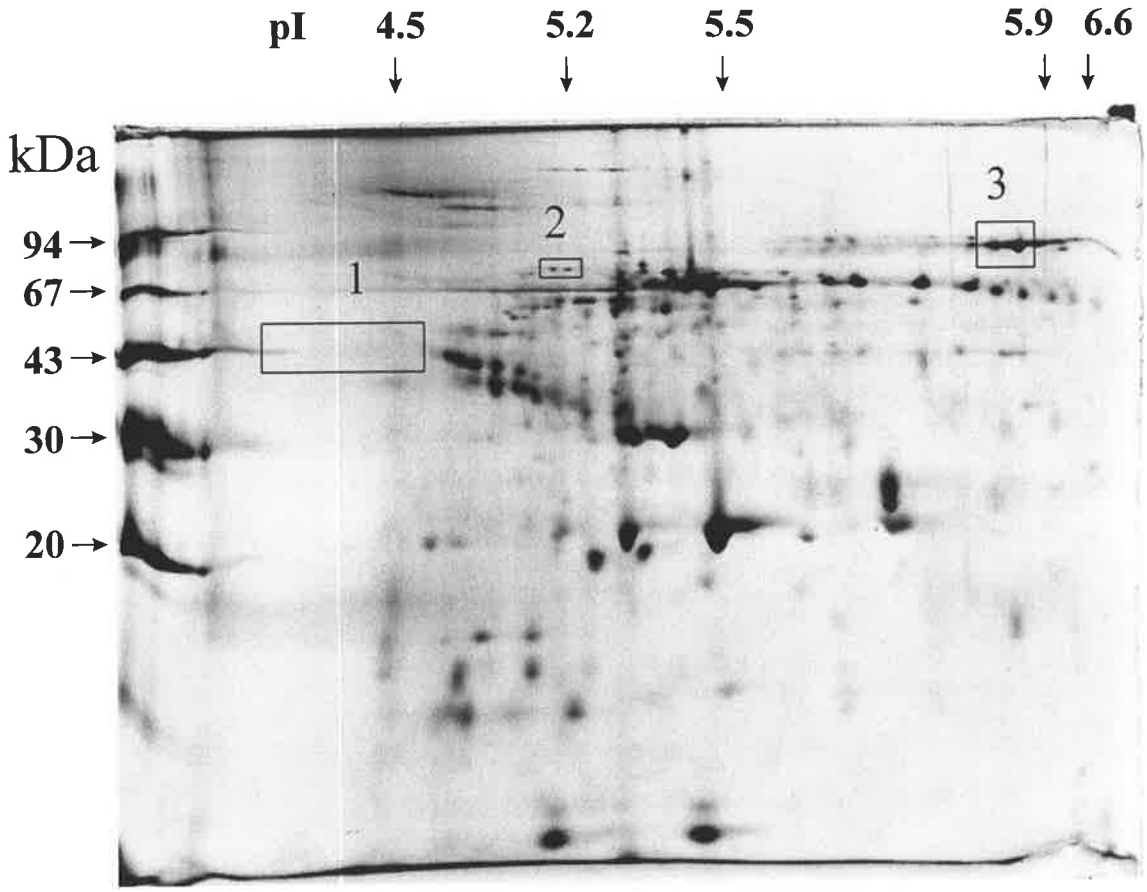

Figure 5.7 Silver stained Red Dye flow through, lysosomal membrane proteins separated by 2-DE, with SAT-1 cross-reactive proteins indicated.

Approximately 40 µg of chloroform/methanol (2:1) extracted Red Dye flow through protein was focused in a 7.5 cm tube IEF-gel containing 5% 3-10 ampholytes (*Section 2.2.6.2*). The second dimension (SDS-PAGE) was resolved on a mini 12.5% acrylamide gel as described in *Section 2.2.6.1*. Open boxes indicate the proteins and regions identified by Western blot analysis. The pI range was determined by separating standards under the same conditions on an identical 2-DE gel (not shown).

5.4.2.6 Identification of proteins by *N*-terminal sequencing.

Proteins in the Red Dye flow through fraction were separated by 2-DE and a number of proteins were sequenced (*Table 5.3*). The protein (80 kDa, pI 6) detected by the anti-SAT-1 antibody was serotransferrin (*Figure 5.7*). The 80 kDa protein detected in the insoluble fraction (*Figure 5.6*) was most probably also serotransferrin. The mature form of serotransferrin has been found to be insoluble in Triton X-100 (Cerneus *et al.* 1993). Serotransferrin transports iron and is known to cycle to the plasma membrane from endosomes, although it has not previously been found in lysosomes (Cerneus and van der Ende 1991). Serotransferrin has been found to be abundant amongst the luminal lysosomal proteins of placenta (Chataway *et al.* 1998), and speculated to be transferred into lysosomes from endosomes due to the saturation of this trafficking pathway.

N-terminal sequence was also obtained from four other Red Dye flow through proteins. These were prominent proteins when stained with Coomassie blue (R-250) after separation by 2-DE. Although there was no antibody cross-reactivity with these proteins, they were enriched from lysosomal membrane proteins, which were further enriched with Con A-Sepharose followed by Red Dye matrix. These four proteins (see *Table 5.3* for details) were all placental alkaline phosphatase (PLAP) which varied slightly in pI. PLAP is thought to function as a receptor transferring IgG from mother to foetus, and was found to be abundant in clathrin-coated vesicles prepared from placenta (Makiya and Stigbrand 1992a-c; Makiya *et al.* 1992). PLAP attaches to membranes by a glycosylphosphatidylinositol anchor and was not abundant enough to be detected in the Con A eluate. Like serotransferrin, PLAP is also found in the lysosomes, which is possibly due to saturation of the endocytic pathway. The tissue specific abundance of PLAP and its membrane association may also contribute to a slow turnover of this protein.

Table 5.3 ***N-terminal sequence from Red Dye non-binding lysosomal-enriched membrane proteins.***

ID	kDa	PI	Level	*N*-terminal sequenced	Protein identified	Swiss-Prot ID
M12	67	5.74		IIPVEE(E)N(P)(D)	Placental alkaline phosphatase	PPB1_HUMAN
M13	67	5.75		IIPVEEEN(P)D(F)	Placental alkaline phosphatase	PPB1_HUMAN
M14	67	5.76	2.0 pmol	IIPVEEENPD(F)(N)(N)X(E)	Placental alkaline phosphatase	PPB1_HUMAN
M15	67	5.8	0.5 pmol	IIPVEEENP(D)	Placental alkaline phosphatase	PPB1_HUMAN
M21	80	5.8-6.2	1.8 pmol	VPDKTVRXXAV(S)(E)	Serotransferrin	TRFE_HUMAN

5.4.3 Search for the lysosomal sulphate transporter and the human SAT-1 protein using a unique region of the human SAT-1 sequence.

Dr. Lorne A. Clarke of the Department of Medical Genetics, University of British Columbia, Vancouver, Canada very kindly provided the unpublished human SAT-1 sequence.

The human SAT-1 sequence was revealed by personal communication from Dr. Lorne Clarke. With this knowledge a unique sequence to this protein could be determined. All work done up to this point in the study relied on the rat SAT-1 sequence. At this point, with the addition of the human SAT-1 sequence, this family of proteins consisted of three human proteins (SAT-1, DRA and DTDST) and one rat protein (SAT-1).

5.4.3.1 Design of a peptide antigen unique to the human SAT-1 protein.

A fourth member (excluding orthologs) of the SAT-1 protein family (Pendrin) was found after the unique peptide was designed, and is included in the alignment which follows. The four human members of the SAT-1 family, which included the unpublished human SAT-1 sequence, were aligned and a unique region in a hydrophilic domain chosen from the human SAT-1 sequence (*Figure 5.8*). A BLAST search of this sequence against the NR databases only found homology with the rat SAT-1 sequence. The unique thirteen residue peptide (FDPSQDGLQPGAC) in the second extra-membranous loop on the extracellular side of the membrane, was coupled to diphtheria toxoid and used to raise antibodies in rabbit as described in *Section 5.3.2.1.*

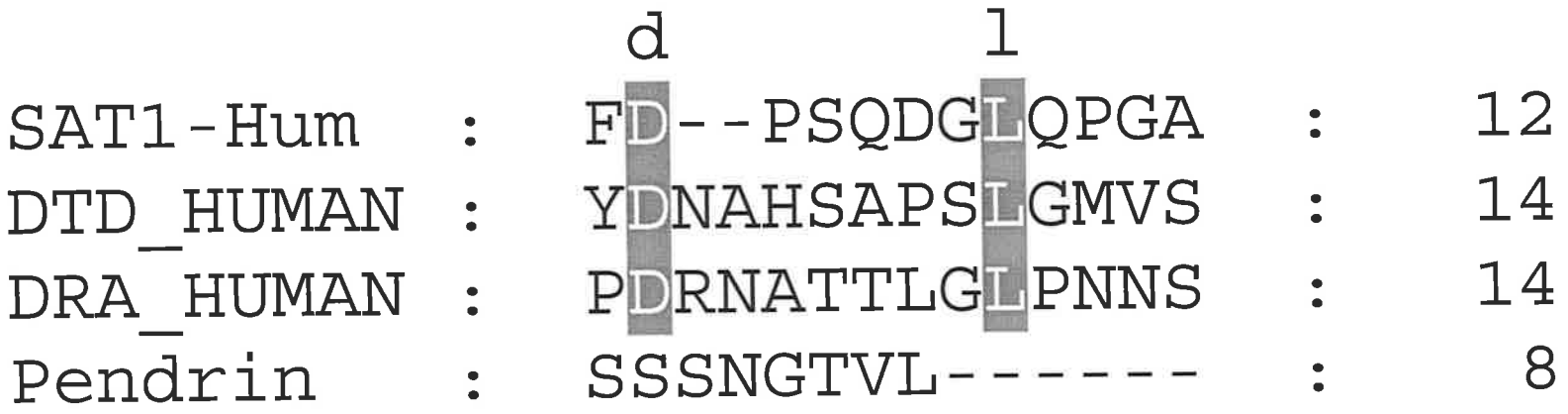

Figure 5.8 Unique peptide to the human SAT-1 protein.

The amino acid sequences of three human sulphate transporters, DTD-Hum, DRA-Hum and Pendrin were aligned with the human SAT-1 sequence. The amino acids of this hydrophilic region of the alignment correspond to numbering used in by the Swiss-Prot database entries: 185-198 for DTD_HUMAN, 150-163 for DRA_HUMAN and 158-171 for Pendrin. The human SAT-1 residues were 144-157. The alignment was performed with the GCG* program Pileup, with an open gap penalty of 3.0, a gap extension penalty of 0.1 using the Blosum 62 scoring matrix. The program GenDoc (Version 2.0.004 by Karl B. Nicholas) was used to present this part of the alignment. The number of residues within each protein in this region is indicated to the right.

* Genetics Computer Group, Inc. WISCONSIN PACKAGE, Version 8.1-UNIX, August 1995 and the EGCG extensions to the WISCONSIN PACKAGE, Version 8.1.0, March 1996.

5.4.3.2 Affinity purification of antibodies to the conserved and unique peptide sequences.

Non-specific antibodies are generated during polyclonal antibody production, resulting in non-specific cross-reactivities, such as those detected with the anti-SAT-1 antibodies (*Section 5.4.2.6*). Non-specific antibodies generated against the carrier protein (diphtheria toxoid) were therefore, adsorbed by passing the antibodies over diphtheria toxoid (18 mg) coupled to Affi-Gel 15 (5 mL). The coupling was 72% efficient as calculated from the recovery of diphtheria toxoid (DT). The DT-Affi-Gel 15 was treated with urea, before passing the polyclonal serum through the column (*Section 5.3.2.2.1*). Adsorbing the polyclonal antibody with denatured DT was found to reduce cross-reactivity with DT, more than that with non-denatured DT (data not shown). To measure the effectiveness of the DT adsorption and to investigate the cross-reactivities of these antibodies a third antibody was employed. The three antibodies were against peptides coupled to DT, the unique human SAT-1 (FDPSQDGLQPGAC), the conserved rat SAT-1 (FATSAALSKTLVKIATGC) sequences, and the human lysosomal-associated membrane protein (LAMP-1) (CLVGRKRSHAGYQTI) sequence which was another unrelated negative control. The cross-reactivities of these antibodies before adsorption against diphtheria toxoid is shown in *Figure 5.9*.

Figure 5.9 Cross-reactivities of the conserved and unique anti-SAT-1, and anti-LAMP-1 antibodies to each other.

Wells were coated with 10 µg/mL of BSA (×); diphtheria toxoid (○); conserved SAT-1 diphtheria toxoid antigen (□); unique SAT-1 diphtheria toxoid antigen (△); LAMP-1 diphtheria toxoid antigen (◇). The primary polyclonal antibodies were against the conserved SAT-1 diphtheria toxoid antigen (**A**); unique SAT-1 diphtheria toxoid antigen (**B**); and LAMP-diphtheria toxoid antigen (**C**). Coating of plates, primary and secondary antibody incubations, and colour development were performed as described in *Section 2.2.10.1.3.* The ELISA plates were read at 10.5, 10.5 and 9.5 min respectively, after the addition of colour development substrate.

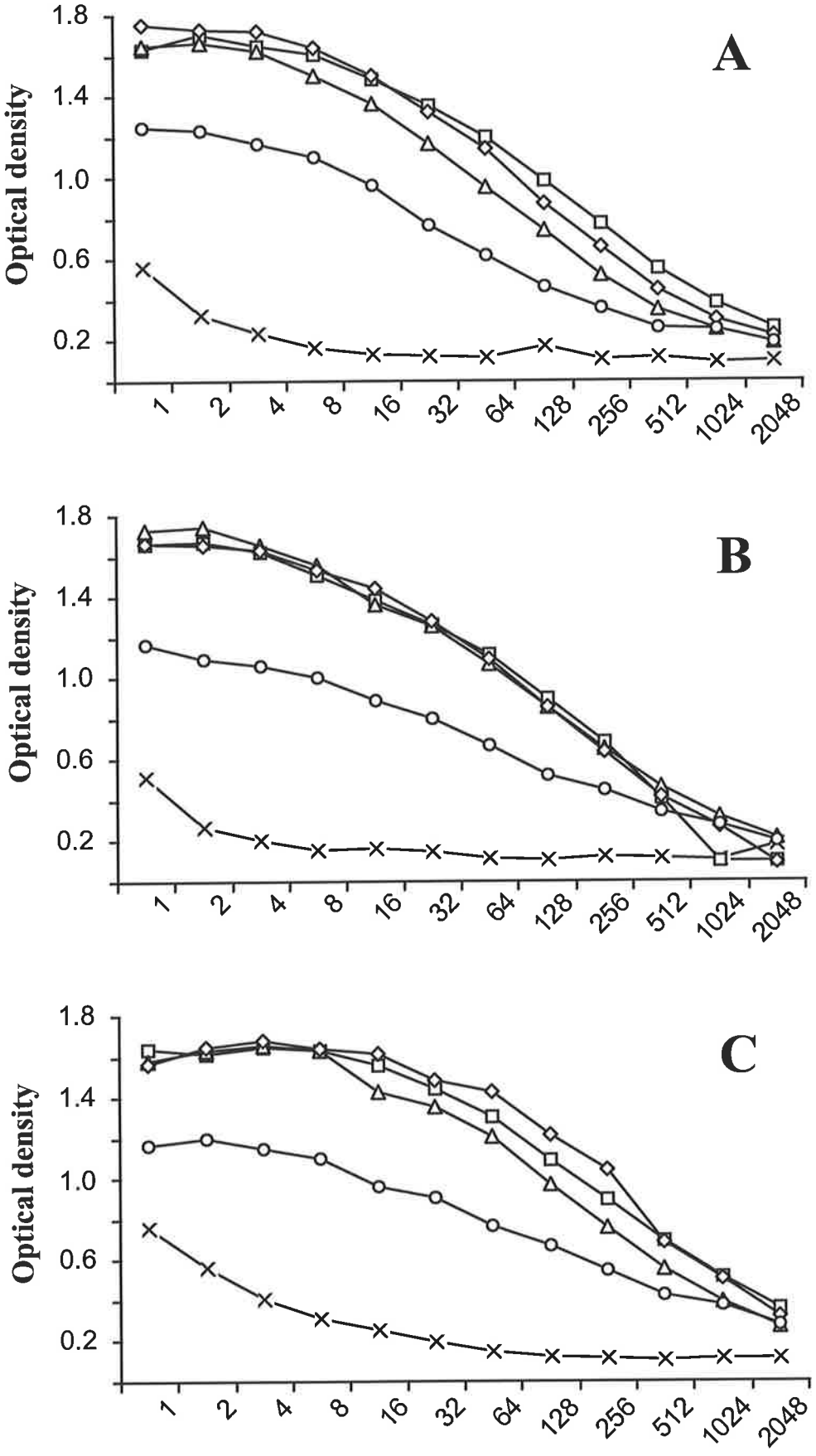
A
B
C
Optical density
1.8
1.4
1.0
0.6
0.2
1
2
4
8
16
32
64
128
256
512
1024
2048
Primary antibody dilution (x 1:1000)

After diphtheria toxoid adsorption the antibodies did not cross-react with the carrier-protein, but they did cross-react with all three peptides coupled to the carrier (*Figure 5.10*). The peptides coupled (Mimotopes Pty. Ltd, Australia) to diphtheria toxoid were based on the method of Lee *et al.* (1980). This method uses the bifunctional reagent 6-maleimido caproic acyl *N*-hydroxy succinimide ester (MCS) which is first coupled to an amino group of a carrier. The MCS-modified carrier containing maleimido reactive groups is then conjugated to peptides containing a thiol group. A possible remaining common antigen between the antibodies after diphtheria toxoid adsorption may have been the peptide-carrier bridge. Cross-reactivities between peptide-carrier conjugates were found in a study (Briand *et al.* 1985) where chaos coupling reagents such as glutaraldehyde were used. The cross-reactivities were found to be to specific to the modifications made to the carrier by the coupling reagent. This was shown by cross-reactivities to different carriers modified by the same coupling reagent, but not between the same carriers modified by different coupling reagents. The coupling reagent used by Mimotopes Pty. Ltd., known as 6-(*N*-maleimido)-*n*-hexanoate (MHS) however, was reported to show almost no reactivity (Peeters *et al.* 1989). The more flexible non-aromatic linkage from MHS was the reason why this coupling reagent did not induce the high linker-specific antibody levels, other constrained maleimide type coupling reagents did.

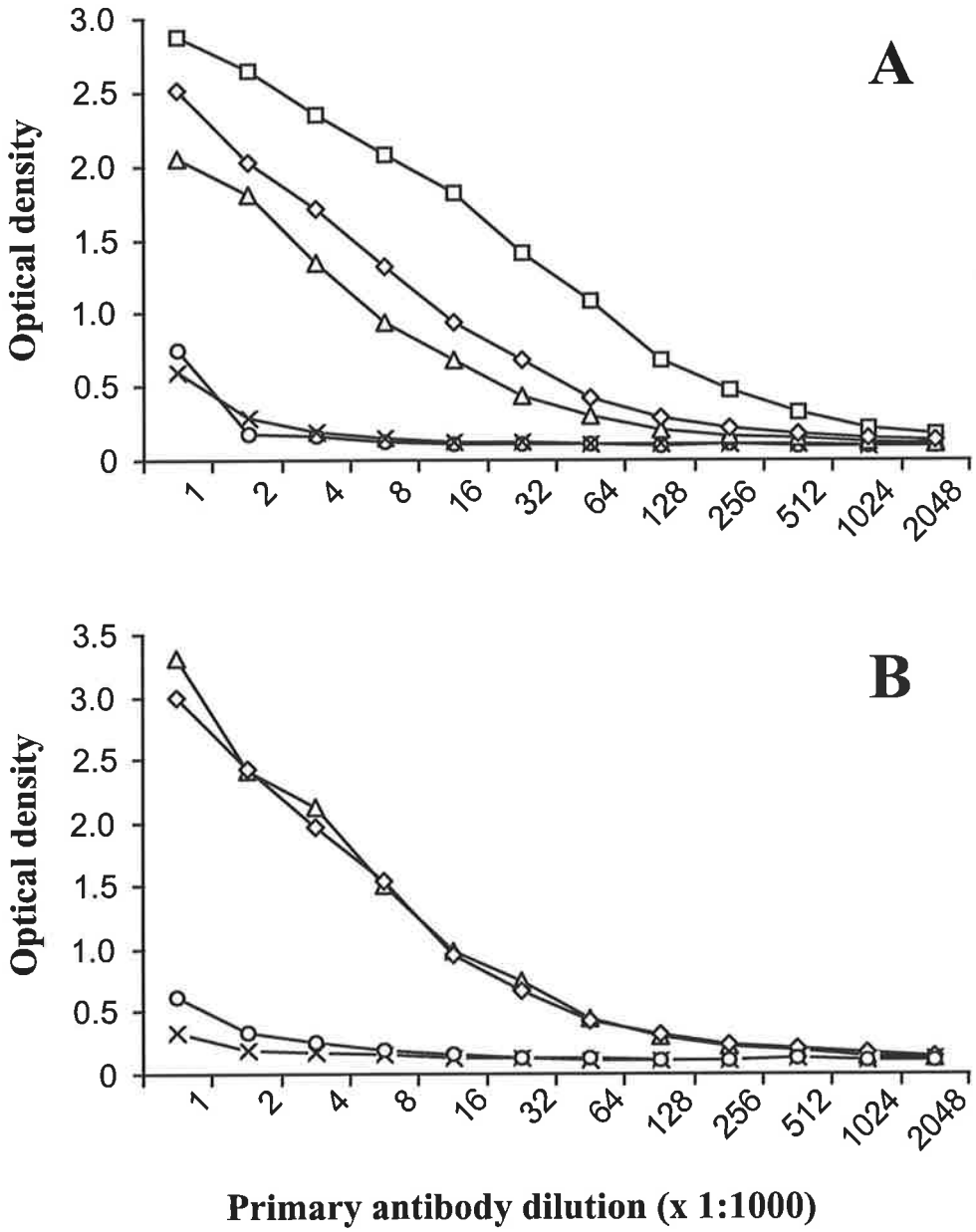

Figure 5.10 Cross-reactivities of diphtheria toxoid adsorbed antibodies.

Wells were coated with 10 µg/mL of BSA (×); diphtheria toxoid (○); conserved SAT-1 diphtheria toxoid antigen (□); unique SAT-1 diphtheria toxoid antigen (△); and LAMP-1 diphtheria toxoid antigen (◇). The primary polyclonal antibodies were against the conserved SAT-1 diphtheria toxoid antigen (**A**); unique SAT-1 diphtheria toxoid antigen (**B**). Coating of plates primary and secondary antibody incubations, and the colour development were performed as described in *Section 2.2.10.1.3.* The ELISA plates were read at 20 and 10.5 min respectively, after the addition of colour development substrate.

To remove the non-specific cross-reactivities the polyclonal antibodies against the SAT-1 conserved and unique peptides were affinity purified peptides coupled to thiopropyl-Sepharose 6B (see *Section 5.3.2.2.2*). The purified antibodies were quantified (*Table 5.4*) and visualised with silver on an SDS-PAGE gel (not shown). The anti-conserved SAT-1 antibody was at background level against conserved SAT-1, and LAMP-1 antigens conjugated to DT with a 40-fold dilution, while cross-reacting with the conserved SAT-1 antigen with a 10240-fold dilution. The anti-unique SAT-1 antibody did not cross-react with the conserved SAT-1 or LAMP-1; DT conjugated antigens with a dilution greater than 80-fold, while it did cross-react with the unique SAT-1 antigen with a 1280-fold dilution.

Table 5.4 Quantities of affinity purified antibodies.

Antibody protein was quantified by the BCA assay with a BSA standard and converted to μg of IgG by dividing by 1.12.

	Conserved SAT-1 antibody FATSAALSKTLVKIATGC	**Unique SAT-1 antibody FDPSQDGLQPGAC**
Serum	1 mL	3 mL
Low pH elution	150 μg	540 μg
High pH elution	10 μg	1175 μg

5.4.3.3 Identification of human SAT-1 cross-reactive proteins.

Western blot analysis with affinity purified antibodies against the conserved and unique SAT-1 peptides detected many fewer proteins. The anti-SAT-1 antibodies against the conserved peptide detected a 53 kDa protein in the lysosomal Con A-Sepharose flow through, and a 31 and 55 kDa in the Con A-Sepharose eluate. The anti-SAT-1 antibody against the unique peptide detected a 52 kDa protein in the Con A-Sepharose flow through, and a 57 kDa protein in the lysosomal Con A-Sepharose eluate. The 55 and 57 kDa proteins detected may

have been the same protein with the relative molecular mass difference due to gel-to-gel variation. The molecular weight difference of 2-5 kDa between the proteins detected at approximately 56 kDa in the Con A-Sepharose -flow through and -eluate is probably due to a difference in glycosylation. The slightly larger protein is present in the Con A-Sepharose eluate.

Not enough of the protein detected at approximately 56 kDa in the Con A eluate was purified to obtain *N*-terminal sequence. If the amount of protein used to isolate the candidate proteins were simply increased, it would not increase the relative amounts of candidate proteins. A different approach would therefore be required. A future strategy to isolate enough protein to sequence candidate sulphate transport proteins, could be to enrich candidate proteins from cultured cells. There would be a number of advantages in using cultured cells; a cell line could be chosen that is abundant in lysosomes; there would not be the variation experienced between protein fractions prepared from tissues; there would be no contaminating serum proteins; and less total protein species would be contained in each fraction.

Figure 5.11 Western blot analysis with affinity purified anti-SAT-1 antibodies.

Membrane (1 and 2), Con A-Sepharose flow through (3 and 4), and Con A-Sepharose eluate (5 and 6) proteins; that were either lysosomal (1, 3 and 5) or mitochondrial-enriched (2, 4 and 6) were separated by SDS-PAGE (12.5% polyacrylamide mini-gel), electrophoresed at a constant 200 V (*Section 2.2.6.1*). The protein samples (20 µg) were transferred (250 mA, 1.75 h) to a PVDF filter (*Section 2.2.10.2.2*) and incubated with antibodies affinity purified to the conserved region of SAT-1 (A) and the unique region of SAT-1 (B). The PVDF filter was incubated overnight at 4°C with primary antibodies (5 µg/mL), then with the secondary anti-rabbit antibodies (diluted 2000 fold) for 1 h, and then visualised by ECL (*Section 2.2.11*).

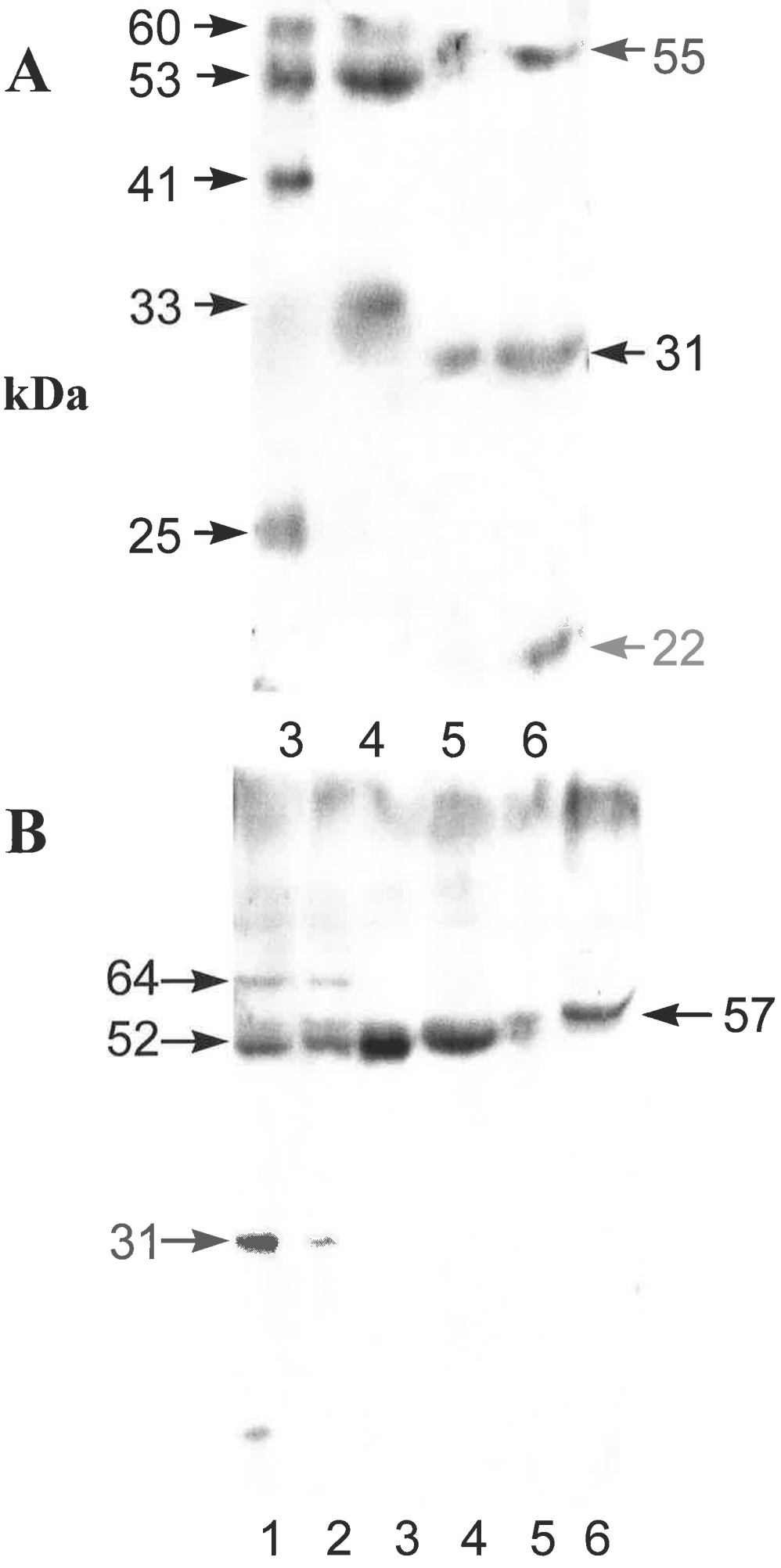
A
60
53
41
33
25
kDa
55
31
22
3 4 5 6
B
64
52
31
57
1 2 3 4 5 6

5.4.4 SAT-1 family sequence analysis.

Analysis of the SAT-1 related proteins has not been reported. The human SAT-1 protein was not available from the public databases (checked February 2000) and the publications reporting the SAT-1 like sulphate transporters have focused on the protein's possible function. The most recent member of the SAT-1 family, Pendrin, which was cloned since completion of this study (*Section 1.5.2.4*) has been included in the sequence analysis. New orthologs found since completion of this study have also been included.

5.4.4.1 Database searching.

Sequences with homology to members of the SAT-1 family were found by database searches. The FastA (Pearson and Lipman 1988), BLASTP (Altschul *et al.* 1990) and PSI-BLAST (Altschul *et al.* 1997) algorithms were used to search the non-redundant (NR) protein databases*. These included the Swiss-Prot (Bairoch and Apweiler 2000), GenPept (Benson *et al.* 2000) and the Protein Information Resource (PIR) (George *et al.* 1997) databases. To search for both closely and distantly related sequences, the three point accepted mutation (PAM) matrices PAM40, PAM120 and PAM250 (Dayhoff *et al.* 1978) were used, with the k-turple or word lengths set to one.

* Australian National Genomic Information Service (ANGIS) NR database consists of data collated from GenPept, Swiss-Prot and PIR. GenPept is an ANGIS database generated by translating GenBank coding sequences. Swiss-Prot is a database compiled predominantly from the translation of DNA sequences from EMBL, with other sequences from the literature and submissions by researches. The Protein Information Resource (PIR) is an American collaboration with the German MIPS and Japanese JIPID protein databases. ANGIS is located at The University of Sydney (http://www.angis.org.au).

5.4.4.2 Sequence alignments and phylogenetic analysis.

Proteins found from searching databases with the human SAT-1 protein (*Section 5.4.4*) that had an E value* less than 0.05 were aligned using ClustalW (Thompson *et al.* 1994). ClustalW was run with its pairwise similarity scores calculated from slow, accurate, global alignments using a dynamic programming method.

A phylogenetic tree was produced using the 'distance matrix' method. The 'maximum parsimony' method was not used as it does not use branch length information, and the 'maximum likelihood' method was not used as it is too computationally intensive. The 'distance matrix' method was performed sequentially by the programs Seqboot (bootstraps), Protdist (creates a distance matrix), Kitsch (predicts a phylogenetic tree), and Consense (calculates a consensus tree). These programs are part of the widely used Phylogeny Inference Package (PHYLIP), version 3.2 (Felsenstein 1989), which uses an alignment of sequences such as that produced by ClustalW.

The ClustalW alignment was used to produce a set of 500 bootstrapped† alignments, which were used to produce a set of 500 bootstrapped phylogenetic trees using Protdist. Kitsch was run to generate a data set of rooted trees. A rooted tree, in addition to displaying branch lengths (representative of the degree of relatedness), also indicates the ancestral order of genes, with the oldest at the root of the tree. Consense was used to generate a consensus tree from the set of 500 trees (*Figure 5.12*).

The rule of thumb for statistical interpretations of phylogenetic trees is that if the branching pattern has greater than 70% bootstrap support, then the branching is likely to be correct at the

---

* An E value indicates the statistical significance of an alignment, based upon the extreme value distribution.

† Determination of statistical likelihood of an alignment or branch decisions in a phylogenetic tree.

95% level (Hillis and Bull 1993). The phylogenetic tree suggests that the bacteria at the bottom of the tree have the most primitive sulphate transporters which are most closely related to the unicellular eukaryotic yeasts and fungi, followed by the nematode worm (*Caenorhabditis elegans*), mammals, *Drosophila*, blue green algae and cyanobacterium, and then plants.

In viewing the tree, however, it must be appreciated that the sodium-independent sulphate transporter family consists of transporters that range from low to high affinity transporters. The phylogenetic tree has a number of orthologs, some of which occur within the one species, while in other species only one sulphate transporter was known. The bacterial proteins at the bottom of the tree are low affinity transporters and those towards the top are high affinity transporters. The fungi proteins are sulphate permeases and the sulphate transporters in mammals are not divided into high and low affinity transporters. The mammalian transporters were found to be expressed in a tissue-specific manner.

The weakest consensus in bifurcations of the tree occurs where the single cell and multicellular eukaryotic clades branch (28%), and the division between the plants and cyanobacteria (29%). The reduced statistical certainty of these bifurcations reflects the evolutionary distance between animals, plants and the single cell organisms. Seventy-six percent of the 55 bifurcations were highly significant with a 95% confidence level.

The protein sequences aligned and illustrated in the phylogenetic tree (*Figure 5.12*) are listed in *Appendix A*. For a short list of these proteins, whose functions are well described or representative from different clades of the phylogenetic tree, *see Table 5.5*.

Figure 5.12 Rooted phylogenetic tree of proteins homologous to human SAT-1.

A set of proteins homologous to human SAT-1 were analysed as described in *Section 5.4.4.2*. The tree root is on the left, bifurcations are to the right, ending with the tree tips. TreeView© (Page 1996) was used to display the tree ladderised to the left. The number at each fork indicates the number of phylogenetic trees out of 500 bootstrapped sets whose bifurcation occurred as shown. The number of bifurcations with 95% confidence are not displayed.

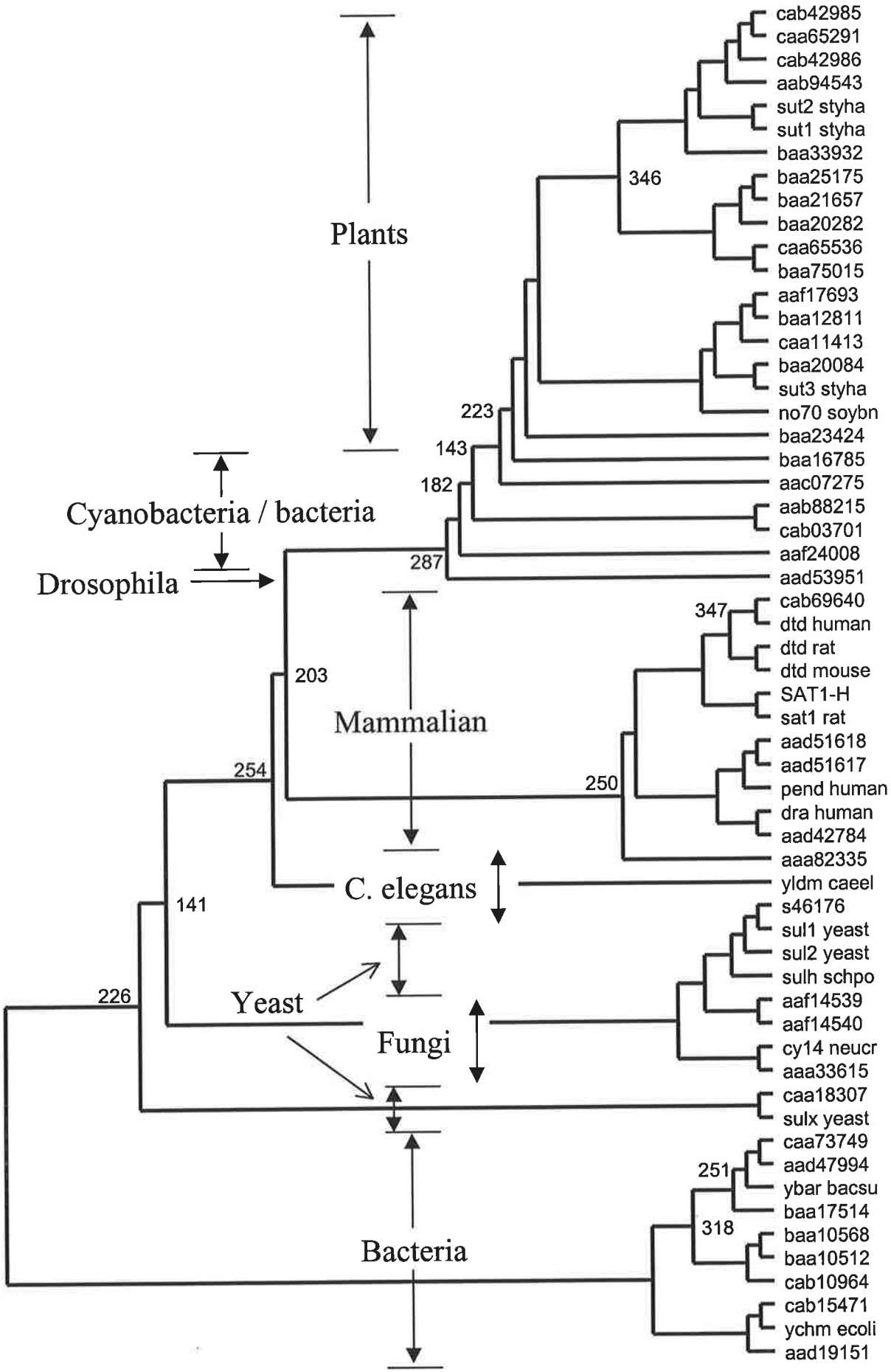
Plants
Cyanobacteria / bacteria
Drosophila
Mammalian
C. elegans
Yeast
Fungi
Bacteria
346
223
143
182
287
203
254
250
347
141
226
251
318
cab42985
caa65291
cab42986
aab94543
sut2 styha
sut1 styha
baa33932
baa25175
baa21657
baa20282
caa65536
baa75015
aaf17693
baa12811
caa11413
baa20084
sut3 styha
no70 soybn
baa23424
baa16785
aac07275
aab88215
cab03701
aaf24008
aad53951
cab69640
dtd human
dtd rat
dtd mouse
SAT1-H
sat1 rat
aad51618
aad51617
pend human
dra human
aad42784
aaa82335
yldm caeel
s46176
sul1 yeast
sul2 yeast
sulh schpo
aaf14539
aaf14540
cy14 neucr
aaa33615
caa18307
sulx yeast
caa73749
aad47994
ybar bacsu
baa17514
baa10568
baa10512
cab10964
cab15471
ychm ecoli
aad19151

Table 5.5 Proteins included in the phylogenetic analysis illustrated in Figure 5.12.

Swiss Prot ID	Description	Organism	Reference
DTD_RAT	Sulphate transporter (ortholog of DTD_HUMAN)	Rattus norvegicus	Satoh *et al.* 1998
DTD_MOUSE	Sulphate transporter (ortholog of DTD_HUMAN)	Mus musculus	Kobayashi *et al.* 1997
DTD_HUMAN	Sulphate transporter (diastrophic dysplasia protein)	Homo sapiens	Hastbacka *et al.* 1994
SAT1_RAT	Sulphate anion transporter 1 (canalicular sulphate transporter) (sulphate/carbonate antiporter)	Rattus norvegicus	Bissig *et al.* 1994
Human SAT-1*	Sulphate transporter (ortholog of SAT1_RAT)	Homo sapiens	Clarke *et al.* 1994
DRA_HUMAN	Sulphate transporter (down-regulated in adenoma)	Homo sapiens	Schweinfest *et al.* 1993
PEND_HUMAN	Sulphate transporter (pendrin)	Homo sapiens	Everett *et al.* 1997
YLDM_CAEEL	Hypothetical 85.0 kd protein F41D9.5 in chromosome X.	Caenorhabditis elegans, nematode worm.	Submitted to EMBL/ GenBank/DDBJ databases
SUT1_STYHA	High affinity sulphate transporter 1. Belongs to the sulphate permease family	Stylosanthes hamata tropical forage, legume	Smith *et al.* 1995a
SUT2_STYHA	High affinity sulphate transporter 2	Stylosanthes hamata	Smith *et al.* 1995a
SUT3_STYHA	Low affinity sulphate transporter 3	Stylosanthes hamata	Smith *et al.* 1995a
NO70_SOYBN	Early nodulin 70	Glycine max, soybean	Kouchi and Hata 1993

(table continued next page...)

* This protein sequence is not available from a database.

(table continued...)

Swiss Prot ID	Description	Organism	Reference
SULX_YEAST	Putative sulphate transporter YPR003C	Saccharomyces cerevisiae	Submitted To Badcock K. Bowman S. Churcher C.M. Pearson D. Rajandream M.A. Walsh S.V. Barrell B.G. (Apr-1996) to the EMBL/ GenBank/ DDBJ Databases
YCHM_ECOLI	Hypothetical 58.4 kDa protein in PTH-PRSA intergenic region	Escherichia coli.	Blattner *et al.* 1997
YBAR_BACSU	Hypothetical 46.4 kDa protein in RRNG-FEUC intergenic region	Bacillus subtilis.	Submitted by Liu H. Yasumoto K. Haga K. Ohashi Y. Yoshikawa H.Takahashi H. (APR-1996) to the EMBL/ GenBank/ DDBJ databases.
CY14_NEUCR	Sulphate permease II	Neurospora crassa.	Ketter *et al.* 1991
SULH_SCHPO	Probable sulphate permease SPBC3H7.02	Schizosaccharomyces pombe	Submitted by Lyne M. Rajandream M.A. Barrell B.G. Jimenez Martinez J. (AUG-1998) to the EMBL/ GenBank/ DDBJ databases.
SUL1_YEAST	Sulphate permease 1 (high-affinity sulphate transporter 1)	Saccharomyces cerevisiae	Smith *et al.* 1995b
SUL2_YEAST	Sulphate permease 2 (high-affinity sulphate transporter 2)	Saccharomyces cerevisiae	Submitted by Johnston M. et al. (APR-1996) to the EMBL/ GenBank/ DDBJ databases.
YG35_YEAST	Hypothetical 117.0 kDa protein in ASN2-PHB1 intergenic region	Saccharomyces cerevisiae	Van Dyck *et al.* 1997
YA7B_SCHPO	Hypothetical 107.1 kDa protein C24H6.11C in chromosome I	Schizosaccharomyces pombe	Submitted by Barrell B.G. Rajandream M.A. Walsh S.V. (SEP-1995) to the EMBL/ GenBank/ DDBJ databases.

5.5 Discussion.

The iduronidase PCR described in *Section 5.4.1.2* showed (*Figure 5.2B*) the expected size product of 225 bp and the additional 84 bp product resultant from alternative splicing. The lack of SAT-1 product in the human liver and fibroblast cDNA could have been due to a lack of homology between the rat and human sequence in the region to which the primers were designed.

Antibodies to a conserved peptide sequence of the rat SAT-1 protein and a unique peptide to the human SAT-1 protein were raised in rabbits. These antibodies were found to be more specific after affinity purification. The first antibodies (conserved) detected a 55 kDa protein and the second (unique) antibody a 57 kDa protein in lysosomal Con A-Sepharose flow through and eluate fractions, respectively. Disappointingly, not enough of these cross-reactive candidate proteins could be isolated to obtain *N*-terminal sequence. Another approach beginning with less protein species, may be required to purify enough enriched lysosomal sulphate transport proteins to enable *N*-terminal amino sequence to be obtained

A phylogenetic analysis of 58 members of the sodium-independent sulphate transporter family revealed these transporters are conserved across many species while performing a range of functions. Plants have high affinity sulphate transporters involved in nutrient uptake, while animal, yeast and fungi require sulphate transported for biochemical and metabolic purposes.

The DTDST has turned out to be the most widely expressed of this family of sulphate transporters. The DTDST sequence may have been used in preference to that of SAT-1 considering its tissue distribution. This is not to say SAT-1 is not widely distributed, as only

eight tissues had been tested with four positives for SAT-1 expression (*Table 5.6*). The SAT-1 sequence was especially attractive with it being partly coded for on the antisense DNA strand of the lysosomal enzyme iduronidase.

Table 5.6 Summary of sulphate transporter distribution

Tissue	SAT-1	DRA	DTDST	Pendrin
liver	✓	×	✓	×
kidney	✓	×	✓	×
skeletal muscle	✓		✓	×
brain	✓	×	✓	×
small intestine	×		✓	×
proximal and distal colon	×	✓	✓	
heart	×	×	✓	×
lung	×	×	✓	×
placenta		×	✓	×
spleen		×	✓	
peripheral blood leucocytes		×	✓	
testis		×	✓	×
ovary		×	✓	
thymus		×	✓	×
prostate			✓	
thyroid				✓
pancreas		×		×
bone marrow		×		
adrenal medulla				×
adrenal cortex				×
stomach				×

The most recently discovered sulphate transporter, Pendrin (Everett *et al.* 1997), was reported to overlap with the sulphate transporter DRA. Pendrin has only been found to be expressed in thyroid, and DRA in colon. Pendrin is attributed to 10% of congenital deafness while DRA is involved in colon adenoma. These findings suggest that the overlap of the two transporters, more than likely is coincidental and not functional. As described earlier SAT-1 and iduronidase are also overlapping genes. This rare juxtaposition of sulphate transporters on the opposite DNA strand of other genes may be a consequence of some property of the gene's sequence and duplication during evolution. The next chapter examines the possibility of any consequences for lysosomal sulphate transport if the iduronidase gene is altered in the region of the SAT-1 gene.

6. Investigation of sulphate transport in human skin fibroblasts.

6.1 Introduction

Prior to these studies placental material had been used to study the involvement of the SAT-1 protein in lysosomal sulphate transport. A number of observations, however, prompted the investigation of sulphate transport in human skin fibroblasts. These observations were the coincidence that the SAT-1 and iduronidase genes overlap (*Section 1.5.2.1*), and the availability of α-L-iduronidase mutant cell lines, one of which contains it's mutation in this overlapping region.

The α-L-iduronidase mutation (Q70X) in the overlapping region of the SAT-1 gene is in the 3' untranslated region of SAT-1. A difference in the clinical severity between the iduronidase Q70X and W402X genotypes, both of which are null mutations, has been observed (*personal communication John Hopwood*). The difference in phenotype may relate to the impairment of sulphate transport due to the Q70X mutation, which occurs in the overlapping regions of the two genes.

The study of sulphate transport in these cell lines may therefore, reveal differences between Q70X and W402X that relate to a defect in SAT-1 expression. Human skin fibroblasts with an α-L-iduronidase deficiency also provide an advantage over placental material in that they can be loaded with sulphate in the form of glycosaminoglycan (GAG) stored within the lysosome and that sulphate can be released by the addition of iduronidase into the culture media.

Transport studies were performed to determine whether the common mutation to iduronidase (Q70X) and SAT-1 affected sulphate transport across either the plasma or lysosomal membrane. Although the mutation falls in the 5' untranslated region of SAT-1 it was thought the mutation common to both genes may be responsible for the extreme clinical severity seen in this MPS I phenotype. This relatively frequent mutation causes the 70th amino acid residue to become a premature stop codon. Another frequent MPS I mutation W402X, like Q70X has no detectable iduronidase enzyme or activity (*personal communication* John Hopwood) but does not lie in the overlapping region. Disease progression of individuals with the Q70X mutation is significantly worse than the W402X phenotype and consequently coined 'galloping' Hurler (Scott *et al.* 1992; *personal communication,* John Hopwood 1998). The hypothesis therefore, is that the Q70X mutation is more severe than the W402X mutation, because this mutation also in the SAT-1 gene affects sulphate transport.

6.2 Methods.

6.2.1 Fibroblast cultures.

Fibroblast cultures were established by Kathy Nelson, Department of Chemical Pathology, Women's and Children's Hospital, Adelaide, South Australia.

Human diploid fibroblasts were established from skin biopsies submitted to the Women's and Children's Hospital for diagnosis (Hopwood *et al.* 1982). Fibroblasts were grown to confluence with basal medium Eagle's (BME) and 10% (v/v) foetal calf serum (FCS) at 37°C with 5% CO_2 and 95% humidity. Culture flasks (75 mL) were split or harvested by washing with 3 mL PBS, incubation for 4 min with 2 mL versine/trypsin and tapped on the palm of the hand several times to detach cells, which was verified under a microscope. Cells were collected and the flasks rinsed with PBS to increase cell recovery. Pooled cells were pelleted at 400 ***g*** (1500 rpm), for 5 min at 4°C in bench top centrifuge and washed once with PBS.

6.2.2 Sulphate uptake in fibroblasts.

Cells were grown in six-well (3.5 cm diameter) Corning™ plates. Fibroblasts were washed twice with 1 mL PBS and pre-incubated for 1 h in 150 mM NaCl, 4 mM hemi-magnesium gluconate, 300 μM sulphate, 10 mM HEPES titrated to pH 7.5 with Tris. Fibroblasts were then washed once with 1 mL fresh pre-incubation medium and 1 mL of uptake medium consisting of 150 mM NaCl, 4 mM hemi-magnesium gluconate, 25 mM MES, 50 μM sodium [^{35}S]-sulphate titrated to pH 5.5 with HCl. Uptake was stopped by aspiration of the uptake medium followed by six 1.5 mL ice-cold PBS washes. Fibroblasts were solubilised with 1 mL 0.1 M NaOH rocking for 1 h at 20°C. Sulphate uptake was then quantitated by scintillation counting 200 μL of the solubilised cells.

6.2.3 Lysosomal storage, degradation and quantification of radio-labelled glycosaminoglycans.

*Recombinant iduronidase was produced by Kay Beckman (*Unger *et al.* 1994), *Department of Chemical Pathology, Women's and Children's Hospital, North Adelaide, South Australia.*

Fibroblasts were grown in 75 mL (large) flasks with BME until confluent. Each flask was washed with 5 mL PBS and incubated for 24 h with 5 mL Ham's F12 containing 10% dialysed FCS and 75 μL sodium [^{35}S]-sulphate (2 μCi/mL). Flasks were aspirated and fibroblasts grown in BME with 10% FCS for 48 h to remove sulphate not incorporated into glycosaminoglycans.

To degrade and clear the stored lysosomal glycosaminoglycans 1 μL (1 μg) recombinant iduronidase (8965 nmol/min/mg) was added to each 75 mL flask and returned to the incubator for various times. To quantitate the sulphate-labelled material in the lysosome, the fibroblasts in each flask were harvested and dissolved in 1 mL 0.1 M NaOH before scintillation counting.

6.2.4 Separation of glycosaminoglycans from sulphate.

Samples of solubilised fibroblasts (100 μL) were neutralised with 0.1 M HCl and 0.5 mL of 0.5 M NaCl, 20 mM sodium phosphate, pH 7 was added. Samples were then chromatographed on Sephadex G10 (1 x 30 cm), Biogel P2 (1 x 29 cm) or an Econo-Pac anion exchange Q cartridge.

6.2.4.1 Sephadex G10 chromatography.

A 1 x 30 cm column packed with Sephadex G10 was blocked with 1 mg sodium heparan in 10 mL of application buffer (0.5 M NaCl and 20 mM sodium phosphate, pH 7) and washed with 100 mL of application buffer. Samples were applied and eluted from the column at

1 mL.min^{-1} with application buffer. Fractions (1 mL) were collected, of which 200 µL was counted with 4 mL of scintillant.

6.2.4.2 Biogel P2 chromatography.

A 1 x 30 cm column was packed with 23 mL of Biogel P2. Samples were applied and run at 0.15 mL.min^{-1} (11.4 cm.hr^{-1}) in 0.5 M NaCl, 20 mM sodium phosphate, pH 7. Fractions of 0.75 mL were collected, of which 200 µL was counted with 4 mL of scintillant.

6.2.4.3 Econo-Pac anion exchange Q cartridge.

A Bio-Rad® cartridge containing 1 mL of a strongly basic anion exchanger with a $-N^{+}(CH_3)_3$ functional group was prepared as described in the instructions (washing with a low-salt buffer (10 mM NaCl, 20 mM Tris-HCl, pH 7.4) for 2 min at 2 mL.min^{-1}, with a high-salt buffer (3 M NaCl, 20 mM Tris-HCl, pH 7.4) 10 min at 6 mL.min^{-1}, and then with the low-salt buffer for 10 min at 6 mL.min^{-1}). The column was equilibrated and samples applied at 1 mL.min^{-1} in low-salt buffer. The column was eluted step-wise with high-salt, then with 100 mM Na_2SO_4 also buffered with. Fractions of 1 mL were collected and mixed with 4 mL of scintillant and counted.

6.2.5 Separation of glycosaminoglycans from proteins.

Cells were labelled with sodium [^{35}S]-sulphate as described in *Section 6.2.3*. The solubilised cells were titrated to pH 3.5 with 1 M sodium phosphate, pH 2.5, and placed at 4°C for 1 h. The protein was pelleted by microfuge at 13,000 ***g*** for 15 min, and the supernatant was desalted on a Sephadex G10 column (1 x 10 cm) at 1.5 mL.min^{-1} with 10% (v/v) aqueous ethanol. The glycosaminoglycan fractions (0.5 mL) detected by scintillation counting (50 µL) were pooled and freeze dried.

6.2.6 Gradient SDS-PAGE of glycosaminoglycans.

Glycosaminoglycans were kindly electrophoresed by Enzo Ranieri, Department of Chemical Pathology, Women's and Children's Hospital, North Adelaide, South Australia. Molecular weight standards were a gift from Jeremy Turnbull, School of Biochemistry, University of Birmingham, Edgbaston, England.

The glycosaminoglycans prepared as described in *Section 6.2.5* were resolved by a linear 30-40% gradient non-reducing, non-denaturing PAGE as described by Turnbull *et al.*. GAG samples were assayed for uronic acid (Blumenkrantz and Asboe-Hansen 1973), and 0.5 μg of uronic acid equivalent loaded in 10% (v/v) glycerol. Electrophoresis was performed at 150 V for 30 min until samples had entered the resolving gel, then 350 V for 16 h (Byers *et al.* 1998). The gel was stained with 1% (w/v) Alcian Blue for 30 min in 2% (v/v) acetic acid, washed in 20% ethanol, 10% acetic acid for 15 min and rinsed in water (Merril *et al.* 1981). The gel was then silver stained as described in *Section 2.2.7.2*.

6.3 Results and Discussion.

6.3.1 Sulphate uptake in MPS I fibroblasts.

To investigate whether the Q70X mutation affected sulphate transport across the plasma membrane, sulphate uptake was compared in normal, W402X and Q70X fibroblasts (*Figure 6.1*). No significant difference in sulphate uptake was measured. This sulphate uptake was inhibited in all three fibroblast types assayed by the anion exchange inhibitor SITS (*Table 6.1*). No significant difference therefore, was found in sulphate transport across the plasma membrane, suggesting that the Q70X mutation does not affect sulphate transport at the plasma membrane.

Table 6.1 Inhibition of sulphate uptake in fibroblasts.

Cells were grown to confluence and incubated in the presence and absence of 1.45 mM SITS for 1 min in sulphate uptake buffer. The amount of uptake was determined as described in *Section 6.2.2*.

Genotype	Percent inhibition
Wild type	59.5
Q70X	75.4
W402X	81.6

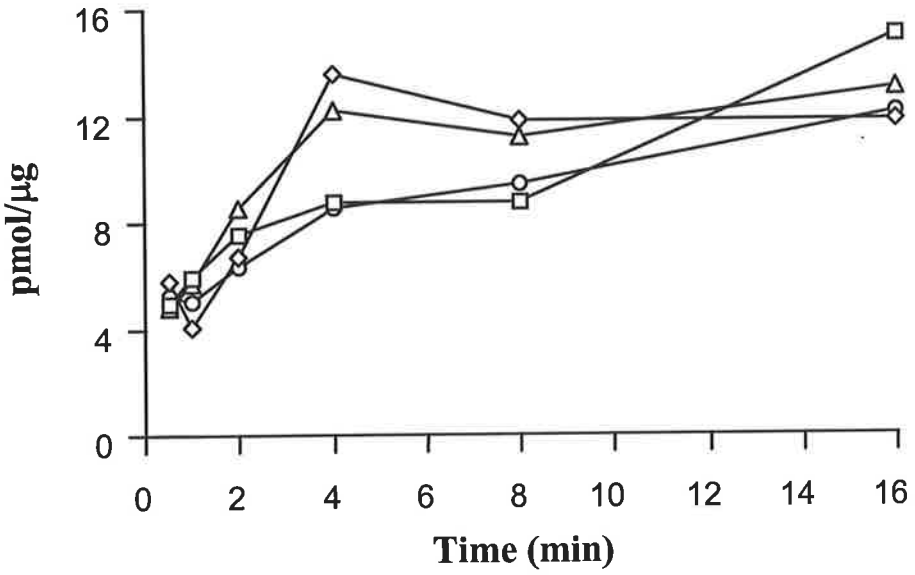

Figure 6.1 Sulphate uptake across the plasma membrane.

Wild type fibroblasts SF4260 (○) and SF4543 (□), and MPS I fibroblasts W402X, SF3125 (△), and Q70X, SF1229 (◇) were grown to confluence in six-well plates (35 mm in diameter). Cells were then washed twice with PBS and incubated for 1 h in pre-incubation medium (150 mM NaCl, 4 mM hemi-magnesium gluconate, 300 µM sulphate, 10 mM HEPES titrated to pH 7.5 with Tris). Fibroblasts were then washed once with 1 mL fresh pre-incubation medium and 1 mL of uptake medium (150 mM NaCl, 4 mM hemi-magnesium gluconate, 25 mM MES, 50 µM sodium [^{35}S]-sulphate titrated to pH 5.5 with HCl) was added. Uptake was stopped by aspiration of the uptake medium followed by six 1.5 mL ice-cold PBS washes. Fibroblasts were solubilised and the sulphate taken-up was quantitated as described in *Section 6.2.2.*

6.3.2 *In-situ* lysosomal sulphate efflux.

If the lysosomal sulphate transporter is unable to allow the efflux of sulphate, sulphate may accumulate in the lysosome. To determine whether sulphate accumulated in the lysosomes of MPS I fibroblasts with the Q70X mutation, fibroblasts were grown in the presence of radio-labelled sulphate to label the stored glycosaminoglycans. Fibroblasts were then treated with recombinant iduronidase to degrade the stored glycosaminoglycans and determine if the liberated inorganic sulphate was retained in the lysosome.

Fibroblasts were labelled with $Na_2{}^{35}SO_4$ (*Section 6.2.3*); after which the were harvested and subcultured with trypsin/versine (*Section 6.2.1*) and allowed to attach in fresh media for 3.5 h; before treating with iduronidase and the measurement of storage clearance over 2 h (data not shown). The radio-labelling and iduronidase treatment of fibroblasts was repeated, allowing cells to attach overnight before the addition of iduronidase (*Figure 6.2*) which was monitored over 4 h. The increased time between treatment with trypsin and iduronidase did not appear to increase the rate of storage removal, which may have increased due to an increase in cell surface receptors and iduronidase uptake. The wild type fibroblasts did not store labelled sulphate as expected, although both the Q70X and the W402X MPS I fibroblasts did retain labelled sulphate, which showed more clearance when iduronidase treatment was extended to 4 h. The amount of apparent labelled storage material contained within the Q70X and W402X fibroblasts was more than that seen in the wild type fibroblasts. Iduronidase treatment reduced the amount of stored material in both of the mutant cell lines, which did not appear significantly different from each other.

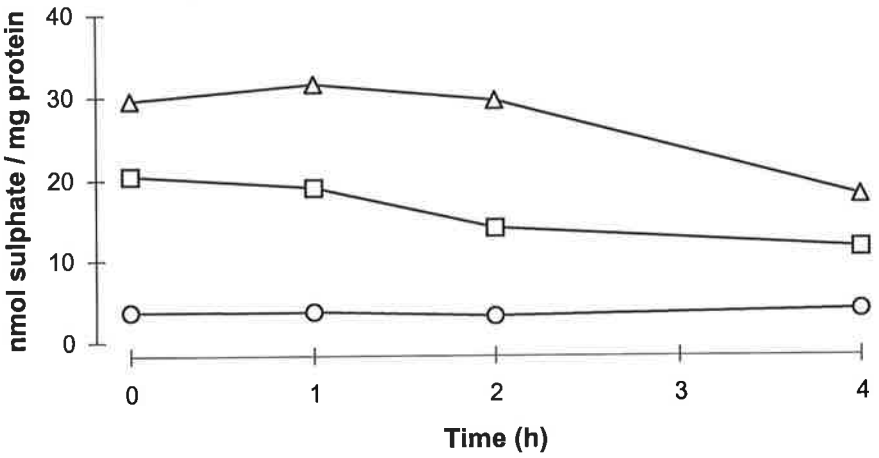

Figure 6.2 Iduronidase treatment of fibroblasts labelled with [^{35}S]-sulphate.

Fibroblasts were grown to confluence in a large flask (75 cm^2), then labelled with $Na_2{}^{35}SO_4$ for 24 h and chased for 48 h. The wild type (○), Q70X (□), and W402X (△) fibroblasts, in each flask were then harvested and subcultured into four smaller (25 cm^2) flasks and returned to 37°C to allow attachment for 16 h. Recombinant iduronidase (1 μg) was introduced for 0, 1, 2 and 4 h, before the cells were washed with ice-cold PBS, harvested with trypsin and washed with PBS (*Section 6.2.1*). The cell pellet was then solubilised with 1 mL of 0.1 N NaOH and the cell lysate mixed with 4 mL of scintillant and the remaining labelled sulphate quantitated by scintillation counting. Wild type, Q70X and W402X fibroblasts were SF4620, SF1229 and SF3125 cell lines respectively.

6.3.3 Determination of sulphate storage.

If sulphate is unable to efflux from the lysosome because its sulphate transporter is defective, treatment with recombinant iduronidase would result in the accumulation of inorganic sulphate; this in turn may inhibit the degradation of GAG. To determine how much of the labelled sulphate was inorganic and how much was incorporated into GAG the labelled materials required fractionation. It could then be determined whether the Q70X genotype resulted in the lysosomal storage of inorganic sulphate.

To separate the stored GAG from sulphate the mass of the GAG was determined. This was achieved by isolating labelled GAGs stored in fibroblast lysosomes and resolving them by gradient PAGE (*Figure 6.3*). The molecular mass of the bulk of the material ranged between a dodeca and a fourteen disaccharide unit, which was approximately 6 kDa.

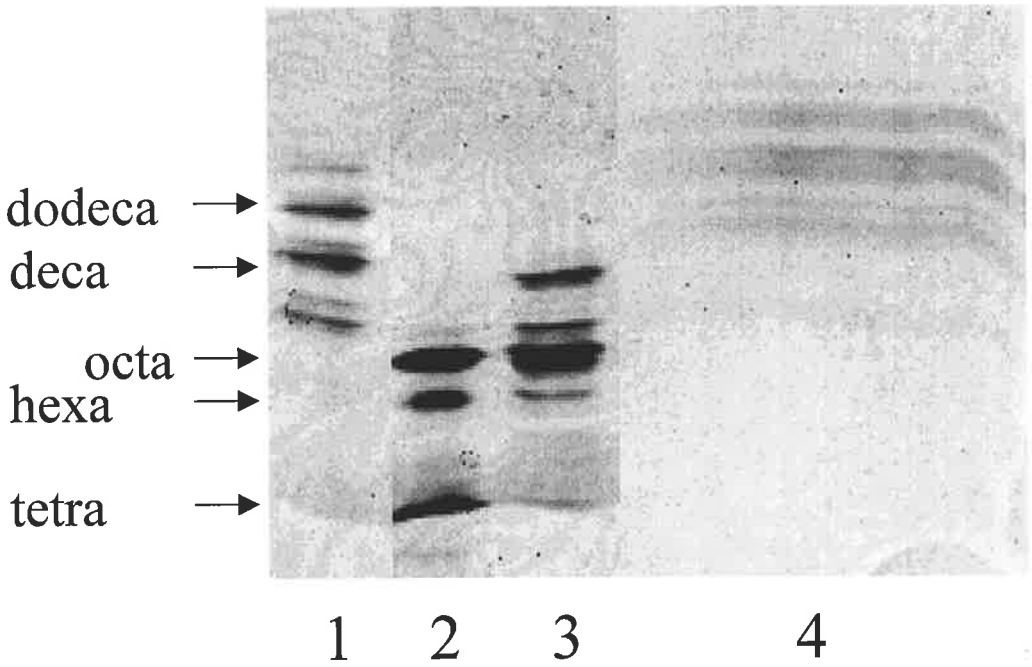

Figure 6.3 Electrophoresis of labelled storage product.

Molecular weight standards (1, 2, and 3): are a mixture of DS and CS disaccharide chains isolated from human MPS 6 urine (1 and 3); and heparan isolated from bovine lung (2). From mutant iduronidase (Q70X) fibroblasts labelled (*Section 6.2.3*) with sodium [^{35}S]-sulphate, GAG was isolated as described in *Section 6.2.5*. The isolated GAG (4) was loaded (0.5 μg of uronic acid equivalents) onto and separated by PAGE on a linear 30-40% gradient, non-reducing, non-denaturing gel (10 x 14 cm wide). Samples were loaded in 10% (v/v) glycerol and electrophoresis performed at 150 V for 30 min to allow samples to enter the resolving gel, and then 350 V for 16 h. Heat was dissipated by circulating tap water through a refrigeration unit. The gel was then fixed and stained with Alcian Blue then silver (*Section 6.2.6*).

6.3.4 Separation of inorganic sulphate from glycosaminoglycans.

[H^3]-heparan sulphate was kindly provided by Dr. Peter Meikle, Department of Chemical Pathology, Women's and Children's Hospital, North Adelaide, South Australia.

Several methods were explored for the separation of inorganic sulphate from GAG by using [^{35}S] sulphate and [^{3}H] heparan sulphate. These included size exclusion chromatography on either Sephadex G10, Biogel P2 and anion exchange chromatography on an Econo Q cartridge. The Q cartridge was found to give the best separation. It was found with the Q cartridge that sulphate eluted with about 30 mM Na_2SO_4 while heparan sulphate did not elute with 100 mM Na_2SO_4.

The separation of [^{35}S]-sulphate and [^{3}H]-heparan sulphate is shown in *Figure 6.4*. The use of different isotopes and dual scintillation counting established that sulphate and heparan sulphate were able to be clearly separated by this method. The fibroblast storage material (GAG and sulphate) was then successfully separated by the same method using wild type and MPS I fibroblasts. All the samples separated cleanly into two peaks, as demonstrated in the sulphate and heparan sulphate experiment. An example of the separation of inorganic sulphate and GAG is shown in *Figure 6.5*.

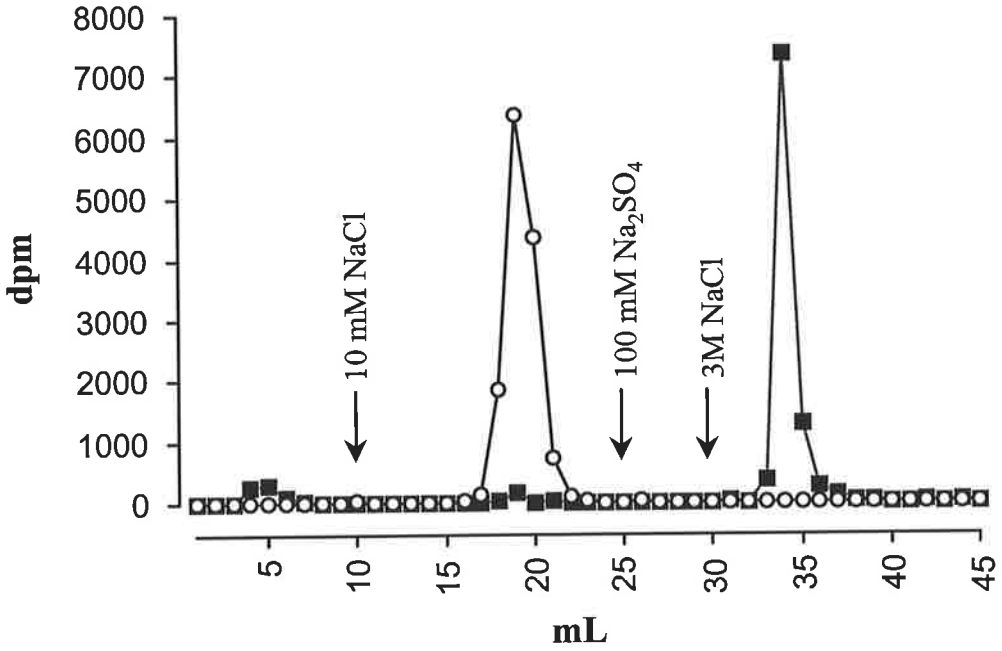

Figure 6.4 Separation of [^{35}S] sulphate and [^{3}H] heparan sulphate by anion exchange chromatography.

Approximately 14,000 dpm each of $Na_2{}^{35}SO_4$ (○) and [^{3}H] labelled heparan sulphate (■) were mixed and loaded onto a 1 mL Econo Q cartridge at 1.0 mL.min^{-1} in a low-salt buffer (10 mM NaCl, 20 mM Tris-HCl, pH 7.4). The cartridge was washed with 10 mL of low-salt buffer then eluted with a linear gradient to 100 mM Na_2SO_4 in 20 mM Tris-HCl, pH 7.4, over 15 min, followed by 5 mL of 100 mM Na_2SO_4, 20 mM Tris-HCl, pH 7.4, and then a step elution of 3 M NaCl, 20 mM Tris-HCl, pH 7.4. Fractions of 1 mL were collected of which 0.1 mL aliquots were mixed with 4 mL of scintillation fluid and counted.

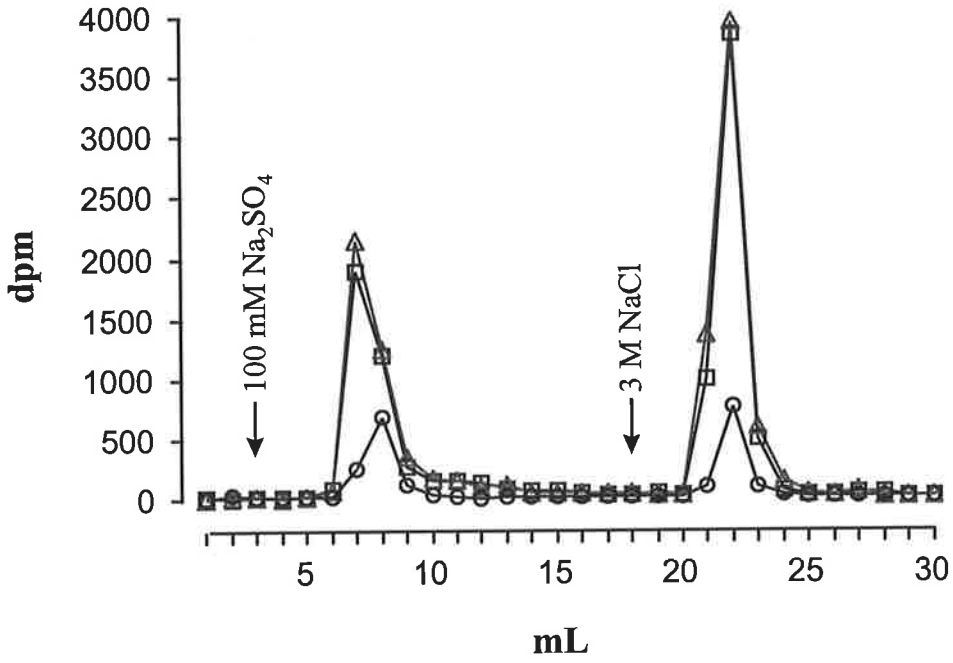

Figure 6.5 Separation of stored sulphate and GAG from fibroblasts by anion exchange chromatography.

Wild type (○), Q70X (□) and W402X (△) fibroblasts were labelled with [^{35}S]-sulphate and solubilised as described in *Section 6.2.3*. An aliquot (200 µL) of the solubilised material was added to 1 mL of low-salt buffer (10 mM NaCl, 20 mM Tris-HCl, pH 7.4) and loaded onto an Econo Q cartridge at 1 mL.min^{-1}. The cartridge was washed with a further 3 mL of low-salt buffer prior to a step elution with 15 mL of 100 mM Na_2SO_4, 20 mM Tris-HCl, pH 7.4 and then a step elution with 5 mL of 3 M NaCl, 20 mM Tris-HCl, pH 7.4. The amount of sample loaded in each 200 µL was 26, 57 and 43 µg of protein, respectively, of the wild type, Q70X and W402X solubilised fibroblasts. The dpm of each 1 mL fraction was determined by liquid scintillation counting with 4 mL of scintillant.

6.3.4.1 Separation of sulphate and GAG from iduronidase-treated fibroblasts.

If the Q70X fibroblasts were not able to transport sulphate from the lysosome due to a defective sulphate transporter, the degradation of labelled GAG stored in the lysosome followed by its isolation and separation would enable the relative measurement of untransported sulphate.

The separation of the labelled storage products from inorganic sulphate in wild type, W402X and Q70X fibroblasts after treatment with iduronidase for 0, 1, 2 and 4 h was performed (*Table 6.2*). No significant difference could be seen between Q70X and W402X in the ratio of GAG stored to free sulphate. The ratio of GAG to sulphate in wild type fibroblasts was approximately 1.0 and did not significantly alter with iduronidase treatment. The ratios observed with the W402X and Q70X fibroblasts was about 1.5 before iduronidase treatment and about 1.1 after 4 h treatment with iduronidase.

Table 6.2 Ratio of sulphate to glycosaminoglycans in iduronidase-corrected fibroblasts.

Wild type, Q70X and W402X fibroblasts were labelled with [^{35}S]-sulphate, treated for 0, 1, 2 and 4 h with iduronidase and solubilised as described in *Section 6.2.3*. As illustrated in *Figure 6.5* an aliquot (200 µL) of each solubilised sample (30-60 µg protein) was added to 1 mL of low-salt buffer (10 mM NaCl, 20 mM Tris-HCl, pH 7.4) and loaded onto an Econo Q cartridge at 1 mL.min^{-1}. The cartridge was washed with a further 3 mL of low-salt buffer prior to a step elution with 15 mL of 100 mM Na_2SO_4, 20 mM Tris-HCl, pH 7.4, to recover the inorganic sulphate fraction, and then a step elution with 5 mL of 3 M NaCl, 20 mM Tris-HCl, pH 7.4, to recover the GAG fraction. The dpm of each 1 mL fraction was determined by liquid scintillation counting with 4 mL of scintillant.

	Sample	sulphate dpm/mg	GAG dpm/mg	GAG/sulphate Ratio
0 h Iduronidase treatment				
	Wild type	42846	38461	0.9
	Q70X	63098	95774	1.52
	W402X	92406	142149	1.54
1 h Iduronidase treatment				
	Wild type	30858	27979	0.91
	Q70X	66675	84644	1.27
	W402X	101347	148510	1.47
2 h Iduronidase treatment				
	Wild type	31518	32658	1.04
	Q70X	48677	57177	1.17
	W402X	102032	126181	1.24
4 h Iduronidase treatment				
	Wild type	37467	36923	0.99
	Q70X	44849	47682	1.06
	W402X	60934	69982	1.15

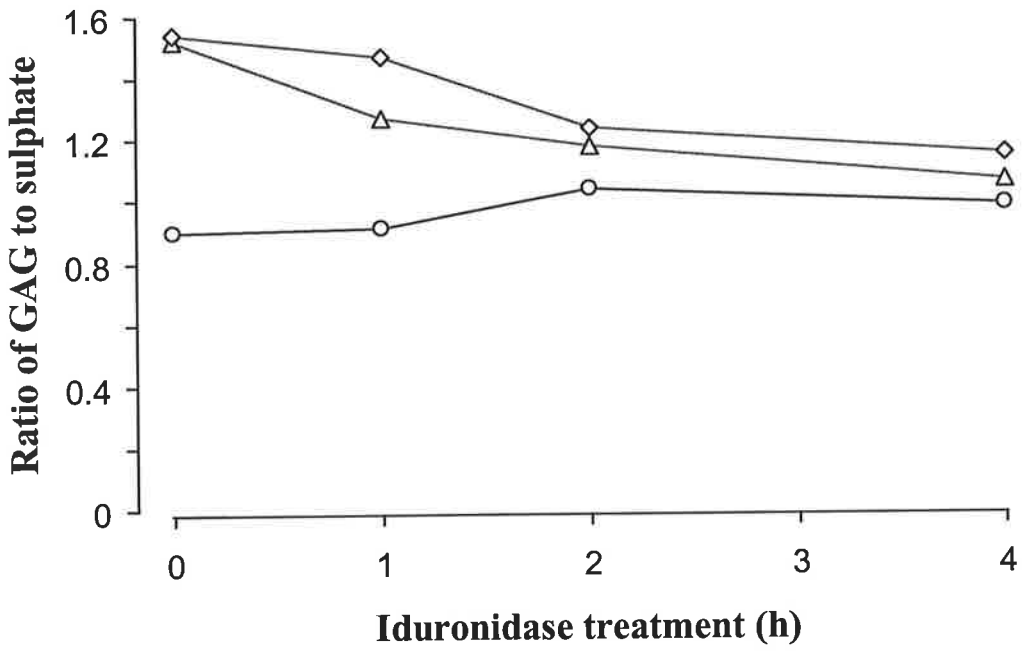

Figure 6.6 Ratio of labelled sulphate to GAG stored after fibroblasts were treated with iduronidase.

Wild type (○), Q70X (△) and W402X (◇) fibroblasts were labelled with [^{35}S]-sulphate, treated with iduronidase and solubilised as described in *Section 6.2.3.* The sulphate and GAG contents were fractionated on an Econ Q cartridge and quantitated (data shown in *Table 6.2*).

6.4 Summary

The iduronidase Q70X mutation, which is in the region that overlaps the SAT-1 gene, appears not to effect sulphate transport across either the plasma or lysosomal membrane. Hence, the more severe clinical phenotype of the Q70X mutation, when compared with the W402X mutation, does not appear to be due to impaired sulphate transport at either of these membranes, and is most probably not related to any effect of the expression of the SAT-1 protein.

7. Concluding remarks

7.1 A historical perspective.

Sulphate transport was studied at a physiological level in erythrocytes in the mid 1980s (Milanick and Gunn 1984, 1986). The erythrocyte anion exchanger also known as Band 3 allows the passage of sulphate, and has been widely studied due to its physiological importance. During this period lysosomal transporters were also being characterised.

Sulphate transporters were divided into sodium dependent and independent transporters, the lysosomal sulphate transporter (LST) belonging to the latter group. The first sulphate transporters from both groups were cloned in the same year, the sodium dependent rat renal transporter (Markovich *et al.* 1993), and the sodium independent transporter in human colon, known as DRA (Schweinfest *et al.* 1993). These two transporters were not homologous and the DRA transporter was not recognised to have a role in either transport or sulphate. At this point in time the Band 3 transporter was characteristically the most similar to the LST. The approach to isolate the LST therefore, was immunological cross-reactivity to Band 3 based on their functional similarities.

The following year another two sodium independent sulphate transporters were cloned, the SAT-1 from rat (Bissig *et al.* 1994), and the human DTDST (Bissig *et al.* 1994). The homology of these transporters with DRA, revealed the function of DRA. It was also found in this year that SAT-1 overlapped with a region of the lysosomal enzyme α-L-iduronidase (Clarke *et al.* 1994). The approach to isolate the LST at this point switched from Band 3 to the SAT-1 protein. The serendipity of the SAT-1 and iduronidase genes overlapping, posed the question of whether they are transcribed at the same time, due to a functional requirement that they be expressed at the same time in the lysosome. A mutation in the region of the

iduronidase gene (Q70X) that overlapped with the SAT-1 gene resulted in a more severe Hurler phenotype, than a mutation in a non-overlapping region (W402X). Neither of these genotypes had any detectable iduronidase activity, therefore the mutation in the SAT-1 gene was investigated as to whether it contributed to this more severe phenotype. The new group of SAT-1 like sulphate transporters remains characteristically the most closely related to the LST. Since the experimental part of this study was completed another member of the sodium independent sulphate transporter family was cloned, and is known as Pendrin (Everett *et al.* 1997).

The way lysosomes have been isolated has changed over time. Prior to this study, lysosomes were isolated from rat liver, after altering their density by pre-treatment of the animals with the detergent Triton WR-1339 (Ohkuma *et al.* 1982). In addition to affecting the density of the organelles, Triton made the lysosomal proton-pump uncharacteristically sensitive to inhibition by *N,N'*-dicyclohexylcarbodiimide (DCCD) and azide. Rat liver lysosomes were later isolated using methionine methyl ester, which caused their swelling and rupture (Symons and Jonas 1987). This thesis isolated lysosomes from human placentae and not rat liver. Density centrifugation was also employed, although neither detergent nor methionine methyl ester was used to alter density, which may have effected lysosomal sulphate transport.

7.2 Evolution of methodologies.

The technical challenges of purifying a membrane protein changed over the course of this study. Some of the techniques used for such pursuits were reconstitution and 2-D electrophoresis. A number of molecular biological techniques, including expression cloning have also been used to identify the genes of membrane proteins.

The lysosomal sialic acid carrier from rat liver was reconstituted into proteoliposomes (Mancini *et al.* 1992). The lysosomal sulphate transporter was reported to be reconstituted after the lysosomal membranes were ruptured by swelling with methionine during their isolation (Koetters *et al.* 1995b). Although this technique has shown some of these proteins characteristics, neither protein nor nucleic sequence of these carriers have been elucidated.

The separation of proteins by 2D-electrophoresis was performed by the labour intensive tube gel method, which formed pI gradients during the focusing steps. Now the more easily reproducible immobilised gradients are readily available from commercial sources. It has been reported however, that membrane proteins may focus better in tube gels.

Molecular biological techniques, such as expression cloning and linkage analysis of pedigrees, have increasingly replaced classical protein purification techniques. The completion of the human genome project, and more powerful bioinformatics methods have made available further approaches for gene searching. It has been these latter techniques which enabled SAT-1, DRA, DTDST and Pendrin to be cloned. All orthologs of this family except SAT-1 were discovered because of disease. These diseases are colon adenoma, diastrophic dysplasia and congenital deafness respectively.

More recently, the field of proteomics has extended from maps of proteins in different cell types to mapping proteins at an organelle level. Proteomics is now aided by tandem mass spectrometry, robotics and microarray technology. These new technologies will reduce the time taken to identify proteins of interest.

7.3 Significance of this study.

Lysosomes were isolated from human placenta delivered by caesarean section, after finding lysosomes from vaginally delivered placentae inferior for both proton and sulphate transport assays. Lysosomal membranes were successfully reconstituted, however, sulphate readily bound to the phosphatidylcholine used for unilamelar vesicle formation.

Initially the erythrocyte anion exchanger (Band 3) was most akin (of known transporters) to the LST. During the search for the LST using antibodies against Band 3, lysosomal membrane proteins were enriched chromatographically and resolved by 2-DE. The amount of membrane protein that could be resolved by 2-DE was increased to enable the *N*-terminal sequencing of some of the identified proteins.

A new family of sulphate anion transporters (SAT) was then discovered which characteristically were more similar to the LST than that of Band 3. The search continued therefore, with antibodies against peptide sequences from the SAT family. Two proteins (55 and 57 kDa) were identified, but they were unable to be *N*-terminally sequenced as not enough protein was isolated due to their low abundance. No affect of the iduronidase mutation (Q70X) in the overlapping region of the SAT-1 gene could be found on sulphate transport at either the plasma membrane or the lysosome.

7.4 Future work.

There were a number of inherent problems in purifying the LST. It resides in a heterogenous organelle that is difficult to isolate and is an integral membrane protein. Integral membrane proteins generally become inactive when removed from their phospholipid environment and transporters need to be reconstituted in order to be assayed. The locations of the cellular sulphate pools, which affect *in-vivo* transport studies, are still to be elucidated.

Further more, unlike cystinosis or Salla disease, no known naturally occurring disease involving this transporter has as yet presented itself. The human SAT-1 family members have been discovered mainly as a consequence of serious disease. DRA, the first gene isolated, is responsible for colon adenoma and congenital chloride diarrhoea; mutations in the DTDST gene have resulted in three types of chondrodysplasias. The dysfunction of Pendrin expressed in thyroid results in congenital deafness and goitre. The likelihood of the LST presenting itself clinically is low and a more probable route of discovery will begin at a genomic level.

Elucidation of the LST could be continued with a tissue or cell type higher in lysosomal number. As tissues are often composed of multiple cell types, purification from cultured cells would eliminate many contaminating proteins, including those that are up-regulated by ligands (eg. hormones) from other tissues. Due to the nature of the lysosome's degradative function, non-lysosomal proteins were isolated along with lysosomal proteins. The isolation of proteins from tissue had a quantitative advantage at the expense of purity. The quantitative advantage of using cultured cells, however, may be lost, making the isolation of a low abundant protein difficult.

The discovery of the LST will be most probably achieved by a number of steps. The genomic information will need to be found and identified by homology studies, which is the most difficult step. This information could be used to express and tag the protein, which may confirm its cellular location, and function.

8. Bibliography.

Addison, R. and Scarborough, G.A. (1982). Conformational changes of the Neurospora plasma membrane H+ATPase during its catalytic cycle. *Journal of Biological Chemistry* **257** (17), 10421-10426.

Adra, C.N., Zhu, S., Ko, J.L., Guillemot, J.C., Cuervo, A.M., Kobayashi, H., Horiuchi, T., Lelias, J.M., Rowley, J.D. and Lim, B. (1996). LAPTM5: a novel lysosomal-associated multispanning membrane protein preferentially expressed in hematopoietic cells. *Genomics* **35**, 328-337.

Akamine, A., Tsukuba, T., Kimura, R., Maeda, K., Tanaka, Y., Kato, K. and Yamamoto, K. (1993). Increased synthesis and specific localization of a major lysosomal membrane sialoglycoprotein (LGP107) at the ruffled border membrane of active osteoclasts. *Histochemistry* **100** (2), 101-108.

Alper, S.L. (1991). The band 3-related anion exchanger (AE) gene family. *Annual Review of Physiology* **53**, 549-564.

Altschul, S.F., Gish, W., Miller, W., Myers, E.W. and Lipman, D.J. (1990). Basic local alignment search tool. *Journal of Molecular Biology* **215**, 403-410.

Altschul, S.F., Madden, T.L., Schaffer, A.A., Zhang, J., Zhang, Z., Miller, W. and Lipman, D.J. (1997). Gapped BLAST and PSI-BLAST: a new generation of protein database search programs. *Nucleic Acids Research* **25**, 3389-3402.

Andersson, G.N., Torndal, U.B. and Eriksson, L.C. (1989). Decreased vacuolar acidification capacity in drug-resistant rat liver preneoplastic nodules. *Cancer Research* **49** (14), 3765-3769.

Applegarth, D.A., Dimmick, J.E. and Hall, J.G. (1997). Lysosomal disorders. Organelle Diseases. Edited by Applegarth, D.A., Dimmick, J.E. and Hall, J.G. **Part 1**, Chapman and Hall, London.

Arai, K., Shimaya, A., Hiratani, N. and Ohkuma, S. (1993). Purification and characterization of lysosomal H(+)-ATPase. An anion-sensitive v-type H(+)-ATPase from rat liver lysosomes. *Journal of Biological Chemistry* **268** (8), 5649-5660.

Bairoch, A. and Apweiler, R. (2000). The SWISS-PROT protein sequence database and its supplement TrEMBL in 2000. *Nucleic Acids Research* **28**, 45-48.

Barrueco, J.R. and Sirotnak, F.M. (1991). Evidence for the facilitated transport of methotrexate polyglutamates into lysosomes derived from S180 cells. Basic properties and specificity for polyglutamate chain length. *Journal of Biological Chemistry* **266** (18), 11732-11737.

Batt, R.M. and Mann, L.C. (1983). Evaluation of preformed Percoll and reorientating sucrose density gradient centrifugation for the analytical subcellular fractionation of dog liver. *Research in Veterinary Science* **34** (3), 272-279.

Ben David, E. and Shemesh, M. (1990). Ultrastructural localization of cytochrome P-450scc in the bovine placentome using protein A-gold technique. *Biology of Reproduction* **42** (1), 131-138.

Benet, L.Z. and Sheiner, L.B. (1985). Pharmacokinetics: the dynamics of drug absorption, distribution, and elimination. The Pharmacological Basis of Therapeutics. Seventh Edition. Edited by Gilman, A.G., Goodman, L.S., Rall, T.W. and Murad, F. pp 17-21. Macmillan Publishing Company, New York.

Benson, D.A., Karsch-Mizrachi, I., Lipman, D.J., Ostell, J., Rapp, B.A. and Wheeler, D.L. (2000). GenBank. *Nucleic Acids Research* **28** (1), 15-18.

Bernar, J., Tietze, F., Kohn, L.D., Bernardini, I., Harper, G.S., Grollman, E.F. and Gahl, W.A. (1986). Characteristics of a lysosomal membrane transport system for tyrosine and other neutral amino acids in rat thyroid cells. *Journal of Biological Chemistry* **261** (36), 17107-17112.

Bhattacharyya, T., Karnezis, A.N., Murphy, S.P., Hoang, T., Freeman, B.C., Phillips, B. and Morimoto, R.I. (1995). Cloning and subcellular localization of human mitochondrial hsp70. *Journal of Biological Chemistry* **270**, 1705-1710.

Bird, S.J. and Lloyd, J.B. (1990). Evidence for a dipeptide porter in the lysosome membrane. *Biochimica et Biophysica Acta* **1024**, 267-270.

Bissig, M., Hagenbuch, B., Stieger, B., Koller, T. and Meier, P.J. (1994). Functional expression cloning of the canalicular sulfate transport system of rat hepatocytes. *Journal of Biological Chemistry* **269**, 3017-3021.

Black, S.M., Harikrishna, J.A., Szklarz, G.D. and Miller, W.L. (1994). The mitochondrial environment is required for activity of the cholesterol side-chain cleavage enzyme, cytochrome P450scc. *Proceedings of the National Academy of Sciences of the United States of America* **91** (15), 7247-7251.

Blattner, F.R., Plunkett G, 3.r.d., Bloch, C.A., Perna, N.T., Burland, V., Riley, M., Collado Vides, J., Glasner, J.D., Rode, C.K., Mayhew, G.F., Gregor, J., Davis, N.W., Kirkpatrick, H.A., Goeden, M.A., Rose, D.J., Mau, B. and Shao, Y. (1997). The complete genome sequence of Escherichia coli K-12. *Science* **277** (5331), 1453-1474.

Blumenkrantz, N. and Asboe-Hansen, G. (1973). New method for quantitative determination of uronic acids. *Analytical Biochemistry* **54**, 484-489.

Bond, C.S., Clements, P.R., Ashby, S.J., Collyer, C.A., Harrop, S.J., Hopwood, J.J. and Guss, J.M. (1997). Structure of a human lysosomal sulfatase. *Structure* **5** (2), 277-289.

Briand, J.P., Muller, S. and Van Regenmortel, M.H. (1985). Synthetic peptides as antigens: pitfalls of conjugation methods. *Journal of Immunological Methods* **78** (1), 59-69.

Busch, A.E., Waldegger, S., Herzer, T., Biber, J., Markovich, D., Murer, H. and Lang, F. (1994). Electrogenic cotransport of Na+ and sulfate in Xenopus oocytes expressing the cloned Na+SO4(2-) transport protein NaSi-1. *Journal of Biological Chemistry* **269**, 12407-12409.

Byeon, M.K., Westerman, M.A., Maroulakou, I.G., Henderson, K.W., Suster, S., Zhang, X.K., Papas, T.S., Vesely, J., Willingham, M.C., Green, J.E. and Schweinfest, C.W. (1996). The down-regulated in adenoma (DRA) gene encodes an intestine-specific membrane glycoprotein. *Oncogene* **12** (2), 387-396.

Byers, S., Rozaklis, T., Brumfield, L.K., Ranieri, E. and Hopwood, J.J. (1998). Glycosaminoglycan accumulation and excretion in the mucopolysaccharidoses: characterization and basis of a diagnostic test for MPS. *Molecular Genetics and Metabolism* **65**, 282-290.

Carlsson, S.R., Roth, J., Piller, F. and Fukuda, M. (1988). Isolation and characterization of human lysosomal membrane glycoproteins, h-lamp-1 and h-lamp-2. Major sialoglycoproteins carrying polylactosaminoglycan. *Journal of Biological Chemistry* **263**, 18911-18919.

Casey, J.R. and Reithmeier, R.A. (1991). Analysis of the oligomeric state of Band 3, the anion transport protein of the human erythrocyte membrane, by size exclusion high performance liquid chromatography. Oligomeric stability and origin of heterogeneity. *Journal of Biological Chemistry* **266** (24), 15726-15737.

Castellucci, M. and Kaufmann, P. (1995). Basic structure of the villous trees and nonvillous parts of the placenta. Pathology of the Human Placenta. Third Edition. Edited by Benirschke, K. and Kaufmann, P. **57**, p 182. Springer-Verlag, New York, Berlin, Heidelberg.

Cerneus, D.P., Ueffing, E., Posthuma, G., Strous, G.J. and van der Ende, A. (1993). Detergent insolubility of alkaline phosphatase during biosynthetic transport and endocytosis. Role of cholesterol. *Journal of Biological Chemistry* **268**, 3150-3155.

Cerneus, D.P. and van der Ende, A. (1991). Apical and basolateral transferrin receptors in polarized BeWo cells recycle through separate endosomes. *Journal of Cell Biology* **114**, 1149-1158.

Chang, H.W. and Bock, E. (1980). Pitfalls in the use of commercial nonionic detergents for the solubilization of integral membrane proteins: sulfhydryl oxidizing contaminants and their elimination. *Analytical Biochemistry* **104** (1), 112-117.

Chataway, T.K. and Barritt, G.J. (1995). Purification of histidine-tagged ras and its use in the detection of ras binding proteins. *Molecular and Cellular Biochemistry* **144**, 167-173.

Chataway, T.K., Whittle, A.M., Lewis, M.D., Bindloss, C.A., Davey, R.C., Moritz, R.L., Simpson, R.J., Hopwood, J.J. and Meikle, P.J. (1998). Two-dimensional mapping and microsequencing of lysosomal proteins from human placenta. *Placenta* **19**, 643-654.

Cherest, H., Davidian, J.C., Thomas, D., Benes, V., Ansorge, W. and Surdin Kerjan, Y. (1997). Molecular characterization of two high affinity sulfate transporters in *Saccharomyces cerevisiae*. *Genetics* **145** (3), 627-635.

Chomczynski, P. and Sacchi, N. (1987). Single-step method of RNA isolation by acid guanidinium thiocyanate-phenol-chloroform extraction. *Analytical Biochemistry* **162**,156-159.

Chou, H.F., Passage, M. and Jonas, A.J. (1998). Lysosomal sulphate transport is dependent upon sulphydryl groups. *Biochemical Journal* **330** (Pt 2), 713-717.

Chou, H.F., Vadgama, J. and Jonas, A.J. (1992). Lysosomal transport of small molecules. *Biochemical Medicine and Metabolic Biology* **48**, 179-193.

Chung, B.C., Matteson, K.J., Voutilainen, R., Mohandas, T.K. and Miller, W.L. (1986). Human cholesterol side-chain cleavage enzyme, P450scc: cDNA cloning, assignment of the gene to chromosome 15, and expression in the placenta. *Proceedings of the National Academy of Sciences of the United States of America* **83** (23), 8962-8966.

Clarke, L.A., Nasir, J., Zhang, H., McDonald, H., Applegarth, D.A., Hayden, M.R. and Toone, J. (1994). Murine alpha-L-iduronidase: cDNA isolation and expression. *Genomics* **24** (2), 311-316.

Clarke, L.A., Russell, C.S., Pownall, S., Warrington, C.L., Borowski, A., Dimmick, J.E., Toone, J. and Jirik, F.R. (1997). Murine mucopolysaccharidosis type I: targeted disruption of the murine alpha-L-iduronidase gene. *Human Molecular Genetics* **6** (4), 503-511.

Clements, P.R., Brooks, D.A., Saccone, G.T. and Hopwood, J.J. (1985). Human alpha-L-iduronidase. 1. Purification, monoclonal antibody production, native and subunit molecular mass. *European Journal of Biochemistry* **152**, 21-28.

Collarini, E.J., Pisoni, R.L. and Christensen, H.N. (1989). Characterization of a transport system for anionic amino acids in human fibroblast lysosomes. *Biochimica et Biophysica Acta* **987** (2), 139-144.

Cooperstein, S.J. and Lazarow, A. (1951). A microspectrophotometric method for the determination of cytochrome oxidase. *Biochemical Journal* **189**, 665-670.

Coughtrie, M.W., Sharp, S., Maxwell, K. and Innes, N.P. (1998). Biology and function of the reversible sulphation pathway catalysed by human sulphotransferases and sulphatases. *Chemico-Biological Interactions* **109** (1-3), 3-27.

Crompton, M., Palmieri, F., Capano, M. and Quagliariello, E. (1974). The transport of sulphate and sulphite in rat liver mitochondria. *Biochemical Journal* **142** (1), 127-137.

Crompton, M., Palmieri, F., Capano, M. and Quagliariello, E. (1975). A kinetic study of sulphate transport in rat liver mitochondria. *Biochemical Journal* **146** (3), 667-673.

Cuppoletti, J., Goldinger, J., Kang, B., Jo, I., Berenski, C. and Jung, C.Y. (1985). Anion carrier in the human erythrocyte exists as a dimer. *Journal of Biological Chemistry* **260** (29), 15714-15717.

Curtis, C.G. (1982). The origins of intracellular sulphate for conjugation reactions. Sulfate Metabolism and Sulfate Conjugation. Proceedings of an International Workshop held at Noordwijkerhout, The Netherlands 1981. Edited by Mulder, G.J., Caldwell, J., Van Kempen, G.M. and Vonk, R.J. pp 67-71. Taylor and Francis Ltd., London.

D'Souza, M.P., Ambudkar, S.V., August, J.T. and Maloney, P.C. (1987). Reconstitution of the lysosomal proton pump. *Proceedings of the National Academy of Sciences of the United States of America* **84** (20), 6980-6984.

David, C. and Ullrich, K.J. (1992). Substrate specificity of the luminal Na(+)-dependent sulphate transport system in the proximal renal tubule as compared to the contraluminal sulphate exchange system. *Pflugers Archiv European Journal of Physiology* **421** (5), 455-465.

Dayhoff, M.O., Schwartz, R.M. and Orcutt, B.C. (1978). A model of evolutionary change in protein matrices for detecting distant relationships. Atlas of Protein Sequence Structure. Edited by Dayhoff, M.O. **5**, pp 345-358. National Biomedical Research Foundation, Washington DC.

Domanico, S.Z., DeNagel, D.C., Dahlseid, J.N., Green, J.M. and Pierce, S.K. (1993). Cloning of the gene encoding peptide-binding protein 74 shows that it is a new member of the heat shock protein 70 family. *Molecular and Cellular Biology* **13** (6), 3598-3610.

Domingo, A. and Marco, R. (1989). Visualization under ultraviolet light enhances 100-fold the sensitivity of peroxidase-stained blots. *Analytical Biochemistry* **182** (1), 176-181.

Drenckhahn, D., Schluter, K., Allen, D.P. and Bennett, V. (1985). Colocalization of band 3 with ankyrin and spectrin at the basal membrane of intercalated cells in the rat kidney. *Science* **230** (4731), 1287-1289.

Esko, J.D., Elgavish, A., Prasthofer, T., Taylor, W.H. and Weinke, J.L. (1986). Sulfate transport-deficient mutants of Chinese hamster ovary cells. Sulfation of glycosaminoglycans dependent on cysteine. *Journal of Biological Chemistry* **261** (33), 15725-15733.

Estep, J.A., Zorn, J.P. and Marin, M.G. (1981). Kinetics of sulfated mucous glycoprotein secretion in dog trachea in vitro. *Journal of Applied Physiology* **50** (2), 383-391.

Everett, L.A., Glaser, B., Beck, J.C., Idol, J.R., Buchs, A., Heyman, M., Adawi, F., Hazani, E., Nassir, E., Baxevanis, A.D., Sheffield, V.C. and Green, E.D. (1997). Pendred syndrome is caused by mutations in a putative sulphate transporter gene (PDS). *Nature Genetics* **17**, 411-422.

Fan, M.-Y. and Templeton, D.M. (1992). Sulfate metabolism in experimental diabetes. *Diabetes and Metabolism* **18**, 98-103.

Fath, M.J. and Kolter, R. (1993). ABC transporters: bacterial exporters. *Microbiological Reviews* **57**, 995-1017.

Felsenstein, J. (1989). PHYLIP -- Phylogeny Inference Package (Version 3.2). *Cladistics* **5**, 164-166.

Fiermonte, G., Dolce, V., Arrigoni, R., Runswick, M.J., Walker, J.E. and Palmieri, F. (1999). Organization and sequence of the gene for the human mitochondrial dicarboxylate carrier: evolution of the carrier family. *Biochemical Journal* **344 Pt 3**, 953-960.

Finean, J.B., Coleman, R. and Michell, R.H. (1984). Lipid components. Membranes and their Cellular Functions. Third Edition. Edited by Finean, J. pp 27-37. Blackwell Scientific Publications, Oxford, Boston, Melbourne.

Florin, T., Neale, G., Gibson, R.R., Christl, S.U. and Cummings, J.H. (1991). Metabolism of dietary sulfate: absorption and excretion in man. *Gut* **32**, 766-773.

Forgac, M., Cantley, L., Wiedenmann, B., Altstiel, L. and Branton, D. (1983). Clathrin-coated vesicles contain an ATP-dependent proton pump. *Proceedings of the National Academy of Sciences of the United States of America* **80** (5), 1300-1303.

Forsbeck, K., Ericsson, J., Birgegard, G., Malmgren, M. and Nilsson, K. (1986). Subcellular characterization of the transferrin-transferrin receptor and iron accumulating system of established human erythroid and monoblastoid tumour cell lines. *Acta Pathologica, Microbiologica, et Immunologica Scandinavica Section A, Pathology* **94** (4), 245-252.

Frates, R.C., Kaizu, T.T. and Last, J.A. (1983). Mucus glycoprotiens secreted by respiratory epithelial tissue from cystic fibrosis patients. *Pediatric Research* **17**, 30-34.

Fujita, H., Takata, Y., Kono, A., Tanaka, Y., Takahashi, T., Himeno, M. and Kato, K. (1992). Isolation and sequencing of a cDNA clone encoding the 85 kDa human lysosomal sialoglycoprotein (hLGP85) in human metastatic pancreas islet tumor cells. *Biochemical and Biophysical Research Communications* **184**, 604-611.

Fukuda, M. (1991). Lysosomal membrane glycoproteins. Structure, biosynthesis, and intracellular trafficking. *Journal of Biological Chemistry* **266** (32), 21327-21330.

Gahl, W.A., Bashan, N., Tietze, F., Bernardini, I. and Schulman, J.D. (1982). Cystine transport is defective in isolated leukocyte lysosomes from patients with cystinosis. *Science* **217** (4566), 1263-1265.

Gahl, W.A., Bashan, N., Tietze, F. and Schulman, J.D. (1984). Lysosomal cystine counter-transport in heterozygotes for cystinosis. *American Journal of Human Genetics* **36** (2), 277-282.

Gahl, W.A., Reed, G.F., Thoene, J.G., Schulman, J.D., Rizzo, W.B., Jonas, A.J., Denman, D.W., Schlesselman, J.J., Corden, B.J. and Schneider, J.A. (1987). Cysteamine therapy for children with nephropathic cystinosis. *New England Journal of Medicine* **316** (16), 971-977.

Gahl, W.A. (1992). Lysosomal transport of amino acids: lysosomal cysteine transport. Pathophysiology of Lysosomal Transport. Edited by Thoene, J.G. pp 45-71. CRC Press, London Tokyo.

Gahl, W.A., Schneider, J.A. and Aula, P.P. (1998). Lysosomal transport disorders: cystinosis and sialic acid storage disorders. The Metabolic and Molecular Bases of Inherited Disease. Seventh Edition. Edited by Scriver, C.R., Beaudet, A.L., Sly, W.S. and Valle, D. **1**, pp 3763-3797. McGraw-Hill, New York London Sydney.

Garavito, R.M., Picot, D. and Loll, P.J. (1996). Stategies for crystalizing membrane proteins. *Journal of Bioenergetics and Biomembranes* **28** (1), 13-27.

Gartner, E.M., Liebold, K., Legrum, B., Fasold, H. and Passow, H. (1997). Three different actions of phenylglyoxal on band 3 protein-mediated anion transport across the red blood cell membrane. *Biochimica et Biophysica Acta* **1323** (2), 208-222.

Geck, P. and Heinz, E. (1976). Coupling in secondary transport. Effect of electrical potentials on the kinetics of ion linked co-transport. *Biochimica et Biophysica Acta* **443** (1), 49-63.

Geck, P., Heinz, E. and Pietrzyk, C. (1978). Sodium-dependent transport processes influence each other over the sodium-gradient. *Journal of Physiology* **285**, 8P-9P.

Geck, P. and Heinz, E. (1989). Secondary active transport: introductory remarks. *Kidney International* **36** (3), 334-341.

Geier, C., von Figura, K. and Pohlmann, R. (1989). Structure of the human lysosomal acid phosphatase gene. *European Journal of Biochemistry* **183**, 611-616.

Gennis, R.B. (1989). Channels verses transporters. Biomembranes. Molecular Structure and Function. Edited by Cantor, C.R. **8.11**, pp 272-276. Springer Verlag, New York.

George, D.G., Dodson, R.J., Garavelli, J.S., Haft, D.H., Hunt, L.T., Marzec, C.R., Orcutt, B.C., Sidman, K.E., Srinivasarao, G.Y., Yeh, L.S.L., Arminski, L.M., Ledley, R.S., Tsugita, A. and Barker, W.C. (1997). The Protein Information Resource (PIR) and the PIR-International Protein Sequence Database. *Nucleic Acids Research* **25**, 24-28.

Getz, H.P., Thom, M. and Maretzki, A. (1994). Monoclonal antibodies as tools for the identification of the tonoplast sucrose carrier from sugarcane stalk tissue. *Journal of Plant Physiology* **144**, 525-532.

Geuze, H.J., Stoorvogel, W., Strous, G.J., Slot, J.W., Bleekemolen, J.E. and Mellman, I. (1988). Sorting of mannose 6-phosphate receptors and lysosomal membrane proteins in endocytic vesicles. *Journal of Cell Biology* **107**, 2491-2501.

Golabek, A.A., Kaczmarski, W., Kida, E., Kaczmarski, A., Michalewski, M.P. and Wisniewski, K.E. (1999). Expression studies of CLN3 protein (battenin) in fusion with the green fluorescent protein in mammalian cells in vitro. *Molecular Genetics and Metabolism* **66**, 277-282.

Hamill, O.P., Marty, A., Neher, E., Sakmann, B. and Sigworth, F.J. (1981). Improved patch-clamp techniques for high-resolution current recording from cells and cell-free membrane patches. *Pflugers Archiv European Journal of Physiology* **391** (2), 85-100.

Hare, J.F. and Huston, M. (1985). Degradation of exogenous membrane proteins implanted into the plasma membrane of cultured hepatoma cells. *Experimental Cell Research* **161**, 331-341.

Hart, G.W. (1978). Glycosaminoglycan sulfotransferases of the developing chick cornea. *Journal of Biological Chemistry* **253** (2), 347-353.

Hastbacka, J., de la Chapelle, A., Mahtani, M.M., Clines, G., Reeve Daly, M.P., Daly, M., Hamilton, B.A., Kusumi, K., Trivedi, B. and Weaver, A. (1994). The diastrophic dysplasia gene encodes a novel sulfate transporter: positional cloning by fine-structure linkage disequilibrium mapping. *Cell* **78**, 1073-1087.

Hastbacka, J., Superti-Furga, A., Wilcox, W.R., Rimoin, D.L., Cohn, D.H. and Lander, E.S. (1996). Atelosteogenesis type II is caused by mutations in the diastrophic dysplasia sulphate-transporter gene (DTDST): evidence for a phenotypic series involving three chondrodysplasias. *American Journal of Human Genetics* **58**, 255-262.

Hawkesford, M.J., Davidian, J.C. and Grignon, C. (1993). Sulphate/proton cotransport in plasma-membrane vesicles isolated from roots of *Brassica napus L.*: increased transport in membranes isolated from sulphur-starved plants. *Planta (Heidelberg)* **190**, 297-304.

Hayashi, H., Niinobe, S., Matsumoto, Y. and Suga, T. (1981). Effects of Triton WR-1339 on lipoprotein lipolytic activity and lipid content of rat liver lysosomes. *Journal of Biochemistry* **89** (2), 573-579.

Heinz, E., Geck, P. and Wilbrandt, W. (1972). Coupling in secondary active transport. Activation of transport by co-transport and-or counter-transport with the fluxes of other solutes. *Biochimica et Biophysica Acta* **255** (2), 442-461.

Hell, R. (1997). Molecular physiology of plant sulfur metabolism. *Planta* **202** (2), 138-148.
Henning, R. and Heidrich, H.-G. (1974). Membrane lipids of rat liver lysosomes prepared by free-flow electrophoresis. *Biochimica et Biophysica Acta* **345**, 326-335.

Hill, W.G. (1995). Sulphation of glycosaminoglycans in cystic fibrosis. Ph.D. Thesis, The University of Adelaide.

Hill, W.G., Harper, G.S., Rozaklis, T., Boucher, R.C. and Hopwood, J.J. (1997a). Organ-specific over-sulfation of glycosaminoglycans and altered extracellular matrix in a mouse model of cystic fibrosis. *Biochemical and Molecular Medicine* **62** (1), 113-122.

Hill, W.G., Harper, G.S., Rozaklis, T. and Hopwood, J.J. (1997b). Sulfation of chondroitin/dermatan sulfate by cystic fibrosis pancreatic duct cells is not different from control cells. *Biochemical and Molecular Medicine* **62** (1), 85-94.

Hille-Rehfeld, A. (1995). Mannose 6-phosphate receptors in sorting and transport of lysosomal enzymes. *Biochimica et Biophysica Acta* **1241**, 177-194.

Hillis, D.M. and Bull, J.J. (1993). An empirical test of bootstrapping as a method for assessing confidence in phylogenetic analyses. *Systematic Biology* **42**, 182-192.

Hoglund, P., Haila, S., Socha, J., Tomaszewski, L., Saarialho Kere, U., Karjalainen Lindsberg, M.L., Airola, K., Holmberg, C., de la Chapelle, A. and Kere, J. (1996). Mutations of the Down-Regulated in Adenoma (DRA) gene cause congenital chloride diarrhoea. *Nature Genetics* **14** (3), 316-319.

Holmberg, E.G., Verkman, A.S. and Dix, J.A. (1989). Mechanism of acridine orange interaction with phospholipids and proteins in renal microvillus vesicles. *Biophysical Chemistry* **33**, 245-256.

Holness, C.L. and Simmons, D.L. (1993). Molecular cloning of CD68, a human macrophage marker related to lysosomal glycoproteins. *Blood* **81**, 1607-1613.

Honing, S., Griffith, J., Geuze, H.J. and Hunziker, W. (1996). The tyrosine-based lysosomal targeting signal in lamp-1 mediates sorting into Golgi-derived clathrin-coated vesicles. *EMBO Journal* **15** (19), 5230-5239.

Hopwood, J.J. and Brooks, D.A. (1997). An introduction to the basic science and biology of the lysosome and storage disease. Organelle Diseases. Edited by Applegarth, D.A., Dimmick, J.E. and Hall, J.G. **Chapter 2**, pp 7-35. Chapman and Hall, London.

Hopwood, J.J. and Morris, C.P. (1990). The mucopolysaccharidoses diagnosis, molecular genetics and treatment. *Molecular Biology and Medicine* **7**, 381-404.

Hopwood, J.J., Muller, V., Harrison, J.R., Carey, W.F., Elliott, H., Robertson, E.F. and Pollard, A.C. (1982). Enzymatic diagnosis of the mucopolysaccharidoses: experience of 96 cases diagnosed in a five-year period. *Medical Journal of Australia* **1** (6), 257-260.

Horuk, R., Rodbell, M., Cushman, S.W. and Simpson, I.A. (1983). Identification and characterization of the rat adipocyte glucose transporter by photoaffinity crosslinking. *FEBS Letters* **164**, 261-266.

Humphries, D.E., Silbert, C.K. and Silbert, J.E. (1986). Glycosaminoglycan production by bovine aortic endothelial cells cultured in sulfate-depleted medium. *Journal of Biological Chemistry* **261** (20), 9122-9127.

Iacobazzi, V., Palmieri, F., Runswick, M.J. and Walker, J.E. (1992). Sequences of the human and bovine genes for the mitochondrial 2-oxoglutarate carrier. *DNA Sequence* **3**, 79-88.

Idriss, J.M. and Jonas, A.J. (1991). Vitamin B12 transport by rat liver lysosomal membrane vesicles. *Journal of Biological Chemistry* **266** (15), 9438-9441.

Idriss, J.M., Koetters, P. and Jonas, A. (1991). Lysosomal transport and recycling of biotin. Poster 479, 8th International Congress of Human Genetics. *American Journal of Human Genetics* **49**, 100.

Ihrke, G., Gray, S.R. and Luzio, J.P. (2000). Endolyn is a mucin-like type I membrane protein targeted to lysosomes by its cytoplasmic tail. *Biochemical Journal* **345 Pt 2**, 287-296.

Imai, Y., Yanagishita, M. and Hascall, V.C. (1994). Measurement of contribution from intracellular cysteine to sulfate in phosphoadenosine phosphosulfate in rat ovarian granulosa cells. *Archives of Biochemistry and Biophysics* **312** (2), 392-400.

Jennings, M.L. and Al Rhaiyel, S. (1988). Modification of a carboxyl group that appears to cross the permeability barrier in the red blood cell anion transporter. *Journal of General Physiology* **92** (2), 161-178.

Jindal, S., Dudani, A.K., Singh, B., Harley, C.B. and Gupta, R.S. (1989). Primary structure of a human mitochondrial protein homologous to the bacterial and plant chaperonins and to the 65-kilodalton mycobacterial antigen. *Molecular and Cellular Biology* **9** (5), 2279-2283.

Jonas, A.J., Conrad, P. and Jobe, H. (1990). Neutral-sugar transport by rat liver lysosomes. *Biochemical Journal* **272**, 323-326.

Jonas, A.J. and Jobe, H. (1990). Sulfate transport by rat liver lysosomes. *Journal of Biological Chemistry* **265** (29), 17545-17549.

Jonas, A.J., Speller, R.J., Conrad, P.B. and Dubinsky, W.P. (1989). Transport of N-acetyl-D-glucosamine and N-acetyl-D-galactosamine by rat liver lysosomes. *Journal of Biological Chemistry* **264** (9), 4953-4956.

Jones, D.B., Coulson, A.F. and Duff, G.W. (1993). Sequence homologies between hsp60 and autoantigens. *Immunology Today* **14** (3), 115-118.

Karp, G. (1999). Lysosomes. Cell and Molecular Biology. Concepts and Experiments. 2nd Edition. pp 323-327. John Wiley & Sons Inc., Brisbane, New York.

Kellokumpu, S., Neff, L., Jamsa Kellokumpu, S., Kopito, R. and Baron, R. (1988). A 115-kD polypeptide immunologically related to erythrocyte band 3 is present in Golgi membranes [published erratum appears in Science 1988 Dec 23; 242 (4886):1624]. *Science* **242** (4883), 1308-1311.

Ketter, J.S., Jarai, G., Fu, Y.H. and Marzluf, G.A. (1991). Nucleotide sequence, messenger RNA stability, and DNA recognition elements of cys-14, the structural gene for sulfate permease II in *Neurospora crassa*. *Biochemistry* **30** (7), 1780-1787.

Kim, D.Y., Cho, D.Y. and Taylor, H.W. (1996). Lysosomal storage disease in an emu (dromaius novaehollandiae). *Veterinary Pathology* **33**, 365-366.

Klionsky, D.J. and Ohsumi, Y. (1999). Vacuolar import of proteins and organelles from the cytoplasm. *Annual Review of Cell and Developmental Biology* **15**, 1-32.

Kobayashi, T., Sugimoto, T., Saijoh, K., Fukase, M. and Chihara, K. (1997). Cloning of mouse diastrophic dysplasia sulfate transporter gene induced during osteoblast differentiation by bone morphogenetic protein-2. *Gene* **198** (1-2), 341-349.

Koetters, P.J., Chou, H.F. and Jonas, A.J. (1995a). Lysosomal sulfate transport: inhibitor studies. *Biochimica et Biophysica Acta* **1235** (1), 79-84.

Koetters, P.J., Chou, H.F. and Jonas, A.J. (1995b). Reconstitution of lysosomal sulfate transport in proteoliposomes. *Biochimica et Biophysica Acta* **1244** (2-3), 311-316.

Koj, A., Frendo, J. and Janik, Z. (1967). [^{35}S]Thiosulphate oxidation by rat liver mitochondria in the presence of glutathione. *Biochemical Journal* **103** (3), 791-795.

Kornfeld, S. (1992). Structure and function of the mannose 6-phosphate/insulinlike growth factor II receptors. *Annual Review of Biochemistry* **61**, 307-330.

Kornilova, E.S., Sorkin, A.D. and Nikol'skii, N.N. (1987). Dinamika kompartmentalizatsii epidermal'nogo faktora rosta v kletkakh A431. (Compartmentalization dynamics of the epidermal growth factor in A431 cells). *Tsitologiia* **29** (8), 904-910.

Kouchi, H. and Hata, S. (1993). Isolation and characterization of novel nodulin cDNAs representing genes expressed at early stages of soybean nodule development. *Molecular and General Genetics* **238** (1-2), 106-119.

Krijgsheld, K.R. and Mulder, G.J. (1982). The availability of inorganic sulfate as a rate-limiting factor in the sulfation of xenobiotics in mammals *in-vivo*. Sulfate Metabolism and

Sulfate Conjugation. Proceedings of an International Workshop held at Noordwijkerhout, The Netherlands 1981. Edited by Mulder, G.J., Caldwell, J., Van Kempen, G.M. and Vonk, R.J. pp 59-66. Taylor and Francis Ltd., London.

Krijgsheld, K.R., Scholtens, E. and Mulder, G.J. (1980). Serum concentration of inorganic sulfate in mammals: species differences and circadian rhythm. *Comparative Biochemistry and Physiology A: Comparative Physiology* **67A**, 683-686.

Krijgsheld, K.R., Scholtens, E. and Mulder, G.J. (1982). The dependence of the rate of sulphate conjugation on the plasma concentration of inorganic sulphate in the rat in vivo. *Biochemical Pharmacology* **31** (24), 3997-4000.

Laemmli, U.K. (1970). Cleavage of structural proteins during the assembly of the head of bacteriophage T4. *Nature* **227**, 680-685.

Leaback, D.H. and Walker, P.G. (1961). Studies on glucosaminidase IV. The fluorometric assay N-acetyl-beta-glucosaminidase. *Biochemical Journal* **78**, 151-156.

Lee, A.C., Powell, J.E., Tregear, G.W., Niall, H.D. and Stevens, V.C. (1980). A method for preparing beta-hCG COOH peptide-carrier conjugates of predictable composition. *Molecular Immunology* **17** (6), 749-756.

Lemons, R.M. and Thoene, J.G. (1991). Mediated calcium transport by isolated human fibroblast lysosomes. *Journal of Biological Chemistry* **266** (22), 14378-14382.

Liau, Y.H. and Horowitz, M.I. (1976). The importance of PAPS in determining sulfation in gastrointestinal mucosa. *Digestion* **14** (4), 372-375.

Liscum, L., Ruggiero, R.M. and Faust, J.R. (1989). The intracellular transport of low density lipoprotein-derived cholesterol is defective in Niemann-Pick type C fibroblasts. *Journal of Cell Biology* **108** (5), 1625-1636.

Lloyd, J.B. and Forster, S. (1991). The lysosomal membrane. *Trends in Biochemical Sciences* **11**, 129.

Lotscher, M., Custer, M., Quabius, E.S., Kaissling, B., Murer, H. and Biber, J. (1996). Immunolocalization of Na/SO_4-cotransport (NaSi-1) in rat kidney. *Pflugers Archiv European Journal of Physiology* **432** (3), 373-378.

MacDonald, M.E., Cheng, S.V., Zimmer, M., Haines, J.L., Poustka, A., Allitto, B., Smith, B., Whaley, W.L., Romano, D.M. and Jagadeesh, J. (1989). Clustering of multiallele DNA markers near the Huntington's disease gene. *Journal of Clinical Investigation* **84** (3), 1013-1016.

Madsen, K.M., Kim, J. and Tisher, C.C. (1992). Intracellular band 3 immunostaining in type A intercalated cells of rabbit kidney. *American Journal of Physiology* **262**, F1015-F1022.

Mahfoudi, A., Beck, L., Nicollier, M., Coosemans, V. and Adessi, G.L. (1991). Progesterone effect on intracellular inorganic sulphate in uterine epithelial cells. *Molecular and Cellular Endocrinology* **79** (1-3), R15-R20.

Makiya, R. and Stigbrand, T. (1992a). Placental alkaline phosphatase is related to human IgG internalization in HEp2 cells. *Biochemical and Biophysical Research Communications* **182**, 624-630.

Makiya, R. and Stigbrand, T. (1992b). Placental alkaline phosphatase as the placental IgG receptor. *Clinical Chemistry* **38**, 2543-2545.

Makiya, R. and Stigbrand, T. (1992c). Placental alkaline phosphatase has a binding site for the human immunoglobulin-G Fc portion. *European Journal of Biochemistry* **205**, 341-345.

Makiya, R., Thornell, L.E. and Stigbrand, T. (1992). Placental alkaline phosphatase, a GPI-anchored protein, is clustered in clathrin-coated vesicles. *Biochemical and Biophysical Research Communications* **183**, 803-808.

Mancini, G.M., Beerens, C.E., Aula, P.P. and Verheijen, F.W. (1991). Sialic acid storage diseases. A multiple lysosomal transport defect for acidic monosaccharides. *Journal of Clinical Investigation* **87** (4), 1329-1335.

Mancini, G.M., Beerens, C.E., Galjaard, H. and Verheijen, F.W. (1992). Functional reconstitution of the lysosomal sialic acid carrier into proteoliposomes. *Proceedings of the National Academy of Sciences of the United States of America* **89** (14), 6609-6613.

Mancini, G.M., Beerens, C.E. and Verheijen, F.W. (1990). Glucose transport in lysosomal membrane vesicles. Kinetic demonstration of a carrier for neutral hexoses. *Journal of Biological Chemistry* **265**, 12380-12387.

Mancini, G.M., de Jonge, H.R., Galjaard, H. and Verheijen, F.W. (1989). Characterization of a proton-driven carrier for sialic acid in the lysosomal membrane. Evidence for a group-specific transport system for acidic monosaccharides. *Journal of Biological Chemistry* **264**, 15247-15254.

Mane, S.M., Marzella, L., Bainton, D.F., Holt, V.K., Cha, Y., Hildreth, J.E. and August, J.T. (1989). Purification and characterization of human lysosomal membrane glycoproteins. *Archives of Biochemistry and Biophysics* **268**, 360-378.

Maneri, L.R. and Low, P.S. (1988). Structural stability of the erythrocyte anion transporter, band 3, in different lipid environments. A differential scanning calorimetric study. *Journal of Biological Chemistry* **263** (31), 16170-16178.

Markello, T.C., Bernardini, I.M. and Gahl, W.A. (1993). Improved renal function in children with cystinosis treated with cysteamine. *New England Journal of Medicine* **328** (16), 1157-1162.

Markovich, D., Bissig, M., Sorribas, V., Hagenbuch, B., Meier, P.J. and Murer, H. (1994). Expression of rat renal sulfate transport systems in *Xenopus laevis* oocytes. Functional characterization and molecular identification. *Journal of Biological Chemistry* **269**, 3022-3026.

Markovich, D., Forgo, J., Stange, G., Biber, J. and Murer, H. (1993). Expression cloning of rat renal $Na^+/SO_4^{(2-)}$ cotransport. *Proceedings of the National Academy of Sciences of the United States of America* **90**, 8073-8077.

Matsuzawa, Y. and Hostetler, K.Y. (1979). Degradation of bis(monoacylglycero)phosphate by an acid phosphodiesterase in rat liver lysosomes. *Journal of Biological Chemistry* **254** (13), 5997-6001.

Matsuzawa, Y. and Hostetler, K.Y. (1980). Studies on drug induced lipidosis: subcellular localisation of phospholipid and cholestrol in the liver of rats treated with chloroquine or 4,4'-bis(diethylaminoethoxy)alpha,beta-diethyldiphenylethane. *Journal of Lipid Research* **21**, 202-214.

McCarthy, J. and Turley, E. (1993). Effects of extracellular matrix components on cell locomotion. *Critical Reviews in Oral Biology and Medicine* **4** (5), 619-637.

McPhee, M.D., Atkinson, S.A. and Cole, D.E.C. (1990). Quantitation of free sulphate and total sulfoesters in human breast milk by ion chromatography. *Journal of Chromatography* **527**, 41-50.

Meikle, P.J., Whittle, A.M. and Hopwood, J.J. (1995). Human acetyl-coenzyme A:alpha-glucosaminide N-acetyltransferase. Kinetic characterization and mechanistic interpretation. *Biochemical Journal* **308** (Pt 1), 327-333.

Merril, C.R., Goldman, D., Sedman, S.A. and Ebert, M.H. (1981). Ultrasensitive stain for proteins in polyacrylamide gels shows regional variation in cerebrospinal fluid proteins. *Science* **211**, 1437-1438.

Milanick, M.A. and Gunn, R.B. (1984). Proton-sulfate cotransport: external proton activation of sulfate influx into human red blood cells. *American Journal of Physiology* **247**,C247-C259.

Milanick, M.A. and Gunn, R.B. (1986). Proton inhibition of chloride exchange: asynchrony of band 3 proton and anion transport sites? *American Journal of Physiology* **250**, C955-C969.

Miskimins, W.K. and Shimizu, N. (1982). Dual pathways for epidermal growth factor processing after receptor-mediated endocytosis. *Journal of Cellular Physiology* **112** (3), 327-338.

Mohapatra, N.K., Cheng, P.W., Parker, J.C., Paradiso, A.M., Yankaskas, J.R., Boucher, R.C. and Boat, T.F. (1993). Sulfate concentrations and transport in human bronchial epithelial cells. *American Journal of Physiology* **264** (5 Pt 1), C1231-C1237.

Morcuende, J.A., Plass, A.H.K. and Kimura, J.H. (1996). Altered functional activity of the sulphate transport channel SAT-1 in a mutant rat chondrosarcoma clone. *42nd Annual Meeting, Orthopaedic Research Society, February 19-22, Atlanta Georgia* p 764.

Moriyama, Y. and Nelson, N. (1987). The purified ATPase from chromaffin granule membranes is an anion-dependent proton pump. *Journal of Biological Chemistry* **262** (19), 9175-9180.

Moriyama, Y., Takano, T. and Ohkuma, S. (1984). Proton translocating ATPase in lysosomal membrane ghosts. Evidence that alkaline Mg2+-ATPase acts as a proton pump. *Journal of Biochemistry* **95** (4), 995-1007.

Morohashi, K., Fujii Kuriyama, Y., Okada, Y., Sogawa, K., Hirose, T., Inayama, S. and Omura, T. (1984). Molecular cloning and nucleotide sequence of cDNA for mRNA of mitochondrial cytochrome P-450(SCC) of bovine adrenal cortex. *Proceedings of the National Academy of Sciences of the United States of America* **81** (15), 4647-4651.

Morohashi, K., Sogawa, K., Omura, T. and Fujii Kuriyama, Y. (1987). Gene structure of human cytochrome P-450(SCC), cholesterol desmolase. *Journal of Biochemistry* **101** (4), 879-887.

Muelder, C.J. and Kuelemans, K. (1978). Metabolism or inorganic sulfate in the isolated perfused rat liver: effect of sulfate concentration on the rate of sulfation of phenol sulfotransferase. *Biochemical Journal* **176**, 959-965.

Mulder, G.J., Caldwell, J., Van Kempen, G.M. and Vonk, R.J. (1982). Preface. Sulfate Metabolism and Sulfate Conjugation. Proceedings of an International Workshop held at Noordwijkerhout, The Netherlands 1981. Edited by Mulder, G.J., Caldwell, J., Van Kempen, G.M. and Vonk, R.J. pp ix-xi. Taylor and Francis Ltd., London.

Nakamura, N., Yamamoto, A., Wada, Y. and Futai, M. (2000). Syntaxin 7 mediates endocytic trafficking to late endosomes. *Journal of Biological Chemistry* **275**, 6523-6529.
Nauseef, W.M. and Clark, R.A. (1986). Separation and analysis of subcellular organelles in a human promyelocytic leukemia cell line, HL-60: application to the study of myeloid lysosomal enzyme synthesis and processing. *Blood* **68** (2), 442-449.

Neher, E. and Sakmann, B. (1976). Single-channel currents recorded from membrane of denervated frog muscle fibres. *Nature* **260** (5554), 799-802.

Noctor, G., Arisi, A.C.M., Jouanin, L., Valadier, M.H., Roux, Y. and Foyer, C.H. (1997). Light-dependent modulation of foliar glutathione synthesis and associated amino acid metabolism in poplar overexpressing gamma-glutamylcysteine synthetase. *Planta* **202**, 357-369.

Norbis, F., Perego, C., Markovich, D., Stange, G., Verri, T. and Murer, H. (1994). cDNA cloning of a rat small-intestinal $Na^{+}/SO_4^{(2-)}$ cotransporter. *Pflugers Archiv European Journal of Physiology* **428** (3-4), 217-223.

Normann, P.T. and Flatmark, T. (1982). Microperoxisomes and mitochondria of brown adipose tissue. Hydrodynamic parameters, isolation and capacity of long-chain fatty acid oxidation. *Biochimica et Biophysica Acta* **712** (3), 621-627.

Norseth, J., Normann, P.T. and Flatmark, T. (1982). Hydrodynamic parameters and isolation of mitochondria, microperoxisomes and microsomes of rat heart. *Biochimica et Biophysica Acta* **719** (3), 569-579.

O'Farrell, P.H. (1975). High resolution two-dimensional electrophoresis of proteins. *Journal of Biological Chemistry* **250**, 4007-4021.

Ohkuma, S., Moriyama, Y. and Takano, T. (1982). Identification and characterization of a proton pump on lysosomes by fluorescein-isothiocyanate-dextran fluorescence. *Proceedings of the National Academy of Sciences of the United States of America* **79** (9), 2758-2762.

Ohkuma, S. and Poole, B. (1978). Fluorescence probe measurement of the intralysosomal pH in living cells and the perturbation of pH by various agents. *Proceedings of the National Academy of Sciences of the United States of America* **75** (7), 3327-3331.

Okamoto, M., Hiratani, N., Arai, K. and Ohkuma, S. (1996). Properties of H+-ATPase from rat liver lysosomes as revealed by reconstitution into proteoliposomes. *Journal of Biochemistry* **120** (3), 608-615.

Okubo, K., Kang, D., Hamasaki, N. and Jennings, M.L. (1994). Red blood cell band 3. Lysine 539 and lysine 851 react with the same H_2DIDS (4,4'-diisothiocyanodihydrostilbene-2,2'-disulfonic acid) molecule. *Journal of Biological Chemistry* **269** (3), 1918-1926.

Oshima, A., Nolan, C.M., Kyle, J.W., Grubb, J.H. and Sly, W.S. (1988). The human cation-independent mannose 6-phosphate receptor. Cloning and sequence of the full-length cDNA and expression of functional receptor in COS cells. *Journal of Biological Chemistry* **263**, 2553-2562.

Ostedgaard, L.S., Jennings, M.L., Karniski, L.P. and Schuster, V.L. (1991). A 45-kDa protein antigenically related to band 3 is selectively expressed in kidney mitochondria. *Proceedings of the National Academy of Sciences of the United States of America* **88** (3), 981-985.

Page, R.D. (1996). TreeView: an application to display phylogenetic trees on personal computers. *Computer Applications in the Biosciences* **12**, 357-358.

Palmgren, M.G. (1991). Acridine orange as a probe for measuring pH gradients across membranes: mechanism and limitations. *Analytical Biochemistry* **192** (2), 316-321.

Parenti, G., Meroni, G. and Ballabio, A. (1997). The sulfatase gene family. *Current Opinion in Genetics and Development* **7** (3), 386-391.

Pearson, W.R. and Lipman, D.J. (1988). Improved tools for biological sequence comparison. *Proceedings of the National Academy of Sciences of the United States of America* **85**, 2444-2448.

Peeters, J.M., Hazendonk, T.G., Beuvery, E.C. and Tesser, G.I. (1989). Comparison of four bifunctional reagents for coupling peptides to proteins and the effect of the three moieties on the immunogenicity of the conjugates. *Journal of Immunological Methods* **120** (1), 133-143.

Pertoft, H., Warmegard, B. and Hook, M. (1978). Heterogeneity of lysosomes originating from rat liver parenchymal cells. Metabolic relationship of subpopulations separated by density-gradient centrifugation. *Biochemical Journal* **174**, 309-317.

Pisoni, R.L., Acker, T.L., Lisowski, K.M., Lemons, R.M. and Thoene, J.G. (1990). A cysteine-specific lysosomal transport system provides a major route for the delivery of thiol to human fibroblast lysosomes: possible role in supporting lysosomal proteolysis. *Journal of Cell Biology* **110**, 327-335.

Pisoni, R.L., Flickinger, K.S., Thoene, J.G. and Christensen, H.N. (1987). Characterization of carrier-mediated transport systems for small neutral amino acids in human fibroblast lysosomes. *Journal of Biological Chemistry* **262** (13), 6010-6017.

Pisoni, R.L., Thoene, J.G. and Christensen, H.N. (1985). Detection and characterization of carrier-mediated cationic amino acid transport in lysosomes of normal and cystinotic human fibroblasts. Role in therapeutic cystine removal? *Journal of Biological Chemistry* **260** (8), 4791-4798.

Pisoni, R.L. and Thoene, J.G. (1989). Detection and characterization of a nucleoside transport system in human fibroblast lysosomes. *Journal of Biological Chemistry* **264** (9), 4850-4856.

Pisoni, R.L. (1991). Characterization of a phosphate transport system in human fibroblast lysosomes. *Journal of Biological Chemistry* **266** (2), 979-985.

Ploug, M., Jensen, A.L. and Barkholt, V. (1989). Determination of amino acid compositions and NH2-terminal sequences of peptides electroblotted onto PVDF membranes from tricine-sodium dodecyl sulfate-polyacrylamide gel electrophoresis: application to peptide mapping of human complement component C3. *Analytical Biochemistry* **181**, 33-39.

Pohl, T.M., Zimmer, M., MacDonald, M.E., Smith, B., Bucan, M., Poustka, A., Volinia, S., Searle, S., Zehetner, G. and Wasmuth, J.J. (1988). Construction of a NotI linking library and isolation of new markers close to the Huntington's disease gene. *Nucleic Acids Research* **16** (19), 9185-9198.

Pohlmann, R., Nagel, G., Schmidt, B., Stein, M., Lorkowski, G., Krentler, C., Cully, J., Meyer, H.E., Grzeschik, K.H. and Mersmann, G. (1987). Cloning of a cDNA encoding the human cation-dependent mannose 6-phosphate-specific receptor. *Proceedings of the National Academy of Sciences of the United States of America* **84**, 5575-5579.

Pritchard, J.B. (1987). Sulfate-bicarbonate exchange in brush-border membranes from rat renal cortex. *American Journal of Physiology* **252** (2 Pt 2), F346-F356.

Ramaswamy, K., Harig, J.M., Kleinman, J.G., Harris, M.S. and Barry, J.A. (1989). Sodium-proton exchange in human ileal brush-border membrane vesicles. *Biochimica et Biophysica Acta* **981**, 193-199.

Rasmussen, H., Sallis, J., Fang, M., DeLuca, H.F. and Young, R. (1964). Parathyroid hormone and anion uptake in isolated mitochondria. *Endocrinology* **74**, 388-394.

Recasens, M. and Mandel, P. (1979). Similarities between cysteinesulphinate transaminase and aspartate aminotransferase. *Ciba Foundation Symposium* **72**, 259-270.

Rechid, R., Vingron, M. and Argos, P. (1989). A new interactive protein sequence alignment program and comparison of its results with widely used algorithms. *Computer Applications in the Biosciences* **5**, 107-113.

Reinhart, W.H., Wyss, E.J., Arnold, D. and Ott, P. (1994). Hereditary spherocytosis associated with protein band 3 defect in a Swiss kindred. *British Journal of Haematology* **86** (1), 147-155.

Reizer, J., Reizer, A. and Saier Jr, M.H. (1994). A functional superfamily of sodium/solute symporters. *Biochimica et Biophysica Acta* **1197** (2), 133-166.

Renlund, M., Aula, P.P., Raivio, K.D., Autio, S., Sainio, K., Rapola, J. and Koskela, S.L. (1983). Salla disease: a new lysosomal storage disorder with disturbed sialic acid metabolism. *Neurology* **33**, 57-66.

Renlund, M., Tietze, F. and Gahl, W.A. (1986). Defective sialic acid egress from isolated fibroblast lysosomes of patients with Salla disease. *Science* **232** (4751), 759-762.

Rodgers, R.J., Waterman, M.R., Simpson, E.R. and Magness, R.R. (1988). Immunoblot analysis of cholesterol side-chain cleavage cytochrome P-450 and adrenodoxin in corpora lutea of cyclic and late-pregnant sheep. *Journal of Reproduction and Fertility* **83** (2), 843-850.

Rodgers, R.J. (1990). Steroidogenic cytochrome P450 enzymes and ovarian steroidogenesis. *Reproduction, Fertility, and Development* **2** (2), 153-163.

Rome, L.H. and Hill, D.F. (1986). Lysosomal degradation of glycoproteins and glycosaminoglycans. Efflux and recycling of sulphate and N-acetylhexosamines. *Biochemical Journal* **235**, 707-713.

Rosenblatt, D.S., Hosack, A., Matiaszuk, N.V., Cooper, B.A. and Laframboise, R. (1985). Defect in vitamin B12 release from lysosomes: newly described inborn error of vitamin B12 metabolism. *Science* **228** (4705), 1319-1321.

Rothwell, J.T., Harper, P.A.W., Hartley, W.J., Gumbrell, R.C. and Meischke, H.R.C. (1990). Lysosomal storage disease in Kangaroo. *Journal of Wildlife Diseases* **26**, 275-278.

Rumpho, M.E. and Sack, F.D. (1989). Fluorescence microscopy and radiolabeling of C3 and C4 chloroplasts using diisothiocyanatostilbene disulfonic acid as a marker for the phosphate translocator. *Planta* **179**, 137-147.

Sabatini, D.D. and Adesnik, M.B. (1998). The biogenesis of membranes and organelles. The Metabolic and Molecular Bases of Inherited Disease. Seventh Edition. Edited by Scriver, C.R., Beaudet, A.L., Sly, W.S. and Valle, D. **1**, pp 459-464. McGraw-Hill, New York London Sydney.

Saris, N.E. (1980). Sulphate transport by H+ symport and by the dicarboxylate carrier in mitochondria. *Biochemical Journal* **192** (3), 911-917.

Satoh, H., Susaki, M., Shukunami, C., Iyama, K., Negoro, T. and Hiraki, Y. (1998). Functional analysis of diastrophic dysplasia sulfate transporter. Its involvement in growth regulation of chondrocytes mediated by sulfated proteoglycans. *Journal of Biological Chemistry* **273** (20), 12307-12315.

Scheuring, U., Kollewe, K., Haase, W. and Schubert, D. (1986). A new method for the reconstitution of the anion transport system of the human erythrocyte membrane. *Journal of Membrane Biology* **90** (2), 123-135.

Scheuring, U., Lindenthal, S., Grieshaber, G., Haase, W. and Schubert, D. (1988). The turnover number for band 3-mediated sulfate transport in phosphatidylcholine bilayers. *FEBS Letters* **227** (1), 32-34.

Schmidt, N.D., Peschon, J.J., Chandler, C.J., Renosto, F. and Segel, I.H. (1982). ATP Sulphurylase: An enzyme subject to potent product inhibition. Sulfate Metabolism and Sulfate Conjugation. Proceedings of an International Workshop held at Noordwijkerhout, The Netherlands 1981. Edited by Mulder, G.J., Caldwell, J., Van Kempen, G.M. and Vonk, R.J. pp 5-12. Taylor and Francis Ltd., London.

Schneider, D.L. (1979). The acidification of rat liver lysosomes *in vitro*: a role for the membranous ATPase as a proton pump. *Biochemical and Biophysical Research Communications* **87** (2), 559-565.

Schneider, D.L. (1981). ATP-dependent acidification of intact and disrupted lysosomes. Evidence for an ATP-driven proton pump. *Journal of Biological Chemistry* **256** (8), 3858-3864.

Schneider, D.L. (1983). ATP-dependent acidification of membrane vesicles isolated from purified rat liver lysosomes. Acidification activity requires phosphate. *Journal of Biological Chemistry* **258** (3), 1833-1838.

Schneider, J.A., Bradley, K. and Seegmiller, J.E. (1967). Increased cystine in leukocytes from individuals homozygous and heterozygous for cystinosis. *Science* **157** (794), 1321-1322.

Schweinfest, C.W., Henderson, K.W., Suster, S., Kondoh, N. and Papas, T.S. (1993). Identification of a colon mucosa gene that is down-regulated in colon adenomas and adenocarcinomas. *Proceedings of the National Academy of Sciences of the United States of America* **90** (9), 4166-4170.

Scott, H.S., Blanch, L., Guo, X.H., Freeman, C., Orsborn, A., Baker, E., Sutherland, G.R., Morris, C.P. and Hopwood, J.J. (1995). Cloning of the sulphamidase gene and identification of mutations in Sanfilippo A syndrome. *Nature Genetics* **11** (4), 465-467.

Scott, H.S., Litjens, T., Nelson, P.V., Brooks, D.A., Hopwood, J.J. and Morris, C.P. (1992). alpha-L-Iduronidase mutations (Q70X and P533R) associate with a severe Hurler phenotype. *Human Mutation* **1** (4), 333-339.

Sillaots, S. and Rosenblatt, D.S. (1992). Lysosomal cobalamin transport. Pathophysiology of Lysosomal Transport. Edited by Thoene, J.G. pp 201-230. CRC Press, London Tokyo.

Simon, S.M. and Blobel, G. (1991). A protein-conducting channel in the endoplasmic reticulum. *Cell* **65**, 371-380.

Singh, H. and Poulos, A. (1995). Substrate specificity of rat liver mitochondrial carnitine palmitoyl transferase I: evidence against alpha-oxidation of phytanic acid in rat liver mitochondria. *FEBS Letters* **359**, 179-183.

Smith, F.W., Ealing, P.M., Hawkesford, M.J. and Clarkson, D.T. (1995a). Plant members of a family of sulphate transporters reveal functional subtypes. *Proceedings of the National Academy of Sciences of the United States of America* **92** (20), 9373-9377.

Smith, F.W., Hawkesford, M.J., Prosser, I.M. and Clarkson, D.T. (1995b). Isolation of a cDNA from *Saccharomyces cerevisiae* that encodes a high affinity sulphate transporter at the plasma membrane. *Molecular and General Genetics* **247** (6), 709-715.

Smith, P.K., Krohn, R.I., Hermanson, G.T., Mallia, A.K., Gartner, F.H., Provenzano, M.D., Fujimoto, E.K., Goeke, N.M., Olson, B.J. and Klenk, D.C. (1985). Measurement of protein using bicinchoninic acid [published erratum appears in Anal Biochem 1987 May 15;163(1):279]. *Analytical Biochemistry* **150** (1), 76-85.

Sobue, M., Takeuchi, J., Ito, K., Kimata, K. and Suzuki, S. (1978). Effect of environmental sulfate concentration on the synthesis of low and high sulfated chondroitin sulfates by chick embryo cartilage. *Journal of Biological Chemistry* **253** (17), 6190-6196.

Stanfield, P.R. (1987). Nucleotides such as ATP may control the activity of ion channels. *Trends in Neurosciences* **10**, 335-339.

Stein, W.D. (1986). Channels across the cell membrane; and Facilitated diffusion: the simple carrier. Transport and Diffusion across Cell Membranes. Edited by Stein, W.D. **Chapters 3-4**, pp 114-337. Academic Press, Inc., London Montreal Sydney New York.

Stevens, T.H. and Forgac, M. (1997). Structure, function and regulation of the vacuolar (H+)-ATPase. *Annual Review of Cell and Developmental Biology* **13**, 779-808.

Stewart, B.H., Collarini, E.J., Pisoni, R.L. and Christensen, H.N. (1989). Separate and shared lysosomal transport of branched and aromatic dipolar amino acids. *Biochimica et Biophysica Acta* **987** (2), 145-153.

Stirling, J.W., Coleman, M. and Brennan, J. (1990). The use of inert dehydration and glycol methacrylate embedding for immunogold localisation of glomerular basement membrane components. *Laboratory Investigation* **62** (5), 655-663.

Stirling, J.W. and Graff, P.S. (1995). Antigen unmasking for immunoelectron microscopy: labelling is improved by treating with sodium ethoxide or sodium metaperiodate, then heating on retrieval medium. *Journal of Histochemistry and Cytochemistry* **43** (2), 115-123.

Storrie, B. (1988). Assembly of lysosomes: perspectives from comparative molecular cell biology. *International Review of Cytology* **111**, 53-105.

Sugahara, K. and Schwartz, N.B. (1979). Defect in 3'-phosphoadenosine 5'-phosphosulfate formation in brachymorphic mice. *Proceedings of the National Academy of Sciences of the United States of America* **76** (12), 6615-6618.

Superti-Furga, A. (1994). A defect in the metabolic activation of sulfate in a patient with achondrogenesis type IB. *American Journal of Human Genetics* **55** (6), 1137-1145.

Superti-Furga, A., Hastbacka, J., Cohn, D.H., Wilcox, W.R., van der Harten, H.J., Rimoin, D.L., Lander, E.S., Steinmann, B. and Gitzelmann, R. (1995). Defective sulphation of proteoglycans in achondrogenesis type IB is caused by mutations in the DTDST gene: the disorder is allelic to diastrophic dysplasia. *American Journal of Human Genetics* **57**, A48.

Symons, L.J. and Jonas, A.J. (1987). Isolation of highly purified rat liver lysosomal membranes using two Percoll gradients. *Analytical Biochemistry* **164**, 382-390.

Tanner, M.J.A. (1993). The major integral membrane proteins of the human red cell. *Baillieres Clinical Haematology* **6** (2), 333-356.

Tanner, M.J. (1996). The acid test for band 3. *Nature* **382** (6588), 209-210.
Templeton, D.M. and Wang, A. (1992). Conserved charge of glomerular and mesangial cell proteoglycans: possible role of amino acid-derived sulphate. *Canadian Journal of Physiology and Pharmacology* **70** (6), 843-852.

Terlecky, S.R. and Dice, J.F. (1993). Polypeptide import and degradation by isolated lysosomes. *Journal of Biological Chemistry* **268** (31), 23490-23495.

Thoene, J.G. (1992). Introduction. Pathophysiology of Lysosomal Transport. Edited by Thoene, J.G. pp 1-6. CRC Press, Boca Raton Ann Arbor London Tokyo.

Thompson, J.D., Higgins, D.G. and Gibson, T.J. (1994). CLUSTAL W: improving the sensitivity of progressive multiple sequence alignment through sequence weighting, position-specific gap penalties and weight matrix choice. *Nucleic Acids Research* **22** (22), 4673-4680.

Tietze, F., Seppala, R., Renlund, M., Hopwood, J.J., Harper, G.S., Thomas, G.H. and Gahl, W.A. (1989). Defective lysosomal egress of free sialic acid (N-acetylneuraminic acid) in fibroblasts of patients with infantile free sialic acid storage disease. *Journal of Biological Chemistry* **264** (26), 15316-15322.

Tilly, B.C., Mancini, G.M., Bijman, J., van Gageldonk, P.G., Beerens, C.E., Bridges, R.J., de Jonge, H.R. and Verheijen, F.W. (1992). Nucleotide-activated chloride channels in lysosomal membranes. *Biochemical and Biophysical Research Communications* **187** (1), 254-260.

Tjiong, H.B. and Debuch, H. (1978). Lysosomal bis (monoacylglycero)phosphate of rat liver, its induction by chloroquine and its structure. *Hoppe-Seylers Zeitschrift für Physiologische Chemie* **359** (1), 71-79.

Tjiong, H.B., Lepthin, J. and Debuch, H. (1978). Lysosomal phospholipids from rat liver after treatment with different drugs. *Hoppe-Seylers Zeitschrift f ür Physiologische Chemie* **359** (1), 63-69.

Tokuyasu, K.T. (1984). Immuno-cryoultramicrotomy. Immunolabeling for Electron Microscopy. Edited by Polak, J.M. and Varnel, I.M. p 71. Elsevier Science Publishers, Amsterdam, New York, Oxford.

Towbin, H., Staehelin, T. and Gordon, J. (1979). Electrophoretic transfer of proteins from polyacrylamide gels to nitrocellulose sheets: procedure and some applications. *Proceedings of the National Academy of Sciences of the United States of America* **76**, 4350-4354.

Town, M., Jean, G., Cherqui, S., Attard, M., Forestier, L., Whitmore, S.A., Callen, D.F., Gribouval, O., Broyer, M., Bates, G.P., van't Hoff, W. and Antignac, C. (1998). A novel gene encoding an integral membrane protein is mutated in nephropathic cystinosis. *Nature Genetics* **18** (4), 319-324.

Turnbull, J.E., Hopwood, J.J. and Gallagher, J.T. (1997). Exosequencing of heparan sullphate/heparin saccharides using lysosomal enzymes. A Laboratory Guide to Glycoconjugate Analysis. Edited by Jackson, P. and Gallagher, J.T. Birkhauser Verlag, Basel.

Turner, R.J. (1983). Quantitative studies of cotransport systems: models and vesicles. *Journal of Membrane Biology* **76**, 1-15.

Turrini, F., Arese, P., Yuan, J. and Low, P.S. (1991). Clustering of integral membrane proteins of the human erythrocyte membrane stimulates autologous IgG binding, complement deposition, and phagocytosis. *Journal of Biological Chemistry* **266**, 23611-23617.

Ullrich, K.J. (1994). Specificity of transporters for 'organic anions' and 'organic cations' in the kidney. *Biochimica et Biophysica Acta* **1197** (1), 45-62.

Unger, E.G. Durrant, J. Anson, D.S. Hopwood, J.J. (1994). Recombinant alpha-L-iduronidase: characterization of the purified enzyme and correction of mucopolysaccharidosis type I fibroblasts. *Biochemical Journal* **304** (1), 43-49.

Vadgama, J.V., Chang, K., Kopple, J.D., Idriss, J.-M. and Jonas, A.J. (1991). Characteristics of taurine transport in rat liver lysosomes. *Journal of Cellular Physiology* **147**, 447-454.

Vadgama, J.V. and Jonas, A.J. (1992). Lysosomal transport of inorganic ions: Lysosomal sulphate transport. Pathophysiology of Lysosomal Transport. Edited by Thoene, J.G. pp 133-154. CRC Press, Boca Raton Ann Arbor London Tokyo.

Van Dyck, L., Tettelin, H., Purnelle, B. and Goffeau, A. (1997). An 18.3 kb DNA fragment from yeast chromosome VII carries four unknown open reading frames, the gene for an Asn synthase, remnants of Ty and three tRNA genes. *Yeast* **13** (2), 171-176.

VanBuskirk, A.M., DeNagel, D.C., Guagliardi, L.E., Brodsky, F.M. and Pierce, S.K. (1991). Cellular and subcellular distribution of PBP72/74, a peptide-binding protein that plays a role in antigen processing. *Journal of Immunology* **146**, 500-506.

Varin, L., Marsolais, F., Richard, M. and Rouleau, M. (1997). Sulphation and sulphotransferases 6: Biochemistry and molecular biology of plant sulphotransferases. *FASEB Journal* **11** (7), 517-525.

Venner, T.J., Singh, B. and Gupta, R.S. (1990). Nucleotide sequences and novel structural features of human and Chinese hamster hsp60 (chaperonin) gene families. *DNA and Cell Biology* **9** (8), 545-552.

Verheijen, F.W. Verbeek, E. Aula, N. Beerens, C.E. Havelaar, A.C. Joosse, M. Peltonen, L. Aula, P. Galjaard, H. van der Spek, P.J. and Mancini, G.M. (1999). A new gene, encoding an anion transporter, is mutated in sialic acid storage diseases. *Nature Genetics* **23** (4),462-465.

von Figura, K. (1991). Molecular recognition and targeting of lysosomal proteins. *Current Opinion in Cell Biology* **3**, 642-646.

Walker, B.A., Scott, C.I., Hall, J.G., Murdoch, J.L. and McKusick, V.A. (1972). Diastrophic dwarfism. *Medicine* **51** (1), 41-59.

Wang, D.N., Kuhlbrandt, W., Sarabia, V.E. and Reithmeier, R.A. (1993). Two-dimensional structure of the membrane domain of human band 3, the anion transport protein of the erythrocyte membrane. *EMBO Journal* **12**, 2233-2239.

Wherrett, J.R. and Huterer, S. (1972). Enrichment of bis(monoacylglycerol)phosphate in lysosomes from rat liver. *Journal of Biological Chemistry* **247**, 4114-4120.

Winters, R.W., Delluva, A.M., Deyrup, I.J. and Davies, R.E. (1962). Accumulation of sulfate by mitochondria of rat kidney cortex. *Journal of General Physiology* **45**, 757-775.

Wood, P.G. (1992). The anion exchange proteins: homology and secondary structure. Progress in Cell Research. Edited by Bamberg, E. and Passow, H. **2**, pp 325-352. Elsevier Science Publishers, Amsterdam.

Young, F.M., Luderer, W.B. and Rodgers, R.J. (1995). The antioxidant beta-carotene prevents covalent cross-linking between cholesterol side-chain cleavage cytochrome P450 and its electron donor, adrenodoxin, in bovine luteal cells. *Molecular and Cellular Endocrinology* **109** (1), 113-118.

Zaki, L., Fasold, H., Schuhmann, B. and Passow, H. (1975). Chemical modification of membrane proteins in relation to inhibition of anion exchange in human red blood cells. *Journal of Cellular Physiology* **86** (3 Pt 1), 471-494.

Appendix A. Sequences included in the phylogenetic tree illustrated in *Figure 5.12.*

Accession ID	Database	Species	Transporter
cab42985	GenPept	Triticum	
caa65291	GenPept	H. vulgare	
cab42986	GenPept	Triticum	
aab94543	GenPept		
sut2_styha	Swiss-Prot	Stylosanthes hamata (forage legume)	High affinity sulphate transporter 2
sut1_styha	Swiss-Prot	Stylosanthes hamata	High affinity sulphate transporter 1
baa33932	GenPept		
baa25175	GenPept		
baa21657	GenPept		
baa20282	GenPept	Arabidopsis thaliana (thale cress)	
caa65536	GenPept		
baa75015	GenPept		
aff17693	GenPept		
baa12811	GenPept		
caa11413	GenPept		
baa20084	GenPept		
sut3_styha	Swiss-Prot	Stylosanthes hamata	Low affinity sulphate transporter 3
no70_soybn	Swiss-Prot	Glycine max (soybean)	Sulphate permease
baa23424	GenPept	Arabidopsis thaliana (thale cress)	Sulphate transporter
baa16785	GenPept	Synechocystis sp. (cyanobacterium)	High affinity sulphate transporter
aac07275	GenPept	Aquifex aeolicus (bacterium)	High affinity sulphate transporter
aab88215	GenPept	Synechococcus (cyanobacterium)	Biotin carboxylase
cab03701	GenPept	Mycobacterium tuberculosis	High affinity sulphate transporter
aaf24008	GenPept		
aad53951	GenPept	Drosophila melanogaster	
cab69640	GenPept	Bos taurus	Sulphate transporter
dtd_human	Swiss-Prot	Homo sapiens	Sulphate transporter
dtd_rat	Swiss-Prot	Rattus norvegicus	Sulphate transporter
dtd_mouse	Swiss-Prot	Mus musculus	Sulphate transporter
SAT1_H	None	Homo sapiens	Sulphate transporter
sat1_rat	Swiss-Prot	Rattus norvegicus	Sulphate transporter
aad51618	GenPept		
aad51617	GenPept		
pend_human	Swiss-Prot	Homo sapiens	Sulphate transporter
dra_human	Swiss-Prot	Homo sapiens	Sulphate transporter
aad42784	GenPept	Mus musculus	Sulphate transporter

(appendix continued ...)

(continuation of appendix ...)

Accession ID	Database	Species	Transporter
aaa82335	GenPept	*Caenorhabditis elegans* (worm).	
yldm_caeel	Swiss-Prot	*Caenorhabditis elegans* (worm).	Hypothetical 85.0 kd protein
s46176	PIR		
sul1_yeast	Swiss-Prot	*Saccharomyces cerevisiae*	High affinity sulphate transporter 1
sul2_yeast	Swiss-Prot	*Saccharomyces cerevisiae*	High affinity sulphate transporter 2
sulh_schpo	Swiss-Prot	*Schizosaccharomyces pombe*	Probable sulphate permease
aaf14539	GenPept	*Penicillium chrysogenum* (fungi)	Sulphate permease (Sut B gene)
aaf14540	GenPept	*Penicillium chrysogenum* (fungi)	Sulphate permease (Sut A gene)
cy14_neucr	Swiss-Prot	*Neurospora crassa*	Sulphate permease II
aaa33615	GenPept		
caa18307	GenPept		
sulx_yeast	Swiss-Prot	*Saccharomyces cerevisiae*	Putative sulphate transporter
caa73749	GenPept		
aad47994	GenPept		
ybar_bacsu	Swiss-Prot	*Bacillus subtilis*	Hypothetical 46.4 kDa protein
baa17514	GenPept		
baa10568	GenPept		
baa10512	GenPept		
cab10964	GenPept		
cab15471	GenPept		
ychm_ecoli	Swiss-Prot	*Escherichia coli*	Hypothetical 58.4 kDa protein
aad19151	GenPept		

Addendum

p. xii: par. 2, line 6: "nor any other substrate" should read "nor any other ligand".
p. 4: par. 2, line 3: "electrophysiological data is "should read "electrophysiological data are".
p. 11: next to last line: "due to pathway's" should read "due to ATP sulphurylase's".
p. 17: par. 2, lines 1 and 3: replace "between species" with "among species".
p. 19: par. 2, line 5: replace "unwelcome" with "invading".
p. 21: par. 2, line 3: "but it contains" should read "but also contains".
p. 27: par. 2, line 2: replace "tagged" with "modified".
p. 28: par. 2, line 7: replace "tool for the" with "tool for the purification of the".
p. 30: line 5: "as many" should read "over twenty".
p. 30: line 10: addition "The sialic acid transporter, too, has been cloned (*Section 1.3.3.3*)".
p. 32: footnote: addition; It is uncertain that lysosomal cystine transport is active transport. The finding that ATP stimulates the cystine transporter does not necessarily mean it is active. Cystine probably always moves down a concentration gradient when it leaves the lysosome, since the reducing environment of the cytoplasm rapidly removes the disulphide.
p. 45: section 1.5: "sulphate specific" should read "sulphate-specific".
p. 48: Section 1.5.2, line 2: "More recently the first" should read "The first".
p. 50: par 3, line: 6: replace "widely expressed" with "wide"
p. 50: par. 3, last sentence: replace the first coma with a colon and all subsequent comas with semi-colons.
p. 50: last line: "disequilibrium mapping" should read "linkage disequilibrium mapping".
p. 53: second sentence: replace "analysis of" with "analysis of:" and replace all comas with semi-colons.
p. 98: line 9: replace "osmotic conditions" with "iso-osmotic conditions".
p. 105: the last sentence should read "This supports that the H^+-ATPase activity observed was a measure of lysosomal H^+-ATPase activity".
p. 108: par 2, line 6: after "apoptosis" insert ",however apoptosis is not uniquely defined by these data".
p. 123, Fig. 3.15: insert "Error bars represent standard deviation.".
p. 127, Fig. 3.16: insert "These data reflect an efflux experiment".
p. 136, Fig. 3.19: insert "Valinomycin prevents an electrochemical membrane potential.".
p. 140: par. 2, line 2: should read "This suggests that phospholipid membrane integrity, and not protein structure was compromised".
p. 172: par. 2, line 4: should read "in abundance to be visualised".
p. 176: par. 3, line 4: replace "detergent affects" with "detergent disrupts".
p. 189: par. 1, line 3: replace "cistae" with "cristae".
p. 203: line 11: replace "A lot" with "A substantive amount".
p. 204: Fig. 5.2A, legend: "subject to" should read "subjected to".
p. 206, par. 2: after first sentence insert "The antigenic index was determined by the method by Jameson and Wolf, CABIOS, 4(1), 181-186 (1988)."
p. 211: par. 1, line 6: should read "This demonstrated that the 28 kDa protein detected was not a result of cross-reactivity with Con A-Sepharose".
p. 211: par. 2, line 2: replace: "then" with "than".
p. 226: line 2: "were affinity purified peptides" should read "were affinity purified with peptides".
p. 241: par. 1, next to last line: replace "its" with "it's".
p. 242: line 10: replace "galloping" with "rapidly developing".
p. 249: par. 2, line 1: replace "the" with "they".